DESIGN OPTIMIZATION OF THE ELECTRICALLY PEAKING HYBRID (ELPH) VEHICLE

by

M. Ehsnai, Ph.D., P.E., F. IEEE
Yimin Gao, Ph.D.
K. Butler, Ph.D., P.E.

SWUTC/98/466620-1

This report also serves as a deliverable for the following SWUTC projects:
466600 and 465140

Southwest Region University Transportation Center
Texas Transportation Institute
Texas A&M University System
College Station, Texas 77843-3135

October 1998

Technical Report Documentation Page

1. Report No.	2. Government Accession No.	3. Recipient's Catalog No.
SWUTC/98/466620-1		

4. Title and Subtitle	5. Report Date
Design Optimization of the Electrically Peaking Hybrid (ELPH) Vehicle	October 1998
	6. Performing Organization Code

7. Author(s)	8. Performing Organization Report No.
M. Ehsani, Y. Gao and K. Butler	Research Report 466620-1

9. Performing Organization Name and Address	10. Work Unit No. (TRAIS)
Texas Transportation Institute Texas A&M University System College Station, Texas 77843-3135 PB99-129645	11. Contract or Grant No. CF057

12. Sponsoring Agency Name and Address	13. Type of Report and Period Covered
Southwest Region University Transportation Center Texas Transportation Institute The Texas A&M University System College Station, Texas 77843-3135	14. Sponsoring Agency Code

15. Supplementary Notes

Supported by a grant from the Office of the Governor of the State of Texas, Energy Office

16. Abstract

Electrically Peaking Hybrid (ELPH) is a parallel hybrid electric vehicle propulsion concept that was invented at Texas A&M University, by the advanced vehicle systems research group. Over the past six years, design methodologies, component development, and system optimization work has been going on for this invention.

This project was a first attempt in integrating the above developments into an optimized design of an ELPH passenger car. Design specifications were chosen for a full size passenger car, performing as well as any conventional car, over the EPA-FTP-75 combined city/highway drive cycles.

The results of this design project were two propulsion systems. Both were appropriate for commercial production, from the points of view of cost, availability of the technologies, and components. One utilized regenerative braking and the other did not.

Substantial fuel savings and emissions reductions resulted from simulating these designs on the FTP-75 drive cycle. For example, our ELPH full size car, with regenerative braking, was capable of delivering over 50 miles per gallon in city driving, with corresponding reductions in its emissions.

This project established the viability of our ELPH concept and our design methodologies, in computer simulations. More work remains to be done on investigating more advanced power plants, such as fuel cells, and more advanced components, such as switched reluctance motor drives, for our designs. Furthermore, our design optimization can be carried out to more detailed levels, for prototyping and production.

17. Key Words	18. Distribution Statement
Hybrid-Electric Vehicle, Hybrid Vehicle, Electric Vehicle, Advanced Vehicle, Sustainable Transportation, Fuel Efficient Vehicle, Clean Car, Zero Emission Vehicle, ULEV, ZEV.	No Restrictions. This document is available to the public through NTIS: National Technical Information Service 5285 Port Royal Road Springfield, Virginia 22161

19. Security Classif.(of this report)	20. Security Classif.(of this page)	21. No. of Pages	22. Price
Unclassified	Unclassified	203	

ACKNOWLEDGMENT

This publication was developed as part of the University Transportation Centers Program which is funded 50% in oil overcharge funds from the Stripper Well settlements as provided by the Texas State Energy Conservation Office and approved by the U.S. Department of Energy. Mention of trade names or commercial products does not constitute endorsement or recommendation for use.

Executive Summary

This project was the first attempt at optimizing and designing Electrically Peaking Hybrid (ELPH) vehicle. The ELPH vehicle was invented in our research center, at Texas A&M University. Extensive work had previously been done in developing design methodologies, computer models and controls, toward the realization of the ELPH car. This project used these background works to develop the first viable ELPH car design, which is appropriate for commercial mass production.

The objectives of this project were to optimize and design the ELPH propulsion system for a typical 5-seat full size passenger car that possesses features such as

(1) Comparable performance to conventional vehicles that have similar space and loading capacity,
(2) Similar mass production cost to that for corresponding conventional vehicles,
(3) The same operation as driving conventional vehicles,
(4) Two to three times fuel economy over the conventional vehicles and,
(5) Self sustained battery state-of-charge (The batteries on board do not need to be charged from outside of the vehicle).

The ELPH propulsion system operates based on the Electrically Peaking Hybrid principle developed in our research center, which is described in detail at page 2 of the Technical Report attached

The key issues in the ELPH propulsion system optimization and design are (1) proper selection of the propulsion components, (2) control strategy designs, (3) regenerative braking consideration, (4) driving simulation, and (5) performance prediction.

The car that was designed is a 4-door, 5-seat full size passenger car with front - wheel drive, spark-ignition gasoline engine, induction AC motor and lead/acid batteries on board and

single gear transmission (Please see the design specifications at page 7 of the Technical Report attached).

The engineering data and driving performances obtained from the simulated test drives show that the ELPH vehicle design is very reasonable. This report show that ELPH propulsion system can meet the practical design specifications and is suitable for the mass production. The fuel consumption can be significantly reduced. Emissions of the toxic and green house gases are expected to also be greatly reduced (Please see the Design Results at pages 10 through 14).

Component improvements, design improvements and simulation model improvements are being aggressively continued. Our new discoveries of better electric motor drives, control methods, new power plants and system design methodologies are being individually perfected at the present time. We request continuation of funding of this design optimization effort. In the next phase of this project, we propose to deliver the second-generation ELPH design, incorporating the above developments. Thus, we can produce car propulsion system designs that far surpass the existing technologies, in performance, fuel efficiency emission and cost of manufacturing. Proposals for further study are also briefly mentioned in this report (Please see page 15 through 16 in the Technical report attached).

Table of Contents

List of Figures

Design Optimization of the ELectrically Peaking Hybrid (ELPH) Vehicle

INTRODUCTION

In vehicle development and design, the current major issues are marketability and impact on the environment. Conventional gasoline and diesel fueled vehicles possess the advantages of (1) good performance, (2) long driving range, (3) ease of refueling, (4) light-weight energy source, (5) well known manufacturing technology, and (6) safety. These advantages have enabled the conventional vehicles to dominate the market. However, the conventional vehicles have serious disadvantages in regard to fuel consumption and environment impact. The electric vehicles, which have been under development for many years, are considered to be important substitutes of the conventional vehicles. But the commercialization of the electric vehicles has encountered major obstacles. Due to the heavy and bulky batteries on board, the electric vehicles usually have sluggish performance, limited loading capacity, short driving range, long battery recharging time and high manufacturing cost.

Hybrid electric vehicles under development in recent years, are considered to be the best trade-off between conventional and electric vehicles. In a hybrid vehicle, two power plants are available which commonly are internal combustion engine and electric motor. The inclusion of two power plants provides flexibility to use either internal combustion engine or electric motor or both together for traction, according to their operation characteristics and driving requirement. This configuration increases the potential to optimize the overall drive train operation. It also, however, increases the complexity in the management of the powers supplied by both engine and motor. Therefore, the control strategy of the power plants is a crucial aspect in the development of hybrid electric vehicles.

A hybrid electric propulsion system, with a parallel configuration, referred to as ELectrically Peaking Hybrid (ELPH) propulsion system, was introduced by our group. The principle is illustrated through simulations performed using the V-ELPH software simulation program developed at Texas A&M University[1]. The power plants available in the system are a spark ignition internal combustion engine and an AC induction motor. The power plants are managed (controlled) with electrically peaking manner[2,3,7,8,9]. The objectives of the application of the ELPH propulsion system to a full size car are:

(1) comparable performance to conventional vehicles that have similar space and loading capacity,
(2) similar mass production to that for corresponding conventional one,
(3) the same operation as driving conventional vehicle,
(4) two to three times fuel economy over the conventional vehicles, and
(5) self sustained battery SOC.

ELPH PRINCIPLE

For a full size vehicle, the required acceleration performance usually determines the power capacity of the power plants. For instance, for a vehicle with 1500 kg gross weight, the average power needed to accelerate the vehicle from zero speed to 100 km/h (62.5 mph) in 10 seconds is about 60 kW, and the peak power of the engine needed would reach about 90 to 100 kW. However, in normal driving, the average load power is only 15 to 20 kW. Such low load power results in very low engine fuel efficiency. This conflict between the performance and fuel economy requirements pushes the conventional vehicle design into a dilemma.

Actually, in normal driving, the load power of the vehicle varies randomly as shown in Fig.1. This power profile can be resolved into two components: one representing the average power demand and other representing the dynamic power demand which has a zero average value. With the ELPH principle, an internal combustion engine, which has optimal steady-state operating region in its speed-power characteristics map, is used to supply the average load. The electric traction system (electric motor and batteries) is used to produce the dynamic power[7,8]

With the ELPH principle, engine size can be reduced greatly and the engine can operate mostly in its efficient region, resulting in much more operating efficiency. The electric traction system operates in a dynamic manner, producing the peaking power to meet the peak power demand in acceleration and hill-climbing. The storage energy within the batteries can be maintained in a balanced state by two battery charging approaches. The first approach is to charge the battery by recovering the kinetic energy in decelerating and potential energy of the vehicle in down-hill driving. The second approach is to charge the batteries by the excess power of the engine when the load power demand is less than the power the engine can produce. These two battery-charging approaches can be implemented by using the motor controller to operate the traction motor as a generator. With these approaches, the batteries only function as an energy reservoir. With proper design, the battery state-of-charge can be maintained at a reasonable level in the driving, and the battery size (energy capacity) can be small[2].

CONFIGURATION AND OPERATION MODES OF THE PROPULSION SYSTEM

The ELPH prolusion system proposed has **parallel configuration** as shown in Fig.2 and Fig.3[7,8]. The configuration shown in Fig.2 is the two-shaft configuration, in which, the engine torque, modified by the transmission, and motor torque are added together by a torque summer which may be a set of gears, or chain. The configuration in Fig.3 is single-shaft configuration, in which, the rotor of the motor functions as the torque summer. However, both configurations have the same operation principle. The choice of which is more suitable in physical design depends on the engine and motor characteristics, performance requirement, and convenience to developing the propulsion under hood.

The transmissions in both configurations are used to modify the torques so as to properly match the requirement of the driving. The transmissions may be multi-speed or single speed, depending on the engine and motor size, operation characteristics and performance requirement. Actually, due to the favorable characteristics of the electric motor as a traction power plant, a **sing-gear transmission** may satisfactorily serve the propulsion[2].

The ELPH propulsion can potentially realize several operation modes such as: **(1) motor-only mode, (2) engine-only mode, (3) hybrid traction mode (engine plus motor), (4) regenerative braking mode, and (5) battery charging from the excess power of the engine.** The motor-only operation mode is used when the speed of the vehicle is very low such that the engine can not operate steadily and the battery is fully charged in highway driving. The engine-only operation mode may be used in the case that the battery is fully discharged (if this occurs accidentally). However, this operation mode should be avoided as much as possible. Hybrid traction operation mode is used in a case where the peak power is required, such as acceleration and hill climbing driving. The regenerative braking operation mode is used in braking. In this case, the electric motor functions as a generator to recuperate the kinetic or potential energy of the vehicle into electric energy to charge the batteries on board. The battery charging mode from the excess power of the engine is used when the batteries is not fully charged and the engine has excess power after propelling the vehicle.

A micro-processor based vehicle controller is applied to regulate the engine and motor operations to optimally use the above operation modes according to the driving requirement, engine and motor operation characteristics, battery state-of-charge information. The control target of the control strategies in the vehicle controller is **(1) to meet the tractive effort required by the driver, (2) to maintain the battery SOC at reasonable level, (3) to operate the engine efficiently, and (4) to recover the kinetic and potential energy as much as possible.**

CONTROL STRATEGIES

Maximum Battery SOC Control Strategy

In urban driving, the frequently accelerating–decelerating driving would discharge the batteries quickly. Therefore, Maintaining the battery SOC at high level is crucial for the operation of the vehicle. In this case, the control system should, a priori, charge the batteries to prevent them from complete depleting. Therefore, Maximum battery SOC control strategy would be the best control strategy while the vehicle drives in urban.

The control target of the Maximum Battery SOC control strategy follows the principle that high battery SOC should be maintained in driving as much as possible. This control principle results in the engine being used as much as possible and the electric traction system should be used as little as possible. The details of this control strategy are illustrated in Fig.4, which is explained in detail below.

(1) **Hybrid Traction Mode**: when the traction power required is greater than the power that the engine can supply (this may occur in acceleration and hill-climbing) as shown in Fig. 4 by point A, hybrid traction mode must be used. In this case, the engine and electric motor must supply their power to meet the power requirement. The power distribution between the engine and the motor is to operate the engine at near full load (full throttle, which usually is the optimal fuel economy operation), and to control the electric motor to supply its power equal to the remaining load power. So, output traction power of the electric motor and battery discharge power are expressed as

and

$$P_{mt} = \frac{P_L - P_{eopt}\eta_{T,e}}{\eta_{T.m}} \qquad (1)$$

$$P_{bd} = \frac{P_{mt}}{\eta_m \eta_{bd}} \qquad (2)$$

where, P_L is the load power of the vehicle,

P_{eopt} is the engine power corresponding to its optimal operating line, which is near the full-throttle operation,

$\eta_{T,e}$ is the transmission efficiency from the engine to the driven wheels,

η_m is the efficiency of the traction motor,

η_{bd} is the battery discharge efficiency.

(2) **Engine Alone Traction Mode**: When the traction power required is less than the power that the engine can produced with near full throttle as shown in Fig.4 by point B, the engine can be controlled depending on the battery SOC. If the battery SOC reaches its top level, the engine should be controlled to produce its power that is equal the load power. In this case, the engine output power is

$$P_e = \frac{P_L}{\eta_{T,e}} \qquad (3)$$

and the electric motor and battery power are zero. In ELPH power train design, this operation mode should be avoided as mush as possible, because the partial-load operation will result in low engine operation efficiency.

(3) **Battery Charging Mode from Engine Excess Power**: When the traction power requirement is the same as in (2) represented by point B and the battery SOC does not reach its top level,

the engine should be operated at near full load. The power remaining after propelling the vehicle is used to charge the batteries. In this case, the electric motor will function as a generator and the batteries will absorb energy from the electric motor. The output power of the electric motor and the battery charging power are expressed as

and

$$P_{mg} = (P_{eopt} - \frac{P_L}{\eta_{T,e}})\eta_{T,em}\eta_m \qquad (4)$$

$$P_{bc} = \frac{P_{mg}}{\eta_{bc}} \qquad (5)$$

Where, $\eta_{T,em}$ is the transmission efficiency from the engine to the electric motor,

η_{bc} is battery charging efficiency.

(4) **Motor Alone Traction Mode:** When the vehicle speed is less than the speed which corresponds to the minimum speed of the engine, the engine stands still and the electric motor alone propels the vehicle. In this case, the motor output power is expressed as

and

$$P_{mt} = \frac{P_L}{\eta_{T,m}} \qquad (6)$$

$$P_{dc} = \frac{P_{mt}}{\eta_m \eta_{bd}} \qquad (7)$$

(5) **Hybrid Braking Mode:** In braking operation, if the braking power is greater than the power that the electric system (electric motor and batteries) can absorb, as shown in Fig.4 by point C, and to recuperate the braking energy as much as possible, the electric motor, functioning as a generator, should be controlled at its maximum power. The remaining braking power is supplied by the frictional brake system. The generating power of the electric motor and the battery charging power can be expressed as

$$P_{mg} = P_{mmax} \qquad (8)$$

and

$$P_{bc} = \frac{P_{mg}}{\eta_m \eta_{bc}} \qquad (9)$$

The braking power distribution between the electric braking and mechanical frictional braking will be described in following section.

(6) **Electrically Regenerative Braking Alone Mode**: When the braking power needed is less than the power the electric system can handle, as shown in Fig.4 by point D, the electrically regenerative braking alone is used. The generating power of the electric motor and battery charging power can be expressed as

and $$P_{mg} = P_b \eta_{T,m} \qquad (10)$$

$$P_{bc} = \frac{P_{mg}}{\eta_m \eta_{bc}} \qquad (11)$$

Using the equations above and the control strategy, the engine power, motor power and the battery charging and discharging power can be calculated at any time of a given driving cycle.

Engine Turn-on and Turn-off Control Strategy

When vehicle is driven on the highway, the power and energy supplied by the electric system are much smaller than driving in urban areas, and the load power is usually less than the full-load power capacity of the engine. The batteries, in this case, can easily be fully charged. For avoidance of the inefficient engine operation, the engine should operate in a turn-on and turn-off or duty-cycle manner.

In the engine turn-on and turn-off control strategy, the duty cycle of the engine operation is depends on the battery SOC. Fig.5 shows the relationship between the engine duty cycle and the battery SOC. In the engine turn-on period, the engine alone propels the vehicle and the excess power is used to charge the batteries. Then the battery SOC goes up until reaching its top line. In this way, the engine would operate always near full load. After the battery SOC reaches its top level, the engine is turned off and the vehicle is propelled by the electric system alone. With the engine turn-on and turn off operation manner, the propulsion system would obtain maximum overall efficiency

REGENERATIVE BRAKING AND FRICTIONAL BRAKING

For improving the economy of the vehicle, the power train should recover the kinetic and potential energy of the vehicle as much as possible. In the case that the electric traction system is only available for one drive axle (front or rear) and braking must be applied on two axles (front and rear) for safety season, completely recovering the braking energy is impossible. In this study, a parallel braking system is applied. Parallel braking means that an additional electric braking system is added to the traditional frictional brake system. While braking, both brake systems are

in effect. The braking forces supplied by the electric and frictional brake systems are shown in Fig.6, where front wheel drive is assumed.

Fig.6 shows the frictional brake force, summation of frictional and regenerative braking forces and the ideal braking force curves. The frictional braking forces on the front and rear axles are proportional to the hydraulic pressure in the master brake cylinder. The regenerative braking force developed by the electric motor on the front axle is a preset function of the hydraulic pressure of the master cylinder, and therefore the preset function of vehicle deceleration. The braking operation is divided into three regions according to braking deceleration. First is the region in which the deceleration of the vehicle is less than 0.1g. In this case, the brake force of the vehicle is only applied to the front axle by the electric braking. Second is the region in which the deceleration of the vehicle is greater than 0.1g and less than 0.7g. In this case, the braking force on the rear axle is only supplied by the frictional barking system, and the braking force of the front axle is the summation of the frictional and electric braking forces, as shown in Fig.6. Third is the region in which the deceleration of the vehicle is greater than 0.7g. In this case, the braking forces on the front and rear axles are applied only by the frictional braking system.

PROPULSION DESIGN FOR FULL SIZE PASSENGER CAR

The design targets of the ELPH propulsion are that the full size passenger cars have:

(1) comparable performance to the conventional cars that have similar space and loading capacity,
(2) similar mass production cost to that of the conventional cars,
(3) the same operation as driving conventional cars,
(4) two to three times fuel economy over the conventional cars, and
(5) self sustained battery SOC.

Design Specification

Vehicle Type: 4-door, 5-seat passenger car, front engine/motor and front drive

Overall dimensions:

Overall length:	4.70 ~ 4.80 m
Overall width:	1.70 ~ 1.80 m
Overall height:	1.40 ~1.45 m
Wheel base	2.65 ~ 2.8 m
Tread width	1.55 ~ 1.75 m

Estimated weight

Curb weight:	1500 kg (include traction batteries)
Load	Two person (2×70 kg)+ luggage (60 kg)=200 kg
Total weight;	1700 kg

Weight on front/rear axle: 62% / 38%

Main components:

Engine:	Spark ignition, gasoline fueled internal combustion engine.
Traction Motor:	Electronically controlled induction AC motor.
Batteries:	Lead/acid traction batteries
Transmission:	Single gear, mechanical transmission

Performance specification

Acceleration	12±1 sec. (from 0 to 96 km/h or 60 mph)
Max. gradeability:	>30% and >5% @ 100 km/h
Maximum speed;	
Engine only:	120 km/h (75 mph)
Hybrid traction	160 km/h (100 mph)
Range:	Free from battery energy storage and only rely on fuel tank volume

Estimate of the Propulsion Parameters

In vehicle design, the first step is to estimate the size of the power plant(s) and the transmission parameters according to the design specification. In the ELPH propulsion design, The choices of the engine size, electric motor size and transmission have crucial influence on the vehicle performance, fuel economy, battery size, and driving range.

Engine Size—According to the ELPH operation principle, the engine is used to supply the average load power (the load power in steady driving). Thus, the engine power capacity can be initially determined by the load power demand in steady driving, which can be expressed as

$$P_e = \frac{V}{1000\eta_{T,e}}\left(mgf_r + \frac{1}{2}\rho_a C_D A_f V^2\right) \quad (kW), \qquad (12)$$

where, m is the vehicle gross mass in kg, $\eta_{T,e}$ is the transmission efficiency from the engine to driven wheels, f_r is the rolling resistance coefficient, ρ_a is the air density with $1.205\ kg/m^3$, C_D is the aerodynamic coefficient, A_f is the front area of the vehicle in m^2, and V is vehicle speed in m/s. The values of above parameters used are as follows.

Vehicle mass	1700 kg
Rolling resistance	0.01
Transmission efficiency	0.92
Aerodynamic drag coefficient	0.3

Front area $2.25m^2$

The power demand along the vehicle speed is shown in Fig.7. This figure indicates that about 21 to 33 kW of engine power can meet the power requirement for the speed between 120 to 140 km/h (75 to 87.5 mph) with steady driving. This power demand is much smaller than the power of engines used in conventional passenger cars[2]. Considering the power consumed in accessories, such as lights, audio, power steering, air conditioner and so on, a 28 to 40 kW engine would be needed. The speed – power and speed torque characteristics of a typical gasoline engine are shown in Fig.8.

Electric Motor Size – Based on the ELPH principle, electric motor is used to handle the dynamic load of the vehicle. Therefore, determination of the electric motor size depends on the acceleration and gradeability requirements. In practice, the acceleration is the first consideration in design of passenger cars.

As initial estimate, an assumption would be made that the steady-state load is handled by engine and the dynamic load is handled by electric motor. In this way, the maximum electric motor power needed in the acceleration can be expressed as[4]

$$P_{m\,max} = \frac{30m\delta}{9546\pi t_f}\left(\frac{V_b^2 + V_f^2}{2}\right) \quad (kW), \qquad (13)$$

where, δ is the mass factor of the rotating components in the drive train, V_b is the vehicle speed corresponding to the motor base speed in *m/s*, V_f is the vehicle speed at the end of the acceleration in *m/s*, and t_f is the acceleration time in second. The following parameters are used in the estimate of the maximum power of the electric motor.

Final speed of acceleration:	96 km/h (60 mph)
Acceleration time:	12 Sec.
Mass factor	1.02
Vehicle speed corresponding to motor base speed	37.5 km/h (23.4 mph)

The maximum motor power of about 65 kW is calculated using equation (13) and the parameters above. It should be noted that engine has, actually, some excess power to help electric motor to accelerate the vehicle as shown in Fig 9. This excess engine power to assist the electric motor in acceleration is assumed to be about 10 kW. Thus the maximum power of the electric motor will be 55 kW. It should be noted that this motor power is the peak power needed. The rated power of the electric motor is much smaller that this value (one third or half of the peak power). Fig 10 shows the speed power characteristics of the electric motor.

Transmission – Due to the favorable traction characteristics of the electric motor, a single transmission would meet the performance requirement. Reference [2] has described the principle,

with which, the proper gear ratios from the engine and the electric motor to the drive wheels can be chosen. With the engine characteristics shown in Fig.7 and the maximum vehicle speed specified in the design specification, the gear ratio from the engine to the driven wheels are chosen as 3.90. Similarly, the gear ratio from the electric motor to the driven wheels is also chosen as 6.58.

It should be noted that all the parameters mentioned above are the initial estimated values. They should be verified and confirmed by further performance calculation and driving simulation. If necessary, they should be modified for achieving optimum operation results and meeting the requirements of the design specification.

DESIGN RESULTS

Design of the ELPH propulsion has been performed with the aid of the V-ELPH simulation package developed in ELPH Research Group, Department of Electrical Engineering, Texas A&M University. By running the computer program, and iteratively refining the propulsion parameters, the optimum design can be found, which optimize the fuel economy of the vehicle under the condition of meeting the design specification.

In order to find the influence of the regenerative braking on the vehicle performance and fuel economy. Two designs have been made, one is regenerative breaking available and the other unavailable.

Design Results (Regenerative Braking Unavailable)

In calculation of the vehicle economy in the EPA FTP75 driving cycles (urban and highway) and performance for the propulsion without regenerative braking, the propulsion parameters below are used.

Maximum power of engine	42(kW) (35 kW available for traction)
Maximum power of electric motor	55 kW
Gear ratio from the engine to the driven wheels	3.9
Gear ratio from the traction motor driven wheels	6.58
Transmission efficiency	0.92

Fuel Economy in EPA FTP75 Driving Cycles

Driving in FTP75 Urban cycle – Fig.11 shows the simulation results, which includes vehicle speed, engine power output, electric motor power output and the changes in battery storage energy, in which, the **Maximum battery SOC control strategy** is used. This figure indicates that, with the selected propulsion parameters, the battery storage energy can be balanced at the beginning and end of the driving cycle. This results means that the vehicle can be free from its battery recharging from outside of the vehicle. The fuel economy of the vehicle, in this case, reaches 34.32 mpg (6.89 L/100 km). Fig.12 shows the engine operating points on the characteristic map of

the engine fuel economy. This figure indicates that actual engine operating points coincide to the optimal operating line and the potential of the engine fuel economy can be mostly used.

Driving In FTP75 Highway Driving – Fig.13 shows vehicle speed, engine power output, motor power output and the changes in the battery storage energy versus the driving time with Engine Turn-on and Turn-off control strategy. Fig. 14 shows the actual engine operating points on the characteristic map of the engine fuel economy. In this case, the fuel economy of the vehicle is 42.34 mpg(5.58 L/100 km), and the vehicle can also be free from the outside charging.

Performance

The acceleration performance is shown in Fig.15. This figure show that the time needed for the vehicle to accelerate from zero speed to 96 km/h (60 mph) needs 11.7 seconds and the covered distance is about 174m.

The gradeability and the maximum cruising speed of the vehicle can be found in Fig.16, which is a diagram maximum traction force on the driven wheel versus vehicle speed. The maximum gradeability, represented by point A, is about 18 degrees (32.5%) and the gradeability at the speed of 96 km/h (60 mph) is about 8.5 degrees (15%). The maximum speeds reach 160 and 140 km/h (87.5 and 100 mph) for hybrid traction and engine only traction modes respectively.

Design Results (Regenerative Braking Available)

The regenerative braking can recover the vehicle kinetic and potential energy, therefore reduce the battery charging energy from the engine. Thus the size of the engine can be reduced further. The regenerative braking principle in the design is referred to as parallel braking as shown in Fig.6. The maximum power of the engine is reduced from 35 kW (without regenerative braking to 23 kW (traction available, the maximum power may reaches 30 kW for additionally powering the accessories). The other parameters are the same as above.

Fuel Economy in EPA FTP75 Driving Cycles

Driving in FTP75 Urban cycle – Fig.17 shows the simulation results, which includes vehicle speed, engine power output, electric motor power output and the changes in battery storage energy, in which, the **Maximum battery SOC control strategy** is used. This figure indicates the, even reducing the engine size, the battery storage energy can be balanced at the beginning and end of the driving cycle. The fuel economy of the vehicle, in this case, reaches 50.7 mpg (4.66L/100 km). Fig.18 shows the engine operating points on the characteristic map of the engine fuel economy. This figure indicates that actual engine operating points can coincide to the optimal operating line and the potential of the engine fuel economy can be mostly used.

Driving In FTP75 Highway Driving – Fig.19 shows vehicle speed, engine power output, motor power output and the changes in the battery storage energy versus the driving time with

Engine Turn-on and Turn-off control strategy. Fig. 20 shows the actual engine operating points on the characteristic map of the engine fuel economy. In this case, the fuel economy of the vehicle is 49.8 mpg(4.74L/100 km), and the vehicle can also be free from the outside charging.

Performance

The acceleration performance is shown in Fig.21. This figure show that the time needed for the vehicle to accelerate from zero speed to 96 km/h (60 mph) needs 12.7 seconds and the covered distance is about 205m.

The gradeability and the maximum cruising speed of the vehicle can be found in figure 22. The maximum gradeability, represented by point A, is about 17.5 degrees (31.5%) and the gradeability at the speed of 96 km/h (60 mph) is about 7.8 degrees (13.5%). The maximum speeds reach 160 and 120 km/h (100 and 75 mph) for hybrid traction and engine only traction modes respectively.

Determination of Battery Size

The battery size is determined by two factors, one is the power demand and the other is the storage energy demand. The batteries must be able to supply sufficient power to the electric motor in accelerating driving which means that the peak power the batteries supply must be greater than, at least equal to the peak power of the electric motor (*55 kW*). The modern lead/acid traction batteries show the average specific power of *280W/kg* and power volume density of $470W/dm^3$[9], Thus, the total battery weight needed is about *200 kg* ($55\times10^3/280$) and the total battery volume is about *120* d^{m3} ($55\times10^3/470$).

The batteries must store sufficient energy to maintain the state-of-charge at a reasonable level during driving. Refer to Fig.12 and Fig.14, the maximum change in the battery storage energy is about *0.3 kW.h*. The battery storage energy capacity of the batteries can be obtained by

$$C_b = \frac{\Delta E_b}{SOC_{top} - SOC_{bottom}}$$

Where, ΔE_b is the maximum change in battery storage energy, SOC_{top} and SOC_{bottom} are the top and bottom values of the battery SOC, respectively, which are expected to be maintained in driving.

The battery operating efficiency (discharging and charging) is closely related to the battery state-of-charge as shown in Fig.23. This figure indicates that the range 40% to 60% of the battery state-of-charge is the optimal operating range. Thus, the battery storage energy capacity can be obtained as $C_b=0.3/(0.6-02)=1.5kW.h$.

The specific energy capacity and energy density of modern lead/acid are typically *40 W.h/kg* and *68 W.h/dm^3*. Thus the total weight and total volume of the batteries required by the storage energy are about *37.5 kg (1.5×10^3/40)* and *22 d^{m3} (1.5×10^3/68)* respectively, which are much smaller than those which are required by the peak power. This result implies that in ELPH propulsion, the batteries are used as power source more than as energy source.

Summary of the ELPH propulsion Design

Based on the ELPH principle and the simulation package developed in ELPH Research Group, Department of Electrical Engineering, Texas A&M University, The design results for a full size passenger car are summarized as below

The car without regenerative braking:

Components:	
Maximum engine power (Including powering the accessories)	42 kW (57 hp)
Maximum motor power (1 minute)	55 kW
Transmission	Single gear
Gear ratio from engine to driven wheels	3.9 (37 rpm/(km/h)) or (59 rpm/mph)
Gear ratio from traction motor to driven wheels	6.58 (62.5 rpm/(km/h)) or 100 rpm/mph)
Battery type	Lead/acid
Energy capacity	8 kW.h
Peak power	57 kW
Performance:	
Acceleration time (0 to 96 km/h(60 mph))	11.7 Seconds
Acceleration distance	175m (574 ft.)
Maximum speed	160 km/h (100 mph) with hybrid mode 140 km/h (87.5 mph) with engine-only mode
Gradeability	18 degrees (32.5%) maximum 8.5 degrees(15%) at 96 km/h (100 mph)
Fuel economy	
EPA FTP75 Urban driving	34.3 mpg (6.89L/100 km)
EPA FTP75 Highway driving	42.32 mpg (4.74L/100 km)
Range	Free from battery charging outside of the vehicle

The car with regenerative braking:

Components:	
Maximum engine power (Including powering the accessories)	30 kW (57 hp)
Maximum motor power (1 minute)	55 kW
Transmission	Single gear
Gear ratio from engine to driven wheels	3.9 (37 rpm/(km/h)) or (59 rpm/mph)
Gear ratio from traction motor to driven wheels	6.58 (62.5 rpm/(km/h)) or 100 rpm/mph)
Battery type	Lead/acid
Energy capacity	8 kW.h
Peak power	57 kW
Performance:	
Acceleration time (0 to 96 km/h(60 mph))	12.7 Seconds
Acceleration distance	205 (673 ft.)
Maximum speed	160 km/h (100 mph) with hybrid mode 120 km/h (75 mph) with engine-only mode
Gradeability	17.5 degrees (31.5%) maximum 7.8 degrees(13.7%) at 96 km/h (100 mph)
Fuel economy	
EPA FTP75 Urban driving	50.7 mpg (4.76L/100 km)
EPA FTP75 Highway driving	49.8 mpg (4.74L/100 km)
Range	Free from battery charging outside of the vehicle

Manufacturing Analysis

All the main components of the ELPH vehicles are available in mass production with well known technologies. The engine is a small spark-ignition engine popularly used in modern motor cars and motorcycles. The electric traction motor is a power electronics controlled AC induction motor. Batteries are commonly used lead/acid batteries. And the transmission is a single-gear mechanical speed reducer. The components do not need much R&D effort for application to the ELPH vehicles. These advantages are of vital importance for reduction of manufacturing cost and marketability.

Conclusion

The ELPH propulsion of hybrid electric vehicle, which has parallel configuration and operates with electrically peaking manner, can optimize the overall efficiency and satisfy the performance requirements of the vehicle. When driving inside cities, the Maximum Battery SOC control strategy is used, which can prevent the batteries from being completely depleted. When driving on highway, the Engine Turn-on and Turn-off control strategy is used, which can optimize the overall efficiency of the vehicle.

Simulation results, obtained by running the V-ELPH simulation package, developed by the ELPH Research Group, Department of Electrical Engineering, Texas A&M University, shows that, comparing with conventional gasoline fueled passenger cars, the full size passenger car with ELPH propulsion has comparable performance, similar space and loading capacity, the same driving operation, self sustained battery SOC and two to three times the fuel economy.

Functioning as power source more than as energy source, modern lead/acid batteries, which have good power density and bad energy density, would be the best choice. The ELPH propulsion does not have specific requirement from the electric traction system (traction motor and controller). Therefore, AC induction motor with power electronics controller would be a good selection. The single gear transmission can greatly simplify the construction and control system. Therefore, the cost of mass production is expected not to be higher than that for conventional cars.

Further Study

(1) **Further Study in Regenerative Braking**: As seen in the design results of the ELPH propulsion, availability of the regenerative braking can greatly improve the fuel economy of the vehicle, even though part of the kinetic energy of the vehicle is recovered (for example, in this design, only part of the braking power of the front axle is to be recovered). If the kinetic energy can be completely recovered, it is expected that the overall efficiency would be greatly improved. This may be implemented by adding energy storage devices (electric or mechanical) at the rear axle. Usually, peak value of the braking power is much greater than that the electric system can directly handled. This difficulty may be solved by adding some power leveling devices to reduce the peak value of the braking power (springs, magnetic coils and capacitors, for example). The braking power is stored in the energy storage elements temporarily, and then used to propel the vehicle or send to the batteries. The regenerative braking system may also function as anti-lock brake system (ABS).

(2) **Alternative Power Source:** Based on the ELPH operation principle, one power plant supplies its power to meet the steady load and the other to meet the dynamic load as mentioned in this report. The chemical battery-electric motor may be the most suitable system for dynamic load. But, internal combustion engines used as the power plants in modern vehicles may not be the best power plants to supply the steady load power, due to their very inefficient operation and toxic emissions. Other potential power plants including fuel cell, diesel engine, gas turbine engine, Sterling engine, two stroke engine with fuel ejection system, and so on would be more attractive than common 4-stroke spark-ignition engine

gasoline engine in the application on the ELPH vehicles. Among the potential power plants, the fuel cell may be the most viable one, due to its high efficiency, non-toxic emission advantages and favoring operation in steady state. Combining a better power plant with the ELPH principle, may result in a better propulsion system.

(3) **Driving Pattern Automatic Identification**: For different driving patterns (speed-time profiles, such as urban and highway drivings), the control strategies should be different. For instance, Maximum Battery SOC control strategy for urban driving and Engine Turn-on and turn-off for highway driving as mentioned in this report. The control strategies should be shifted automatically, rather than left to the driver. This may be done by averaging the speed experienced and finding the derivative of the speed, from its average value. The values of the average speed and speed derivative may be taken as the basis for the identification of the driving pattern. Microcomputer based vehicle controller may easily make the decision of which control strategy should be used in the current driving condition.

Reference

1. K. Butler, K. Stevens, and M. Ehsani, "*A Versatile Computer Simulation Tool for Design and Analysis of Electric and HybridDrive Trains*", SAE 970199

2. Yimin Gao, Khwaja M. Rahman, and Mehrdad Ehsani, "*Parametric Design of the Drive Train of Electrically Peaking Hybrid (ELPH) vehicle*", SAE 90294

3. Yimin Gao, Khwaja M. Rahman, and Mehrdad Ehsani, "*The Energy Flow Management and Battery Energy Capacity Determination for the Drive Train of Electrically Peaking Hybrid Vehicle*", SAE 972647

4. M. Ehsani, K. M. Rahman, and H. Toliyat, "*Propulsion System Design of Electric &Hybrid Vehicle*",

5. Martin Endar and Philipp Dietrich, "*Duty Cycle Operation as a Possibility to Enhance the Fuel Economy of an SI engine at Part Load*", SAE 960229

6. Clark G. Hochgraf, Michael J. Ryan, and Herman L. Wiegman, "*Engine Control Strategy for a Hybrid Electric Vehicle Incorporating Load Leveling and Computer Controlled Energy Management*", SAE 960230

7. M. Ehsani, "*Electrically Peaking Hybrid system and Method*", U.S. Patent, Granted 1996

8. J. Howze, M. Ehsani, and D. Buntin, "*Optimization Torque Controller for a Parallel Hybrid Electric Vehicle*", US Patent, Granted 1996

9. M. Ehsani, Y.Gao, and K. Butler, "*Application of Electrically Peaking Hybrid (ELPH) Propulsion System to a Full Size Passenger Car with Simulated Design Verification*", Accepted by IEEE Vehicular Transaction.

10. D. A. J. Rand, R. Woods and R. M. Dell, "*Batteries for Electric Vehicle*", Research Studies Press Ltd. 1998

11. J. W. Wong, "*The theory of Ground Vehicle*", John Wiley & Sons Inc. Press, 1978

12. Stephen Moore and Mehrdad Ehsani, "*An Empirical Based Electrosource Horizon Lead-Acid Battery Model*", SAE paper, 960448.

13. M. Ehsani, K.M. Rahman, M.D. Beller and A. Severinsky, "*Evaluation of Soft Switching for EV and HEV Motor Drives*", IEEE IECON, 1997 New Orleans.

14. K.M. Rahman, B. Fahami, G Suresh and M. Ehsani, "*Advantages of Switched Reluctance Motor for EV and HEV Application: Design and Control Issues*", Accepted for presentation in the IEEE IAS Conference Proceedings, 1998. St. Louis.

15. *Proceedings of ELPH Conference,* Texas A&M University, College Station, Texas, Oct, 1994.

16. Stephen W. Moore, and M. Ehsani, "*Analysis of Electric Vehicle Utilization on Global CO_2 Emission Level*", 99pc-142, Pending on SAE 1999.

17. Stephen W. Moore, and M. Ehsani, "*A Charge Sustaining Parallel HEV Application of the Transmotor*",99p-220, Pending on SAE, 1999

18. Stephen W. Moore, and M. Ehsani, "*Fundamental of Energy and Power Storage and Production in HEV Architectures*", 99-219, Pending on SAE, 1999.

19. Stephen W. Moore, Khwaja, M. Rahman, and M. Ehsani, "*Effect on Vehicle Performance of Extending the Constant Power Region of Electric Drive Motors*", 990-221, Pending on SAE, 1999

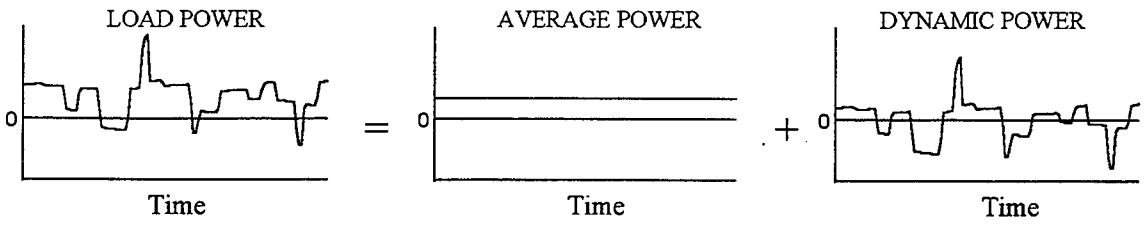

Fig.1 The load power demand and its steady and dynamic components

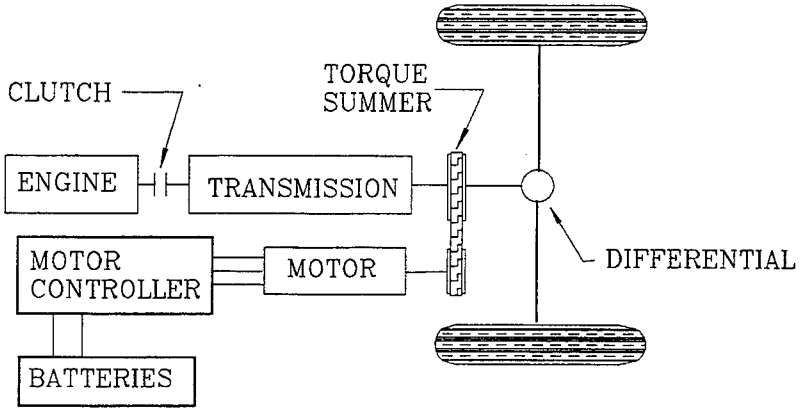

Fig.2 Two-shaft configuration of ELPH propulsion

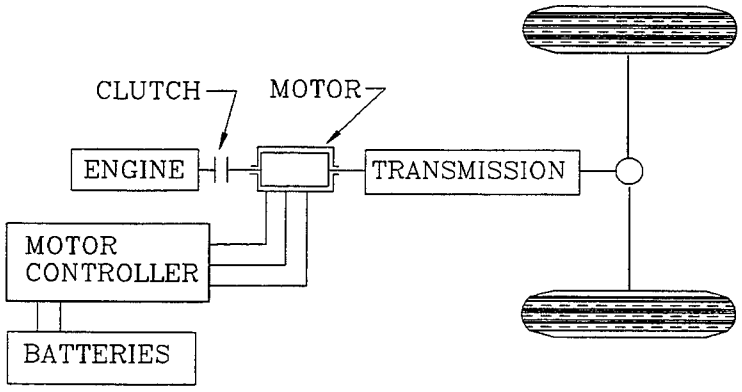

Fig3 Single-shaft configuration of ELPH propulsion

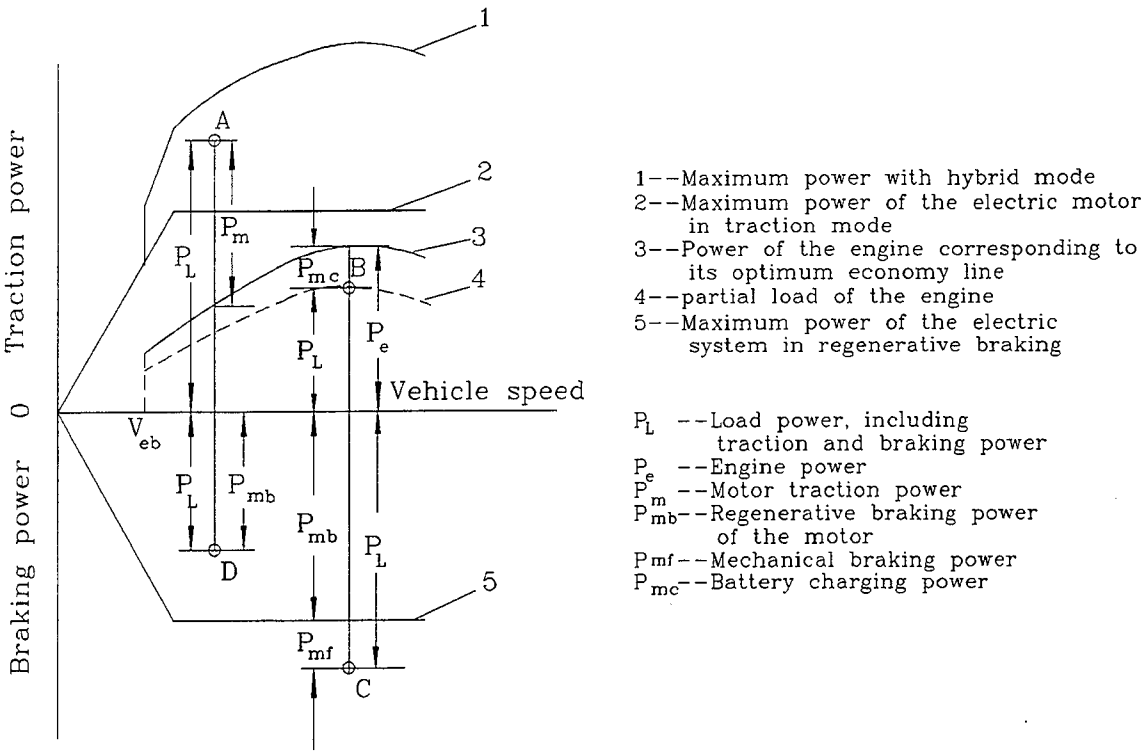

Fig.4 Illustration of the Maximum Battery SOC control strategy

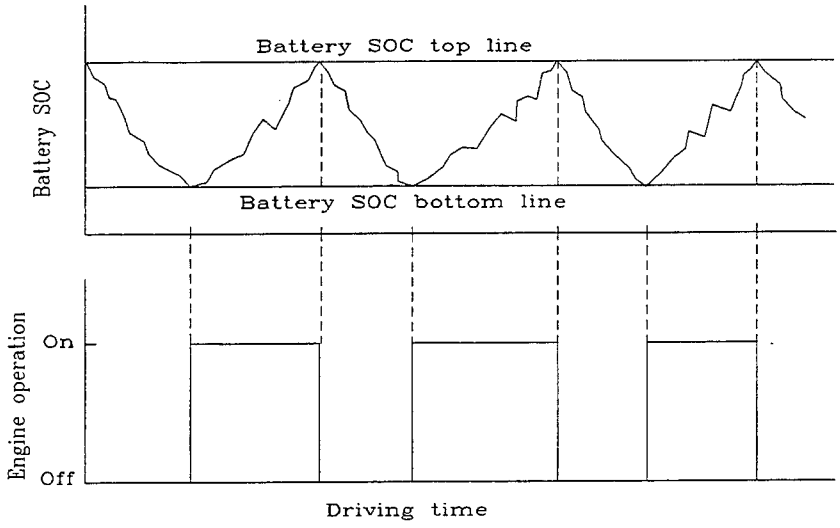

Fig.5 Illustration of the Engine Turn-on and Turn-off operation

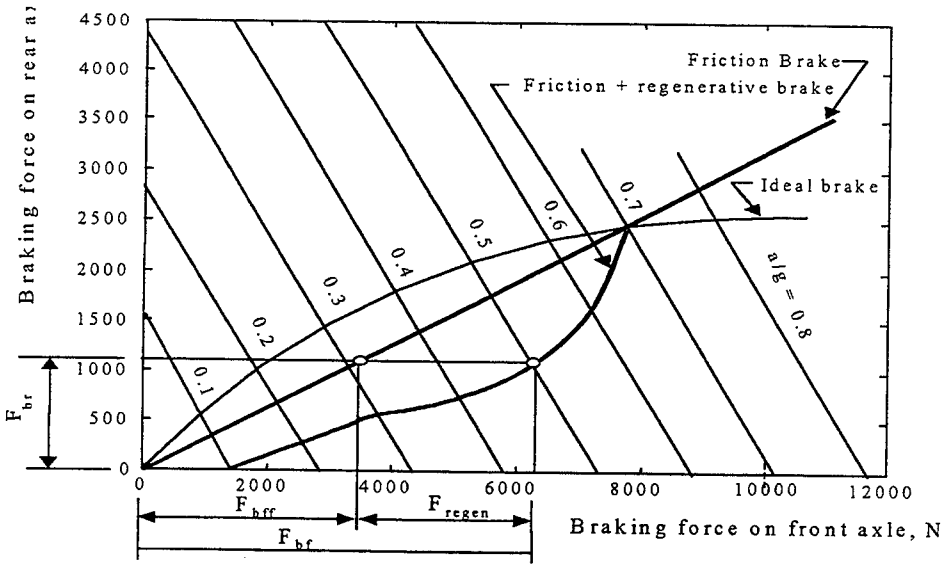

Fig.6 Demonstration of parallel braking principle

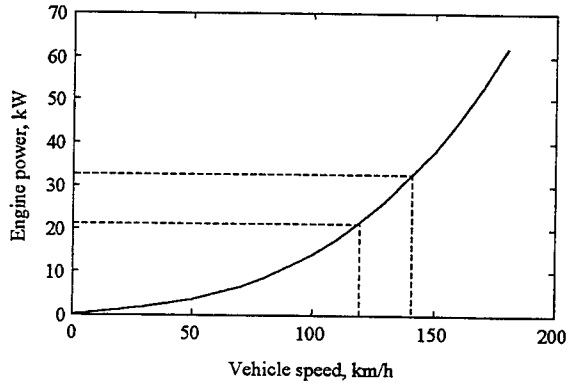

Fig.7 Engine power demand versus vehicle speed in steady driving

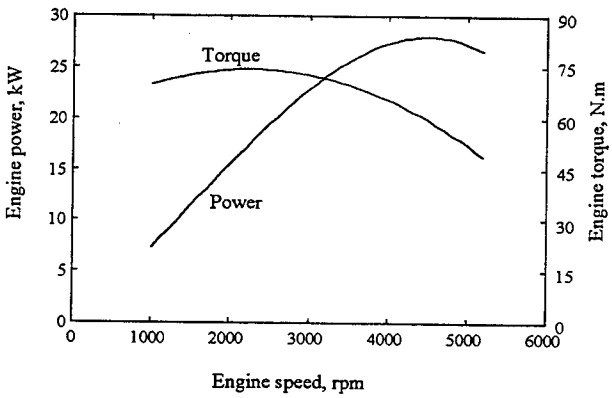

Fig.8 Speed-power and speed torque Characteristics if typical gasine engine

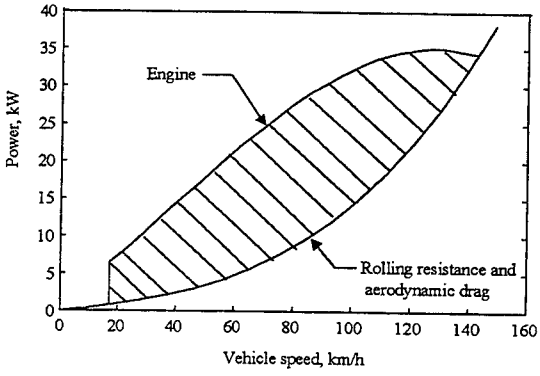

Fig.9 Illustration of the excess power of engine in acceleration

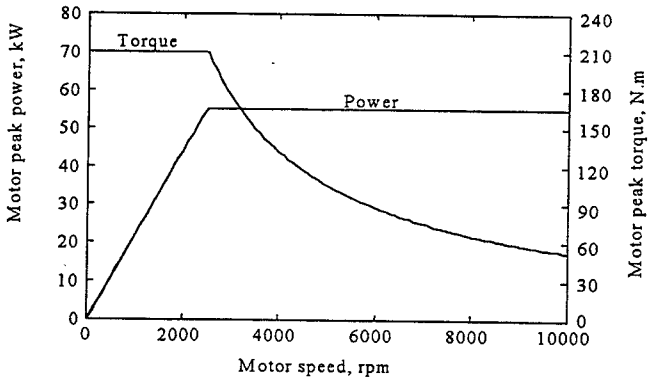

Fig.10 Electric motor characteristics

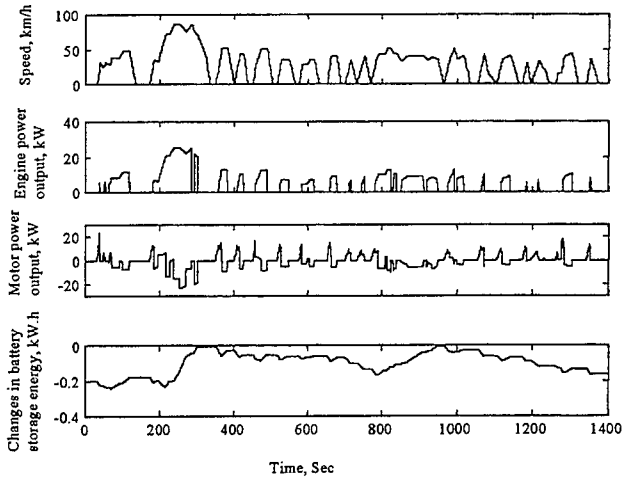

Fig.11 The time history of vehicle speed, engine power output, motor power output, and changes in battery storage energy in EPA FTP75 Urban Driving (regenerative braking unavailable)

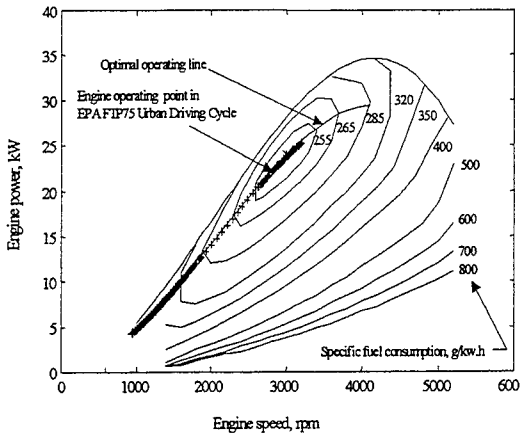

Fig. 12 Engine operating points on the fuel economy characteristics of the engine (regenerative braking unavailable)

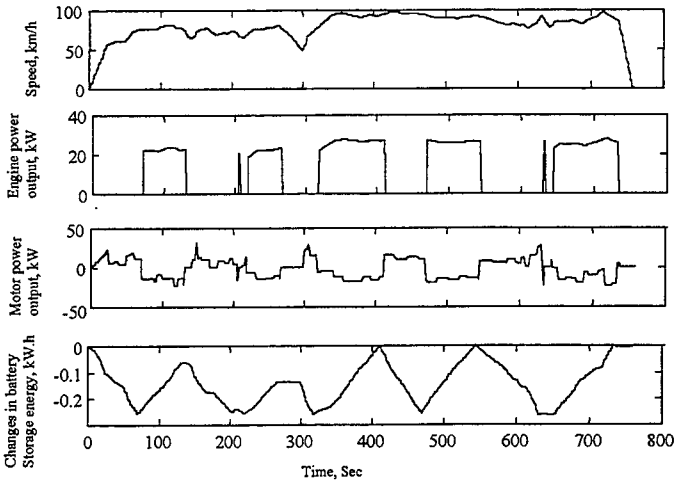

Fig. 13 The time history of vehicle speed, engine power output, motor power output, and changes in battery storage energy in EPA FTP75 Highway Driving (regenerative braking unavailable)

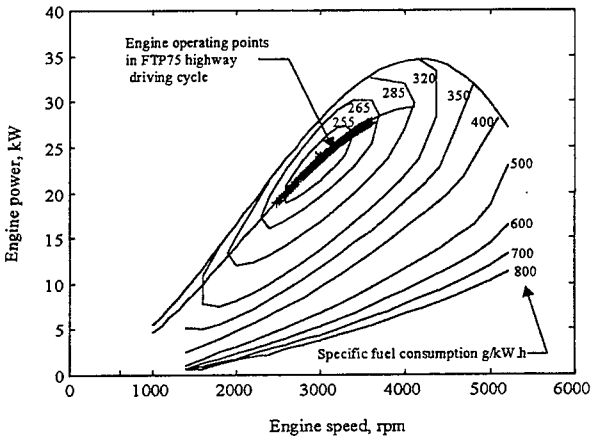

Fig. 14 Engine operating points on the fuel economy characteristics of the engine in EPA FTP75 highway driving (regenerative braking unavailable)

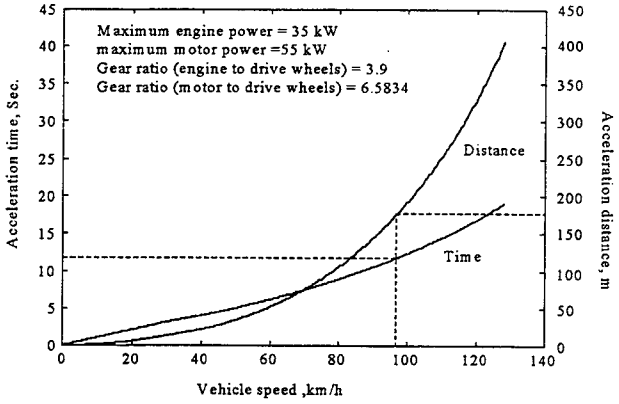

Fig. 15 Acceleration time and distance versus vehicle speed. (regenerative braking unavailable)

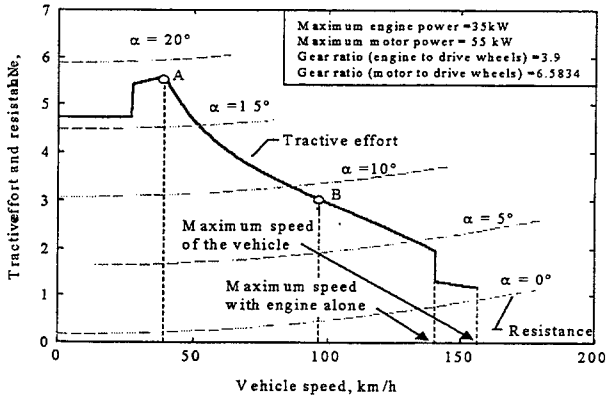

Fig. 16 Tractive effort and resistance on various grade of road versus vehicle speed (regenerative braking unavailable)

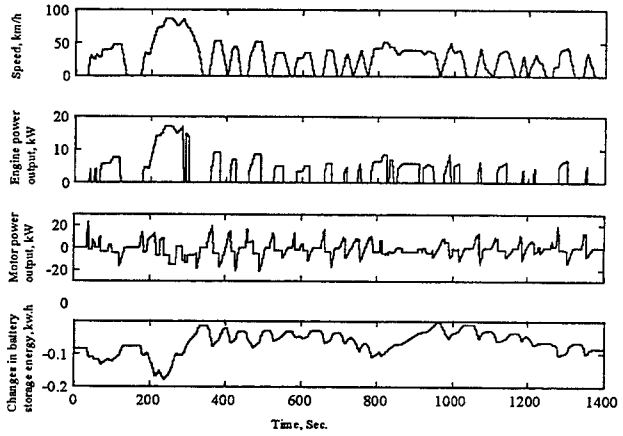

Fig.17 Time history of vehicle speed, engine power, motor power and changes in battery storage energy in EPA FTP75 urban driving cycle (regenerative braking available)

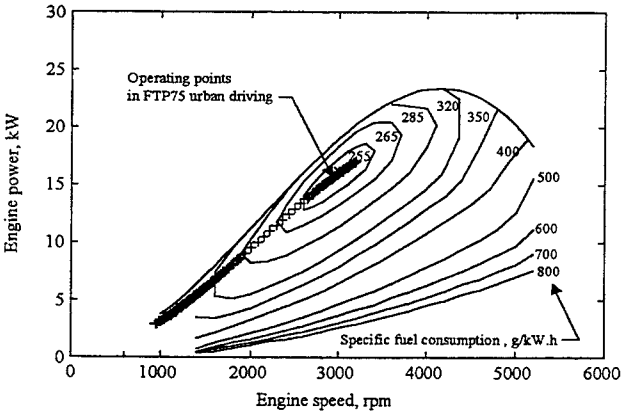

Fig.18 Engine operating points on the fuel economy map (regenerative braking available)

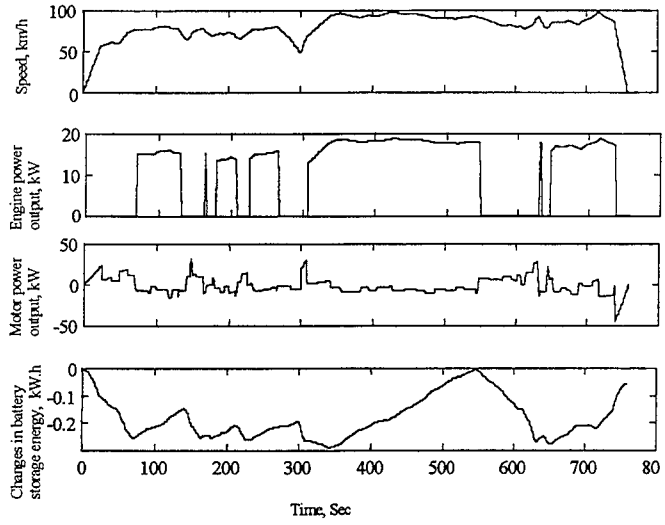

Fig.19 Time history of vehicle speed, engine power, motor power and changes in battery storage energy in EPA FTP75 highway driving cycle (regenerative braking available)

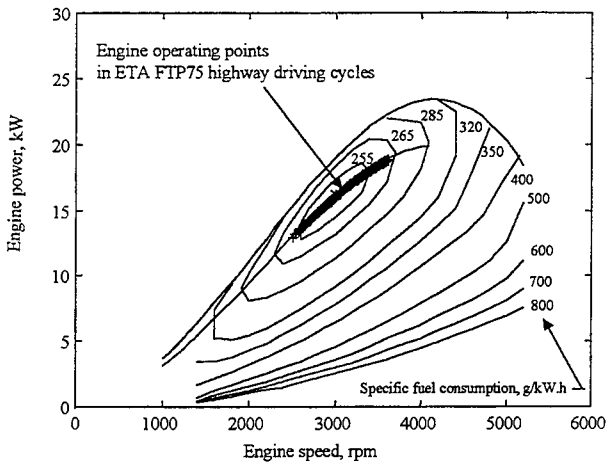

Fig.20 Engine operating points on the engine fuel consumption map. (regenerative braking available)

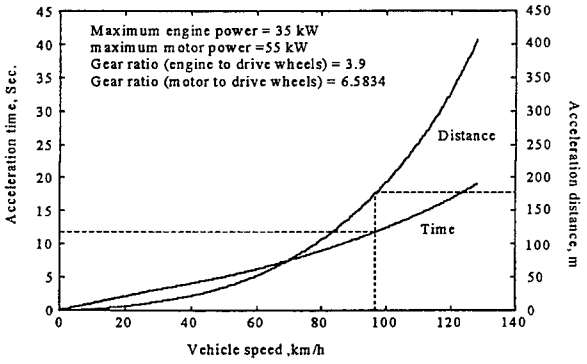

Fig.21 Acceleration time and distance versus vehicle speed (regenerative braking avaialble)

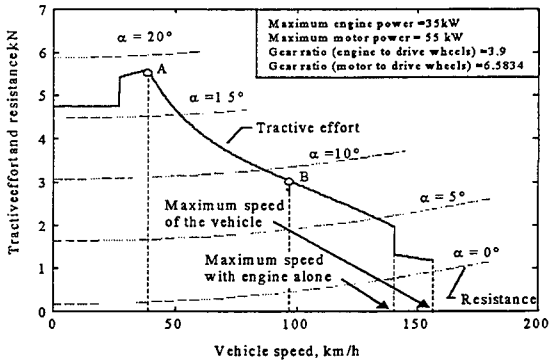

Fig.22 Diagram of vehicle traction effort and resistance versus vehicle speed and road angles (regenerative braking available)

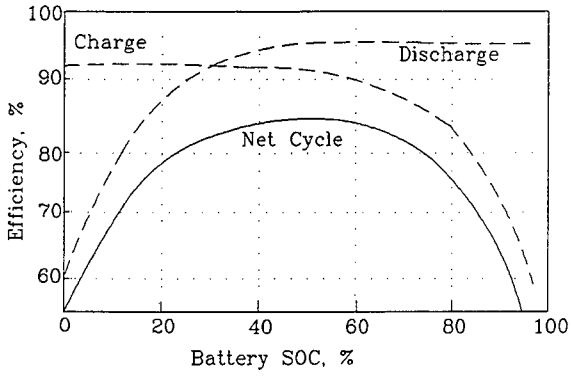

Fig.23 Battery efficiency versus state-of-charge

APPENDIX

972647

THE ENERGY FLOW MANAGEMENT AND BATTERY ENERGY CAPACITY DETERMINATION FOR THE DRIVE TRAIN OF ELECTRICALLY PEAKING HYBRID VEHICLE

Yimin Gao[1], Khwaja M. Rahman, and Mehrdad Ehsani
Texas A&M University

ABSTRACT

In this paper, the configuration of a parallel hybrid vehicle, called electrically peaking hybrid (ELPH) vehicle is introduced. Several operation modes of the engine and electric motor and different control strategies are analyzed. The results show that, with proper selection of the drivetrain parameters, the vehicle can satisfy the urban and highway driving with a small internal combustion engine, a small battery pack and a single gear transmission. Moreover, the vehicle does not need to charge the battery pack from the electricity network for keeping its battery SOC at a reasonable level.

INTRODUCTION

In recent years, increasing concern over air pollution, caused by tailpipe emissions of petroleum-based vehicles, and the dwindling petroleum resources have lead the automotive engineers and automakers to probe the possibility of the zero-emission (ZE) and ultra-low emission (ULE) vehicles. Among all kind possible schemes, electric vehicle (EV) seems to be the most attractive due to their zero emission, petroleum-free energy supply, control flexibility, and simple construction. However, pure electric vehicles suffer from other disadvantages[5, 6].

1. The heavy and bulky battery pack, with very limited energy storage, makes the EV limited in range, and load carrying capacity.

2. Long charging time limits the EV's availability.

Therefore, commercial success of the EV depends entirely on development of advanced high energy batteries. However, progress in batteries over the past several decades has not been adequate.

Hybrid configurations, in which two power sources are applied to propel the vehicles, are now holding the greatest promise. The hybrid electric-internal combustion engine drive train, if properly configured, can combine the advantages of both EV and ICE vehicles with no drawbacks.

The configuration of a parallel hybrid vehicle, called electrically peaking hybrid (ELPH) vehicle is shown in Fig. 1.[7,8,9,10] The internal combustion engine (ICE) and the electric motor are coupled by a set of match gear (or chain) into the input shaft of the transmission. The transmission would be multi-speed or single-speed depending completely on the performance requirement and drivetrain parameters selected.

When the vehicle operates on level road with constant cruising speed, relatively low power is required, but large amount of energy is consumed in a long trip. In this case, a small ICE alone is used to power the vehicle, resulting in an excellent fuel economy due to its operating point being close to the optimal point. When the vehicle experiences an acceleration or a steep hill climbing, the electric motor, functioning as a load leveling device, supplies supplementary power to the drive train to meet the performance requirement. The ELPH configuration has the ability to recover braking energy with the electric motor functioning in regenerating mode. Furthermore, when the vehicle operates with light load, such as at a relatively low constant speed or going down a slight hill, the engine can recharge the battery pack to maintain adequate state-of-charge. More beneficially, this enhances the engine load, for operation close to its optimal point. A well designed ELPH vehicle may never use a wall plug to charge its battery pack and can obtain an excellent fuel economy.

[1] Visiting Scholar from Jilin University of Technology, China

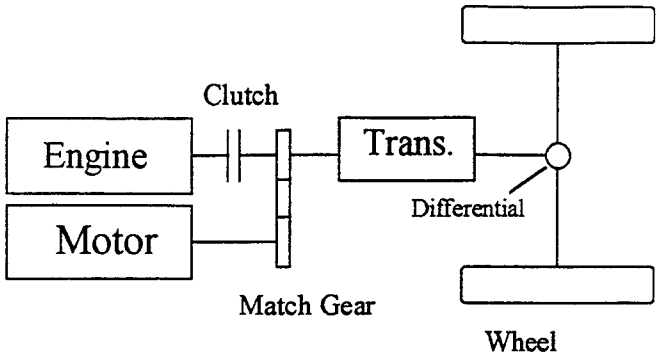

Fig. 1 The Configuration of the ELPH Vehicle

MANAGEMENT OF MOTOR AND ENGINE POWER

The operation of a vehicle can be divided into three basic modes: constant speed (cruising), acceleration (peak power) and deceleration (regeneration). In each mode, the engine and the motor operate with the appropriate behavior to meet the load power requirement and keep proper SOC on the battery.

CRUISING MODE - The cruising mode is the operation mode of the vehicle in which the engine alone can meet the load power requirement, such as operating on a level road with constant speed or with a slight acceleration or a slight hill climbing with constant speed. In this operation mode, the engine and electric motor have several operating status.

Motor-only Tractive Mode - When the speed of the vehicle is less than the speed that is limited by the minimum rpm of engine or greater than the speed that is limited by the engine maximum rpm, all the power required by the load of the vehicle is supplied by the electric motor. The engine must remain at standstill or in idling. In these cases, we have

$$P_e = 0 \tag{1}$$

$$P_m = P_l \tag{2}$$

$$P_b = \frac{P_m}{\eta_{bd}\ \eta_m} \tag{3}$$

where, P_e= power output of engine,
P_m = power output of electric motor,
P_l = load power of the vehicle,
P_b= discharge power of the battery pack,
η_{bd}= discharge efficiency of the battery pack,
η_m= efficiency of the motor.

In this operating mode. All the required energy must be supplied by battery pack.

Battery Pack Charging Mode - When the load power of the vehicle is less than the engine power with wide open throttle, engine has the extra power to charge the battery pack, if necessary. The electric motor functions in the regenerating mode to convert the engine power into electric power to recharge the battery pack. The electric motor power (as a generator), P_m, and battery pack recharging power, P_b, are

$$P_m = -(P_e - P_l) \tag{4}$$

$$P_b = P_m \eta_m \eta_{bc} \tag{5}$$

where; η_{bc}= the battery pack charging efficiency .

Negative P_m means electric motor functioning as generator.

Engine-only Mode - If the battery pack is not required to be recharged, for example, the SOC of the battery pack reaches its top line, the electric motor is idling and the engine power is equal to the load power of the vehicle, that is

$$P_e = P_l \tag{6}$$

PEAK POWER MODE - When the vehicle experiences an acceleration or a steep hill climbing, the load power is much greater than that the engine can produce. Consequently, the motor must work together with the engine to produce enough power to meet the requirement. In this case, the motor power output and battery power output are

$$P_m = P_l - P_e \tag{7}$$

$$P_b = \frac{P_m}{\eta_{bd}\eta_m} \tag{8}$$

REGENERATING MODE - When the vehicle experiences a deceleration or a hill descending, the engine is turned off or idles. The electric motor functions in regenerating mode. The electric motor (generator) power P_m, and battery charging power, P_b, are

$$P_m = \alpha P_l \tag{9}$$

$$P_b = P_m \eta_{tm} \eta_m \eta_{bc} \tag{10}$$

where α = fractional factor of power recovery,
η_{tm} = efficiency from motor to the drive wheels.

In equations (1) to (10), positive P_e, P_m and P_b mean that the engine, motor and battery pack supply powers to the vehicle. In contrast, negative P_m and P_b means that motor and battery pack absorb power from the engine or regenerating braking.

THE ENERGY CHANGE IN THE BATTERY PACK

As explained above, in the peaking power mode, the battery pack must supply energy to the vehicle. Consequently, the stored energy in the battery pack is decreased. On the other hand, when the vehicle operates at low load or in the braking mode, the battery pack absorbs energy from engine or regenerative braking. In a whole drive cycle, if the consumed energy and absorbed energy are balanced, the battery pack will never have to get energy from wall plug. Therefore the range of the vehicle is only limited by the fuel tank as in a conventional vehicle.

The amount of energy change in the battery pack at time t in the drive cycle ($t=0$ represents the beginning of the drive cycle) is expressed by

$$E = -\int_0^t P_b d\tau \qquad (11)$$

The negative sign means that when P_b is positive (battery pack supplies power to the vehicle), the energy in the battery pack is decreased. If, at the end of the drive cycle, the value of E is the same as that at the beginning of the driving cycle, the battery SOC will be kept the same as at the beginning of the drive cycle. Consequently the vehicle will not need wall plug to charge the battery.

CONTROL STRATEGIES OF THE DRIVETRAIN

As explained above, at any time in driving, the sum of the engine power, P_e, and the electric motor power, P_m, should be equal to the vehicle load power P_l (except in the braking mode, in which external braking power may be applied by brake system of the vehicle). In the actual operation, the control system of the drivetrain can determine the power output of each power unit in many ways, provided the total power output meets the requirement. Different control strategies will obtain different fuel economies and different battery energy capacities.

MAXIMUM BATTERY SOC CONTROL STRATEGY - The maximum battery state-of-charge control strategy is consistent with the principle that, at any time, except the battery SOC reaching its top line, the engine should operate with full load (wide-open throttle) to produce maximum power. One part of the engine power is used to counterbalance the vehicle load power, and the remainder is used to charge the battery. This control strategy is illustrated in Fig. 2. In this figure, the segments a and a' represent the battery charging power for high-speed and low-speed gears of the transmission respectively. Similarly, b and b' represent the battery discharging power for higher and lower speed gear of the transmission. *Fig. 2* also implies that a multi-speed transmission is helpful to reduce the size of battery pack. However the penalty is a complicated construction and control system.

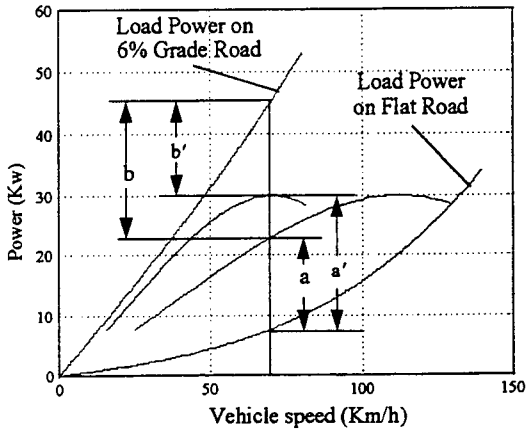

Fig. 2 Battery Charging and Discharging Power

OPTIMAL CONTROL STRATEGY - Fig. 3 shows the fuel consumption map of a typical SI engine with its optimal fuel economy operating line. If operating point of the engine is just on the optimal fuel economy operating line, the engine has a optimal operating efficiency. Fortunately, the power output corresponding to the optimal operating line is just a little smaller than the power output with a full load (wide-open throttle). This implies that, if the control system controls the engine operating on the optimal operating line, the vehicle can not only maintain the battery SOC at a certain level, but also have a good fuel economy, and generally, good emission characteristics.

Generally, the optimal operating line of engine is quite difficult to obtain analytically. It is approximately assumed that power on the optimal fuel economy operating line is proportional to the power output of engine with a wide-open-throttle in a large speed range (see Fig. 3) . Thus

$$P_{eop} = \beta P_{e\,max} \qquad (12)$$

where P_{eop} = power output corresponding to the optimal fuel economy operating line,

β = fractional factor,
P_{emax} = power of the engine with wide open throttle.

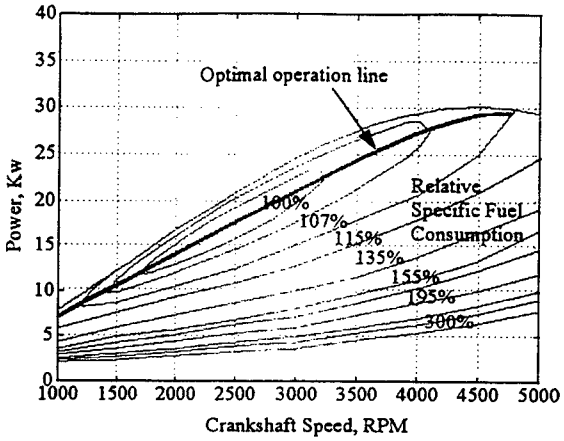

Fig. 3 Specific Fuel Consumption Map Of a Typical SI Engine with Its Optimal Operating Line

DETERMINATION OF BATTERY ENERGY CAPACITY

Proper selection for energy capacity of the battery pack is crucial for the design of the ELPH vehicle. Oversized battery pack would cause vehicle overload, and, undersized battery pack can not supply adequate energy and power for the needs of the vehicle.

The minimal value of E in equation (11) within a drive cycle represents the lowest SOC of the battery, $E=0$ represents the highest SOC of the battery pack

Fig. 4 shows a charge and discharge efficiency of a typical lead-acid battery along with its state -of-charge. This figure suggests that if the SOC of the battery pack is kept within the range of *40%* to *60%*, the cycle efficiency is optimal[1]. Therefore, we set the highest SOC of the battery pack being *60%* and the lowest *40%*..

Thus, we have

$$0.6C_{be} - 0.4C_{be} = |E_{min}| \qquad (13)$$

$$\text{So,} \quad C_{be} = \frac{|E_{min}|}{0.2} \qquad (14)$$

where, C_{be}= the energy capacity of the battery pack with *Kw.h.*

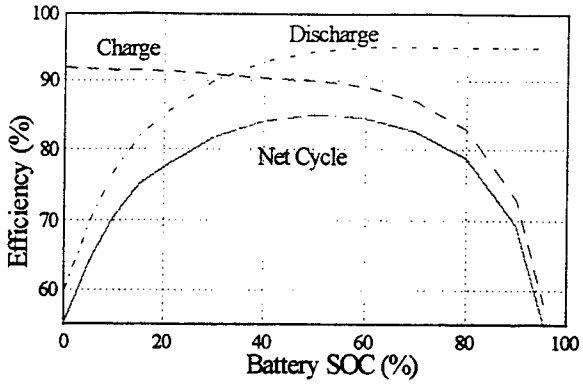

Fig. 4 Battery Efficiency Respect with Battery State-of-Charge [1]

A NUMERICAL EXAMPLE

The specification of the example ELPH vehicle prototype which is being developed at Texas A&M University is listed as below:

Total weight	*1700 Kg,*
Rolling resistance coefficient of tire	*0.013,*
Aero-dynamic drag coefficient	*0.29,*
Frontal area	*2.13 m^2*
Wheel radius	*0.2794 m.*

The following parameters are used in the calculations.

Engine power capacity	*30 Kw*
Differential gear ratio	*4.23*
Single gear transmission, gear ratio	*1.0*
Transmission efficiency from engine and motor to drive wheels	*0.9*
Motor efficiency	*0.85*
Battery charge and discharge efficiency	*0.85*

The engine speed-power characteristic is shown in Fig. 5.

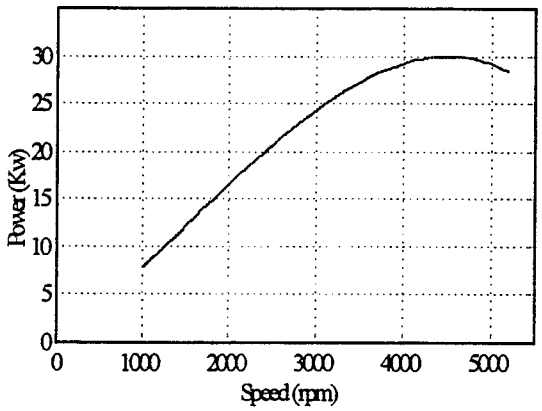

Fig. 5 The Speed-power Characteristic of Engine

Best Battery SOC Control Strategy - Fig. 6 shows the engine power, motor power, battery power and the change of battery energy along with driving time in the urban driving cycle FPT75.

Fig. 6 indicates that E has the same value at the beginning and end of the driving cycle. Therefore, the vehicle does not requires a wall plug to charge the battery pack in urban driving. Fig. 6 also gives a minimal E equal to *0.1421 Kw.h.* Using equation (14) , the energy capacity of the battery pack, C_{be}*=0.7105 Kw.h,* is obtained. This result means that, from the energy point of view, only a very small battery pack is needed.

While operating with highway driving cycle, the engine power, motor power, battery power and energy change in the battery pack are shown in Fig. 7. This figure indicates that engine alone can almost satisfy the requirement except for the transient acceleration at the beginning of the drive cycle. The minimal E is equal to *0.0431 Kw.h.* So, the C_{be}*=0.2155 Kw.h* is enough for this driving cycle.

Optimal Control Strategy - Fig. 8 and Fig. 9 show the time history of the engine power, motor power, battery power and the change in the battery storage energy corresponding to urban and highway driving cycle of FTP 75. The β (see equation (12)) is 0.87 The results show that, even with the frequent start-stop urban driving mode, the vehicle does not need a wall plug to charge its battery pack. The minimal E is equal to 0.1850Kw.h So, the C_{be}= *0.925 Kw.h* This means that, with this control strategy , the battery size is also quite small.

The situation of highway driving with optimal control is quite similar to that with best battery SOC control. The engine alone can almost satisfy the power requirement.

CONCLUSION

The electrically peaking hybrid vehicle has a parallel configuration in which a small internal combustion engine and an electric power peaking motor cooperate. When the vehicle is operating with a light load, the engine can charge the battery pack with the remaining power. When the vehicle operates with high load , the battery pack can supply energy to the drivetrain to meet the requirement of the load power.

The calculation results show that, for a 1700 Kg passenger car ,the combination of a 30 Kw power capacity engine and a small battery pack with a single-gear transmission will satisfy the requirement in both urban and highway driving conditions. With the engine operating point being controlled on the optimal operating line by the optimal control strategy, the vehicle will achieve an excellent fuel economy, and generally good emissions characteristics.

ACKNOWLEDGMENT

The financial support of Texas Higher Education Coordinating Board and Texas Transportation Institute for the ELPH project is gratefully acknowledged.

REFERENCE

1. Clark G. Hochgraf, Michael J. Ryan, and Herman L.Wiegman , *Engine Control Strategy for a Series Hybrid Electric Vehicle Incorporating Load Leveling and Computer Controlled Energy Management,* SAE 960230, 1996

2. Martin Endar and Philipp Dietrich, *Duty Cycle Operation as a Possibility to Enhance the Fuel Economy of an SI Engine at Part Load,* ASE 960229.

3. A.F. Burke, *Battery Availability for Near Term (1998) Electric Vehicle,* SAE 911914.

4. J.Y. Wong , *The Theory of Ground Vehicle* , John Wiley & Sons Inc. Press, 1978.

5. M.Ehsani, K. M. Rahman, and H. Toliyat, *Propulsion System Design of Electric & Hybrid Vehicle,* accepted for publication in the IEEE Tran. of Industrial Electronics.

6. H.A. Toliyat, K. M. Rahman, and M. Ehsani, *Electric Machine in Electric & Hybrid Vehicle Application,* Proceeding of ICPE, 95, Seoul, pp 627--635

7. M.Ehsani, *Electrically Peaking Hybrid System And Method,* U.S. Patent Granted 1996

8. J. Howze, M. Ehsani and D.buntin, *Optimizing Torque Controller for a Parallel Hybrid Electric Vehicle,* U.S. Patent granted, 1996

9. Proceedings of the ELPH Conference, Texas A&M University, College Station, Texas, Oct. 1994

10. Yimin Gao, Khwaja M.Rahman and Mehrdad Ehsani, *Parametric Design of The Drive Train of An Electrically Peaking Hybrid (ELPH) Vehicle,* ASE 970294.

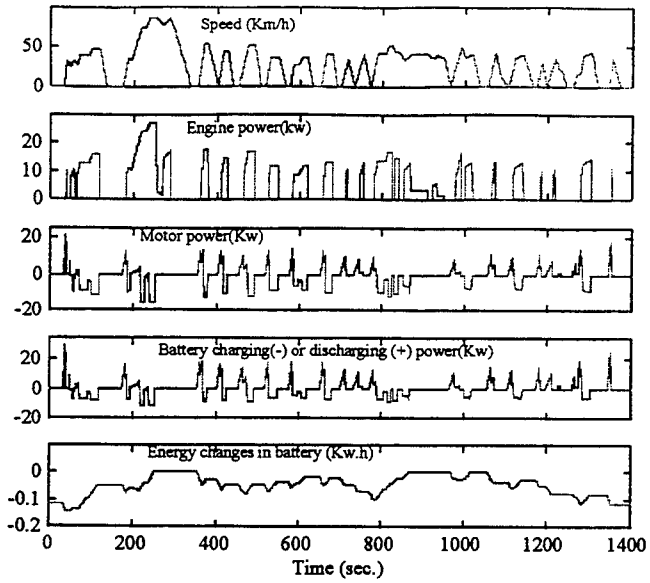

Fig 6. The Time History of Engine Power, Motor Power, Battery Power and Change of Battery Storage Energy Corresponding to FTP75 Urban Driving Cycle with Best Battery SOC Control Strategy

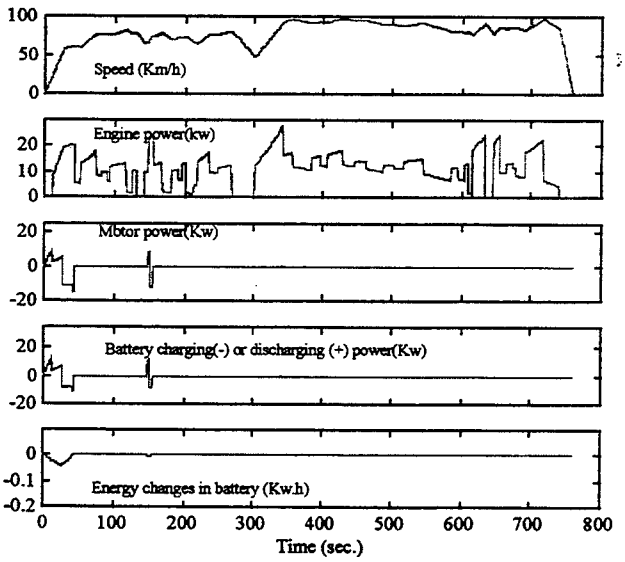

Fig. 7 The Time History of Engine Power, Motor Power, Battery Power and Change of Battery Storage Energy Corresponding to FTP75 Highway Driving Cycle with Best Battery SOC Control Strategy

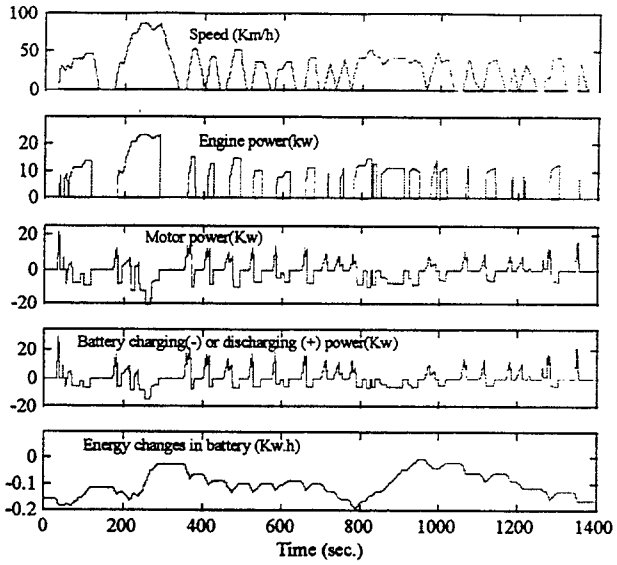

Fig. 8 The Time History of Engine Power, Motor Power, Battery Power and Change of Battery Storage Energy Corresponding to FTP75 Urban Driving Cycle with Optimal Control Strategy)

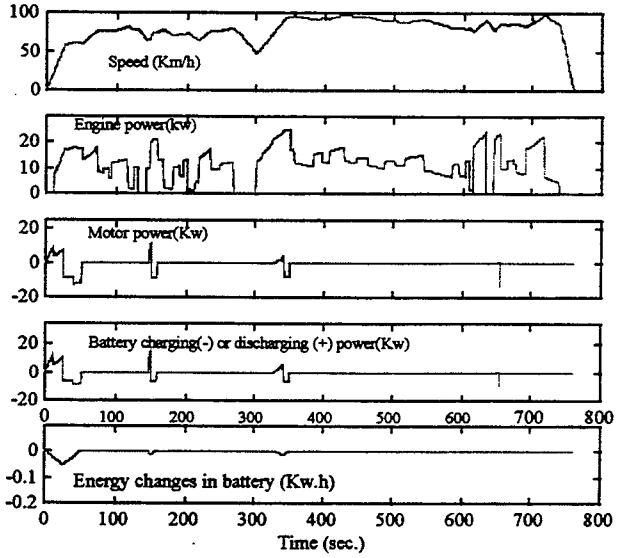

Fig. 9 The Time History of Engine Power, Motor Power, Battery Power and Change of Battery Storage Energy Corresponding to FTP75 Highway Driving Cycle with Optimal Control Strategy

APPLICATION OF ELECTRICLLY PEAKING HYBRID (ELPH) PROPULSION SYSTEM TO A FULL SIZE PASSENGER CAR WITH SIMULATED DESIGN VERIFICATION

M. Ehsani, Y.Gao and K. Butler
Texas A&M University

Abstract

An electrically peaking hybrid electric (ELPH) propulsion system is being developed that has a parallel configuration. A small engine is used to supply power approximately equal to the average load power. The operation of the engine is managed by a vehicle controller and engine controller such that the engine always operates with nearly full load – the optimal economy operation. A induction AC motor is used to supply the peaking power required by the peak load (electrically peaking). The motor can also absorb the excess power of the engine while the load power is less than the peak. This power, along with the regenerative braking power, can be used to charge the batteries on board to maintain the battery state-of-charge at a reasonable level.

With the electrically peaking principle, two control strategies for the drive train have been developed. One is called MAXIMUM BATTERY SOC, by which, the engine and electric motor are controlled so that the battery SOC is maintained at its top level as much as possible. This control strategy may be used in urban driving, in which, accelerating and decelerating driving is common. The other control strategy is called ENGINE TURN-ON AND TURN OFF control, by which, the engine is controlled to operate in turn-on and turn-off manner. This control strategy may be used in highway driving.

Based on the ELPH principles and the drive train control strategies, a drive train for a full size, 5-seat passenger car (1700 kg of gross weight) has been designed and verified using the V-ELPH computer simulation package developed at Texas A&M University. The results show that the ELPH car can easily satisfy the performance requirements and the fuel economy can be improved greatly over conventional vehicles.

Introduction

In vehicle development and design, the major issues are the marketability and the impacts on the environment. Conventional gasoline and diesel fueled vehicles possess the advantages such as, good performance, long driving range, ease in refueling, light-weight energy source. These advantages have enabled the conventional vehicles to dominate the market. However, conventional vehicles have serious disadvantages in regard to energy sources and environment protection, primarily the very inefficient usage of the petroleum sources and serious air pollution. The electric vehicles, which have been under development for many years, are considered to be important substitutes of the conventional vehicles that can overcome their disadvantages. But the acceptability of the electric vehicles in the automobile market has encountered major obstacles. Due to the heavy and bulky batteries on board, the electric vehicles usually have sluggish performance, limited loading capacity, short driving range and long battery recharging time and high manufacturing cost.

Hybrid electric vehicles under development in recent years, are considered to be the best trade-off between conventional and electric vehicles. In a hybrid vehicle, two power plants are available which commonly are an internal combustion engine and electric motor. The inclusion of two power plants provides flexibility to use either internal combustion engine or electric motor or both together for traction, according to their operation characteristics and driving requirement. This configuration increases the potential to optimize the overall drive train operation. It also, however, increases the complexity in the management of the powers supplied by the both engine and motor. Therefore, the control strategy of the power plants is a crucial aspect in the development of hybrid electric vehicles.

In this paper, a hybrid electric propulsion system, with a parallel configuration, referred to as ELectrically Peaking Hybrid (ELPH) propulsion system, is introduced. The principle is illustrated through simulations performed using the V-ELPH software simulation program developed at Texas A&M University[1]. The power plants available in the system are a spark ignition internal combustion engine and an AC induction motor. The power plants are managed (controlled) with electrically peaking manner[2,3,7,8]. The objectives of the application of the ELPH propulsion system to a full size car are: (1) comparable performance to conventional vehicles that have similar space and loading capacity, (2) similar mass production to that for corresponding conventional one, (3) the same operation as driving conventional vehicle, (4) two to three times fuel economy over the conventional vehicles, and (5) self sustained battery SOC.

ELPH Principle

For a full size vehicle, the required acceleration performance usually constraints the reduction of the power capacity of the power plants. For instance, for a vehicle with 1500kg gross weight, the average power needed to accelerate the vehicle from zero speed to 100 km/h (62.5mph) in 10 seconds is about 60kW, and the peak power of the engine needed would reach about 90 to 100kW. However, in normal driving, the average load power is only 15 to 20kW. Such low load power results in very low engine fuel efficiency. This conflict between the performance and fuel economy requirements pushes the conventional vehicle design into a dilemma.

Actually, in normal driving, the load power of the vehicle varies randomly as shown in Fig.1. This power profile can be resolved into two components: one representing the average power demand and other representing the dynamic power demand which has a zero average value. With the ELPH principle, an internal combustion engine, which has optimal steady-state operating region in its speed-power characteristics map, is used to supply the average load. The electric traction system (electric motor and batteries) is used to produce the dynamic power[7,8]

With the ELPH principle, engine size can be reduced greatly and the engine can operate almost in its efficient region, thus resulting in much high operating efficiency. The electric traction system operates in a dynamic manner, producing the peaking power to meet the peak power demand in acceleration and hill-climbing driving. The storage energy within the batteries can be maintained in a balanced state by two battery charging approaches. The first approach is to charge the battery by recovering the kinetic energy in decelerating driving and potential energy of the vehicle in down-hill driving. The second approach is to charge the batteries by the access power of the engine when the load power demand is less than the power the engine can

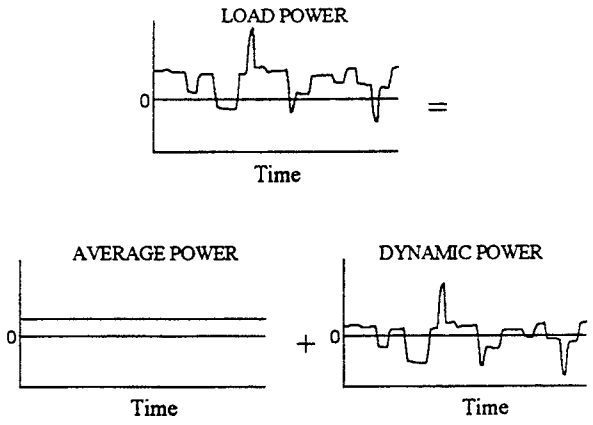

Fig.1 The load power demand and its steady and dynamic components

produce. These two battery-charging approaches can be implemented by using the motor controller to operate the traction motor as a generator. With these approaches, the batteries only function as an energy reservoir. With proper design, the battery state-of-charge can possibly be maintained at a reasonable level in the driving, and the battery size (energy capacity) can be small[2].

Configuration and Operation Modes of the Propulsion System

The ELPH prolusion system proposed has parallel configuration as shown in Fig.2 and Fig.3[7,8]. The configuration shown in Fig.2 is the two-shaft configuration, in which, the engine torque, modified by the transmission, and motor torque are added together by a torque summer which may be a set of gears, or chain. The configuration in Fig.3 is single-shaft configuration, in which, the rotor of the motor functions as the torque summer. However, both configurations have the same operation principle, and which is more suitable in physical design depends on the engine and motor characteristics, performance requirement, and convenience to developing the propulsion under hood.

The transmissions in both configurations are used to modify the torques so as to properly match the requirement of the driving. The transmissions may be multi-speed or single speed, depending on the engine and motor size, operation characteristics and performance requirement. Actually, due to the favorable characteristics of the electric motor as a traction power plant, a sing-gear transmission may satisfactorily serve the propulsion[2].

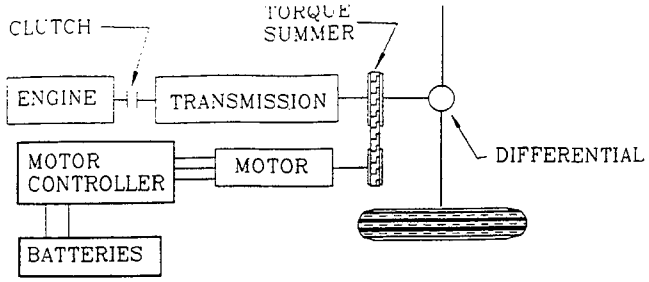

Fig.2 Two-shaft configuration of ELPH propulsion

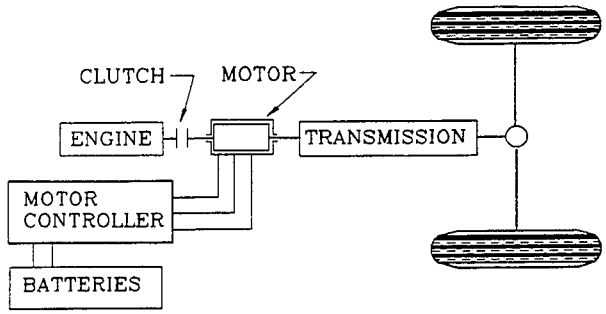

Fig.3 Single-shaft configuration of ELPH propulsion

The ELPH propulsion can potentially realizes several operation modes such as: (1) motor-only mode, (2) engine-only mode, (3) hybrid traction mode (engine plus motor), (4) regenerative braking mode, and (5) battery charging from the excess power of the engine. The motor-only operation mode is used when the speed of the vehicle is very low such that the engine can not operate steadily and the battery is fully charged in highway driving. The engine-only operation mode may be used in the case that the battery is fully discharged (if this occurs accidentally). However, this operation mode should be avoided as much as possible. Hybrid traction operation mode is used in a case where the peak power is required, such as acceleration and hill climbing driving. The regenerative braking operation mode is used in braking driving. In this case, the electric motor functions as a generator to recuperate the kinetic or potential energy of the vehicle into electric energy to charge the batteries on board. The battery charging mode from the excess power of the engine is used when the batteries are not fully charged and the engine has excess power after propelling the vehicle.

A micro-processor based vehicle controller is applied to regulate the engine and motor operations to optimally use the above operation modes according to the driving requirement, engine and motor operation characteristics, battery state-of-charge information. The control target of the control strategies in the vehicle controller is (1) to meet the tractive effort required by the driver, (2) to maintain the battery SOC at reasonable level, (3) to operate the engine efficiently, and (4) to recover the kinetic and potential energy as much as possible.

Control Strategies

Maximum Battery SOC Control Strategy

The control target of the maximum Battery SOC control strategy follows the principle that high battery SOC should be maintained in driving as much as possible. This control principle results in that the engine should be used as much as possible and the electric traction system should be used as less as possible. The details of this control strategy are illustrated in Fig. 4.

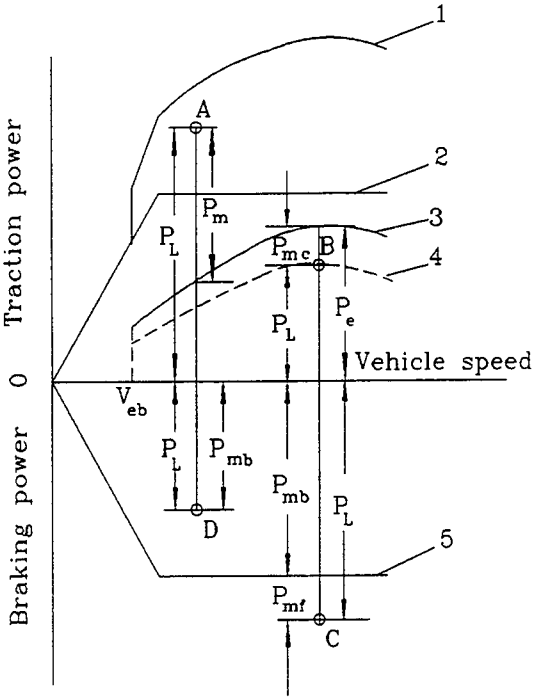

1--Maximum power with hybrid mode
2--Maximum power of the electric motor in traction mode
3--Power of the engine corresponding to its optimum economy line
4--partial load of the engine
5--Maximum power of the electric system in regenerative braking

P_L --Load power, including traction and braking power
P_e --Engine power
P_m --Motor traction power
P_{mb}--Regenerative braking power of the motor
P_{mf}--Mechanical braking power
P_{mc}--Battery charging power

Fig. 4 Illustration of the Maximum battery SOC control strategy

In Fig.4, point *A* represents the traction power that is greater than the power that the engine can supply (this may occur in acceleration and hill-climbing driving), In this case, the engine and electric motor must supply their power to meet the power requirement. The power distribution between the engine and the motor is to operate the engine at near full load (full throttle, which usually is the optimal fuel economy operation), and to control the electric motor to supply its power equal to the remaining load power. Point *B* represents the traction power that is less than the power that the engine can produced with near full throttle. In this case, the engine can be controlled depending on the battery SOC. If the battery SOC dose not reach its top level, the engine should be operated at near full load. The power remaining after propelling the vehicle is used to charge the batteries. If the battery SOC reaches its top level, the engine should be controlled to produce its power that is equal the load power. Point *C* represents the braking power which is greater than the power that the electric system (electric motor and batteries) can absorb. In this case, to recuperate the braking energy as much as possible, the electric motor, functioning as a generator, should be controlled at its maximum power. The remaining braking power is taken by the frictional brake system. Point *D* represents the braking power required by the driver, which is less than the power the electric system can handle. In this case, the electric regenerative braking alone is used. Reference [3] has given the mathematical description in detail.

The Maximum Battery SOC control strategy may suitably match the urban driving, in which, the frequently accelerating–decelerating driving would discharges the batteries quickly. Therefore, Maintaining the battery SOC at high level is crucial for the operation of the vehicle.

Engine Turn-on and Turn-off Control Strategy

When vehicle drives on the highway, the power and energy supplied by the electric system is much smaller than driving in urban and the load power is usually less than the full-load power capacity of the engine. The batteries, in this case, can easily be fully charged. For avoidance of the inefficient engine operation, the engine should operate in a turn-on and turn-off or duty-cycle manner.

In the engine turn-on and turn-off control strategy, the duty cycle of the engine operation is depends on the battery SOC. Fig.5 shows the relationship between the engine duty cycle and the battery SOC. In the engine turn-on period, the engine alone propels the vehicle and the excess power is used to charge the batteries. Then the battery SOC goes up until reaching its top line. In this way, the engine would operate always near full load. After the battery SOC reaches its top level, the engine is turned off and the vehicle is propelled by the electric system alone. With the engine turn-on and turn off operation manner, the propulsion system would obtain maximum overall efficiency

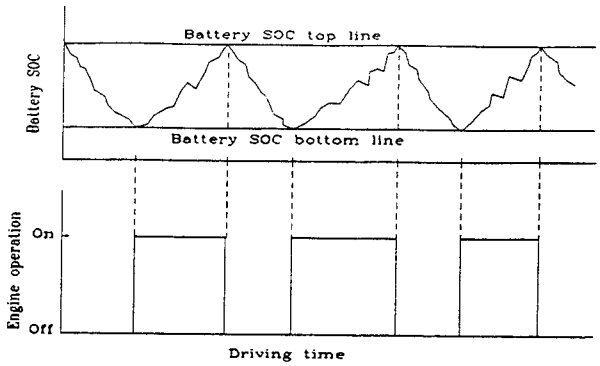

Fig.5 Illustration of the engine turn-on and turn-off operation

Application of the ELPH Propulsion System to Full Size Passenger Car

Below are the specifications of the full-size ELPH passenger car. It is expected that the car has the similar performance and load capacity to conventional gasoline fueled passenger cars with self-sustained battery SOC property. The fuel economy is expected to be two to three times that of conventional cars.

***Vehicle Type**: 4-door, 5-seat passenger car, front engine/moor and front drive*

***Overall dimension**:*

Overall length:	*4.70 ~ 4.80 m*
Overall width:	*1.70 ~ 1.80 m*
Overall height:	*1.40 ~1.45 m*
Wheel base	*2.65 ~ 2.8 m*
Tread width	*1.55 ~ 1.75 m*

Estimated weight

Curb weight:	*1500 kg (include traction batteries)*
Load	*Two person (2x70 kg) + luggage (60 kg)=200 kg*

Total weight; 1700 kg
Weight on front/rear axle:62% / 38%

Main components:

Engine:	*Spark ignition, gasoline fueled internal combustion engine.*
Traction Motor:	*Electronically controlled induction AC motor.*
Batteries:	*Lead/acid traction batteries*
Transmission:	*Single gear, mechanical transmission*

Performance specification

Acceleration *12±1 sec. (from 0 to 96 km/h or 60 mph)*

Max. gradeability:>30% and >5% @ 100km/h

Maximum speed;

Engine only: *140 km/h*

Hybrid traction *160 km/h*

Range: *Free from battery energy storage and only rely on fuel tank volume*

Estimate of Propulsion Parameters

Engine size – As mentioned in the ELPH operation principle, the engine power capacity can be determined by the load power for steady driving, which can be expressed as

$$P_e = \frac{V}{1000\eta_{t,e}}\left(mgf_r + \frac{1}{2}\rho_a C_D A_f V^2\right) \quad (kW), \qquad (1)$$

where, m is the vehicle gross mass in kg, $\eta_{t,e}$ is the transmission efficiency from the engine to driven wheels, f_r is the rolling resistance coefficient, ρ_a is the air density with $1.205kg/m^3$, C_D is the aerodynamic coefficient, A_f is the front area of the vehicle in m^2, and V is vehicle speed in m/s. The values of above parameters used in this paper are as follows.

Vehicle mass	*1700 kg*
Rolling resistance	*0.01*
Transmission efficiency	*0.92*
Aerodynamic drag coefficient	*0.3*
Front area	*$2.25m^2$*

The power demand along the vehicle speed is shown in Fig.6. This figure indicates that about 33 kW is needed for the vehicle speed of 140km/h (87mph). This value is quite much smaller than the power of engines used in conventional passenger cars[2]. Considering the power consumed in accessories, such as lights, audio, power steering, air conditioner and so on, a 40 kW engine is needed. Here a maximum power of 35 kW is assumed being used in traction. The speed – power and speed torque characteristics of the engine are shown in Fig.7.

Estimate of Electric Motor Size – Based on the ELPH principle, the electric motor is used to handle the dynamic load of the vehicle. Therefore, determination of the electric motor size depends on the acceleration and gradeability. In practice, the acceleration is the first consideration in the design of passenger cars.

As the initial estimate, an assumption would be made that the steady-state load is handled by the engine and the dynamic load is handled by electric motor. In this way, the maximum electric motor power needed in the acceleration can be expressed as[4]

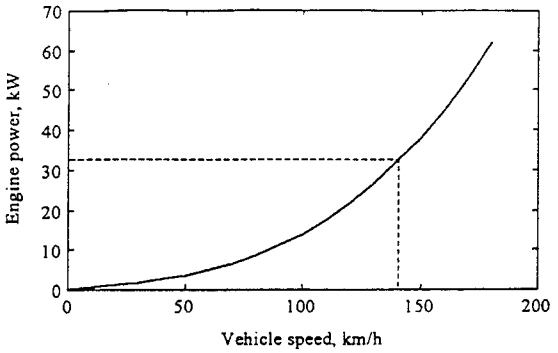

Fig.6 Engine power demand versus vehicle speed in steady driving

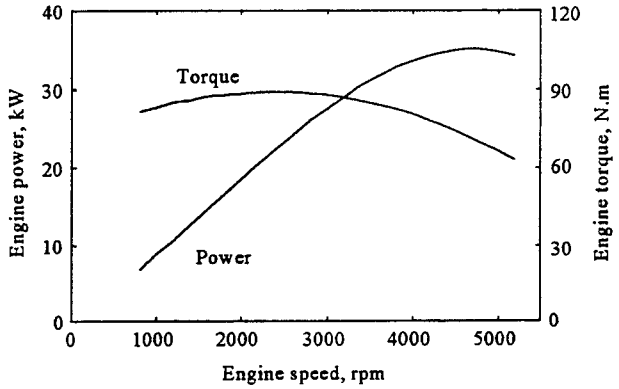

Fig.7 Speed-power and speed-torque characteristics of the engine

$$P_{mmax} = \frac{30m\delta}{9549\pi t_f}\left(\frac{V_b^2 + V_f^2}{2}\right) \quad (kW), \qquad (2)$$

where, δ is the mass factor of the rotating components in the drive train, V_b is the vehicle speed corresponding to the motor base speed in m/s, V_f is the vehicle speed at the end of the acceleration in m/s, and t_f is the acceleration time in second. The following parameters are used in the in the estimate of the maximum power of the electric motor.

Final speed of acceleration:	*96km/h (60mph)*
Acceleration time:	*12 Sec.*
Mass factor	*1.02*
Vehicle speed corresponding to motor base speed	*37.5 km/h (23.4mph)*

The maximum motor power of about 65 kW is calculated using equation (2) and the parameters above. It should be noted that the engine has, actually, some excess power to help the electric motor to accelerate the vehicle as shown in Fig 8. This excess engine power to assist the electric motor in acceleration is assumed to be about 10 kW. Thus the maximum power of the electric motor will be

55kW. It should be noted that this motor power is the peak power needed. The rated power of the electric motor is much smaller that this value (one third or half of the peak power). Fig 9 shows the speed power characteristics of the electric motor.

Transmission – Due to the favorable traction characteristics of the electric motor, a single transmission would meet the performance requirement. Reference [2] has described the principle, with which, the proper gear ratios from the engine and the electric motor to the drive wheels can be chosen. With the engine characteristics shown in Fig.6 and the maximum vehicle speed specified in the design specification, the gear ratio from the engine to the driven wheels are chosen as 3.90. Similarly, the gear ratio from the electric motor to the driven wheels is also chosen as 6.58.

Performance Prediction

The predication of the vehicle performance has been performed using the V-ELPH Simulation Package, which yielded the parameters such as the acceleration performance, gradeability and maximum speed.

Acceleration Performance -- The acceleration performance that resulted from the simulation is shown in Fig 10. This figure shows that the acceleration time and distance covered from 0 to 96km/h (60 mph) are about 12 seconds and 180m respectively. These results perfectly coincide with acceleration performance specified in the design specification.

Gradeability and Maximum Speed – The gradeability and the maximum speed of the vehicle can be obtained from the diagram of vehicle traction effort and resistance versus vehicle speed and road slope angle, as shown in Fig.11. In this figure, the maximum traction effort of the propulsion and the vehicle resistance (rolling resistance and aerodynamic drag), are plotted against vehicle speed for different road slope angles. This figure indicates that the maximum gradeability of the vehicle is about 18.5° (33.5%) and the gradeability at speed of 96km/h (60mph) is about 9° (15.8%). The maximum speeds with engine alone traction and hybrid traction reach 140km/h (87.5mph) and 160km/h (100mph). These results meet the requirements specified in the design specification.

Driving Simulation under EPA FTP75 Driving Cycles

Using the V-ELPH simulation package developed by Hybrid Electric vehicle Research Group, Texas A&M University, data relating the driving of the vehicle to certain driving cycles can be obtained, such as the engine and motor operation states (speed and power versus driving time), battery charging and discharging energy, and fuel

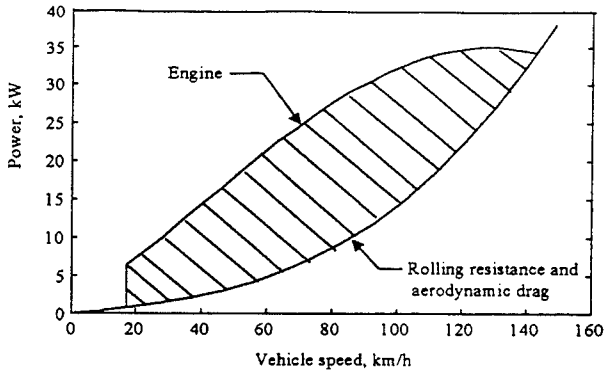

Fig.8 Illustration of the excess power of the engine used in acceleration

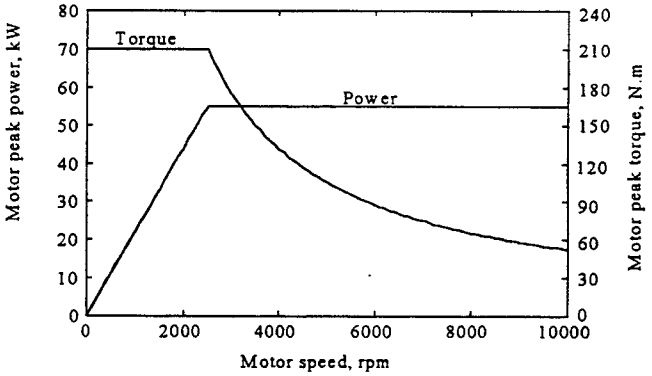

Fig.9 Electric motor characteristics

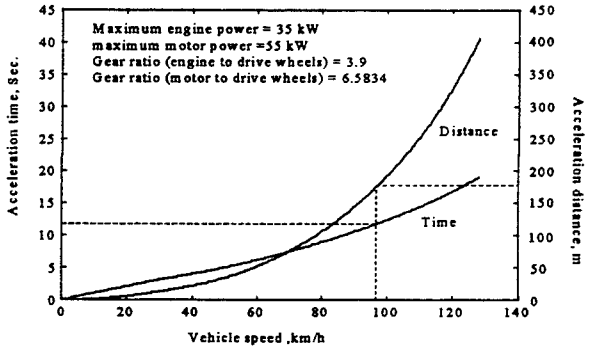

Fig.10 Acceleration performance of ELPH

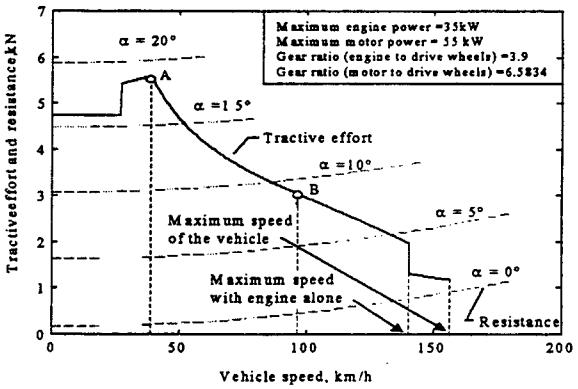

Fig.11 Diagrame of vehicle tration effort and resistenace versus vehicle speed and road angles

consumption. All data related to the operation of the components can be used to verify the design, determine the battery size, etc..

Simulation studies were based on the ELPH control strategies mentioned above. For the simulation of urban driving, the Maximum Battery SOC control strategy was used and for the highway driving, the Engine Turn-on and Turn-off control strategy was used. The regenerative braking was utilized in both urban and highway driving simulations.

Urban Driving Simulation

The EPA FTP75 urban driving cycle, which is described by the profile of vehicle speed versus driving time, is used to emulate the real driving of passenger car in urban area. The simulation program applies the driving cycle second by second, and calculates the engine speed, engine power, motor speed, motor power, regenerative braking power, and the change in the battery storage energy. Fig.12 shows the simulation results generated by the studies using the urban drive cycle with the Maximum Battery SOC Control strategy. Fig.13 shows the engine operation points on its fuel characteristic map.

Fig.12 indicates that with the Maximum Battery SOC control strategy, the battery storage energy can be balanced at the beginning and end of the driving cycle by charging the battery from the excess power of the engine and the regenerative braking. This result shows that the batteries on board do not need to be charged from outside of the vehicle, and the vehicle driving range is limited only by the volume of the fuel tank.

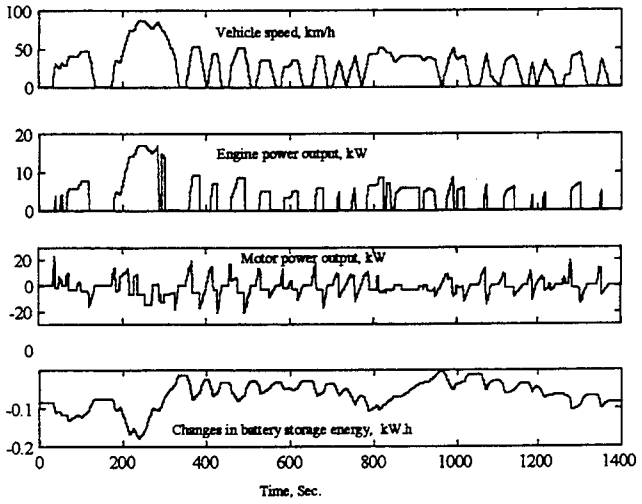

Fig.12 Time history of vehicle speed, engine power output, motor power output and change in the battery storage energy in EPA FTP urban driving cycle.

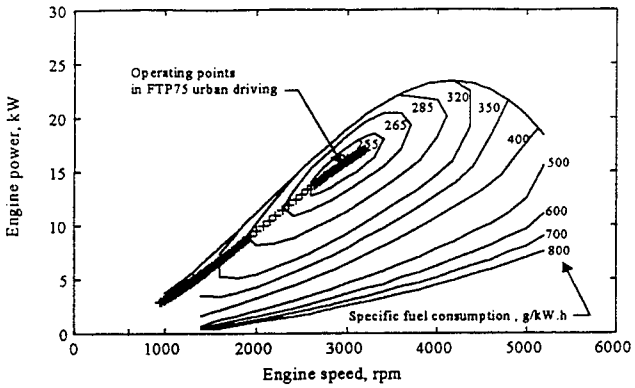

Fig.13 Engine operating points on the fuel characteristic map of the engine

Fig.13 indicates that, with the Maximum battery SOC control strategy and proper selection of the engine size, the engine can almost operate on its optimal operating line. This result is the major reason why the ELPH propulsion can improve the fuel economy greatly. The fuel consumption predicated from the simulation for this design is about 4.66L/100km (50.7mpg). This fuel economy is almost 2.5 times that of conventional passenger car that has a similar performance and load capacity.

Highway Driving Simulation

The EPA ftp highway driving cycle is used to emulate the real driving of passenger cars on highway. Comparing with the urban driving cycle, the highway cycle has a higher average speed and less acceleration–deceleration driving. The Engine Turn-on and Turn-off control strategy is a better control strategy for the highway driving. Using the V-ELPH simulation package, the simulation results generated by the studies using the highway drive cycle with the Engine Turn-on and Turn-off control strategy are shown in Fig. 14 and Fig.15. From these two figures, it can be seen that the battery storage energy can be maintained balanced at beginning and end of the driving cycle and the engine operates almost in its optimal operating region. The fuel economy obtained from the simulation are 4.74 L/100km (50mpg). This value is almost twice the fuel economy of conventional passenger cars with similar performance and load capacity.

Determination of Battery Size

The battery size is determined by two factors, one is the power demand and the other is the storage energy demand. The batteries must be able to supply sufficient power to the electric motor in accelerating driving which means that the peak power the batteries supply must be greater than, at least equal to the peak power of the electric motor (*55kW*). The modern lead/acid traction batteries show the average specific power of *280W/kg* and power volume density of *470W/dm*^{3}[9], Thus, the total battery weight

needed is about *200kg* ($55\times10^3/280$) and the total battery volume is about *120dm*^{3} ($55\times10^3/470$).

The batteries must store sufficient energy to maintain the state-of-charge at a reasonable level during driving. Refer to Fig.12 and Fig.14, the maximum change in the battery storage energy is about *0.3kW.h*. The battery storage energy capacity of the batteries can be obtained by

$$C_b = \frac{\Delta E_b}{SOC_{top} - SOC_{bottom}} \quad , \qquad (4)$$

Where, ΔE_b is the maximum change in battery storage energy, SOC_{top} and SOC_{bottom} are the top and bottom values of the battery SOC, respectively, which are expected to be maintained in driving.

The battery operating efficiency (discharging and charging) is closely related to the battery state-of-charge as shown in Fig.16. This figure indicates that the range 40% to 60% of the battery state-of-charge is the optimal operating range. Thus, the battery storage energy capacity can be obtained as $C_b=0.3/(0.6-02)=1.5kW.h$.

The specific energy capacity and energy density of modern lead/acid are typically *40 W.h/kg* and *68W.h/dm*^{3}. Thus the total weight and total volume of the batteries required by the storage energy are about *37.5kg* ($1.5\times10^3/40$) and *22dm*^{3} ($1.5\times10^3/68$) respectively, which are much smaller than those which are required by the peak power. This result implies that in ELPH propulsion, the batteries are used as power source more than as energy source.

Conclusion

This paper presents an alternative to conventional passenger cars, hybrid electric vehicle with an Electrically Peaking Hybrid (ELPH) propulsion system. Two control strategies, Maximum battery SOC and Engine Turn-on and Turn-off, are discussed for applicability in urban and highway driving, respectively. A full-size hybrid electric passenger car was simulated using the V-ELPH simulation program developed at Texas A&M University. Performance parameters were verified by studies using urban and highway driving cycle.

With parallel configuration and the electrically peaking principle, full size passenger cars can obtain comparable performance and loading capacity to the conventional cars, and the fuel economy of ELPH cars would be increased by 2-3 times. The ELPH cars do not need to be charged from outside of the vehicle. The cost of mass production is expected not to be much higher than that for conventional cars, since all the components in the propulsion are available in industry.

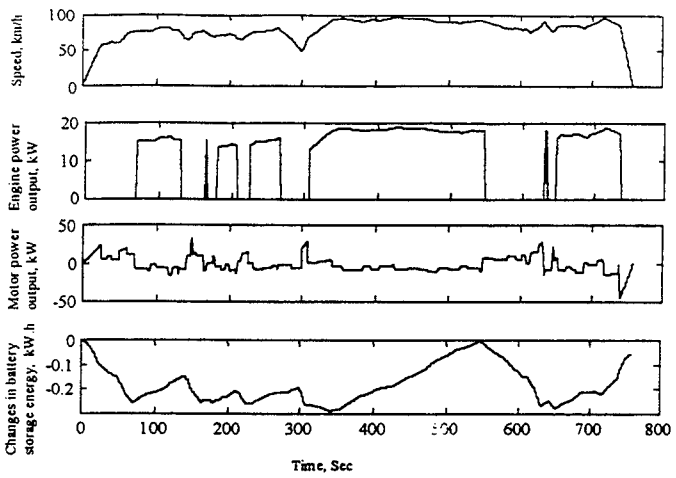

Fig.14 Time history of vehicle speed, engine power, motor power and changes in battery storage energy with the engine Turn-on and Turn-off control strategy in EPA FTP75 highway driving cycle

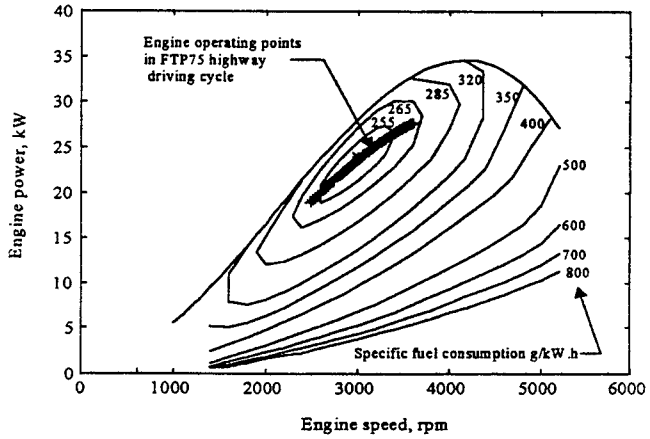

Fig.15 Engine operating points on the engine fuel consumption map in highway driving

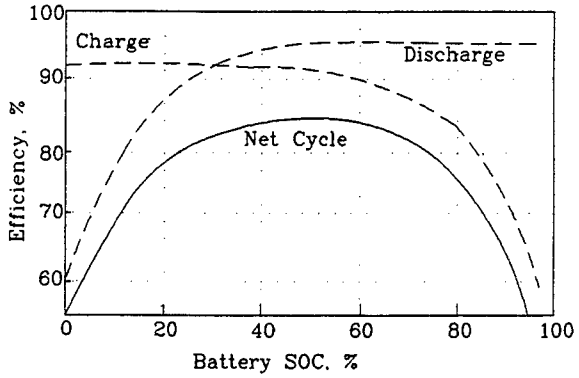

Fig.16 battery efficiency versus state-of-charge

Acknowledgment

The financial support of the Texas Transportation Institute and Texas Higher Education Coordinating Board and for the ELPH project is gratefully acknowledged

Reference

1. K. Butler, K. Stevens, andM. Ehsani, "*A Versatile Computer Simulation Tool for Design and Analysis of Electric and HybridDrive Trains*", SAE 970199

2. Yimin Gao, Khwaja M. Rahman, and Mehrdad Ehsani, "*Parametric Design of the Drive Train of Electrically Peaking Hybrid (ELPH) vehicle*", SAE 90294

3. Yimin Gao, Khwaja M. Rahman, and Mehrdad Ehsani, "*The Energy Flow Management and Battery Energy Capacity Determination for the Drive Train of Electrically Peaking Hybrid Vehicle*", SAE 972647
4. M. Ehsani, K. M. Rahman, and H. Toliyat, "*Propulsion System Design of Electric &Hybrid Vehicle*",

5. Martin Endar and Philipp Dietrich, "*Duty Cycle Operation as a Possibility to Enhance the Fuel Economy of an SI engine at Part Load*", SAE 960229

6. Clark G. Hochgraf, Michael J. Ryan, and Herman L. Wiegman, "*Engine Control Strategy for a Hybrid Electric Vehicle Incorporating Load Leveling and Computer Controlled Energy Management*", SAE 960230

7. M.Ehsani, "*Electrically Peaking Hybrid system and Method*", U.S.Patent, Granted 1996

8. J.Howze, M. Ehsani, and D. Buntin, "*Optimization Torque Controller for a Parallel Hybrid Electric Vehicle*", U.S. Patent, Granted 1996

9. D. A. J. Rand, R. Woods and R. M. Dell, "*Batteries for Electric Vehicle*", Research Studies Press Ltd. 1998

10. J. W. Wong, "*The theory of Ground Vehicle*", John Wiley & Sons Inc. Press, 1978

Analysis of Electric Vehicle Utilization on Global CO_2 Emission Levels

Stephen Moore
Texas A&M University

Mehrdad Ehsani
Texas A&M University

ABSTRACT

The increase of CO_2 emissions in the last quarter of century has risen at an alarming rate. In the U.S.A. alone the CO_2 emissions have increased by 50%, from 1 billion tons of carbon to 1.55 billion tons. The transportation industry contributes currently (1991 figures) 24.7% of the total emissions from the United States. Transportation utilization has grown faster, however, but more efficient vehicles allow for more travel without increasing the CO_2 proportionally. The advancements made in the 1980s have reduced emissions by 21 million tons of CO_2 per year on average.

Electric Vehicles have been a proposed method of reducing the CO_2 emissions due to transportation. Electric vehicles produce no emissions while driving, making them ideal candidates for heavily polluted and concentrated areas such as urban locations. However, it is debatable if electric vehicles are feasible on the global scale of CO_2 reduction. This study compares the amount of emissions produced charging the electric vehicles with the amount of emissions produced by operating a conventional vehicle for equivalent usage. Conclusions are drawn about the advantages and the emissions reductions (if any) that are found by electric vehicle usage.

INTRODUCTION

This portion of the paper will focus of the ratio of the total energy usage (and thus CO_2 production) and transportation energy consumption in the United States. Because the U.S. is globally the foremost producer of emissions from transportation, such is a study is crucial to initial understanding of the problem. The transportation industry in the U.S. has now consumes over 27% of the total energy in 1991, and that number has most certainly increased since then, vs. less than 25% in 1970. With transportation consuming a larger share of the energy budget, any changes in CO_2 production due to technological advancements such as electric vehicles will have a greater impact.

With multiple other countries approaching the CO_2 emission levels of the United States such as Canada, France, Germany, Italy and UK the impact of electric and/or advanced vehicle technology can be extended from the U.S. study. Large developed countries such as the former Soviet Union republics, the People's Republic of China, and India represent a very large share of the next century's transportation energy budget as well.

TRENDS OF U.S. CO_2 EMISSIONS

The total CO_2 emissions from the United States alone have increased by half from 1 billion tons of carbon in 1970 to 1.55 billion tons in 1992. This increase represents multiple sources, including electric plants, transportation, and industrial sources. This increase reflects a total energy consumption increase of about 1% per year between 1970 to 1991. The transportation industry energy use increased at a rate of 1.6% per year in the time span, faster than the average total energy annual growth rate. This is reflected in that the transportation industry gained a greater share of the transportation energy budget from 24.5% in 1970 to 27.3% in 1991. In 1993, the U.S. transportation energy reached 22.8 quadrillion Btu.

A direct correlation can be drawn between energy production and CO_2 emissions. CO_2 is a unique greenhouse gas because it has a stable physical relationship to energy use. Emissions such as NOx and Sulfates can be reduced by combustion techniques and exhaust technologies such as catalytic converters. However, fossil fuels contain a fixed amount of carbon, thus releasing a fixed amount of CO_2 upon utilization. Thus, CO_2 emissions trends closely follow energy trends (this concept is covered in more detail with Table 3 later on). A note must be made that hydroelectric and nuclear power are exceptions.

Between 1970 and 1991 the U.S. emissions from energy use increased with an annual growth rate of 0.8%, from 5,554 million tons (mmt) to 6566 mmt in 1991. During the same period the CO_2 emissions from transportation rose at a growth rate of 1.67%, rising from 1146 mmt to 1624 mmt. Thus, the total amount of transportation emissions rose from 20.6% to 24.7% [1].

Table 1. Increase of Energy Use by the Transportation Industry

	1970	1991	Δ	% Change
Total CO_2 Emissions	5554 mmt	6566 mmt	+1012 mmt	+0.80%
Transportation CO_2	1146 mmt	1624 mmt	+478 mmt	+1.67%
% Share of Emissions	20.6%	24.7%	+4.1%	
% Share of Energy	24.5%	27.3%	+2.8%	

Inspecting Table 1, the most striking feature is that the transportation industry claimed 27.3% of the energy and only contributed 24.7% of the emissions. This is primarily due to the fact that the electric utility industry uses coal, which is significantly higher in carbon content than the fuels used in transportation. Note must be taken on this fact when considering electric vehicles because any emissions that are avoided by using an electric vehicle is deferred to the coal-burning electric utilities used to charge the vehicle's battery.

Even though overall energy production produced more CO_2 than the transportation energy production, non-CO_2 producing power generation such as hydroelectric or nuclear has increased in the United States from 16.9% to 28.5% [2]. Thus with the evaluation of more statistics, it can be proven that the CO_2 emissions per unit energy produced as a whole has declined. Diesel fuel has increased popularity as a transportation fuel from 18.8% in 1970 to 23.69% in 1991 [3]. Since diesel fuel contains more carbon per unit Btu, there was an increase of CO_2 production per unit of transportation energy use.

TRANSPORTATION GROWTH TRENDS

Personal and freight transportation has increased tremendously in the past two decades due to several factors. The United States has maintained an almost constant population growth rate of +1% per year over the last decades, from 205 million in 1970 to 252.2 million in 1991 (18.7% increase). During the same amount of time, personal transportation has increased from 2245 billion passenger-miles (pm) to 3998 billion at a growth rate of 2.8% per year, a 43.84% increase. An interesting fact is that light truck personal transportation has increased at a rate of 5.9% per year, indicating the popularity of the pickup truck for commuter applications [4]. Taking into account the population growth, the per capita increase of commuter miles has been from 10,950 miles per capita to 15,822 miles over the same period of time.

Table 2. Passenger Transportation Trends (U.S.)

	1970	1991	Δ	%
Population	$205x10^6$	$252.2x10^6$	$47.2x10^6$	+18.7%
U.S. GNP	$\$2702x10^9$	$\$4528x10^9$	$\$1826x10^9$	+40.3%
Miles per Capita	10950	15822	4872	+30.8%
Total pm	$2245x10^9$	$3998x10^9$	$1753x10^9$	+43.8%

It is obvious that from this table the increase in transportation is not because there are more people (18.7% population growth vs. 43.8% increase of miles driven). However, the increase of transportation seems to mirror the increase of GNP more closely (40.3% GNP growth correlates to a 43.8% increase of miles driven). Thus two contributing factors of increasing transportation energy usage can be attributed to population growth and economic growth.

Freight transportation increased at a more rapid rate than personal transportation, from 2467 billion ton miles (tm) to 3689 billion tm, a 49.5% increase at a rate of 1.9% per year. It should be noted that air freight now handles 8.86 billion tm, growing at a rate of 5.3% per year. In comparison, truck freight handles 1150 billion tm per year.

IMPROVEMENTS IN TRANSPORTATION EFFICIENCY

Technological advancements in the transportation industry have resulted in a variety of efficiency improvements. Many of these improvements are driven by availability of advanced technology that increases marketable performance while increasing efficiency. Other improvements are brought on by government, public opinion, or legislation. More details on these factors will be brought up in section 3. The Bureau of Transportation Statistics ranks several different types of vehicles based upon their average energy efficiency, expressed as Btu per passenger-mile. It must be pointed out that this statistic reflects how much energy is required to transport one person per mile. A crowded city bus scores high marks in this category compared to a pickup truck with one commuter driver, because the city bus carries more passengers per unit energy than the commuter vehicle (Figure 1):

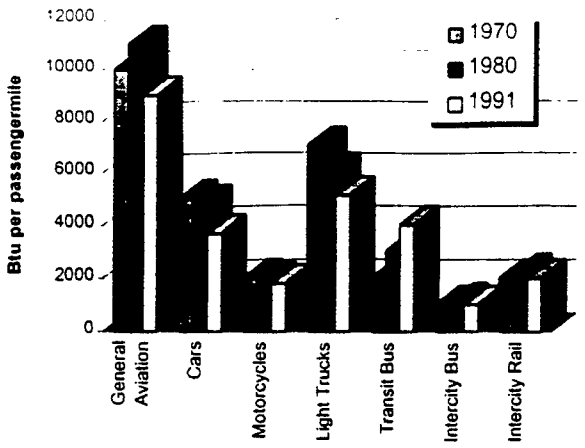

Figure 1. Btu per Passenger-Mile [5]

An interesting note is that the transit bus passenger-mile energy efficiency has decreased. This can be attributed to a general propensity to travel in personal commuter vehicles rather than in public transit busses.

CHANGES IN TRANSPORTATION ENERGY USAGE

The preceding sections detailed the increase of the transportation sector and its attributing causes, which are important to realize if this analysis is to be applied on a global scale in order to make observations about future trends. Next, a scientific and statistical analysis needs to be done to compute the weights and effects of the energy usage in the transportation sector. The beginning of this study is to examine the carbon content of various fossil fuels and rank them accordingly:

Table 3. Common fossil fuels and carbon content [6]

Fuel	Grams of CO_2/gJ	Tons of CO_2/billion Btu
Hard Coal	94.2	99.2
Ship Oil	78.1	82.4
Diesel	73.8	77.9
Aviation Gas	71.2	75.1
Gasoline	71.2	75.1
Jet Aviation Fuel	70.8	74.7
Rail Diesel	70.0	73.9
Natural Gas	56.1	59.2

Conversion was made based on 1 Btu = 1055 joules. All hydrocarbon bound carbon is assumed to be eventually converted to CO_2. True combustion does not result in 100% conversion because incomplete combustion can result in CO (which is rapidly converted to CO_2 in the atmosphere) and CH_4, an important greenhouse gas. It is assumed that the amount of CO_2 produced by incomplete combustion is not significant, even more so considering the advanced engine technologies available presently.

The amount of CO_2 produced by combustion of each fuel is governed a fixed physical relationship based on the carbon content per Btu yield. When undergoing incomplete combustion, utilization of fossil fuels can result in emission of long-chain hydrocarbons, which break down into methane and CO_2. Thus the actual 'greenhouse' emission is not only based on the carbon content but combustion method. The combustion technology combined with the exhaust technology also can result in a wide range of NOx and sulfate emissions.

Next, a table was constructed using the values of Table 3 to compute the actual CO_2 production resulting from each factor (Table 4):

Table 4. Breakdown of driving forces in terms of CO_2 emissions [1]

Increase of CO_2 production for each decade	1970-1980	1980-1991
	mmts CO_2	Mmts CO_2
Efficiency	-54.33	-177.80
Transportation Mode	37.96	1.89
Economic Growth (GDP)	79.80	191.13
Population Growth	87.01	100.21
Other Interactions	-20.73	-37.41
Changes from Passenger Transportation	**129.70**	**78.02**

Increases of Btu use for each decade	1970-1980	1980-1991
	Trillion Btu	Trillion Btu
Efficiency	-725.98	-2369.35
Transportation Mode	508.20	27.91
Economic Growth (GDP)	1062.76	2545.30
Population Growth	1158.78	1334.55
Other Interactions	-277.06	-498.01
Changes from Passenger Transportation	**2333.37**	**1040.41**

During the period of 1970-1980 the transportation sector increased CO_2 production by 315.75 million metric tons (mmt) per year. Because of primarily efficiency gains in personal automotive technology, CO_2 production was reduced to average 162.223 mmt per year. This is key in the study of electric vehicles because for an electric vehicle to compete with standard combustion types there must be a clear advantage. With vehicle technology increasing efficiency and reducing emissions at the current pace, it will remain to be seen if EVs will hold a clear advantage.

Notice again, it is indicated that the economic growth as seen with the GDP contributes largely to the increased use of passenger transportation. Population growth (thus more individuals owning vehicles or using public transportation systems) was the second largest contributing cause.

CONCLUSIONS ABOUT CO_2 PRODUCTION IN THE TRANSPORTATION SECTOR

The most significant observations obtained in this section are listed below:

- Passenger transportation has increased at a rate of 2.8% per year whereas the population increase is only 1.0% per year.
- Per capita miles traveled per year has increased 30.9% between 1970 and 1991.
- Transportation CO_2 emissions only accounted for 20.6% of the total emissions in 1970. In 1991 that number increased by 4.1% to 24.7%.
- Transportation consumed 24.5% of the total energy consumed in the United States in 1970 and 27.3% of the total energy in 1991, a difference of 2.8%.

Passenger transportation technological advancements have saved 227 trillion Btu of energy and 21 million tons of CO_2 per year on average from 1980 to 1991.

TRENDS OF GLOBAL CO_2 PRODUCTION

As automotive technology continues to advance and transportation becomes more available, the economy and society is dictating people to travel more now than ever before. This is not only true for the United States but also in almost every country in the world. Considering that transportation accounted for 24.7% of total CO_2 emissions in the U.S., other countries are facing similar statistics. Table 5 lists several major transportation-related CO_2 contributing countries. Notice that some omissions include China, India, and the former Soviet Union republics due to lack of available data.

Table 5. Some major transportation-related CO_2 contributing countries [7]

	Emissions (mmt/year)		
	CO_2	HC	NOx
Canada	9928	2100	1942
USA	76000	22800	20300
Japan	*5013*	*1503*	1339
Austria	1126	251	211
Belgium	839	*356*	317
Denmark	602	106	241
Finland	660	112	284
France	5200	2185	2567
Germany	8960	1860	3090
Greece	695	82	196
Ireland	497	62	71
Italy	4036	496	1550
Netherlands	1368	452	500
Norway	632	158	125
Portugal	533	91	248
Spain	3780	739	778
Sweden	1250	410	328
Switzerland	711	311	196
Turkey	3707	201	380
UK	5127	1954	1932

GOVERNMENT AND PUBLIC INITIATIVES

Government policy toward CO_2 regulation, especially in the transportation sector, has oscillated dramatically in the last decade. Early optimism about the technology associated with electric vehicles resulted in numerous 'mandates' that a certain percent of the automobile fleet in particular countries be electric. As electric vehicles became a reality and their poor performance, range and cost became obvious these mandates were delayed, decreased, or in some cases, removed altogether.

The low oil prices in the 1980s have also contributed to the loss of interest in electric vehicles. The economy in the 1970s drove technology to search for alternative and possibly cheaper transportation that was not dependent on an imported fuel that looked like was in a shortage. A slight resurgence of research is now underway to develop vehicle technology to reduce urban pollution.

Governments in USA, Japan and some European countries have developed ways to encourage further research [8]. Some particular government regulations regarding CO_2 vehicle emissions include (1993 data).

Some notable U.S. trends include:

- Some U.S. state governments (most notably California due to severe urban pollution) have required a sales percentage of ultra low emission vehicles (ULEVs) or electric vehicles. Many local governments have developed incentives (e.g., tax) for fleets and individuals to operate ULEVs or EVs.
- The U.S. federal government aggressively funds hybrid electric (HEV) and electric vehicle research at both national laboratories and independent research facilities.

Japan has integrated a very aggressive plan called the 'Electric Vehicle Market Expansion Program' that specifically targets government and private fleets:

- Government fleet vehicles of Tokyo and Osaka have been targeted to migrate to electric vehicle use, and private enterprises offered financial incentives to switch to EVs.

- Financial incentives and government subsidies are offered to private utility companies and delivery firms to migrate to EVs.
- Future incentives are planned for individual automobile owners. In 1993, these incentives were only 4% of the cost of an electric vehicle, which is not a significant amount compared to how much more expensive an EV is in comparison to a standard automobile.

All major automotive industries in Europe now have electric vehicle programs, many of them offering electric versions of existing models. In 1993, there were in excess of 25,000 EVs operating in Europe, primarily in UK.

- UK, Germany and Denmark impose a vehicle tax based on vehicle weight, which discourages the use of EVs. Temporary tax measures have been put in place to avoid this problem.
- Many European countries tax vehicles on engine size, which is EV operators avoid.
- The European Community has determined that based upon current EV development, EVs will have the capability of reducing urban pollution by 20-30% [9].
- The German government aggressively funds EV development and offers tax exemption for EV operators.
- In France 90% of electricity is produced by nuclear power or hydroelectric thus any use of electric vehicles will yield a major reduction of CO_2 emissions. Local governments are offered substantial subsidies to migrate to EV use.

An optimistic forecast [10] from the European Community has deterimined that the combined markets for electric vehicles will reach 2.1 million vehicles by 2010:

Table 6. Forecast of electric vehicle sales

		2000	2005	2010
USA	Total	16,860,000	17,290,000	17,360,000
	Evs	163,500	721,500	1,007,300
	ICE	16,696,500	16,568,500	16,352,700
Japan	Total	7,560,000	7,590,000	7,630,000
	Evs	73,500	266,500	485,500
	ICE	7,486,500	7,323,500	7,144,500
Europe	Total	17,410,000	18,110,000	18,640,000
	Evs	37,800	222,800	612,200
	ICE	17,372,200	17,887,200	18,027,800

This table is surprising in that it predicts electric vehicle production in the U.S. will increase from 1,000 vehicles (approximately current rate) to 163,500 in the year 2000. The developers of this table probably were considering the California air restrictions board legislation, which required a certain percentage of vehicles sold in California to be electric. This legislation has been reduced and some measures have even been removed. Thus the year 2000 estimate for electric vehicles sales is not probable. However, the Japanese market has indicated that it is moving toward electric vehicles at a rapid pace.

IMPACT OF ELECTRIC VEHICLES ON CURRENT CO_2 EMISSION LEVELS

The bulk of the data contained in this section is derived from a joint effort study done by the U.S. Department of Energy (DoE) and the Electric Power Research Institute (EPRI) [11]. This study concentrated on *four basic scenarios of EV market penetration compared to two basic scenarios of gasoline vehicle development.* The study forecasts automotive emissions for each of the scenarios and generates emissions savings potentials. The goal of the analysis is to discover the benefit of displacing fossil fuel consumption from individual automobiles to centralized electric generation facilities.

It should be noted emissions from EV battery recycling could be a potential concern. About 85% of used automotive batteries are collected and of those 95% are recycled. The process used to recycle batteries generally produces about 1g of NOx and 3.7g of CO_2 per ordinary automobile battery [12]. Assuming an EV battery on average is 120 times the size of the ordinary automobile battery (420 W-hr vs. 50 KW-hr capacity), an EV battery would require 120g of NOx and 450g of CO_2 per battery recycled. Considering the battery would have a usable lifetime of 400 charging cycles at 80 miles per charge (30,000+ mile battery lifetime, optimistic), the recharging emissions of 0.0001 g/mile of NOx and 0.014 g/mile of CO_2 would have to be entered into the total emissions computations. These numbers correspond to about 1% of that an ordinary automobile produces per mile.

MODEL SCENERIOS

Emission levels from six scenarios were computed for comparison purposes [11]:

a. Electric and Hybrid Vehicle (EHV) are assumed to be high efficiency and electric utilities are assumed to have average emission rates. This is the best case scenario.
b. EVH are assumed to have marginal efficiency and electric utilities to have average emission rates.
c. EVH are assumed to have high efficiency and electric utilities to have marginal emissions rates.
d. EVH are assumed to have marginal efficiency and electric utilities to have marginal emission rates. This is the worst case scenario for EVHs.
e. Conventional Vehicles (CV) are assumed to be low efficiency. This is the worst case control scenario with (no EVHs and low efficiency CVs).
f. Conventional Vehicles are assumed to have high efficiency. Good case control scenario.

The first four scenarios apply to EVHs and the last two are control runs with only ordinary automobiles. Thus conclusions can be drawn when comparing an EVH scenario with a control run. Emissions considered in each case are six pollutants: CO_2, SO_2, CO, VOC (incomplete combustion hydrocarbons), and NOx. It should be noted that SO_2 and NOx are precursors to acid rain, SO_2 creates an localized aerosol that combats greenhouse warming and CO_2 and NOx are greenhouse gasses. The VOCs will decompose eventually into CO_2 or CH_4, which both contributes to greenhouse warming.

Conventional vehicles were modeled assuming that existing vehicles operated at the fuel efficiencies specified on Table 7.1-7.3 for the two control scenarios. The reason behind the decreasing mpg trend in light trucks is due to the increasing popularity of larger and more powerful engine options available. The Moblie4 computer model [13] was used to compute the gasoline vehicle emissions and *the CO_2 production was based on the physical equations of carbon content of fuel, fuel efficiency, CO_2 produced during fuel extraction, refinery operation and distribution.*

Table 7.1. Average vehicle fuel economy (mpg) 'worst case scenario

Year	Automobiles	Light Trucks
1995	22.2	17.0
2000	22.3	16.8
2005	22.6	16.8
2010	22.9	16.9

Table 7.2. Average vehicle fuel economy (mpg) 'good scenario'

Year	Automobiles	Light Trucks
1995	27.8	17.0
2000	27.8	16.8
2005	27.8	16.8
2010	27.8	16.9

Table 4.3. Gasoline/Diesel percent market share for Light Trucks

Year	Gasoline	Diesel
1995	90%	10%
2000	76%	24%
2005	63%	37%
2010	58%	42%

Referring back to Table 3 and assuming that 98% of the carbon content of gasoline is burned in each combustion cycle and 99% conversion of Diesel fuel, the mass of CO_2 produced per gallon of fuel can be computed:

(mass of carbon per gallon) x conversion percent x 44/12 = mass CO_2

Grams per gallon are then converted into grams per mile using the fuel efficiency Tables 7.1-7.3.

The electric vehicle scenarios are divided into two subcategories, the high and low efficiency EVs. Low efficiency EVs require more frequent changing for equivalent miles traveled, thus the demands from the electric utilities are increased. Examining the loads on electric utilities,

Table 8. High and low EV efficiency cases and total annual charging electricity use (GWhw)

	2000	2005	2010
Low Case	3,137	25,332	80,096
High Case	1,511	10,169	26,843

Electric utility plants are modeled by two factors: fuel types and emissions standards. The average and marginal emission calculations were performed using the fuel types (and thus average emissions content) and 1990 CAAA regulations on SO_2 and Nox. Table 9 indicates the breakdown of the different fuel usages.

Table 9. Percent use of different fuel types

Coal	Oil	Gas	Nuclear	Alternative
57.4%	4.43%	6.8%	21.4%	1%

The alternative power utilities include hydroelectric and wind power most (>50%) of this type of power generation is found in the western U.S. Notice that nuclear holds a large portion of power generation in the U.S., but it is not nearly as comparable to France's nuclear efforts of reaching well above 75% of all power is non-fossil fuel. In cases where nuclear power is available, CO_2 production for the use of electric vehicles is significantly reduced.

SCENERIO RESULTS

Because the primary purpose of this review to study the impact of specifically greenhouse gasses, only the CO_2 emission results will be presented. Table 10 shows the model results for CO_2 for each of the six scenarios.

Table 10. CO_2 Emissions in mmt/year for each scenario of EV utilization in the U.S.

	Scenario a	Scenario b	Scenario c
1995	5,197	6,822	6,896
2000	948,572	1,967,166	1,260,386
2005	5,735,672	14,265,967	8,477,902
2010	13,406,344	39,950,717	22,351,069

	Scenario d	Scenario e	Scenario f
1995	9,052	9,757	9,757
2000	2,615,800	2,356,751	2,228,850
2005	21,108,398	19,581,189	17,842,184
2010	66,665,956	64,452,227	54,187,308

There are several pieces of important *general* information to obtain from this table:

- Highly efficient EHVs combined with strict electric utility regulation (Scenario a) can reduce the CO_2 emissions due to transportation over 20%. Because transportation currently is responsible for 24.7% of total CO_2 emissions, it would be a reduction of 5.5% of total U.S. CO_2 emissions.
- Even the worst case scenario (case e) is better than poorly efficient EVHs and marginal utility plants (case d)!
- Conventional vehicles can compete within 25% with poorly efficient EVHs with good efficiency power utilities.

The result of this study indicates that if EVHs are to become (1) a reality and (2) a solution to CO_2 emissions then they must be highly efficient with efficient power generation utility infrastructure. Nuclear energy has a great advantage in this type of study, as does wind energy and hydroelectric systems. However, these types of production are either politically difficult, economically unfeasible, or produce emissions or effluents of their own.

CONCLUSION

There are several important realizations to be made about this study:

- Transportation in the U.S. is increasing at a rapid pace. Population has only increased at a rate of 1.0% per year but total miles traveled has increased by 2.8% per year. Per capita miles traveled has increased by 30.9% since 1970.
- Transportation related CO_2 emissions are responsible for 24.7% of the total CO_2 emissions in the U.S., yet transportation is responsible for 27.3% of the energy usage.
- Conventional gasoline vehicles will continue to compete in CO_2 emissions unless electric or hybrid vehicles and electric power utilities increase efficiency.
- Conventional gasoline vehicles compete favorably to marginally efficient electric vehicles when the electric utility emissions are factored in.
- Conventional vehicles will favorably compete economically unless a technological breakthroughs occurs to lower cost or governments employ financial subsidies initiatives.
- Several governments are funding and/or sponsoring major research efforts for efficient electric or hybrid vehicle technologies.
- Several governments are offering financial incentives or federal subsidies for automobile users to migrate to electric vehicles.

Comparing scenario a to scenario e it can seen that total U.S. CO_2 emissions can be reduced by 5.5% with the use of electric vehicles and efficient power utilities. This is a significant beginning but several things must be considered:

- Advanced electric utilities need to be developed before electric vehicles will become truly useful. At today's present technologies, there is not enough emissions advantage to use electric vehicles because they still need to be charged from emissions-generating power plants.
- Electric vehicle technology today is expensive and battery lifetime is short (~30,000 miles). Electric vehicle technology needs to expand beyond the limitations of electrochemical energy storage before high enough efficiency is to be realized.
- Developing countries and countries such as China, India, and the former Soviet Union republics have to be considered because their share of CO_2 emissions are going to increase considerably. If the U.S. switches to optimal EV usage, the global effect will be small in comparison to the emissions created from other countries. The technology must be universally applied for significant reductions.

CONTACT

Stephen Moore and Dr. Mehrdad Ehsani can be reached by calling the Department of Electrical Engineering, Texas A&M University, at (409) 845-7441, or email smoore@ee.tamu.edu and ehsani@ee.tamu.edu.

REFERENCES

[1] Lakshmanan, T.R., X. Han, "Factors Underlying Transportation CO_2 emissions in the U.S.A.: A Decomposition Analysis," *Transportation Research – D*, Vol. 2, No. 1, pp. 1-15, 1997

[2] Lakshmanan, T.R., X. Han, "Structural Changes and Energy Consumption in the Japanese Economy," *The Energy Journal*, Vol. 15, pp. 165-188, 1994

[3] Bureau of Transportation Statistics, U.S. Department of Transportation (1993), National Transportation Statistics of 1993

[4] Bureau of Census, U.S. Department of Commerce, Census of Transportation, Volume II: Truck Inventory and Use Survey

[5] Bureau of Transportation Statistics, U.S. Department of Transportation (1996), National Transportation Statistics of 1996

[6] "Greenhouse Gas Emissions: The Energy Dimension," *OECD/IEA*, 1991

[7] Green, A.P., C. McGrath, and J. Murray, "Global Opportunities and Risks for Electric and Hybrid Low Emission Vehicles," *Society of Automotive Engineers*, No. 931011, 1993

[8] "MIRA Electric Vehicle Forecast," *MIRA*, 1992

[9] Naunin, D., "The Current Status of Introducing Electric Vehicles into Urban Areas in Germany," EVS11, 1992

[10] "COST 302 – Technical and Economic Conditions for the use of Electric Road Vehicles," *Commission of European Communities*, 1987

[11] "Utility Emissions Associated with Electric and Hybrid Vehicle (EHV) Charging," U.S. Department of Energy, Office of Transportation Technologies, Electric and Hybrid Propulsion Division, 1993

[12] Wang, Quanlu, D.L. Santini, "Magnitude and Value of Electric Vehicle Emission Reductions for Six Driving Cycles in Four U.S. Cities with Varying Air Quality Problems," *72nd Annual Meeting of Transportation Research Board*, 1993

ADDITIONAL SOURCES

[13] DeLuchi, M.D., "Emissions of Greenhouse Gasses from the Use of Transportation Fuels and Electricity," ANL/ESD/TM-22, Vol. 1, Center for Transportation Research, Argonne National Laboratory, 1991

[14] California Air Researches Board (CARB), "Proposed Regulations for Low-Emission Vehicles and Clean Fuels, Technical Support Document," California, 1990

An Open Architecture System for Simulation of Electric and Hybrid Electric Vehicles

Karen L. Butler Mehrdad Ehsani Preyas Kamath Ken Stevens

Texas A&M University
Texas Applied Power Electronics Center
College Station, Texas 77843-3128

ABSTRACT - There has been increased interest by the automobile industry to design zero and near-zero emission automobiles due to the regulations that have been adopted by several states in the U.S. In recent years, computer simulation has provided lower cost and less-time intensive analysis of new design options as compared to the past practice of hardware prototypes. This paper discusses a computer simulation tool, V-Elph, which has been developed to facilitate the design and analysis of electric and hybrid vehicles. V-Elph is composed of detailed models of four major types of components: electric motors, internal combustion engines, batteries, and support components which can be integrated to simulate drive trains having all electric, series hybrid, and parallel hybrid configurations.

The system and component models in V-Elph were developed in a modular manner with standardized interfaces for easy integration of components. A hierarchical, layered design philosophy was adopted for programming V-Elph so that users with different levels of expertise and interests could utilize the tool. It was written in the Matlab/Simulink graphical simulation language and is portable to most computer platforms.

This paper discusses the design methodology, features, and component and system-level functions of V-Elph. The design steps for a series hybrid vehicle are illustrated and simulation results for a sedan vehicle are discussed.

INTRODUCTION

Presently, only electric and low-emissions hybrid vehicles can meet the criteria outlined in the California Air Regulatory Board (CARB) regulations which require a progressively increasing percentage of automobiles to be ultra-low or zero emissions beginning in the year 1998 [1]. Though purely electric vehicles are a promising technology for the long range goal of energy efficiency and reduced atmospheric pollution, their limited range and lack of supporting infrastructure may hinder their public acceptance [2]. Hybrid vehicles offer the promise of higher energy efficiency and reduced emissions when compared with conventional automobiles, but they can also be designed to overcome the range limitations inherent in a purely electric automobile by utilizing two distinct energy sources to provide energy for propulsion. With hybrid vehicles, energy is stored as a petroleum fuel and in an electrical storage device such as a battery pack and is then converted to mechanical energy by an internal combustion engine (ICE) and electric motor, respectively. The electric motor is used for peaking power demands while the ICE provides base power demand. Though many different arrangements of power sources and converters are possible in a hybrid power plant, the two generally accepted classifications are series and parallel [3].

Computer modeling and simulation can be used to reduce the expense and length of the design cycle of hybrid vehicles by testing configurations and energy management strategies before prototype construction begins. Interest in hybrid vehicle simulation began to pick up in the 1970's along side the development of several prototypes which were used to collect a considerable amount of test data on the performance of hybrid drive trains [4]. Also studies have been conducted to study the hybrid electric vehicle concepts [5-7]. Several computer programs have since been developed to describe the operation of hybrid electric power trains, including: Simple Electric Vehicle Simulation (SIMPLEV) from the DOE's Idaho National Laboratory [8], MARVEL from Argonne National Laboratory [9], CarSim from AeroVironment Inc., JANUS from Durham University [10], and ADVISOR from the DOE's National Renewable Energy Laboratory [11]. A previous simulation model, ELPH, developed at Texas A&M University was used to study the viability of an electrically-peaking control scheme and to determine the applicability of computer modeling to hybrid vehicle design [12] but was essentially limited to a single vehicle architecture. Other work conducted by the hybrid vehicle design team at Texas A&M University is reported in [13-17].

V-Elph [18-19] is a system level modeling, simulation and analysis package developed at Texas A&M University using Matlab/Simulink [20] to study issues related to electric vehicle (EV) and hybrid electric vehicle (HEV) design such as component sizing, energy efficiency, fuel economy, and vehicle emissions. The package uses an open architecture so that any type of hybrid electric, electric, or conventional internal combustion engine vehicle configuration can be designed and studied. The framework of the package is general enough that additional features, such as estimates of lifetime vehicle cost or other items of interest can be added without changing the core computer code. It extends the capabilities of previous modeling and simulation efforts by facilitating in-depth studies of power plant configurations, component sizing, energy management strategies, and the optimization of important component parameters for any type of hybrid or electric configuration. Visual programming techniques are used which allow the user to quickly change architectures, parameters, and to view output data graphically. It also includes detailed models of electric motors, internal combustion engines, batteries, and vehicle dynamics developed at Texas A&M University.

In this paper the design methodology, various features, and functions of the V-Elph simulation package are discussed. A series hybrid vehicle is designed to illustrate how the V-Elph package is used to design and study component and control technologies for a vehicle drive train. However, any other propulsion system architecture such as parallel hybrid, electric vehicle, and conventional ICE can be configured and simulated with similar ease.

DESIGN METHODOLOGY

A. Abstraction Levels

The V-Elph software package is organized in a hierarchical and modular manner. Five conceptual levels of abstraction are used in V-Elph to organize a system model and to represent the specific functional levels of a vehicle drive train [18]. The levels are: (1) vehicle control level, (2) power plant control level, (3) configuration level, (4) component level, and (5) coupling level. Defining these levels introduces a hierarchical structure where each level of abstraction encapsulates the functionality of its subsystems while maintaining a common interface to higher levels. Each level of abstraction also isolates a different part of the vehicle design process, allowing systematic analysis.

The highest level of abstraction in the model, the vehicle control level, describes the driver interactions with the vehicle and the environment in which the vehicle operates. It is at this level that the expectations of the driver such as acceleration performance, range, and grade are defined by altering the drive-cycle and/or the driver model. The vehicle control layer separates the actions of the driver from the modeling of the hybrid vehicle plant so that the driver model can be changed without affecting the implementation of the power plant. The vehicle control level receives speed information in km/h and produces a desired torque command which is sent to a power plant controller. A driver can be modeled by matching a reference speed, modeling a driver's behavior through a predetermined course, or by using human input to control vehicle speed.

The power plant control level defines how the components are controlled to meet the torque command produced by the vehicle control level. The implementation of this level is contained within a power plant controller block. By altering the algorithms in the power plant controller block, the vehicle's energy management strategy can be changed for a particular power plant configuration. The power plant controller produces the appropriate signals to be sent to the drive train components to implement the desired control scheme such as ICE throttle command, electric machine torque command, clutch signals, and gear selection signals. The inputs and outputs from the power plant controller vary depending on the information needed to implement a particular control scheme.

The configuration level is not an actual block, but refers to how the components in a drive train interact because of their sizing and how they are arranged. Altering the configuration allows the construction of both series and parallel hybrids and changes the fundamental attributes of a hybrid power plant by changing the components' functional roles; the ICE in a series hybrid plays no direct role in providing torque to the wheels while the ICE in a parallel design is an integral part of propulsion. Sizing components differently within the same arrangement can also drastically change the components' functional roles since the amount of power that they can contribute changes. In a parallel configuration if the electric motor is large and the size of the ICE is small, an ICE based design where the electric motor assists during acceleration results.

The component level describes the local dynamics and control of individual components. The implementation of this level is contained within each of the component blocks in the power plant.

The coupling level defines the interface used to connect components of a certain type. A lumped parameter coupling scheme was chosen to implement V-Elph. All of the components are assumed to be rigidly connected and the component torque and inertia are referred to a single point to calculate the system dynamics. The system acceleration is calculated by summing all of the torques and dividing by the total inertia at a single reference point. The speed of the system is then determined by numerically integrating the acceleration, and this value is passed back to the component models to determine the torque at the next time-step. This scheme was selected because it does not require a small integration time step to capture coupling dynamics and it eliminates the algebraic loops inherently created by the looping of non-integrated signals in the distributed parameter scheme.

B. Buses

The interfaces for electrical and mechanical components are a direct result of implementing the coupling methods described above. Data bussing, a concept borrowed from the computer industry, was used to implement the two-way lumped parameter passing scheme in the model. The concept of a data bus revolves around developing common interfacing specifications which allow different devices to be connected to a common bus regardless of their internal function or implementation. As long as a component's inputs and outputs comply with the interface definition and care is taken to ensure that the model operates within its intended boundaries, it can be attached to the data bus.

The electrical bus concept for the V-Elph is defined as shown in Fig. 1. The electrical bus supplies a voltage to all of the electrical components and then the components determine their current flow based on that voltage. The amount of current drawn or supplied by each electrical energy converter is then passed back to the bus to calculate the voltage at the next time step. The electrical bus usually consists of a storage device such as a battery pack or an ultra-capacitor, which stores electrical energy until it is needed by the electrical components in the systems.

The mechanical bus concept for the V-Elph is defined as shown in fig. 2. The component torque and inertia are combined into a vector to be passed to the rest of the system using a single output line. The friction term is incorporated inside each individual component block since the speed information is available to the component.

C. Control Paradigm

To separate the control of the overall system from the control of each individual component, the master/local control paradigm, shown in Fig. 3, was adopted. The master controller (the power-plant control level) determines how to distribute the driver torque request among the various energy converters in the hybrid power-plant and creates the control signals to implement the desired energy management strategy. The local controller adjusts the component model parameters to meet the demands of the master controller within the component's bounds of operation and then sends information on the status of the component back to the master controller.

The master/local control paradigm helps to encapsulate the inner workings of a component model, limiting outside access through the common interface specification. For example, it separates the functional role of a component as a torque producer from a model's actual implementation and control, allowing a variety of different engines and electric machines to be used without changing the common interface to the rest of the system. The inputs which drive a dc motor and an induction motor are quite different, but by using the master/local control paradigm, which depends on the functional role of the components and not their implementation, a common interface for an electric machine is used for both the dc motor and the induction motor.

D. User Levels

Several levels of depth are available in V-Elph to allow users to take advantage of the features that interest them. At the most basic level, a user can run simulation studies by selecting one the electric vehicles, series or parallel hybrid vehicles, or conventional vehicles provided and display the results using the graphical plotting tools. In addition to being able to change the drive cycle and the environmental conditions under which the vehicle operates, the user can switch components in and out of a model to try different types of engines, motors, and batteries models. The user can also change vehicle characteristics such as size and weight, gear ratios, and the size of the components that make up the drive train.

An intermediate user can create his/her own vehicle configurations using a blank vehicle template and the V-Elph component library. Components can be isolated to run parameter sweeps to create performance maps to assist in component sizing and selection. Given a set of system performance criteria, the performance maps of the components can be used to develop a suitable vehicle design. Finally, advanced users can pursue sophisticated design objectives such as the creation of entirely new component models and the optimization of a power plant by creating add-on features that are compatible with the modeling system interface.

PACKAGE FEATURES

A. Main Menu

The main menu as shown in Fig. 4 provides several options for the user.

- V-Elph – provides information about the V-Elph software and commands to exit the software
- Models – provides facilities for building and sizing electric and hybrid vehicle drivetrains
- Simulation – provides facilities for creating and managing simulation data
- Analysis – provides data analysis tools to organize and plot the information generated during V-Elph simulation
- Help – provides a description of V-Elph.
-

The pull-down entries under each option are stated below.

Models

- Load Vehicle
- Load Component
- Parameter Sweep

Analysis

- Plotter
- Quick Plots
- Data Summary

Simulation

- Setup
- Load Simulation Data
- Save Simulation Data
- Clear Current Data

B. Analysis Tools

There are three major types of analysis tools: *Plotter*, *Quick Plots*, and *Data Summary*. The selection of the *Plotting Tool* icon in the *Analysis* menu brings up the graphical plotter as shown in fig. 5. The user selects the x-axis variable from a menu list of variables generated from the current Matlab workspace. Further the user selects the y-axis from a button list of variables

generated from the current Matlab workspace. The user can also type labels for the x-axis, y-axis and title. Then the user presses the *Plot* button to generate plots of the y-axis variables versus the x-axis variable.

The selection of the *Quick Plots* icon in the *Analysis* menu allows the user to quickly generate several plots. *Quick plot* allows the user to view vital simulation information instantly. When selected, it produces a drop down menu which has the following fields representing parameters related to the major components: *Battery SoC, Battery Voltage, Battery Current,*"*EM Current, EM Torque, Torque* (EM Torque, ICE Torque), *ICE Fuel Consumption , ICE Torque, ICE Emissions* (CO, HC, NOX). The user can plot any of the above variables provided they have been generated during the simulation. The selected variable is then plotted versus time and is labeled accordingly. This tool is useful when running many studies to observe how changes in a parameter effects various outputs.

Another analysis feature of the V-Elph package is the ability to compile the information from a simulation run into a summary of results. To view the simulation results in a summary form, the *Data Summary* icon is selected in the *Analysis* menu, cumulative variables such as total emissions, fuel consumption are calculated and displayed in the data summary output as shown in fig. 6.

COMPONENT LEVEL

A. Interfaces

Data flow within a general component model is shown in fig. 7, where signal connections are used to send information to and from the power plant controller and the power connections represent the physical coupling between components which provide a path for the transfer of energy. The ports for the signal connections are separated from the power connections since the control of each component might be different while the electrical and mechanical coupling mechanisms are the same for all components.

Strict interface definitions are defined for each type of component so that various types of models, e.g. empirical and detailed models, for the same type of component can be included in the V-Elph library of components. The general interface for components utilized in V-Elph is shown in fig. 8. More specifically, the interface for a battery model is shown in fig. 9. All battery models in V-Elph have the same component inputs and outputs and any new model developed by a user must conform to that standard.

B. Library

The component library, as shown in fig. 10, is composed of models of three major components: electric motors, internal combustion engines (ICE), and batteries. Also the library contains models of support components such as vehicle dynamics,

controllers, transmissions, ambient conditions, and drive cycles. The speed at which the simulation executes is highly dependent on the complexity of the component models selected. The various detailed component models currently utilized in the V-Elph package were developed by members of the ELPH research team at Texas A&M University.

C. Design

A user can design new components or utilize existing components to build a hybrid, electric, or conventional drive train system. The component designer should have a detailed understanding of the component technology and can develop a model using empirical data or mathematical equations. The models can be written in Matlab, 'C' programming language, or imported into the package as an executable file.

D. Analysis

A powerful feature of the V-Elph system is the ability to create performance maps of components to help visualize their response characteristics. This feature, a parameter sweep workbench as shown in fig. 11, allows the analysis of the performance of a component over its operating range. Typically one parameter is varied and all other parameters are held constant. The *Constant Parameter* block is connected to the input that will be held constant through a particular sweep and the *Sweep Parameter* block is connected to the input that will be varied during a particular sweep. When the *Setup Sweep* button is selected, the user defines a sweep range of the constant parameter and a sweep time. The plotting tools can be used to observe the behavior of the parameters.

SYSTEM LEVEL

A. Design

The design of a vehicle drive train occurs at each of the five levels of abstraction described earlier. The design process usually begins at the vehicle control level by defining the vehicle mission and the performance that the driver expects from a vehicle of a certain size and a given set of aerodynamic characteristics. The next step is to select a vehicle configuration that meets mission and performance objectives. For example a commuter vehicle which will be driven less than 100 miles a day with access to a land-based charger would require a different configuration than a power-assisted hybrid where the electric motor aids in acceleration to improve fuel economy and emissions while maintaining the battery state of charge. The former defines an electric vehicle while the latter would best be implemented as a parallel hybrid with an electric motor and a downsized ICE. Once a basic

configuration is chosen, the components and gearing is selected to meet the energy requirements of the vehicle. Then a control scheme is selected to meet the performance objectives and the design is iteratively modified until satisfactory performance is achieved.

A system-level model of a drive train can be constructed graphically by connecting the main and support component blocks such as the drive cycle, controller, power plant, and vehicle dynamics from the library of components. The Simulink visual programming methodology is used to connect the appropriate input and output ports. On the other hand, a system-level model can be created from the model section of the main menu which produces the model shown in figure 12 with a blank power plant. The appropriate component models are taken from the library of components to fill in the component blocks.

B. Analysis

Systems can be analyzed by applying a drive cycle to a particular drive train system. Studies may focus on varying component sizes, control strategies, system configurations, etc. The plotting tools and data summary can be used to observe the behavior of the system and component parameters.

CREATING A SERIES HYBRID VEHICLE DRIVE TRAIN

In this section, the design and analysis of a series hybrid electric vehicle drive train using the V-Elph package is discussed. For series hybrid electric vehicles, only one energy converter provides torque to the wheels while the others are used to recharge an energy accumulator, usually a battery pack.

A. Design

The series hybrid vehicle was designed as shown in fig. 13 consisting of a vector controlled induction motor driving the vehicle and an ICE/generator pair connected to the battery to maintain its charge.

A vector controlled induction motor powered by a D.C. battery pack of 156 volts supplies the power at the drive wheels. In addition, there is an A.P.U. (auxiliary power unit) comprising of an ICE driving an induction generator. The A.P.U. supplies power to the battery when the demanded current by the induction motor exceeds a threshold value of 75 amperes. The functionality of the components is based on Hochgraf's work [21]. The local controller is responsible for the following tasks

- demanding a torque (positive or negative) from the induction motor depending on drive cycle requirements.

- for switching on/off the APU.

The torque demanded from the induction motor is positive during acceleration and cruise phases of the drive cycle (motoring mode) and is negative during the deceleration phase of the drive cycle (generator mode). During the motoring mode, current is drawn from the battery (discharging) and during generation mode current is supplied to the battery (charging).

When the APU is on, the ICE is running at its optimum speed and the induction generator supplies charges the battery; in the 'off' mode, the ICE idles. Thus the APU is responsible for decreasing the drain on the battery pack, especially during the acceleration phases of the drive cycle. The ICE control is based on a "constant throttle strategy" which was found to be optimum [21].

The system control strategy for a series hybrid is not required to be as complex as the controller for a parallel hybrid since there is only one torque provider. For the series design discussed in the paper, the classic proportional, integral, and derivative (PID) controller [22] is utilized.

A typical mid-sized family sedan was used as the basis for the vehicle. The vehicle's' components were sized to provide enough power to maintain a cruising speed of 120 km/h on a level road and acceptable acceleration performance of 0 to 100 km/h in 16 seconds for short time intervals. The vehicle was also designed to maintain highway speeds for an extended period of time and provide adequate performance on hills. The sizes of the components for the series hybrid drive train are stated below in Table 1.

TABLE 1
COMPONENTS OF SERIES HYBRID DRIVE TRAIN

ICE	1.2 liter, 40 kW
Motor	Vector controlled, 40 kW
Generator	Vector controlled, 40 kW
Battery	13, 12-volt, lead acid

Recalling fig. 12, the major components such as controller, power plant, and vehicle design must be designed. The propulsion motor must be sized to provide the desired performance and the generator, an ICE/generator pair in this study, to provide the required range for the drive cycle. The steps performed to design the series hybrid vehicle are stated below.

Step 1: Design the Power Plant. The induction motor is connected to the drive shaft of the vehicle. *The SS Model Induction Motor* and *Drive Shaft and Differential* models are dragged from the Library of Components. The *shaft speed*, *inertia* and *road*

speed are passed from the vehicle dynamics to plant and are connected to the *drive shaft and differential* model as shown below. The *drive shaft torque*, *inertia* and gear ratio are multiplexed to the vehicle dynamics model as shown below.

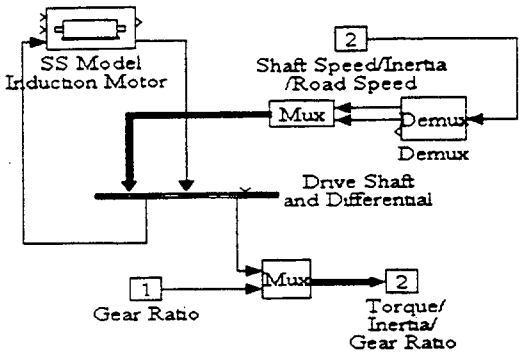

Step 2: Create the ICE/Generator pair connected to the battery. Drag a copy of the *ICE*, the *Horizon Battery*, *SS Induction Generator*, and *Coupling Shaft* from the library of components. The *ICE* and *induction generator* are connected to the *coupling shaft* and arranged as shown below. The *battery pack* and the *induction generator* are connected to the DC bus as shown below. The appropriate sizes for the *ICE*, *induction generator*, and *induction motor* are entered in the dialog box which appears by double-clicking on each model.

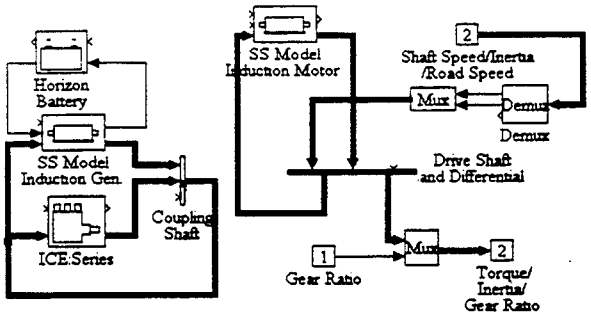

Step 3: Design the controller. The controller determines how the demanded torque of the vehicle is to be met by various devices in the power plant as discussed below. The torque which will be demanded from the Induction Motor and Induction Generator and the throttle angle of the ICE are calculated as stated below.

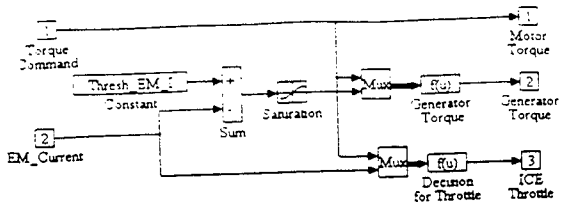

- Motor Torque

  The controller passes the entire torque command to the induction motor that is connected to the drive shaft. Since the induction motor drives the main shaft, it will always try to meet the torque demand of the vehicle.

- Generator Torque

  The torque demanded by the generator depends on the current demanded by the induction motor from the battery pack and the torque demanded by the vehicle. If the torque demanded by the vehicle is positive and the current demanded by the IM exceeds a threshold value, *Thresh_EM_I*, then the induction generator starts demanding a torque from the ICE to which it is coupled. If the demanded torque is negative then the generator cannot demand a torque from the ICE (this logic is embedded in the function block "Generator Torque"). However the torque demanded by the generator cannot exceed a threshold value, *Max_Gen_Trq*, otherwise it may stall the ICE to which it is coupled; this action is the function of the saturation block.

- ICE throttle

  The ICE is operated at a constant throttle strategy. Whenever the ***IM_current*** is greater than the threshold current, *Thresh_EM_I*, (which indirectly implies that the drain on battery is increasing) and the demanded torque is positive, the *ICE throttle* is set to 80 degrees otherwise it is set to 10 degrees. This logic is written in the function block called *Decision for Throttle*.

Step 4: The blocks are grouped into a single subsystem as shown above. The subsystem block is renamed to controller. A mask of the subsystem is built by entering the information as shown in the dialog box below. In the future, when one clicks on the controller subsystem, a dialog box pops up where the values of *Maximum Generator Torque* and *Threshold EM Current* can be entered.

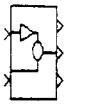

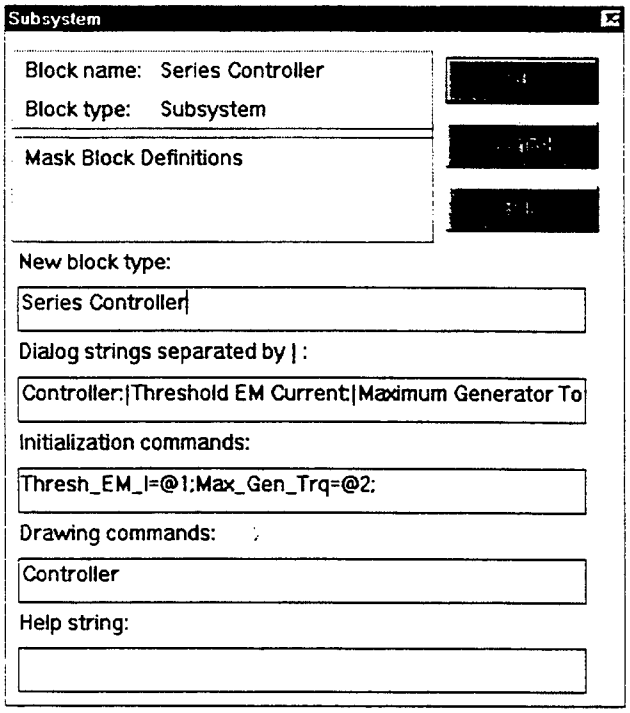

Step 5: The *ICE*, *induction generator*, *battery*, *induction motor* and *controller* are connected in the power plant as shown below. The *Clutch* and *Brake Torque* are multiplexed from the plant as shown.

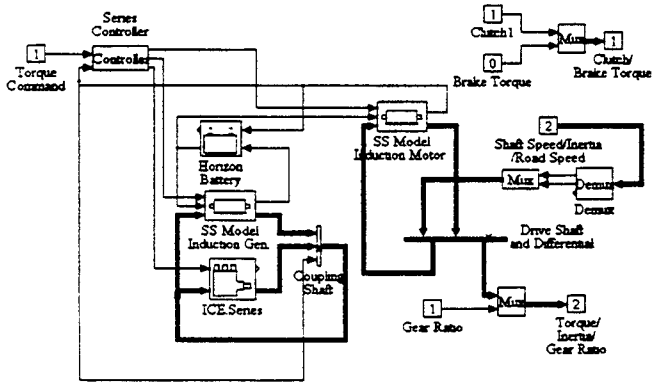

B. Analysis

The results of applying the federal highway and federal u ..n [23] drive cycles are illustrated and discussed below. Figs. 14 shows the federal highway drive cycle. Figs. 15-17 illustrate a few of the outputs generated during the simulation of the federal highway drive cycle applied to the series hybrid vehicle. Plots of the EM, ICE, and Generator torques are shown in Figs. 15 and 16. As can be seen in Fig. 15, the EM torque is relatively constant in the sections where there is a cruising speed demand in the highway drive cycle. Fig. 17 shows a summary of the components' performance. In particular, it gives the fuel consumption and emissions of the ICE engine and the change in the battery SoC resulting from the simulation.

Fig. 18 shows the urban drive cycle. Figs. 19-22 illustrate the application of the urban drive cycle to the series hybrid drive train. In fig. 19, the EM torque has many transients between 200 Nm and -200 Nm due to the many quick acceleration and deceleration demands of the urban drive cycle. In comparing fig. 16 and fig. 20, the generator is used more on the urban drive cycle than the highway drive cycle. This point is also illustrated by comparing the fuel consumption generated during the application of the highway drive cycle in fig. 21 of 21.89 km/l to the fuel consumption of 19.68 km/l generated during the application of the urban drive cycle.

Figs. 21 and 22 show that when the EM current goes above 75 amperes, the generator is used. One such case is seen at 250 seconds which occurs as a result of the steep acceleration in speed demanded in the urban drive cycle.

CONCLUSION

This paper discussed a new system-level modeling, simulation and analysis package developed at Texas A&M University using Matlab/Simulink to study issues related to electric vehicle (EV) and hybrid electric vehicle (HEV) design such as energy efficiency, fuel economy, and vehicle emissions. The package uses visual programming techniques, allowing the user to quickly change architectures, parameters, and to view output data graphically. It also includes detailed models of electric motors, internal combustion engines, and batteries.

The V-Elph package design and user features are discussed. Further the design process for a series hybrid drive train is stated. Simulation results from the application of federal highway and urban drive cycles to the series hybrid drive train are discussed. These results illustrate the flexibility of the package for studying various issues related to electric and hybrid electric vehicle design. The simulation package developed at Texas A&M University runs on PC and Unix-based workstations platforms.

ACKNOWLEDGMENTS

Support for this work was provided by the Texas Higher Education Coordinating Board Advanced Technology Program (ATP), the Office of the Vice President for Research and Associate Provost for Graduate Studies, through the Center for Energy and Mineral Resources, Texas A&M University, and the Texas Transportation Institute.

REFERENCES

[1] M. J. RIEZENMAN, "ELECTRIC VEHICLES," *IEEE SPECTRUM*, PP. 18-101, NOV. 1992.

[2] V. Wouk, "Hybrids: then and now," *IEEE Spectrum*, pp. 16-21, July 1995.

[3] A. Kalberlah, "Electric Hybrid Drive Systems for Passenger Cars and Taxis," *Tech. Rep. 910247, SAE*, 1991.

[4] B. Bates, "On the road with a Ford HEV," *IEEE Spectrum*, pp. 22-25, July 1995.

[5] M. Hayashida, and et al, "Study on Series Hybrid Electric Commuter-Car Concept," *SAE Journal SP-1243, Paper No. 970197*, Feb. 1997.

[6] A. Nikopoulos, H. Hong, and T. Krepec, "Energy Consumption Study for a Hybrid Electric Vehicle," *SAE Journal SP-1243, Paper No. 970198*, Feb. 1997.

[7] R.D. Senger, "Validation of ADVISOR as a Simulation Tool for a Series Hybrid Electric Vehicle using the Virginia Tech Future Car Lumina," Master's Thesis, Virginia Tech University, 1997.

[8] G. Cole, "Simple Electric Vehicle Simulation (SIMPLEV) v3.1," DOE Idaho National Engineering Laboratory.

[9] W.W. Marr and W.J. Walsh, "Life-cycle Cost Evaluations of Electric/Hybrid Vehicles," *Energy Conversion Management*, vol. 33:9, pp. 849-853, 1992.

[10] J.R. Bumby and et al, "Computer Modeling of the Automotive Energy Requirements for Internal Combustion Engine and Battery Electric-Powered Vehicles," *in Proceedings of IEE Pt. A*, vol. 132:5, pp. 265-79, 1985.

[11] K. B. Wipke and M. R. Cuddy, "Using an Advanced Vehicle Simulator (ADVISOR) to Guide Hybrid Vehicle Propulsion System Development," *http://www.heb.doe.gov*.

[12] D. Buntin, *Control System Design for a Parallel Hybrid Electric Vehicle*, Master's thesis, Texas A&M University, College Station, Texas, 1994.

[13] M. Ehsani, K.M. Rahman, and H.A. Toliyat, "Propulsion System Design of Electric and Hybrid Vehicles," *IEEE Transactions on Industrial Electronics*, vol. 44, Feb. 1997, pp. 19-27.

[14] H. A. Toliyat, K. M. Rahman, and M. Ehsani, "Electric Machine in Electric and Hybrid Vehicle Application," *Proceeding of ICPE ' 95*, Seoul, pp. 627-635.

[15] M. Ehsani, *Electrically Peaking Hybrid System and Method*, U.S. Patent granted in 1996.

[16] J. Howze, M. Ehsani, and D. Buntin, *Optimizing Torque Controller for a Parallel Hybrid Electric Vehicle*, U.S. Patent granted in 1996.

[17] *Proceedings of the ELPH Conference*, Texas A&M University, College Station, Texas, October 1994.

[18] K. M. Stevens, *A Versatile Computer Model for the Design and Analysis of Electric and Hybrid Drive Trains*, Master's thesis, Texas A&M University, College Station, Texas, 1994.

[19] K. L. Butler, K. M. Stevens, and M. Ehsani, "A Versatile Computer Simulation Tool for Design and Analysis of Electric and Hybrid Drive Trains," 1997 SAE Proceedings *Electric and Hybrid Vehicle Design Studies,* Book # SP 1243, Paper # 970199. pp. 19-25, February 1997, Detroit, MI.

[20] *Matlab/Simulink*, Version 4.2c.1/1.3c, The Mathworks Inc., Natick, Mass.

[21] C. G. Hochgraf, M.J. Ryan, and H.L. Wiegman, "Engine Control Strategy for a Series Hybrid Electric Vehicle Incorporating Load-Leveling and Computer Controlled Energy Management," *SAE Journal SAE/SP-96/1156*, p. 11-24.

[22] G. Franklin, J. D. Powell, and M. Workman, *Digital Control of Dynamic Systems*, pp. 222-229, 1990, Addison-Wesley.

[23] U. Adler, ed., *Automotive Handbook*, Stuttgart, Germany: Robert Bosch GmbH, 2 ed., 1986.

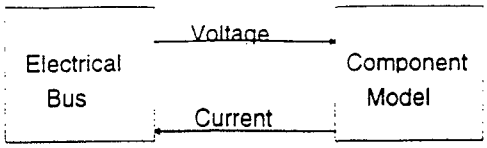

Fig. 1 Electrical Bus

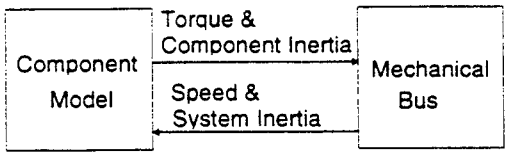

Fig. 2 Mechanical Bus

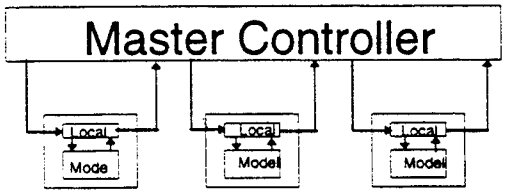

Fig. 3 Master/Control Paradigm

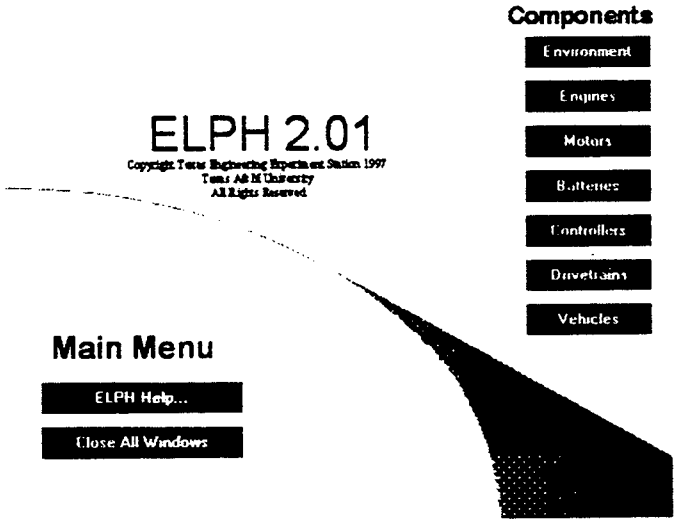

Fig. 4 Main Menu

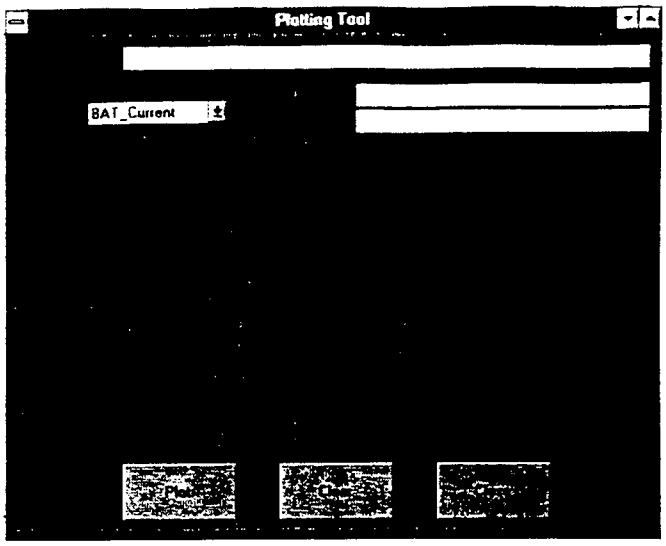

Fig. 5 Plotting Tool

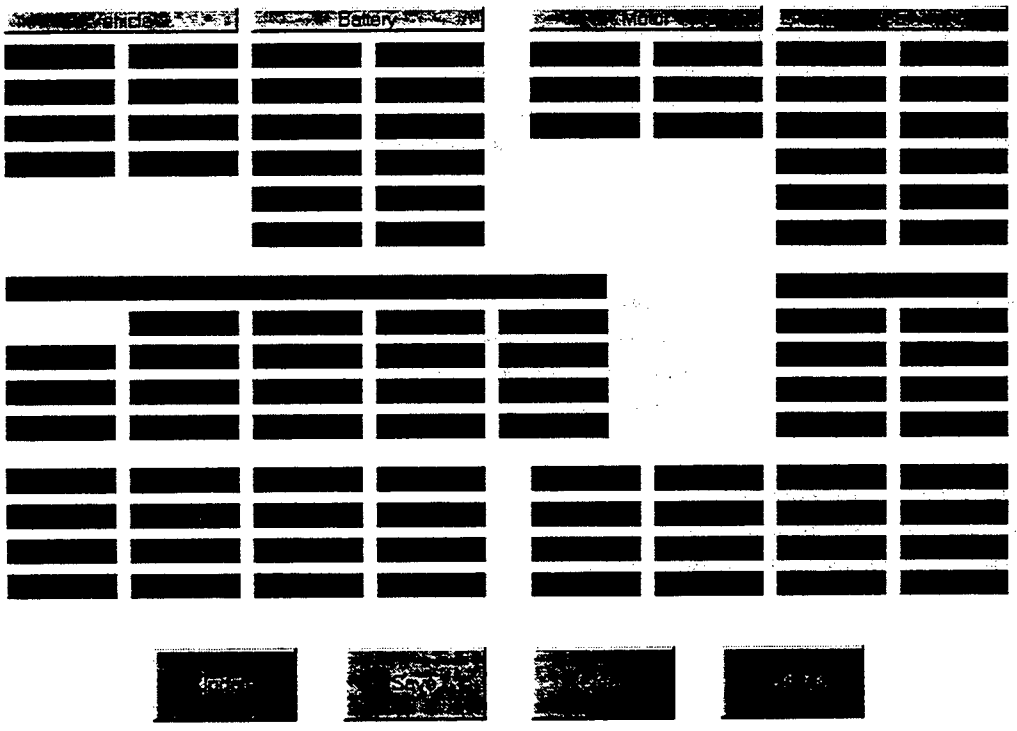

Fig. 6 Data Summary Tool

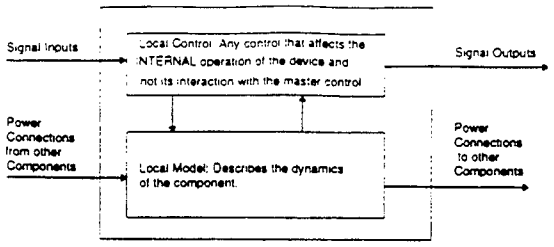

Fig. 7 Data flow through a component model

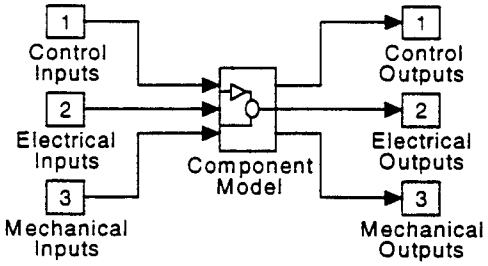

Fig. 8 General Input / Output Interface for a Component Model

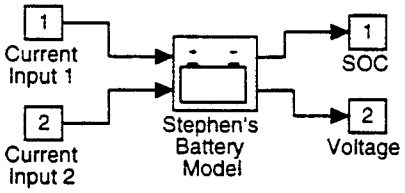

Fig. 9 Interface for a Battery Model

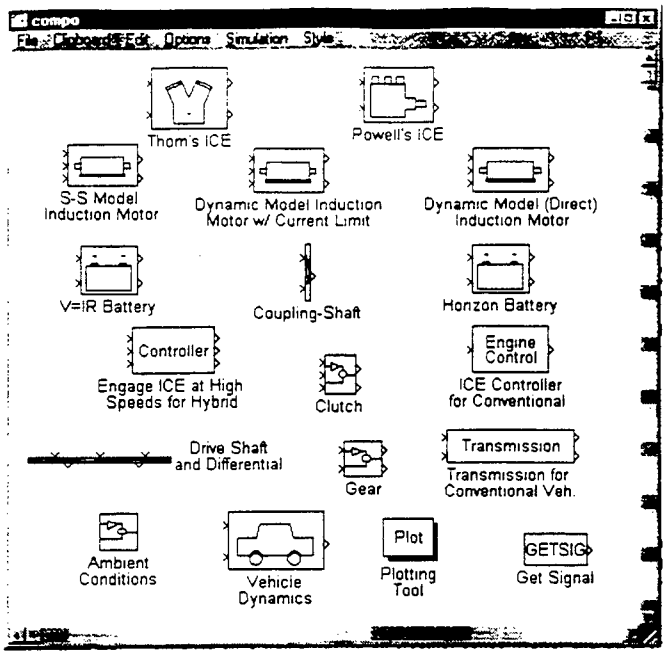

Fig 10. Library of Components

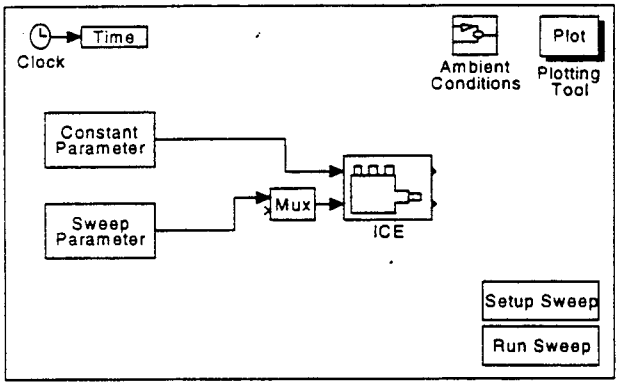

Fig. 11 Parameter sweep workbench

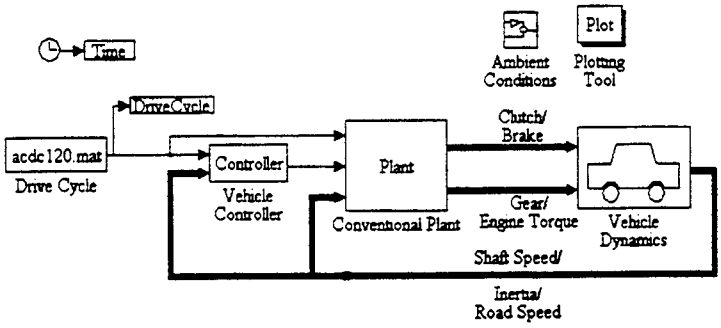

Fig. 12. System level representation of a general vehicle drive train in V-Elph

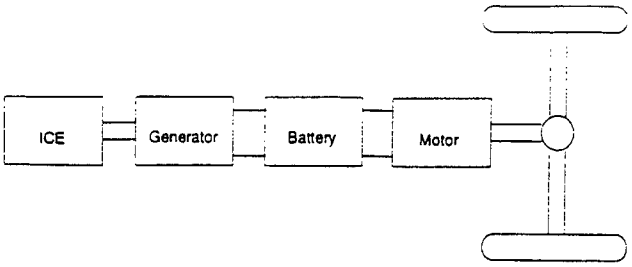

Fig. 13 Series Hybrid Drive Train

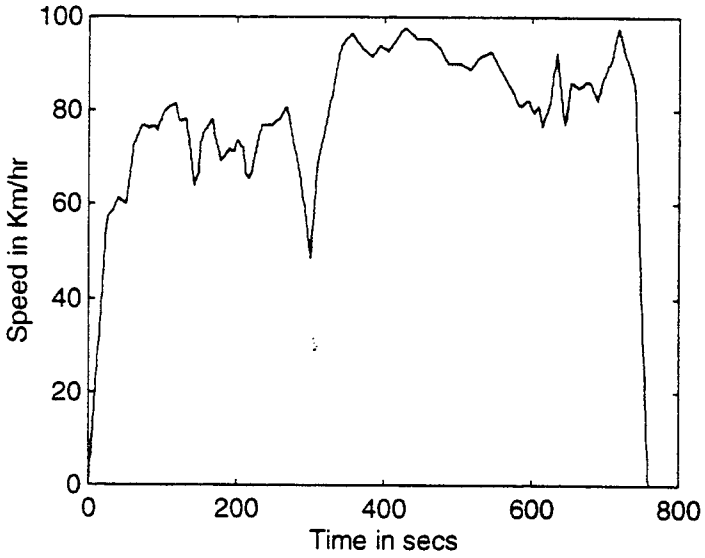

Fig. 14 Federal highway drive cycle

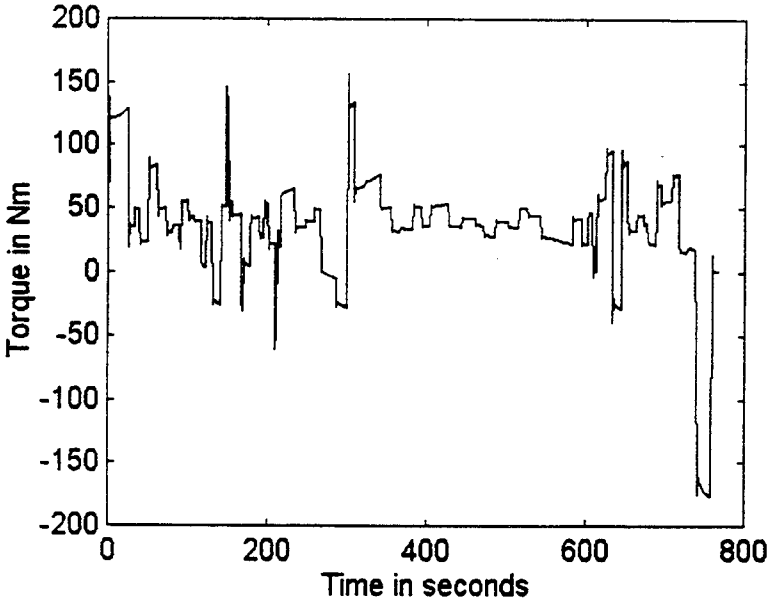

Fig. 15. EM torque for FTP highway applied to series HEV

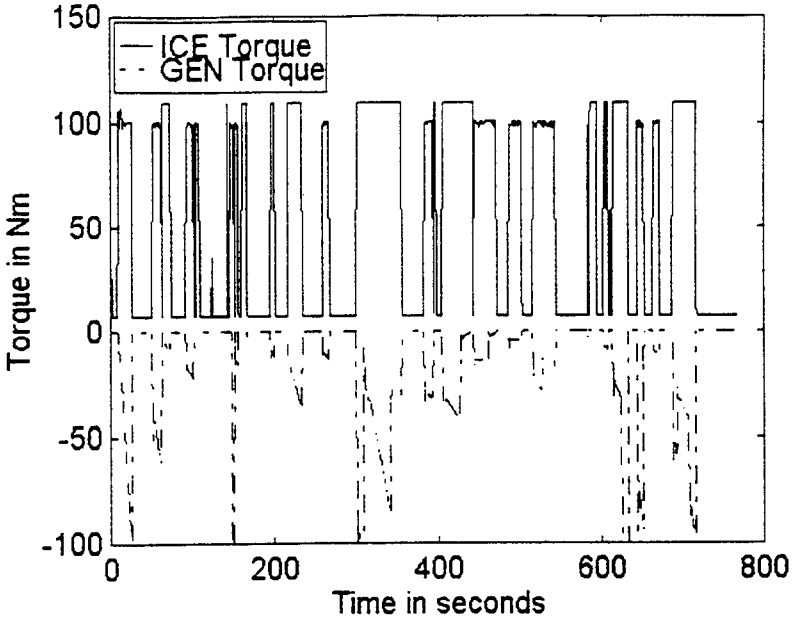

Fig. 16. ICE and generator torques for FTP highway applied to series HEV

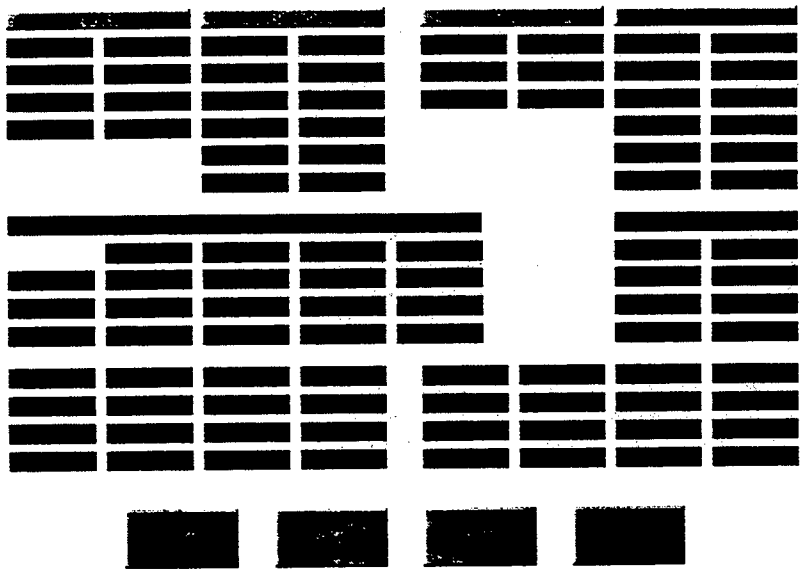

Fig. 17. Data summary for FTP highway applied to series HEV

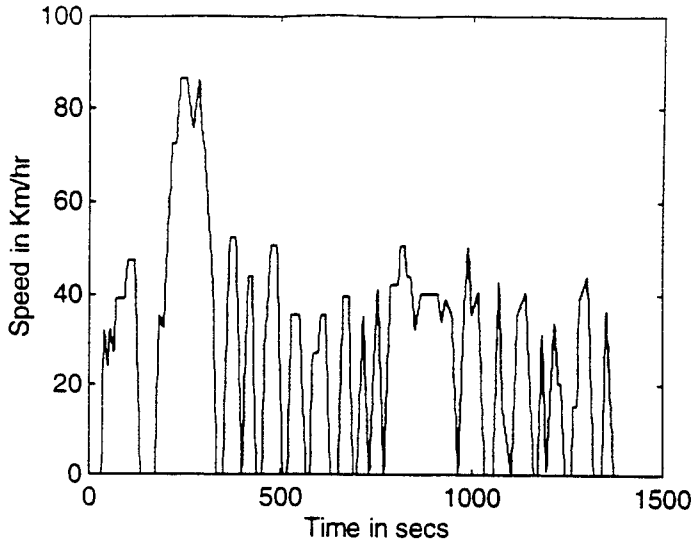

Fig. 18 FTP-75 Urban drive cycle

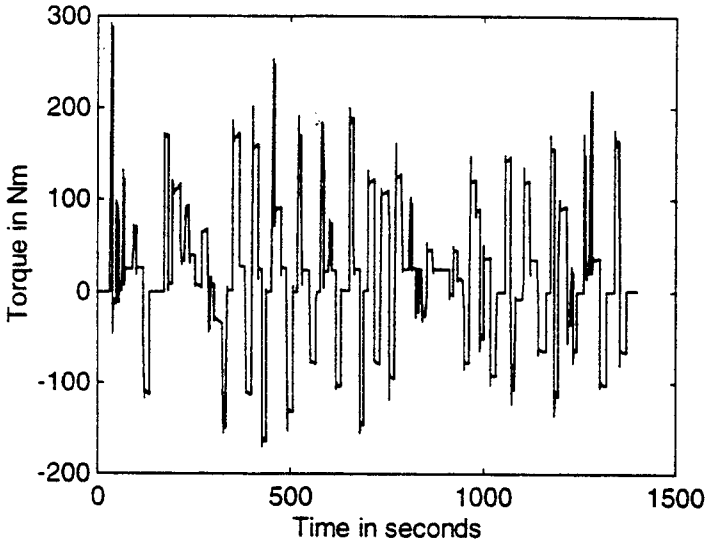

Fig. 19. EM torque for urban drive cycle applied to series HEV

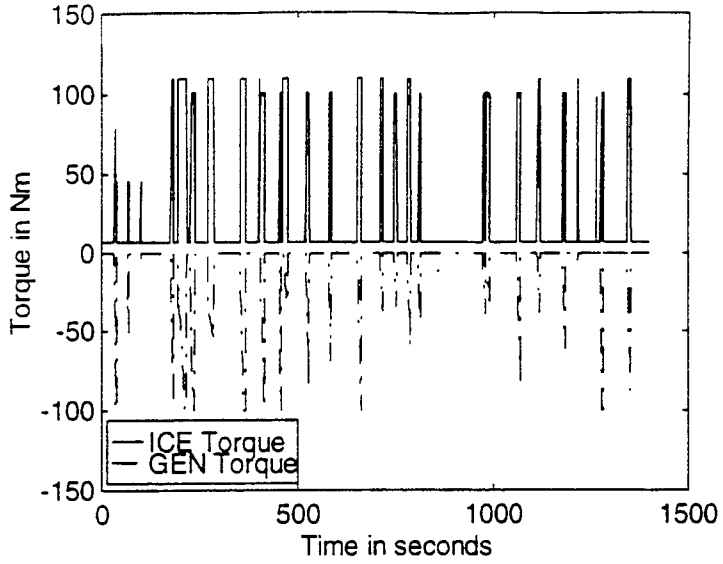

Fig. 20. ICE and generator torque for urban drive cycle applied to series HEV

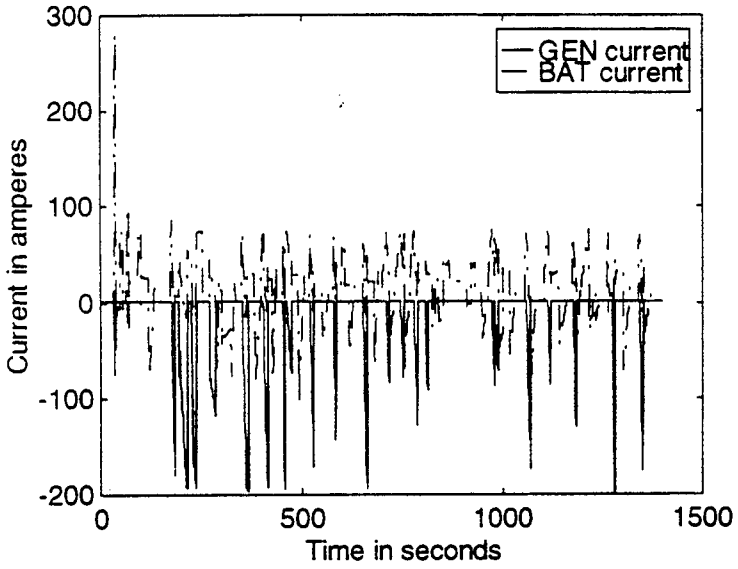

Fig. 21 Generator and battery current for urban drivecycle applied to series HEV

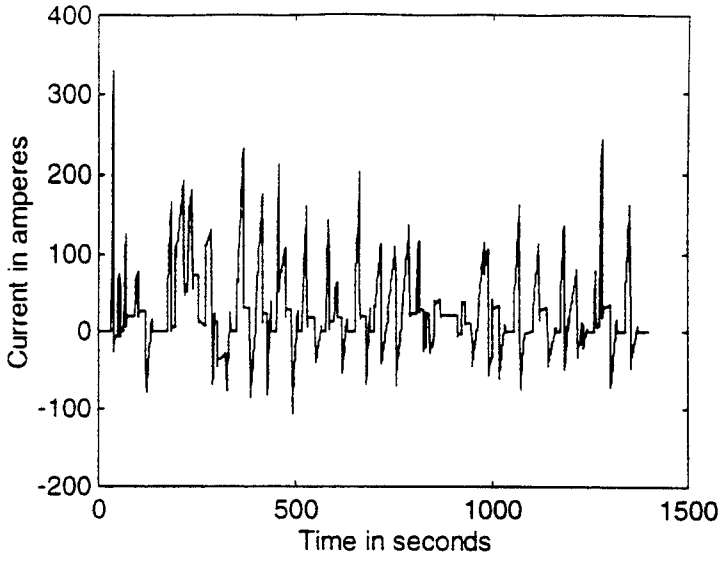

Fig. 22 EM current for urban drivecycle applied to series HEV

Propulsion System Design of Electric and Hybrid Vehicles

Mehrdad Ehsani, *Fellow, IEEE*, Khwaja M. Rahman, *Student Member, IEEE*, and Hamid A. Toliyat, *Member, IEEE*

Abstract—**There is a growing interest in electric and hybrid-electric vehicles due to environmental concerns. Recent efforts are directed toward developing an improved propulsion system for electric and hybrid-electric vehicles applications. This paper is aimed at developing the system design philosophies of electric and hybrid vehicle propulsion systems. The vehicles' dynamics are studied in an attempt to find an optimal torque-speed profile for the electric propulsion system. This study reveals that the vehicles' operational constraints, such as initial acceleration and grade, can be met with minimum power rating if the power train can be operated mostly in the constant power region. Several examples are presented to demonstrate the importance of the constant power operation. Operation of several candidate motors in the constant power region are also examined. Their behaviors are compared and conclusions are made.**

Index Terms—**Electric vehicle, hybrid electric vehicle, motor drives, road vehicle electric propulsion, road vehicle propulsion.**

I. Introduction

THE CONCEPT of the electric vehicle (EV) was conceived in the middle of the previous century. After the introduction of the internal combustion engine (ICE), EV's remained in existence side by side with the ICE for several years. The energy density of gasoline is far more than what the electrochemical battery could offer. Despite this fact, the EV continued to exist, especially in urban areas due to its self-starting capability. However, soon after the introduction of the electric starter for ICE's early this century, despite being energy-efficient and nonpolluting, the EV lost the battle completely to the ICE due to its limited range and inferior performance. Since then, the ICE has evolved, improved in design, and received widespread acceptance and respect. Although this essentially is the case, EV interest never perished completely and whenever there has been any crisis regarding the operation of ICE automobiles, we have seen a renewed interest in the EV. The early air quality concerns in the 1960's and the energy crisis in the 1970's have brought EV's back to the street again. However, the most recent environmental awareness and energy concerns have imposed, for the first time since its introduction, a serious threat to the use of ICE automobiles.

The ICE automobile at the present is a major source of urban pollution. According to figures released by the U.S. Environmental Protection Agency (EPA), conventional ICE vehicles currently contribute 40%–50% of ozone, 80%–90% of carbon monoxide, and 50%–60% of air toxins found in urban areas [1]. Besides air pollution, the other main objection regarding ICE automobiles is their extremely low efficiency use of fossil fuel. Hence, the problem associated with ICE automobiles is threefold: environmental, economical, as well as political. These concerns have forced governments all over the world to consider alternative vehicle concepts. The California Air Resource Board (CARB) is among the few that acted first through the declaration of the Clear Air Act of September 1990. This act requires that 52% of all vehicles sold in that state be either low-emission vehicles (LEV's)—48%, ultralow-emission vehicles (ULEV's)—2%, or zero-emission vehicles (ZEV's)—2%, by 1998 [2]. Similar measures are being considered in other states and nations as well.

EV's and hybrid-electric vehicles (HEV's) offer the most promising solutions to reduce vehicular emissions. EV's constitute the only commonly known group of automobiles that qualify as ZEV's. These vehicles use an electric motor for propulsion and batteries as electrical-energy storage devices. Although there have been significant advancements in motors, power electronics, microelectronics, and microprocessor control of motor drives, the advancement in battery technology has been relatively sluggish. Hence, the handicap of short range associated with EV's still remains. Given these technology limitations, the HEV seems to be the viable alternative to the ICE automobile at the present. HEV's qualify as ULEV's and do not suffer from the range limitations imposed by EV's. These vehicles combine more than one energy source to propel the automobile. In heat engine/battery hybrid systems, the mechanical power available from the heat engine is combined with the electrical energy stored in a battery to propel the vehicle. These systems also require an electric drivetrain to convert electrical energy into mechanical energy, just like the EV. Hybrid-electric systems can be broadly classified as series or parallel hybrid systems [3].

In series hybrid systems, all the torque required to propel the vehicle is provided by an electric motor. On the other hand, in parallel hybrid systems the torque obtained from the heat engine is mechanically coupled to the torque produced by an electric motor [3]. In the EV, the electric motor behaves exactly in the same manner as in a series hybrid. Therefore, the torque and power requirements of the electric motor are roughly equal for an EV and series hybrid, while they are lower for a parallel hybrid.

Manuscript received February 26, 1996; revised April 17, 1996.

The authors are with the Texas Applied Power Electronics Center, Department of Electrical Engineering, Texas A&M University, College Station, TX 77843-3128 USA.

Publisher Item Identifier S 0278-0046(97)00069-5.

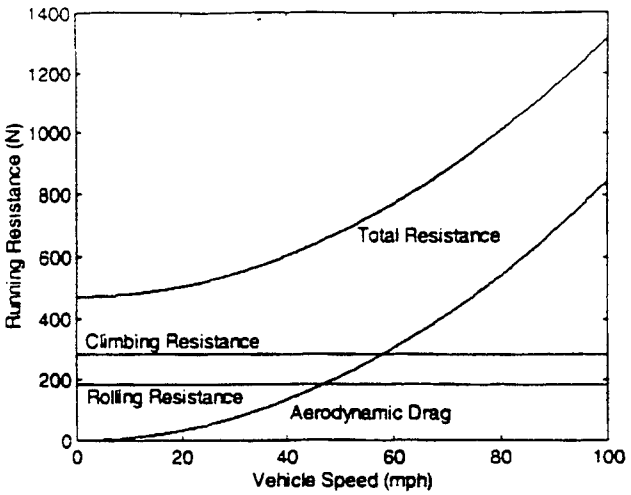

Fig. 1. Typical road load characteristics as a function of vehicle speed.

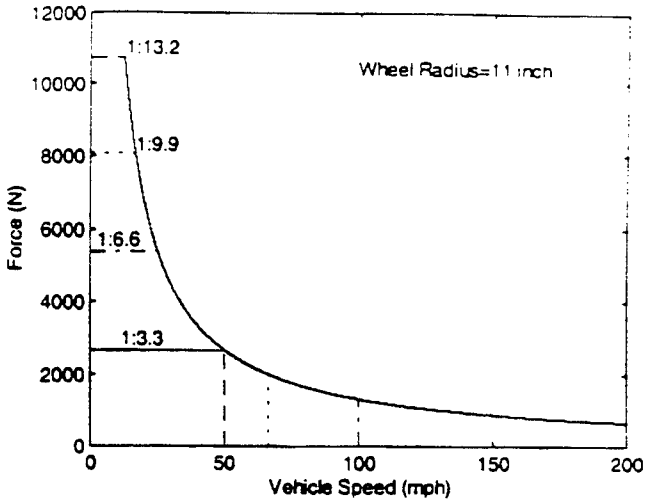

Fig. 2. Torque-speed diagram of an electrical motor in terms of tractive force and vehicular speed with gear size as the parameter.

These assumptions will be used in the analysis presented in the following sections, unless otherwise specified. These assumptions do not change the general trend of the solution and can be easily relaxed.

The motive force F available from the propulsion system is partially consumed in overcoming the road load, F_W. The net force, $F - F_W$, accelerates the vehicle (or decelerates when F_W exceeds F). The acceleration is given by

$$a = \frac{F - F_W}{k_m \cdot m} \tag{5}$$

where k_m is the rotational inertia coefficient to compensate for the apparent increase in the vehicle's mass due to the onboard rotating mass.

III. EV System Design

The main component of the EV drivetrain is its electric motor. The electric motor in its normal mode of operation can provide constant-rated torque up to its base or rated speed. At this speed, the motor reaches its rated power limit. The operation beyond the base speed up to the maximum speed is limited to this constant power region. The range of the constant power operation depends primarily on the particular motor type and its control strategy. However, some electric motors digress from the constant power operation, beyond certain speed, and enter the natural mode before reaching the maximum speed. The maximum available torque in the natural mode of operation decreases inversely with the square of the speed. This range of operation is neglected in the analysis presented in this section, unless otherwise specified. It is assumed that the electric motor operates in the constant power region beyond the base speed and up to the maximum speed. Nevertheless, for some extremely high-speed motors the natural mode of operation is an appreciable part of its total torque-speed profile. Inclusion of this natural mode for such motors may result in a reduction of the total power requirement. Of course, power electronic controls allow the motor to operate at any point in the torque-speed plane, below the envelope defined by the mentioned limits. However, it is the profile of this envelope that is important in the motor drive selection and design.

In order to free up the motor speed from the vehicle speed, for design optimization, gearing between the motor shaft and the drive shaft is required. In our design, we will make the following assumptions.

1) Single gear ratio transmission operation—power electronic control allows instantaneous matching of the available motor torque with the required vehicle torque, at any speed; therefore, multiple gearing in order to match the motor torque-speed to the vehicle torque-speed is no longer a necessity;
2) Ideal loss free gear—without loss of generality, the gear losses can be incorporated at the end of analysis.

The gear ratio and size will depend on the maximum motor speed, maximum vehicle speed, and the wheel radius. Higher maximum motor speed, relative to vehicle speed, means a higher gear ratio and a larger gear size. The selection criterion for the maximum motor speed will be further discussed later. The torque-speed diagram of a typical motor is drawn in Fig. 2, but in terms of tractive force and vehicular speed for different gear ratios. Notice the electric motor base speed and maximum speed, in terms of the vehicle speed, depend on the gear ratio. A design methodology based on the three regions of operation will now be presented.

A. Initial Acceleration

The force-velocity profile of a typical motor is redrawn in Fig. 3. In this figure, v_{rm} is the electric motor rated speed, v_{rv} is the vehicle rated speed, and $v_{\max}$ is the vehicle maximum speed. The motor maximum speed must correspond to this $v_{\max}$, after the gear ratio transformation. The figure also shows (the dashed curve) the force-velocity profile of the motor in the natural mode. This mode of operation, however, is neglected unless otherwise specified.

The range of operation for initial acceleration is 0–v_{rv}. For now, we will focus our attention only on this interval. For

aerodynamic drag coefficient C_H, etc. The resulting equation can be solved numerically for P_m for a specific motor rated velocity v_{rm}, using any standard root-seeking method such as the secant method [5].

Let us assume that it is desired to obtain P_m for the following case:

- 0–26.82 m/s (0–60 mi/h) in 10 s;
- vehicle mass of 1450 kg;
- rolling resistance coefficient of 0.013;
- aerodynamic drag coefficient of 0.29;
- wheel radius of 0.2794 m (11 in);
- level ground;
- zero head-wind velocity.

A plot of the resulting motor rated power versus motor rated speed, in terms of vehicle speed, is shown in Fig. 4 (the dashed curve).

Examination of Fig. 4 (the dashed curve) results in the following conclusions:

1) rated power versus v_{rm} curve shows the same general trend of the resistanceless case;
2) rated motor power requirement is minimum for continuous constant power operation $v_{rm} = 0$;
3) rated motor power is roughly twice that of continuous constant power operation for constant force (torque) operation $v_{rv} = v_{rm}$;
4) rated motor power remains close to its minimum up to about 20 mi/h of rated motor speed and then grows rapidly.

B. Cruising at Rated Vehicle Velocity

A power train capable of accelerating the vehicle to the rated velocity, v_{rv}, will always have sufficient cruising power at this speed. Hence, the constraint of cruising at rated vehicle speed is automatically met for the case of the EV. Of course, cruising range is another issue related to the battery design which is outside the scope of this paper. However, minimizing the power of the drive will help the battery size.

C. Cruising at Maximum Vehicle Velocity

The power requirement to cruise at maximum vehicle speed can be obtained as

$$P_{v\max} = (f_{ro} + f_{st}) \cdot v_{\max} + f_l(v) \cdot v_{\max}. \qquad (10)$$

Since aerodynamic drag dominates at high speeds, this power requirement increases with the cube of maximum vehicle velocity. If this vehicle power requirement is greater than the motor power calculated previously ($P_{v\max} > P_m$), then $P_{v\max}$ will define the motor power rating. However, in general, P_m will dominate $P_{v\max}$, since modern vehicles are required to exhibit a high-acceleration performance. As mentioned before, some extremely high-speed motors usually have three distinct modes of operation. The initial constant torque operation, followed by a range of constant power operation, then to the maximum speed in natural mode (see Fig. 3). For such a motor it may be advantageous to use the entire constant power range for initial acceleration of the vehicle. The operation beyond that would be in the natural mode. This would allow a longer constant power operation in the initial acceleration. Consequently, the motor power requirement will be lower. This scheme will work provided the motor has adequate torque in natural mode to meet the constraints at the maximum vehicle speed. Otherwise, some part of the constant power operation has to be used for the vehicle operation beyond the rated vehicle speed.

TABLE I
EV POWER REQUIREMENT AS A FUNCTION OF CONSTANT POWER RANGE

	Extended Constant HP Speed Range					
	1:1	1:2	1:3	1:4	1:5	1:6
Motor Rated Power (KW)	110	95	74	67	64	62

Natural mode of motor operation is not the preferred mode beyond the rated vehicle speed. Unfortunately, no control algorithm presently exists to operate some high-speed motors entirely in constant power beyond their base speed. However, the natural mode, if included, can lower the overall power requirement. The speed at which the electric motor can enter the natural mode and still meet the power requirement at maximum vehicle speed is obtained from

$$v_n = v_{\max}\sqrt{\frac{P_{v\max}}{P_m}}. \qquad (11)$$

Note that the initial acceleration power is also a function of v_n (extended constant power range). Hence, v_n and P_m have to be solved iteratively. Also, the gear ratio between the drive shaft and the motor shaft is to be determined by matching v_n with the motor speed at which it enters the natural mode. More discussion about the natural mode of operation appears in Section VI. The rest of the analysis is done assuming constant power operation beyond the base speed up to the maximum speed.

The importance of extending the constant power speed range can be better understood by comparing the required motor power for different constant power speed ranges (as a multiple of its base speed). Table I shows an example of power requirement for several constant power ranges for the following case:

1) maximum motor speed is 10 000 r/m;
2) maximum vehicle speed is 44.7 m/s (100 mi/h);
3) other system variables and constants are the same as the previous example.

Here, the required gear ratio to match the maximum motor speed to the maximum vehicle speed for a wheel radius of 0.2794 m (11 in) is 1:6.55. The results of Table I suggest an extended range of 4–6 times the base motor speed in order to significantly lower the motor power requirement.

Finally, we examine the effect of maximum motor speed and the extended constant power range on the overall system performance. In the context of EV/HEV design, we classify motors with maximum speeds of less than 6000 r/m as low-speed motors, those with speeds of 6000–10 000 r/m as medium-speed motors, and those with speeds of 10 000 r/m

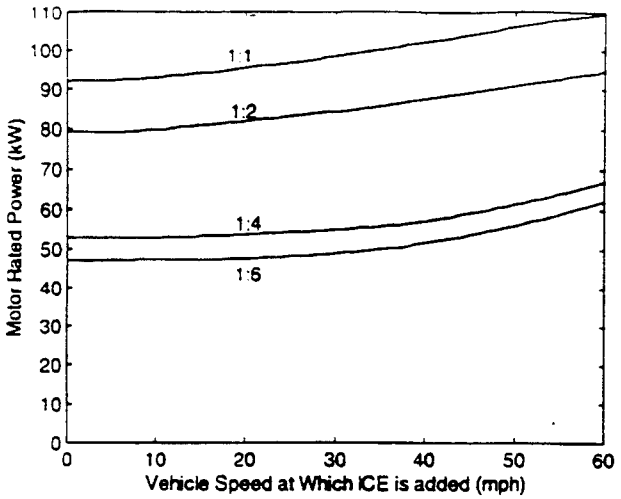

Fig. 8. Acceleration power requirement as a function of vehicle speed at which ICE is added.

example of the road load characteristics on a 3% grade, with other constants remaining the same as before. The figure also shows a series of force-velocity curves of the ICE (the throttle wide open) with the piston displacement as the variable. The correct ICE size can be determined from the intersection of the road load curve with the ICE force-velocity profile at rated velocity, plus allowing a 10% margin for the batterypack recharging. The exact amount of margin needed is the subject of a more complicated analysis involving vehicle driving cycles, battery size, charge/discharge characteristics, etc.

B. Initial Acceleration

The rated power to be delivered by the electric motor is reduced in the case of the parallel HEV due to the mechanical power available from the ICE. An example of the effect of ICE torque blending on the rated power requirement of the electric motor during initial acceleration is shown in Fig. 8. The figure shows four different extended speed range operations of the electric motor. The abscissa is the vehicle speed at which the ICE torque is added. In all of the four cases, the ICE with its low starting torque contributes little up to about the vehicle speed of 20 mi/h. Therefore, this low-speed and low-efficiency operation of the ICE may be avoided without significantly increasing the electric motor power requirement. It is important to note that an extended constant power operation of the electric motor is still a necessity to keep the power requirement low (Fig. 8).

C. Cruising at Maximum Velocity

At maximum vehicle velocity the power requirement is $F_W \cdot v_{max}$. This power is supplied by a combination of the ICE and the electric motor. Once the ICE size is determined, the required electric motor power can be uniquely identified. As mentioned before, this power, in general, would be less than the power requirement for the initial acceleration.

TABLE II
MOTOR DATA

	Rated Speed (rpm)	Maximum Speed (rpm)	Constant Power Range	Power Factor
Induction	1750	8750	1:5	0.82
BLDC	4000	9000	1:2.25	0.93
SRM	4000	20000	1:3 Rest in Natural Mode	0.6

TABLE III
RATED POWER AND CONVERTER VA REQUIREMENTS FOR THE MOTORS OF TABLE II FOR A TYPICAL EV APPLICATION

	Gear Ratio	Power Rating (kW)	Converter Rating (kVA)
Induction	5.7	65	79
BLDC	5.9	86	92
SRM	13	68	113

V. ELECTRIC PROPULSION SYSTEMS FOR EV AND HEV DESIGN

An electric propulsion system is comprised of three main elements: power electronic converter, motor, and its controller. This section is devoted to examining several of the most commonly used motors and their control for EV and HEV propulsion. The importance of extended speed range under motor constant power operation in an EV and HEV was established in the previous sections. This mode of operation is referred to as field weakening, from its origins in dc motor drives. A detailed study of several commonly used motors for EV and HEV propulsion application is presented in [7]. In this section, we present a design example of several motors for the constant power operation. This example will help clarify the capabilities of these motors for vehicle applications.

EV Data:

- vehicle rated speed of 26.82 m/s (60 mi/h);
- required acceleration of 26.82 m/s in 10 s;
- vehicle maximum speed of 44.7 m/s (100 mi/h);
- vehicle mass of 1450 kg;
- rolling resistance coefficient of 0.013;
- aerodynamic drag coefficient of 0.29;
- frontal area of 2.13 m^2;
- wheel radius of 0.2794 m (11 in);
- level ground;
- zero head wind.

The motor data are shown in Table II. The motor data chosen are for the commercially available samples of these motors. Clearly, more specific motors can be designed for vehicle applications, but such data were not available for this paper. Based on the vehicle data, the power requirement to cruise at the maximum speed is 41 kW. The motor power for acceleration and converter volt–ampere (VA) requirement for each motor are shown in Table III.

The extended constant power range available from the induction motor clearly makes it highly favorable for vehicle

TABLE V
COMPARISON OF ELPH PROTOTYPE AND OUR DESIGNED HEV

ELPH Prototype				Our Designed HEV			
Rated Motor Power (kW)	Rated Motor Torque (N-m)	Gear Ratio	Rated Drive Shaft Torque (ICE+ Motor) (N-m)	Rated Motor Power (kW)	Rated Motor Torque (N-m)	Gear Ratio	Rated Drive Shaft Torque (ICE+ Motor) (N-m)
30	136	-	-	50	136	11.45	1733

ELPH prototype is not possible. However, the rated power of the designed HEV matches the actual peak power delivered by the ELPH prototype in the test run (Fig. 9).

Detailed experimental design and evaluation of various motor drives for EV and HEV applications is presently under way on the Stationary Test Bed Laboratory of the Texas Applied Power Electronics Center, Texas A&M University.

VII. CONCLUSIONS

A design methodology for EV and HEV propulsion systems is presented based on the vehicle dynamics. This methodology is aimed at finding the optimal torque-speed profile for the electric power train. The design is to meet the operational constraints with minimum power requirement. The study reveals that the extended constant power operation is important for both the initial acceleration and cruising intervals of operation. The more the motor can operate in constant power, the less the acceleration power requirement will be.

Several types of motors are studied in this context. It is concluded that the induction motor has clear advantages for the EV and HEV at the present. A brushless dc motor must be capable of high speeds to be competitive with the induction motor. The switched reluctance motor may be superior to both of these motors for vehicle application both in size and cost. However, more design and evaluation data is needed to verify this possibility.

The design methodology of this paper was applied to an actual EV and HEV to demonstrate its benefits. Clearly, the detailed design of a vehicle propulsion system is more complicated than in our examples. However, this methodology can serve as the foundation of the detailed design.

REFERENCES

[1] A. Alison, "Searching for perfect fuel . . . in the clean air act," in *Proc. Environ. Veh. Conf.*, Dearborn, MI, 1994, pp. 61–87.

[2] S. Barsony, "Infrastructure needs for EV and HEV," in *NIST Workshop Advanced Components for Electric Hybrid and Electric Veh.*, Gaithersburg, MD, 1993, pp. 14–23.

[3] A. F. Burke, "Hybrid/electric vehicle design options and evaluations," SAE Paper #920447, Feb. 1992.

[4] *Automotive Handbook*. Germany: Robert Bosch Gmbh, 1986.

[5] A. Ralston and P. Rabinowitz, *A First Course in Numerical Analysis*, 2nd ed. New York: McGraw-Hill, 1978.

[6] A. G. Erdman and G. N. Sandor, *Mechanism Design: Analysis and Synthesis, Vol. I*. Englewood Cliffs, NJ: Prentice-Hall, 1984.

[7] H. A. Toliyat, K. M. Rahman, and M. Ehsani, "Electric machines in electric and hybrid vehicle applications," in *Proc. 1995 Int. Conf. Power Electronics*, Seoul, Korea.

Mehrdad Ehsani (S'73–M'75–SM'82–F'96) received the Ph.D. degree in electrical engineering from the University of Wisconsin-Madison, in 1981.

Since 1981, he has been at Texas A&M University, College Station, TX, where he is currently a Professor of electrical engineering and Director of Texas Applied Power Electronics Center (TAPC). He is the author of more than 100 publications concerning pulsed-power supplies, high-voltage engineering, power electronics, and motor drives. He is the co-author of a book on converter circuits for superconductive magnetic energy storage and a contributor to an IEEE guide for self-commutated converters, as well as other monographs. He holds seven U.S. patents. His current research work is in the areas of power electronics, motor drives, and hybrid vehicles and their control systems.

Dr. Ehsani has been a member of the IEEE Power Electronics Society AdCom, past Chairman of the PELS Educational Affairs Committee, past Chairman of the IEEE-IAS Industrial Power Converter Committee, and past Chairman of the IEEE Myron Zucker Student–Faculty Grant program. He was the General Chair of the 1990 IEEE Power Electronics Specialist Conference and is an IEEE Industrial Electronics Society Distinguished Speaker. He was the recipient of the Prize Paper Award in static power converters and motor drives at the IEEE Industry Applications Society Annual Meetings in 1985, 1987, and 1992. In 1984, he was named the Outstanding Engineer of the Year by the Brazos chapter of the Texas Society of Professional Engineers. In 1992, he was named the Halliburton Professor in the College of Engineering at Texas A&M University. In 1994, he was also named the Dresser Industries Professor at the same college. He is a Registered Professional Engineer in the State of Texas.

Khwaja M. Rahman (S'94) received the B.Sc. degree from Bangladesh Engineering University, Dhaka, Bangladesh, and the M.S. degree from Texas A&M University, College Station, TX, both in electrical engineering, in 1987 and 1992, respectively. He is currently working toward the Ph.D. degree at Texas A&M University..

From 1987 to 1990, he was with the Electrical Engineering Department of Bangladesh Engineering University as a Lecturer. His research interests include adjustable speed drives, electric and hybrid-electric propulsion systems, and microcomputer control of drives.

Mr. Rahman is a member of Phi Kappa Phi.

Hamid A. Toliyat (S'87–M'91) received the B.S. degree from Sharif University of Technology, Tehran, Iran, in 1982, the M.S. degree from West Virginia University, Morgantown, WV, in 1986, and the Ph.D. degree from the University of Wisconsin-Madison, in 1991, all in electrical engineering.

Between 1982 and 1984, he worked for power companies in Iran. In 1991, he joined the faculty of Ferdowsi University of Mashhad, Mashhad, Iran, as an Assistant Professor of electrical engineering. In March 19[illegible] he joined the Department of Electrical Engineering, Texas A&M University, College Station, TX, in the same capacity. His main research interests and experience include variable speed drives, analysis and design of electrical machines, fault diagnosis of electric machines, electric and hybrid vehicle traction systems, and power systems and control. He is actively involved in presenting short courses in his area of expertise to various corporations, including General Motors, Texas Instruments, LeTourneau, etc.

Dr. Toliyat is a member of the IEEE Industrial Applications, Industrial Electronics, Power Electronics, and Power Engineering Societies. He also serves on several IEEE Committees and Subcommittees. He is a member of Sigma Xi.

970199

A Versatile Computer Simulation Tool for Design and Analysis of Electric and Hybrid Drive Trains

K. L. Butler, K. M. Stevens, and M. Ehsani
Texas A&M Univ.

ABSTRACT

This paper discusses a new computer simulation tool, V-Elph, which extends the capabilities of previous modeling and simulation efforts by facilitating in-depth studies of any type of hybrid or all electric configuration or energy management strategy through visual programming and by creating components as hierarchical subsystems which can be used interchangeably as embedded systems. V-Elph is composed of detailed models of four major types of components: electric motors, internal combustion engines, batteries, and vehicle dynamics which can be integrated to simulate drive trains having all electric, series hybrid, and parallel hybrid configurations. V-Elph was written in the Matlab/Simulink graphical simulation language and is portable to most computer platforms.

A simulation study of a sustainable, electrically-peaking hybrid-electric vehicle was performed to illustrate the applicability of V-Elph to hybrid and electric vehicle design.

INTRODUCTION

Presently, only electric and low-emissions hybrid vehicles can meet the criteria outlined in the California Air Regulatory Board (CARB) regulations which require a progressively increasing percentage of automobiles to be ultra-low or zero emissions beginning in the year 1998 [1]. Though purely electric vehicles are a promising technology for the long range goal of energy efficiency and reduced atmospheric pollution, their limited range and lack of supporting infrastructure may hinder their public acceptance [2]. Hybrid vehicles offer the promise of higher energy efficiency and reduced emissions when compared with conventional automobiles, but they can also be designed to overcome the range limitations inherent in a purely electric automobile by utilizing two distinct energy sources to provide energy for propulsion. In this paper, the terms hybrid vehicle and hybrid-electric vehicle are used interchangeably and refer to a hybrid vehicle in which energy is stored as a petroleum fuel and in an electrical storage device such as a battery pack and is then converted to mechanical energy by an internal combustion engine (ICE) and electric motor respectively. The electric motor is used to improve energy efficiency and vehicular emissions while the ICE provides extended range capability. Though many different arrangements of power sources and converters are possible in a hybrid power plant, the two generally accepted classifications are series and parallel [3].

Computer modeling and simulation can be used to reduce the expense and length of the design cycle of hybrid vehicles by testing configurations and energy management strategies before prototype construction begins. Interest in hybrid vehicle simulation began to pick up in the 1970's along side the development of several prototypes which were used to collect a considerable amount of test data on the performance of hybrid drivetrains [4]. Several computer programs have since been developed to describe the operation of hybrid power trains, including: Simple Electric Vehicle Simulation (SIMPLEV) from the DOE's Idaho National Laboratory [5], MARVEL from Argonne National Laboratory [6], CarSim from AeroVironment Inc., and JANUS from Durham University [7]. A previous simulation model, ELPH, developed at Texas A&M University was used to study the viability of an electrically-peaking control scheme and to determine the applicability of computer modeling to hybrid vehicle design [8] but was essentially limited to a single vehicle architecture.

V-Elph is a system level simulation and analysis package programmed in Matlab/Simulink [9] which was developed at Texas A&M University primarily to study energy efficiency, fuel economy, and vehicular emissions issues in hybrid drive trains. The framework of the package is general enough that additional features, such as estimates of lifetime vehicle cost or other items of interest can be added without changing the core computer code. It extends the capabilities of previous modeling and simulation efforts by facilitating in-depth studies of power plant configurations, component sizing, energy management strategies, and the optimization of important component parameters for any type of hybrid or all-electric configuration or energy management strategy. It uses visual programming techniques, allowing the user to quickly change architectures, parameters, and to view output data graphically. It also

includes detailed models of electric motors, internal combustion engines, batteries, and vehicle dynamics.

In this paper, a system description of V-Elph is discussed. A sustainable, electrically-peaking hybrid-electric vehicle design is developed using V-Elph to illustrate its performance. Also, the results of the application of a simulation case to this design are presented.

ELPH CONCEPT

The sustainable, electrically peaking hybrid vehicle (ELPH) concept was introduced by Ehsani [10] at Texas A&M. The driving performance of this vehicle can match or exceed that of the traditional ICE-based automobile while improving both fuel consumption and emissions. Also, an ELPH vehicle is able to maintain highway speeds for an extended period of time and provide adequate performance on hills. This design eliminates the need for land-based battery charging by maintaining the state of charge with the onboard systems during vehicle operation using widely available fuels such as gasoline, diesel, or CNG.

DRIVETRAIN DESIGN

Five conceptual levels of abstraction are used in V-Elph to organize the system model and to represent the specific functional levels of a hybrid vehicle drivetrain [11]. The vehicle control level describes driver interactions with the vehicle and defines the ambient operating environment, the power plant control level determines the energy management strategy for the vehicle power plant, the configuration level describes the manner in which components interact because of their sizing and how they are arranged, the component level defines individual component dynamics and control, and the coupling level defines the interfaces between the different types of components. Defining these levels introduces a hierarchical structure where each level of abstraction encapsulates the functionality of its subsystems while maintaining a common interface to higher levels. Each level of abstraction also isolates a different part of the hybrid vehicle design process, allowing systematic analysis. A system diagram of a hybrid vehicle implemented in the V-Elph modeling system is given in figure 1.

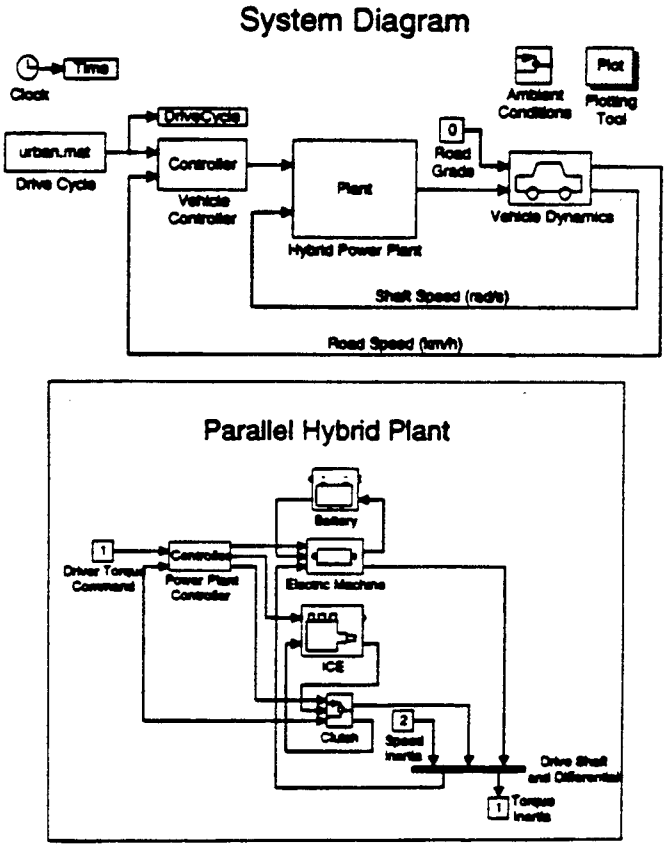

Figure 1. System level and power plant representation of hybrid vehicle in V-Elph

V-Elph permits the user to design an all electric, hybrid series or parallel hybrid power plant. In a series hybrid, only one energy converter provides torque to the wheels while the others are used to recharge an energy accumulator, usually a battery pack. In a typical series hybrid design, an ICE/generator pair charges the batteries and only the motor actually provides propulsion. In a parallel configuration both the ICE and the electric motor can provide torque at the drive wheels and the total power plant torque is controlled by blending the two torques according to a prescribed energy management algorithm. The power plant is designed through an interconnection of component models and support components such as shown in the bottom part of figure 1 for a parallel hybrid power plant.

Data flow within a general component model is given in figure 2, where signal connections are used to send information to and from the power plant controller and the power connections represent the physical coupling between components which provide a path for the transfer of energy. The ports for the signal connections are separated from the power connections since the control of each component might be different while the electrical and mechanical coupling mechanisms are the same for all components.

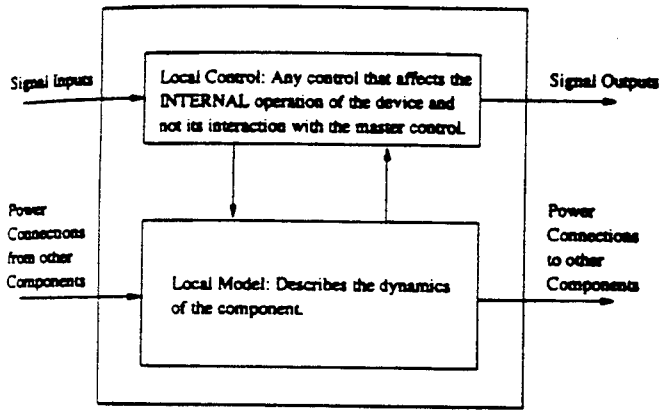

Figure 2. Data flow through a component model

Strict interface definitions were defined for each type of component so that various empirical and detailed models could be included in the V-Elph library of components. For example, in the motor library there are models such as a detailed steady-state as well as dynamic model of a vector controlled induction motor and a detailed model of a dc motor. Each motor model has the same global inputs and outputs.

Several levels of depth are available in V-Elph to allow users to take advantage of the features that interest them. At the most basic level, a user can run simulation studies by selecting one of the series or parallel hybrid vehicles provided and display the results using the graphical plotting tools. In addition to being able to change the drive cycle and the environmental conditions under which the vehicle operates, the user can switch components in and out of the model to try different types of engines, motors, and batteries models. The user can also change vehicle characteristics such as size and weight, gear ratios, and the size of the components that make up the hybrid drive train.

An intermediate user can create his/her own hybrid vehicle configurations using a blank vehicle template and the V-Elph component library. Components can be isolated to run parameter sweeps to create performance maps to assist in component sizing and selection. Given a set of system performance criteria, the performance maps of the components can be used to develop a suitable hybrid vehicle design. Finally, advanced users can pursue sophisticated design objectives such as the creation of entirely new component models and the optimization of the hybrid power plant by creating add-on features that are compatible with the modeling system interface.

SIMULATION STUDIES

To demonstrate the capabilities of the V-Elph package, a parallel configuration was studied to achieve the blending of torques from both the ICE and the electric machine which could provide adequate performance and maintain the state of charge of the battery in an electrically peaking (Elph)-type hybrid. The design of a vehicle takes place at each of the five levels of abstractions described above. The design process usually begins at the vehicle control level by defining the vehicle mission and the performance that the driver expects from a vehicle of a certain size and a given set of aerodynamic characteristics. Next, a vehicle configuration is selected which meets mission and performance objectives. Then the components and gearing must be selected to meet the energy requirements of the vehicle. A control scheme is selected to meet the performance objectives and the design is modified iteratively until satisfactory performance is achieved.

The ICE was sized to provide enough power to maintain a cruising speed of [illegible] on a level road and the electric machine was sized to provide acceptable acceleration performance of 0 to 100 km/h in 16 seconds for short time intervals. The vehicle was also designed to maintain highway speeds for an extended period of time and provide adequate performance on hills. The vehicle configuration in figure 3 which was implemented in V-Elph as shown in figure 1 is based on a typical mid-sized family sedan with a gross weight of 1800 Kg including the additional batteries used in the hybrid power plant. The various detailed component models utilized to design the hybrid drivetrain were developed by the members of the ELPH team at Texas A&M University.

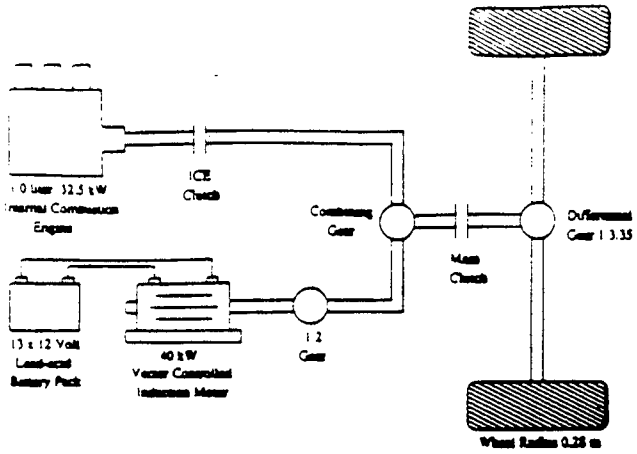

Figure 3. Proposed hybrid vehicle configuration

ICE MODEL - The ICE model used in this study is based on work by [illegible] Powell from Ford Motor Company [12]. For this ELPH-type hybrid, the ICE was sized to meet or barely exceed the steady-state road load requirements at all speeds within the operating range of the ICE. An engine displacement of 1 liter and power of 32.5 kW (43.5 hp) were chosen for this study so that the ICE, running at full throttle, could maintain a speed of 120 km/h on a level road without aid from the electric machine. The comparison of ICE torque and the road load referred to the shaft of the ICE given in figure 4 indicates that the ICE torque is exactly equal to the road load at 120 km/h. It is possible for the vehicle to go faster than this, but it would require the use of the electric motor in tandem with the ICE, draining the battery. The ICE also meets or exceeds the base load requirement for all speeds over 38 km/h (1250 rpm at the ICE shaft). Since there is no traditional transmission in the vehicle, the electric motor will need both the acceleration and road load requirements at speeds below this threshold since ICE performance degrades quickly at low speeds.

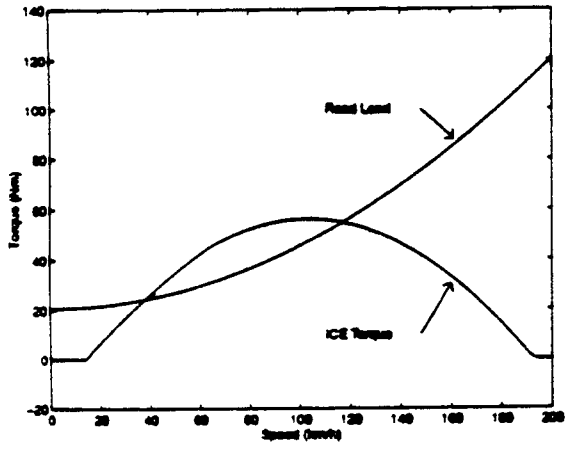

Figure 4. Comparison of ICE torque and total road load to maintain a steady speed of 120 km/h

ELECTRIC MACHINE MODEL - The steady state version of a vector controlled induction machin model used in this study was developed by the motc drives development team at Texas A&M University [13 The induction machine performs two functions in th drive train; as a motor it provides torque at the wheels t accelerate the vehicle and as a generator it recharge the battery during deceleration (regenerative braking) o whenever the torque produced by the power plan exceeds the demand from the driver. Regenerativ braking recaptures some of the energy that woul otherwise be dissipated as heat in the brakes, improvin the overall system efficiency. Vector control extends th constant power region of the motor, making it possible t run the motor over a wide speed range. The motor ca provide the requested torque up to the constant powe threshold at speeds above the base speed of the moto operation beyond this point is restricted to avo exceeding the motor's power rating. The efficiency c the motor is poor at very low speeds, peaks at the bas speed, and then droops slowly as the speed increases Although it is inevitable that the electric machine wi operate in the low efficiency region since it provides all c the vehicle torque at low speeds, the 1:2 gear place between the machine and the drive-shaft pushes th machine into the higher efficiency operating region. Th gear also helps to improve efficiency by reducing th torque load on the electric machine since the torque a the shaft of the machine needs to only be one half c what is required at the drive-shaft. Thus, the propose design utilizes the wide speed range of the vecto controlled induction motor to improve the overall syste efficiency.

BATTERY MODEL - The battery model used i this study was developed by the battery mode development team at Texas A&M University and i based on empirical tests of ElectroSource Horizon lead acid batteries [14]. For this study, thirteen, 12-V batter cells were used to provide power to the electric moto The battery model uses the current load and batter state of charge to determine dc bus voltage. Voltag tends to drop as the state of charge decreases and a the amount of current drawn from the battery increases At low currents, the battery efficiency is reasonably hig regardless of the state of charge. As the amount o current drawn from the pack increases, the batter efficiency drops rapidly to about 75% for a 400 A drain At current levels up to about 100 A the battery recharg efficiency is relatively high but quickly drops off abov this threshold because the physical and chemica processes in the battery can not react quickly enough t absorb the energy, resulting in battery degradation. It i thus desirable to perform battery charging at curren levels of 100 A or less whenever possible.

ANALYSIS OF ELPH-TYPE HYBRID VEHICLE

Using the information obtained from parameter sweep of the components, an energy management strategy wa devised that takes advantage of the characteristics o

each of the individual drivetrain components. The objective of this study was to refine the power plant control algorithm until the battery state of charge at the end of the drive cycle equals the beginning state of charge.

An approach was investigated to improve the overall efficiency of the hybrid power plant by focusing on the efficient conversion of gasoline to mechanical energy. To run the ICE as efficiently as possible, it should only be operated in the high speed and high throttle angle region since the fuel economy of an ICE generally improves as throttle angle increased. In a sustainable, ELPH-type design, the torque requested by the driver is separated into two components. The torque required to maintain the steady-state speed is produced by the ICE and the peaking torque for acceleration is provided by the electric machine. This appropriation smoothes out the ICE torque requirement, improving both fuel economy and emissions. By combining the torque-speed characteristics of the electric machine and the ICE into a single power plant as shown in figure 5, adequate torque can be provided over the entire speed range without a multiple gear transmission, reducing vehicle weight. Since the ICE provides very little torque at low speeds, two regions of vehicle operation are defined. In the low-speed region only the electric machine is used to provide torque at the wheels while in the high-speed region the ICE and the electric machine are use in tandem to propel the vehicle.

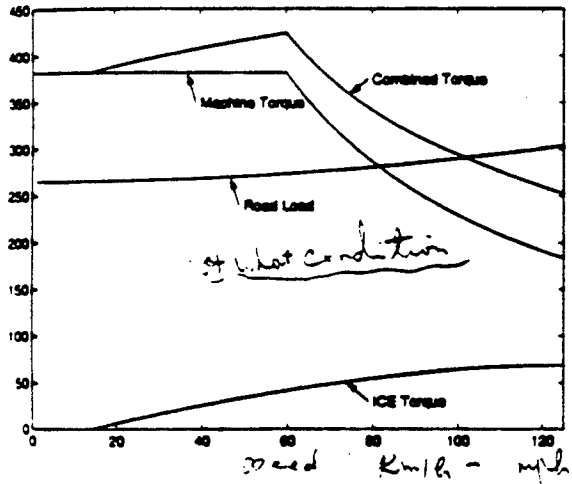

Figure 5. ICE torque, electric machine torque, combined power-plant torque, and total vehicle load including torque required for maximum acceleration referred to the main drive shaft

The control strategy is implemented such that the ICE runs at a constant fuel throttle angle and the electric machine makes up the difference between the torque requested by the driver and the torque produced by the ICE. This approach minimizes the amount of time that the ICE is in use by maximizing the speed at which the ICE is engaged to the wheels while still maintaining the battery state of charge over the drive cycle.

A constant, high throttle angle of 80° is used in this control scheme when the ICE is engaged. The equation used to produce the electric machine torque command depends on the driver torque command T_c, ICE torque T_{ICE}, and vehicle speed v and is given by:

$$T_e = \begin{cases} T_c - T_{ICE} & \text{if } v \geq 60\ km/h \text{ and } T_c \geq 0 \\ T_c & \text{otherwise} \end{cases}$$

The equation that produces the ICE throttle angle command depends only on the vehicle speed v and is given by:

$$\theta_{ICE} = \begin{cases} 80^o & \text{if } v \geq 60\ km/h \\ 10^o & \text{otherwise} \end{cases}$$

The ICE clutch is engaged whenever the ICE throttle angle is 80° and is disengaged otherwise. The main clutch is always engaged in this control scheme but can be used to disengage the power plant from the wheels to charge the battery pack while the vehicle is at a stand still.

SIMULATION RESULTS - A short drive cycle consisting of a gradual acceleration to 120 km/h, cruise, and then a deceleration back to stop is shown in figure 6. The control signals produced by the power plant controller over this drive cycle are given in figure 7 to demonstrate the minimum ICE use control of the power plant over the entire speed range of the vehicle.

A commuter drive cycle shown in figure 8 is 65.25 km long and was developed by combining three FTP-75 urban drive cycles with two federal highway drive cycles [15]. The two highway cycles are inter-spaced between each of the urban cycles. By adjusting the speed at which the ICE engages until the battery state of charge is exactly maintained over the commuter drive cycle, a sustainable hybrid was implemented. The results of several simulations are given in figure 9 showing that the ICE should be engaged at 60 km/h to maintain the battery state of charge over this particular drive cycle.

Graphs of the electric machine and ICE torques produced by the minimum ICE use control scheme over the commuter drive cycle in figure 8 is given in figure 10. Since the battery state of charge at the beginning and end of the drive cycle are the same, all of the energy to run the vehicle must have come from the gasoline. The minimum ICE use control scheme is effective in smoothing the torque required from the ICE and providing transient torque with the electric machine. It is also effective in reducing the amount of time that the ICE is in operation.

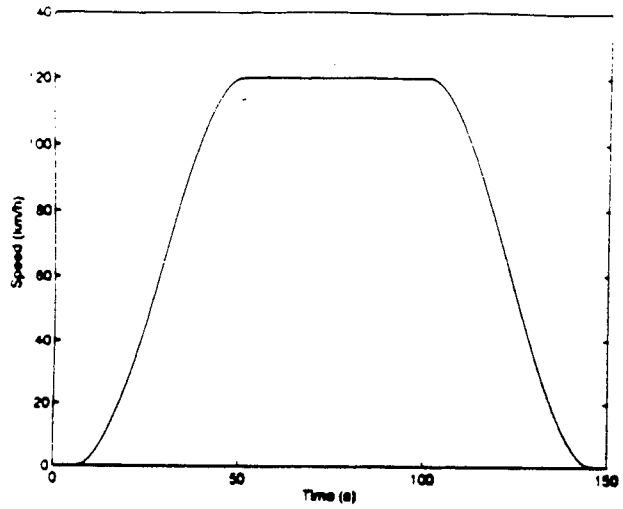

Figure 6. Drive cycle consisting of acceleration, cruise, and deceleration

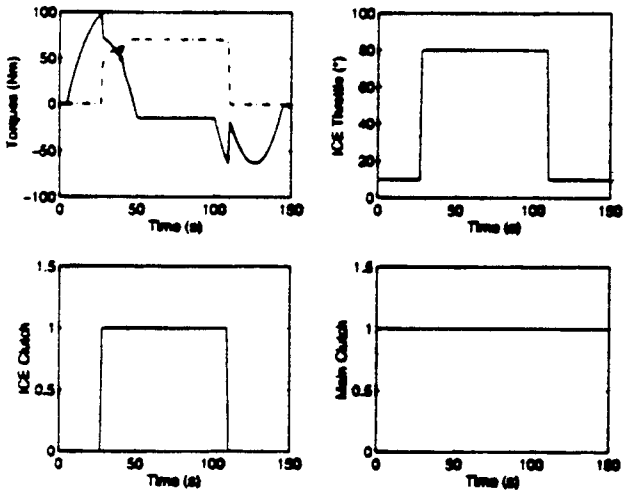

Figure 7. Control signals for the minimum ICE use control schemes for the drive cycle shown in figure 6.

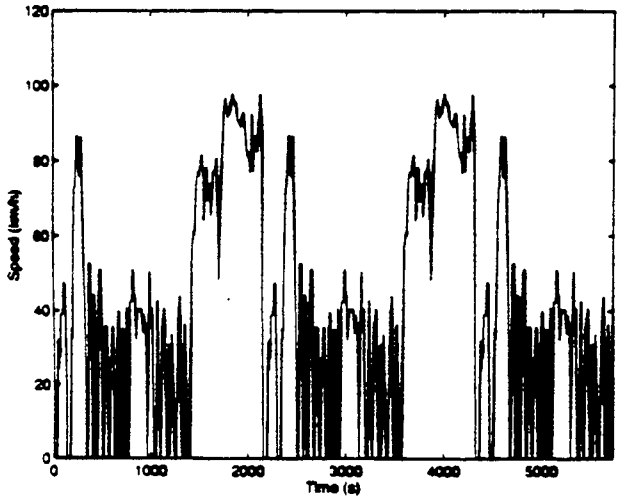

Figure 8. Commuter drive cycle

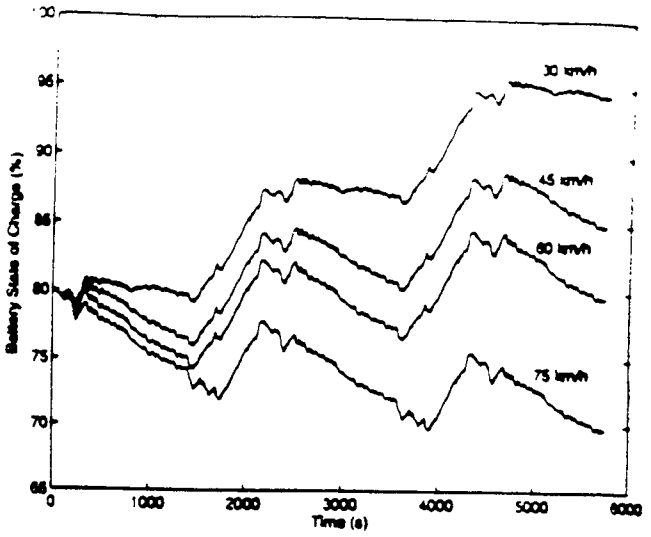

Figure 9. Battery state of charge vs. time for various ICE engagement speeds

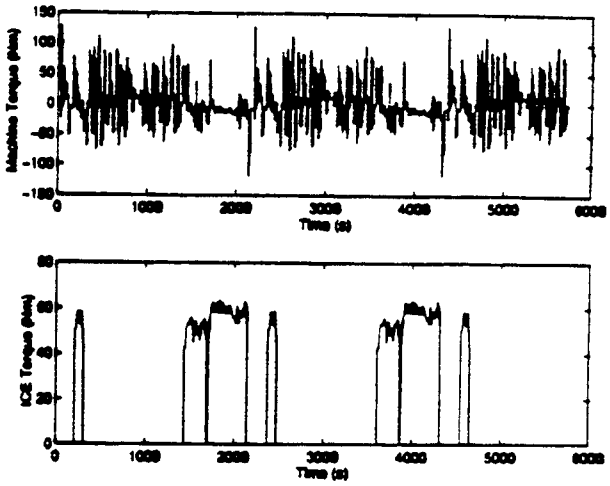

Figure 10. Electric machine and ICE torque for the minimum ICE use control scheme

CONCLUSION

The two main objectives of the work presented in this paper were to create a versatile computer model and simulation package, V-Elph, for the design and analysis of hybrid drivetrains and to demonstrate its use in a simple case of hybrid vehicle design. V-Elph proved to be extremely useful and versatile for vehicle design, allowing the user to try different configurations and control strategies to identify promising concepts before prototype construction begins. Also the analysis features allow the results to be easily conveyed in a visual manner. Finally, V-Elph shows great promise as a tool for advancing the knowledge of hybrid vehicle technologies.

ACKNOWLEDGMENTS

The authors acknowledge the support of the Texas Higher Education Coordinating Board Advanced Technology Program (ATP) and Texas A&M Office of the Vice President for Research.

REFERENCES

[1] M. J. Riezenman, "Electric Vehicles," *IEEE Spectrum*, pp. 18-101, Nov. 1992.

[2] V. Wouk, "Hybrids: then and now," *IEEE Spectrum*, pp. 16-21, July 1995.

[3] A. Kalberlah, "Electric Hybrid Drive Systems for Passenger Cars and Taxis," *Tech. Rep. 910247, SAE*, 1991.

[4] B. Bates, "On the road with a Ford HEV," *IEEE Spectrum*, pp. 22-25, July 1995.

[5] G. Cole, "Simple Electric Vehicle Simulation (SIMPLEV) v3.1," DOE Idaho National Engineering Laboratory.

[6] W.W. Marr and W.J. Walsh, "Life-cycle Cost Evaluations of Electric/Hybrid Vehicles," *Energy Conversion Management*, vol. 33:9, pp. 849-853, 1992.

[7] J.R. Bumby and et al, "Computer Modeling of the Automotive Energy Requirements for Internal Combustion Engine and Battery Electric-Powered Vehicles," *in Proceedings of IEE Pt. A*, vol. 132:5, pp. 265-79, 1985.

[8] D. Buntin, *Control System Design for a Parallel Hybrid Electric Vehicle*, Master's thesis, Texas A&M University, College Station, Texas, 1994.

[9] *Matlab/Simulink*, Version 4.2c.1/1.3c, The Mathworks Inc., Natick, Mass.

[10] M. Ehsani and et al, "Introduction to ELPH: A Parallel Hybrid Vehicle Concept," in *Proceedings of the ELPH Conference*, 1994.

[11] K. M. Stevens, *A Versatile Computer Model for the Design and Analysis of Electric and Hybrid Drive Trains*, Master's thesis, Texas A&M University, College Station, Texas, 1994.

[12] B.K. Powell, "A Dynamic Model for Automotive Engine Control Analysis," in *Proceedings of the 18th IEEE Conference on Decision and Control*, pp. 120-126, 1979.

[13] M. Ehsani, K.M. Rahman, and H.A. Toliyat, "Propulsion System Design of Electric and Hybrid Vehicles," accepted for publication in *IEEE Transactions on Industrial Electronics*.

[14] S. Moore and M. Ehsani, "An Empirically Based Electrosource Horizon Lead-Acid Battery Model," *SAE Journal SP-1156, Paper No. 960448*, Feb. 1996.

[15] U. Adler, ed., *Automotive Handbook*, Stuttgart, Germany: Robert Bosch GmbH, 2 ed., 1986.

BIOGRAPHY

K.L. Butler received the Ph.D. degree in May 1994 in electrical engineering from Howard University where she was a NASA fellow. She received the B.S.E.E. degree in 1985 and M.S.E.E. degree in 1987 from Southern University in Baton Rouge and University of Texas in Austin, respectively. She is currently an assistant professor at Texas A&M University. She is a recent recipient of an NSF Faculty Early Career Development (CAREER) Award.

Dr. Butler was a member of technical staff at Hughes Aircraft Company from 1988-89. Her research interests are in the areas of intelligent systems, modeling and simulation, power distribution automation and system protection.

PERFORMANCE ANALYSIS OF ELECTRIC MOTOR DRIVES FOR ELECTRIC AND HYBRID ELECTRIC VEHICLE APPLICATIONS

Khwaja M Rahman
Student Member, IEEE

Mehrdad Ehsani
Fellow, IEEE

Texas Applied Power Electronics Center
Department of Electrical Engineering
Texas A&M University
College Station, TX 77843-3128
Fax: (409) 845-6259

Abstract:

Our recent study has revealed that high speed motors capable of performing extended constant power operation are best suited for electric and hybrid vehicle application. In that study we have shown that vehicle's operational constraints such as: initial acceleration and gradability can be met with minimum power rating if the powertrain can be operated mostly in constant power region. The purpose of this paper is to make a performance analysis of several most commonly used motors based on those findings. In this study, induction motor is found to be best suited for vehicle application. Permanent magnet (PM) motors, owing to their restrictive speed range, are found to be not as suitable for vehicle applications. On the other hand, Switched Reluctance Motors (SRM), despite their poor power factor of operation, may be proven to be superior to both of these motors, both in size and cost. An attempt has also been made to define the standards for some of the vehicle motor design parameters such as: motor rated speed, motor maximum speed, extent of constant power operation.

I. Introduction

A. An overview of Electric and Hybrid Electric Vehicle

The concept of EV was conceived in the middle of previous century. After the introduction of internal combustion engine (ICE), EVs remained in existence side by side with ICE for several years. The energy density of gasoline is far more than what the electrochemical battery could offer. Despite this fact, the EV continued to exist, especially in the urban areas due to its self starting capability. However, soon after the introduction of electric starter for ICE early this century, despite being energy efficient and nonpolluting, EV lost the battle completely to ICE due to its limited range and inferior performance. Since then ICE has evolved, improved in design, and received wide spread acceptance and respect. Nevertheless, EV interest never perished completely, and whenever there has been any crisis regarding the operation of ICE automobiles, we have seen a renewed interest for EV The early air quality concerns in the 60's and the energy crisis in the 70's have brought EVs back to the street again. However, the most recent environmental awareness and energy concerns have imposed, for the first time since its introduction, a serious threat to the use of ICE automobiles.

The ICE automobile at the present is a major source of urban pollution. According to figures released by the US Environmental Protection Agency (EPA), conventional ICE vehicles currently contribute 40-50% of ozone, 80-90% of carbon monoxide, and 50-60% of air toxins found in urban areas [1]. Besides air pollution, the other main objection regarding ICE automobiles is its extremely low efficiency use of fossil fuel. Hence, the problem associated with ICE automobiles are three fold, environmental, economical, as well as political. These concerns have forced governments all over the world to consider alternative vehicle concepts. The California Air Resource Board (CARB) is among the few who acted first through the declaration of the Clear Air Act of September, 1990. This act requires that 52% of all vehicles sold in that state be either Low Emission Vehicles (LEV's)- 48%, Ultra Low Emission Vehicles (ULEV's)- 2%, or Zero Emission Vehicles (ZEV's)- 2%, by the year of 1998 [2]. Similar measures are considered in other states and nations, as well.

Electric and Hybrid-Electric Vehicles offer the most promising solutions to reduce vehicular emission. Electric vehicles constitute the only commonly known group of automobiles that qualify as ZEVs. These vehicles use an electric motor for propulsion, and batteries as electrical energy storage devices. Although, there have been significant advancements in

motors, power electronics, microelectronics, and microprocessor control of motor drives, the advancement in battery technology has been relatively sluggish. Hence, the handicap of short range, associated with EV's still remains. Given these technology limitations, Hybrid electric vehicle seems to be the viable alternative to ICE automobile at the present. Hybrid electric vehicles (HEVs) qualify as ULEVs, and do not suffer from the range limitations imposed by the EVs. These vehicles combine more than one energy source to propel the automobile. In heat engine/battery hybrid systems, the mechanical power available from the heat engine is combined with the electrical energy stored in a battery to propel the vehicle. These systems also require an electric drivetrain to convert electrical energy into mechanical energy, just like the EV. Hybrid-Electric systems can be broadly classified as series or parallel hybrid systems [3].

In series hybrid systems, all the torque required to propel the vehicle is provided by an electric motor. On the other hand, in parallel hybrid systems the torque obtained from the heat engine is mechanically coupled to the torque produced by an electric motor [3]. In the electric vehicle, the electric motor behaves exactly in the same manner as in a series hybrid. Therefore, the torque and power requirements of the electric motor are roughly equal for an EV and series hybrid, while they are lower for parallel hybrid.

B. Road Load Characteristics

The road load (F_w) consists of rolling resistance (f_{ro}), aerodynamic drag (f_l), and climbing resistance (f_{st}) [4].

$$F_w = f_{ro} + f_l + f_{st} \quad (1)$$

The rolling resistance (f_{ro}) is caused by the tire deformation on the road:

$$f_{ro} = f \cdot m \cdot g \quad (2)$$

where f is the tire rolling resistance coefficient. It increases with vehicle velocity, and also during vehicle turning maneuvers. Vehicle mass is represented by m, and g is the gravitational acceleration constant.

Aerodynamic drag, f_l, is the viscous resistance of air acting upon the vehicle.

$$f_l = 0.5\xi C_W A(v + v_0)^2 \quad (3)$$

where ξ is the air density, C_W is the aerodynamic drag coefficient, A is the vehicle frontal area, v is the vehicle speed, and v_0 is the head wind velocity.

The climbing resistance (f_{st} with positive operational sign) and the down grade force (f_{st} with negative operational sign) is given by

$$f_{st} = m \cdot g \cdot \sin\alpha \quad (4)$$

where α is the grade angle.

A typical road load characteristic as a function of vehicle speed is shown in Fig. 1. The following assumptions are made in the plot

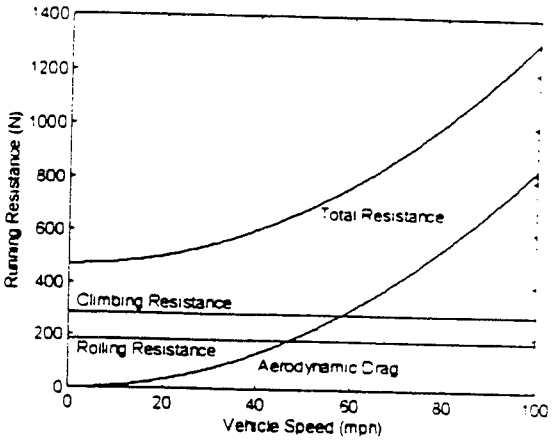

Fig. 1. Typical road load characteristics as a function of vehicle speed.

(i) velocity independent rolling resistance
(ii) zero head wind velocity
(iii) level ground

These assumptions will be used in the analysis presented in the following sections, unless otherwise specified. These assumptions do not change the general trend of the solution and can be easily relaxed.

The motive force F available from the propulsion system is partially consumed in overcoming the road load, F_W. The net force, $F-F_W$, accelerates the vehicle (or decelerates when F_W exceeds F). The acceleration is given by

$$a = \frac{F - F_W}{k_m \cdot m} \quad (5)$$

where k_m is the rotational inertia coefficient to compensate for the apparent increase in the vehicle's mass due to the on-board rotating mass.

C. Contribution of this Paper

The new abstract concept of a power source has been defined as a circuit element whose i-v curve obeys the following equation [5]

$$vi = P = \text{constant} \quad |v| < \infty \quad |i| < \infty \quad (1)$$

The mechanical counterpart of this definition is

$$\omega T = P = \text{constant} \quad |T| < \infty \quad |\omega| < \infty \quad (2)$$

where, ω is the speed and T is the torque.

Figures 2(a) and 2(b) plot the, i-v curve for an electrical power source, and ω-T curve for a mechanical power source, respectively. Our recent study has revealed that, a vehicle, in order to meet its operational constraint such as initial acceleration and gradability with minimum power, needs a power source [6]. The power rating of the motor that is deviating from the power source regime can be as much as two times that of a motor operating as a power source through out its

speed range in a vehicle [6]. Fig. 2(b), therefore, represents theoretically the optimal torque-speed profile of any motor drive for vehicle application.

This paper makes a comprehensive study of several most commonly used motor drives and their

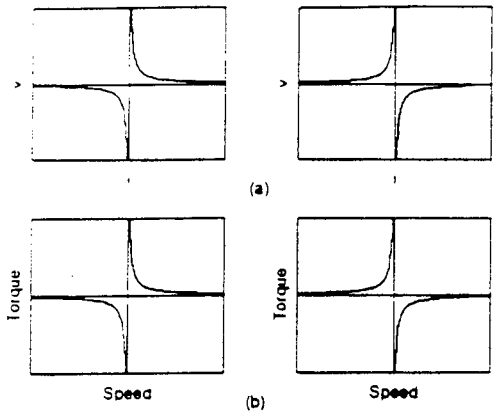

Fig. 2. Electrical (a) and mechanical (b) power source element.

control for vehicle application. Design examples are presented describing the capabilities of these motors. By considering several practical considerations, such as wheel shaft torque, gear torque (single gear), motor drive shaft torque, this paper will also make an attempt to define the vehicle motor selection criteria based on motor design variables such as motor rated speed, motor maximum speed, and the extent of constant power operation.

II. EV and HEV System Design

A detailed study of the EV and HEV system design can be obtained from [6]. Only some key results, pertinent to the present analysis, will be discussed in this section. This discussion will include the effects of, i) extent of electric machine constant power range, ii) electric machine base speed, and iii) electric machine maximum speed, on the overall EV and HEV system design.

The main component of EV and HEV drivetrain is its electric motor. The electric motor in its normal mode of operation can provide constant rated torque up to its base or rated speed. At this speed, the motor reaches its rated power limit. The operation beyond the base speed up to the maximum speed is limited to this constant power region (Fig. 3.). The range of the constant power operation depends primarily on the particular motor type and its control strategy. However, some electric motors digress from the constant power operation, beyond certain speed, and enter the natural mode before reaching the maximum speed. The maximum available torque in the natural mode of operation decreases inversely with the square of the speed. Although machine torque in the natural mode decreases inversely with the square of the

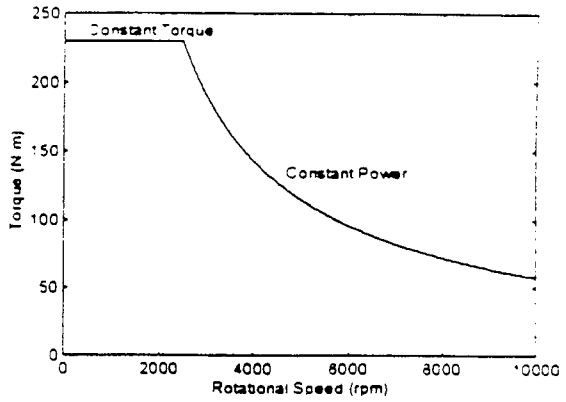

Fig. 3. Typical torque-speed characteristics of an electric motor.

speed, for some extremely high speed motors the natural mode of operation is an appreciable part of its total torque-speed profile. Inclusion of this natural mode for such motors may result in a reduction of the total power requirement. Of course, power electronic controls allow the motor to operate at any point in the torque speed plane, below the envelop defined by the mentioned limits. However, it is the profile of this envelop that is important in the motor drive selection and design.

In order to free up the motor speed from the vehicle speed, for design optimization, gearing between the motor shaft and the drive shaft is required. Power electronic control allows instantaneous matching of the available motor torque with the required vehicle torque, at any speed. Therefore, multiple gearing in order to match the motor torque-speed to the vehicle torque-speed is no longer a necessity.

The gear ratio and size depend on the maximum motor speed, maximum vehicle speed, and the wheel radius. Higher maximum motor speed, relative to vehicle speed, means a higher gear ratio and a larger gear size. The torque speed diagram of Fig. 3 is redrawn in Fig. 4, but in terms of tractive force and vehicular speed for different gear ratios. Notice now the electric motor base speed and maximum speed, in terms of the vehicle speed, depend on the gear ratio.

Extended speed constant power operation has a pronounced effect on the motor rated power to meet the vehicle acceleration requirement. The importance of extending the constant power speed range can be best described by comparing the required motor power for different constant power speed ranges (as a multiple of its base speed). Table I shows an example of power

0-7803-3292-X/96/$5.00 © 1996 IEEE

requirement for several constant power ranges for the

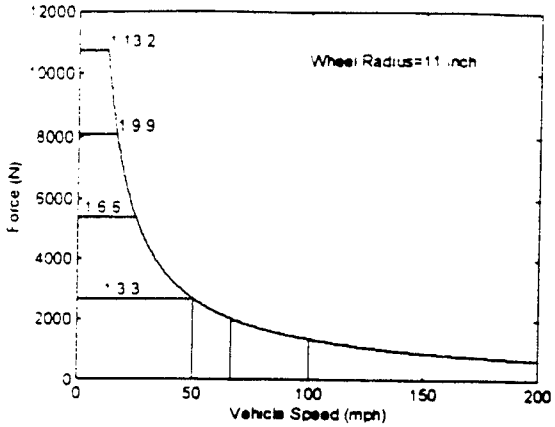

Fig. 4. Torque-speed diagram of an electrical motor in terms of tractive force and vehicular speed with gear size as the parameter.

following vehicular acceleration requirement:

- 0 to 26.82 m/s (0-60 mph) in 10 seconds.
- vehicle mass of 1450 kg.
- rolling resistance coefficient of 0.013.
- aerodynamic drag coefficient of 0.29.
- wheel radius of 0.2794 m (11 inch).
- level ground.
- zero head wind velocity.
- Maximum motor speed is 10,000 rpm.
- Maximum vehicle speed is 44.7 m/s (100 mph).

Here, the required gear ratio, to match the maximum motor speed to the maximum vehicle speed, for a wheel radius of 0.2794 m (11 inches), is 1:6.55. The results of Table I suggest an extended range of 4 to 6 times the base motor speed in order to significantly lower the motor power requirement.

In the context of EV/HEV design, we classify motors with maximum speed of less than 6000 rpm as low speed motors, 6000-10000 rpm as medium speed motors, and 10,000 rpm and beyond as high speed motors. The power requirement is not a function of the motor maximum speed. Motor maximum speed only affects the gear size. However, maximum speed has a pronounced effect on the rated torque of the motor. An example of this is illustrated in the surface plot of Fig. 5. Low speed motors with extended constant power speed range have a much higher rated shaft torque. Consequently, they need more iron to support this higher flux and torque. Furthermore, higher torque is associated with higher motor and power electronics

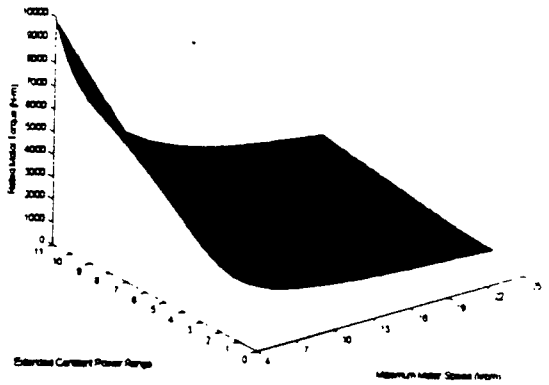

Fig. 5. Rated motor shaft torque as a function of maximum motor speed.

currents. This will also impact the power converter silicon size and conduction losses. Extended speed range, however, is necessary for initial acceleration as well as for cruising intervals of operation. Therefore, the rated motor shaft torque can only be reduced through picking a high speed motor. This would however affect the gear ratio. A good design is the result of a trade off between maximum motor speed and the gear size. However, this tends to be more in favor of selecting a medium or high speed motors. For an extremely high speed motor, a sophisticated gear arrangement might be necessary for speed reduction. Planetary gear arrangement [7] could be the choice, that is compact but allows high speed reduction. Extended constant power range, on the other hand, will increase drive shaft torque and gear torque, as can be seen in Fig. 6. Hence, another design tradeoff is involved between the gear stress and the extended constant power range. It can be seen from the results of table I that after a certain point there is not any appreciable power reduction with extended constant power range. Any further extension of constant power range beyond this point will only adversely affect the gearing and drive shaft appreciably without reducing

Table I.

	Extended Constant HP Speed Range					
	1:1	1:2	1:3	1:4	1:5	1:6
Motor Rated Power (KW)	110	95	74	67	64	62

the power requirement. This will set the upper limit of the extended range of the constant power operation.

In view of these findings, the capabilities of several potential EV and HEV motors are discussed in the following section.

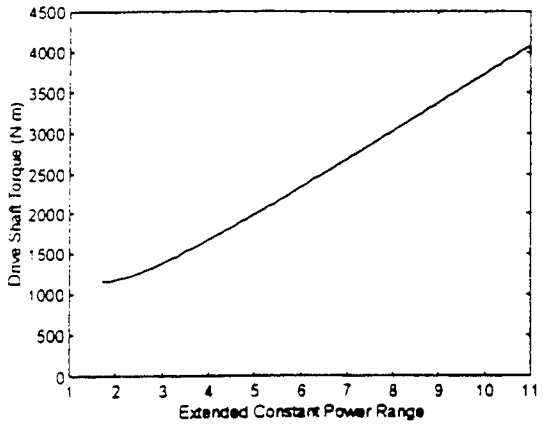

Fig. 6. Drive shaft torque as a function of extended constant power range.

III. Electric Propulsion Systems for EV and HEV Design

An electric propulsion system is comprised of three main elements: power electronic converter, motor, and its controller. This section is devoted to examining several most commonly used motors and their control for EV and HEV propulsion. The importance of extended speed range, under constant power operation of electric motors in EV and HEV system design was discussed in the previous sections. This mode of operation is referred to as field weakening, from its origin in dc motor drives. Therefore, this section will concentrate mainly on the field weakened extended speed operation of the EV and HEV motors. A more detailed study of these motors for EV and HEV propulsion application is presented in [8].

A. DC Commutator Motor

Separately excited dc commutator motor is inherently suited for field weakened operation, due to its decoupled torque and flux control characteristics [9]. Extended constant power operation is possible with this motor through its separate field weakening. However, the presence of mechanical commutators imposes a severe restriction on the maximum speed of the dc motor. As was shown, this low speed and extended constant power operation would necessitate higher motor shaft torque (Fig. 5). Consequently, more motor iron is needed. This makes the motor more bulky, heavy and expensive. This would make the application of this motor less suitable for vehicles, especially with single gear transmission operation.

B. Induction Motor

Field orientation control (FOC) [10] of induction motor can decouple its torque control from field control. This allows the motor to behave in the same manner as a separately excited dc motor. Thus motor, however, does not suffer from the same speed limitations as in the dc motor. Extended speed range operation beyond base speed is accomplished by flux weakening, once the motor has reached its rated power capability. The presence of breakdown torque somewhat limits this extended constant power operation. Nevertheless, a properly designed induction motor, e.g., spindle motor, with field oriented control can achieve field weakened range of 3-5 times the base speed [11]. This approach, however, results in an increased breakdown torque thereby resulting in an oversizing of the motor. A special winding changeover technique of a field orientation controlled induction motor is also reported which demonstrates extremely long field weakened operation [12]. This approach, however, requires winding tap changing and contactors. A contactorless control scheme for extending the speed range of a four pole induction motor was presented most recently in [13]. This scheme uses two inverters each of half the rated power rating that, in theory, can extend the constant power operation range to 4 times the base speed, for a motor, that would otherwise be limited to 2 times the base speed. It may be mentioned here that the torque control in induction motor is achieved through PWM control of the current. In order to retain the current control capability in the extended speed constant power range, the motor is required to enter the field weakening range before reaching the base speed, so that it has adequate voltage margin to control the current [14]. This would, however, oversize the motor slightly. Current regulation with synchronous current regulator [15] may be the preferred choice. It can regulate current with lower voltage margin. The availability of a long field weakened range, obviously, makes the induction motor very suitable for vehicle application. This motor, according to our classification in section II, qualifies as a medium to high speed motor.

C. Permanent Magnet (PM) Brushless DC (BLDC) Motor

The PM BLDC motor is specifically known for its high efficiency and high power density. However, this motor suffers from a rather limited field weakening capability. This is due to the presence of the PM field which can only be weakened through production of a stator field component which opposes the rotor magnetic field. Nevertheless, extended constant power operation is possible through the advancing of the commutation angle [16]. This has been demonstrated in

Fig. 7 for a typical BLDC motor with 120° stator current conduction per phase. The extended range in this case is less than 2 times the base speed. Phase current of the simulated motor in this extended speed

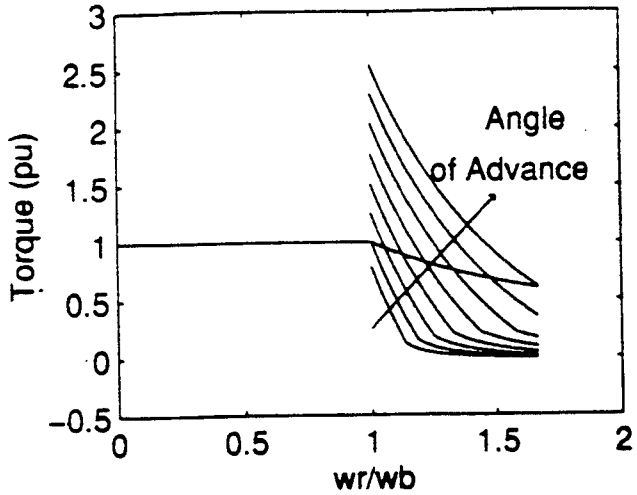

Fig. 7. Torque-speed response of a BLDC motor with phase advance angle as the parameter.

range of operation is shown in Fig. 8. This almost square wave like phase current, even in the extended speed range of operation, results in a high torque per ampere. The simulation result shows that the power

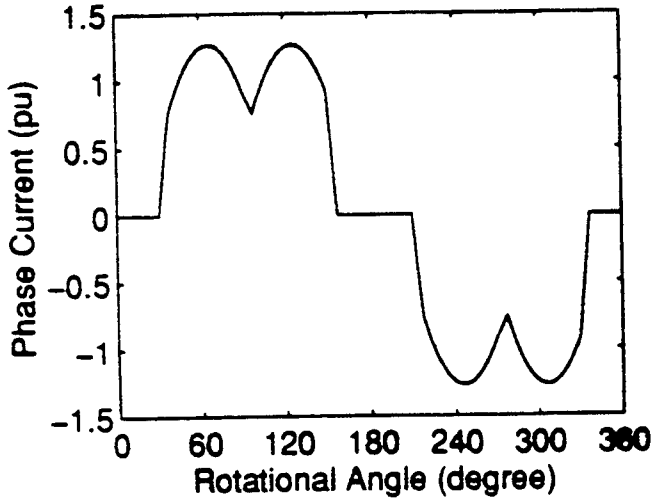

Fig. 8. Phase current of BLDC motor in the extended speed constant power operation.

factor is as high as 0.93 in this extended speed range of operation. This high power factor operation of the BLDC motor reduces the volt-ampere rating of the converter. The range of the constant power operation can be extended a bit further through 180° conduction [16]. This would, however, result in a much higher torque ripple than the 120° conduction. A method of extending the constant power range is also demonstrated in [17] by modulating the converter conduction and the phase angle. Some researchers have shown that higher phase inductance, in the BLDC motor helps extend the constant power operation [18]. This is indeed the case in Chan's BLDC motor [19]. The absence of mutual coupling between the phase windings in this motor was shown to result in an extended power operation as high as 4 times the base speed. However, the range was only 2.5 times the base speed in their actual test result. This may be due to the presence of some unavoidable coupling between the phases.

Current regulation in BLDC motor is necessary for the control of torque below base speed. The integrated current regulator presented in [20] may be particularly suitable for a BLDC motor drive designed for vehicle application. This regulator does not require any current sensors. The current feedback signal is obtained from the integrated MOSFET power transistors (SENSEFETs). Moreover, this regulator has fault current protection capability. This fault current may not be detectable from the DC bus side in a PM BLDC motor. A variation of this regulator with four quadrant operation capability is presented in [21]. A successful commutation of BLDC motor requires

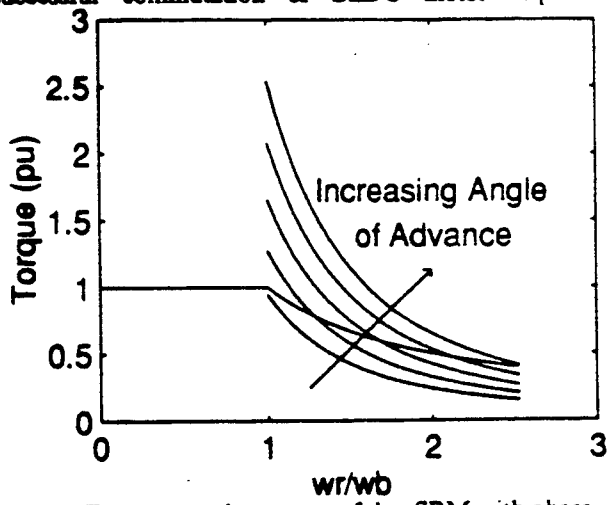

Fig. 9. Torque-speed response of the SRM with phase advance angle as the parameter.

absolute position information. Position encoder is therefore necessary . Obviously EV and HEV design would prefer the sensorless operation of this motor. Sensorless operations have been reported in the literature [22,23].

The surface mounting of the permanent magnets in BLDC motor somewhat limits its maximum speed of operation. However, by proper manufacturing methods, medium to high speed operation is possible.

D. Switched Reluctance Motor (SRM)

Because of its simple construction and the absence of rotor conductors, the SRM is capable of extremely high speeds. Operation in constant power is

made possible in this motor by the phase advancing of stator current conduction angle until overlapping between the successive phases occurs [24]. An extended

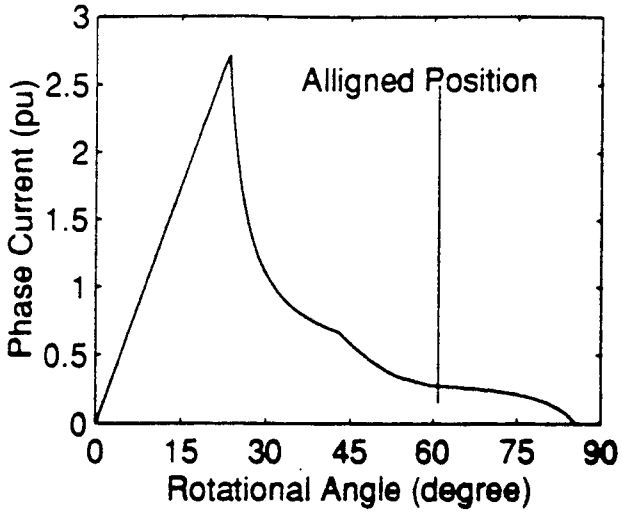

Fig. 10. Phase current of SRM in the extended speed constant power operation.

range of 2-3 times the base speed is usually possible using this control, as detailed in the simulation result shown in Fig. 9. The extended range for this particular motor is 2.5 times the base speed. Phase current of the simulated motor in this extended speed range of operation is shown in Fig. 10. This peaky nature of the current response, as detailed in Fig. 10, results in a high torque pulsation. The power factor for this mode of operation is poor. The simulation result shows that the pf increases monotonically from 0.58 to 0.62 over the range of the constant power operation. This is a drawback of SRM which can penalize the converter in some cases. But, the existence of a long tail of natural mode of operation, beyond the constant power range, can offset some of this disadvantage by making the motor power rating smaller. This will be illustrated in the following example. SRM very easily qualifies as a high speed motor.

Commutation requirement in SRM also necessitates the installation of an absolute position sensor on the motor shaft. Sensorless operations with various modulation techniques are, however, reported [25,26].

E. Design Example

We present a design example of the above motors in the constant power region. This example will help clarify the capabilities of these motors for vehicle applications.

EV data:

- Vehicle Rated Speed of 26.82 m/s (60 mph)
- Required acceleration of 26.82 m/s in 10 seconds.
- Vehicle maximum speed of 44.7 m/s (100 mph).
- Vehicle mass of 1450 kg.
- Rolling resistance coefficient of 0.013.
- Aerodynamic drag coefficient of 0.29.
- Frontal Area of 2.13 m^2.
- Wheel radius of 0.2794 m (11 inch).
- level ground.
- zero head wind.

Table II.

	Rated Speed (rpm)	Maximum Speed (rpm)	Constant Power Range	Power Factor
Induction	1750	8750	1:5	0.82
BLDC	4000	9000	1:2.25	0.93
SRM	4000	20000	1:3 Rest in Natural Mode	0.6

Table III

	Gear Ratio	Power Rating (kW)	Converter Rating (kVA)
Induction	5.7	65	79
BLDC	5.9	86	92
SRM	13	68	113

The motor data are shown in Table II. The motor data chosen are for the commercially available samples of these motors. Clearly, more specific motors can be designed for vehicle applications, but such data were not available for this paper. Based on the vehicle data, the power requirement to cruise at the maximum speed is 41 kW. The motor power for acceleration and converter volt-ampere (VA) requirement for each motor are shown in Table III.

The extended constant power range available from the induction motor clearly makes it highly favorable for vehicle application. The limited constant

0-7803-3292-X/96/$5.00 © 1996 IEEE

power range of the BLDC motor makes it appear inferior to the induction motor, despite its high power factor and high efficiency. The extremely high speed operation of the SRM and its relatively longer constant power range helps it to overcome some of the difficulty associated with its lower power factor operation. Furthermore, the SRM converter is simpler and easier to control.

IV. Conclusion

A comprehensive study of several most commonly used motors for possible EV and HEV application is presented. This study is based on our recent EV and HEV design principles presented in [6]. Several types of motors are studied in this context. It is concluded that the induction motor has clear advantages for EV and HEV, at the present. Brushless dc motor must be capable of high speeds to be competitive with the induction motor. The switched reluctance motor may be superior to both of these motors, for vehicle application, both in size and cost. However, more design and evaluation data is needed to verify this possibility.

V. References

[1] A. Alison, "Searching for perfect fuel ... in the clean air act", *Conference Proceedings of Environmental Vehicles*, 94, pp. 61-87, Dearborn, Jan, 1994.

[2] Barsony, "Infrastructure needs for EV and HEV", *NIST Workshop on Advanced Components for Electric and Hybrid Electric Vehicles*, pp. 14-23, Gaithersburg, MD, Oct., 1993.

[3] A. F. Burke, "Hybrid/Electric vehicle design options and evaluations", SAE paper # 920447, Feb., 1992.

[4] Automotive Handbook, Robert Bosch Gmbh, Germany, 1986.

[5] S. Singer and R. W. Erickson, "Power source element and its properties," *IEE Proc. Circuits Devices Syst.*, Vol. 141, No. 3, pp. 220-226, June, 1994.

[6] M. Ehsani, K. M. Rahman, and H. Toliyat, "Propulsion system design of electric and hybrid vehicles," to be published in *IEEE Trans. Industrial Electronics*.

[7] A. G. Erdman, G. N. Sandor, Mechanism Design: Analysis and Synthesis, Vol. I, New Jersy, Prentice-Hall, 1984.

[8] H. A. Toliyat, K. M. Rahman, and M. Ehsani, "Electric machines in electric and hybrid vehicle applications," *ICPE*, Seoul, Korea, 1995.

[9] P. C. Sen, Principles of Electric Machines and Power Electronics, New York, John Wiley and Sons, 1987.

[10] Andrezej M. Trzynadlowski, *The Field Oriented Principles in the Control of Induction Motor*, Kluwer Academic Publisher, Boston, 1994.

[11] A. Boglietti, P. Ferraris, and M. Lazzari, "A new design criteria for spindles induction motors controlled by field oriented technique", *Electric Machines and Power Systems*, vol. 21, pp. 171-182, 1993.

[12] T. Kume, T. Iwakane, T. Sawa, T. Yoshida, and I. Nagai, "A wide constant power range vector-controlled ac motor drive using winding changeover technique", *IEEE Trans. on Industry Applications*, vol. 27, No. 5, pp. 934-939, Sept./Oct., 1991.

[13] M. Osama and T. A. Lipo, "A new inverter control scheme for induction motor drives requiring wide speed range," *Proceedings of the IEEE-IAS Annual Meeting*, Orlando, 1995, pp. 350-355.

[14] R. J. Kerkman, T. M. Rowan and D. Leggate, "Indirect field-oriented control of an induction motor in the field-weakened region," *IEEE Trans. Industry Applications*, vol. 28, no. 4, pp. 850-57

[15] T. M. Rowan, R. J. Kerkman and T. A. Lipo, "Operation of a naturally sampled current regulators in the transition mode," *IEEE Trans. Industry Applications*, vol. 23, no. 4, pp. 587-595, July/August, 1987.

[16] T. M. Jahns, "Torque production in permanent magnet synchronous motor drives with rectangular current excitation," *IEEE Trans. Industry Application*, vol. 20, no. 4, pp. 803-813, July/Aug., 1984.

[17] R. C. Becerra and M. Ehsani, "High speed torque control of permanent brushless dc motors," *IEEE Trans. Industrial Electronics*, vol. IE-35, no. 3, pp. 402-406, August, 1988.

[18] S. K. Safi, P. P. Acarnley, and A. G. Jack, "Analysis and simulation of the high-speed torque performance of brushless dc motor drives", *IEE Proc. Electr. Power Appl.*, vol. 142, no. 3, May, 1995.

[19] C. C. Chan, J. Z. Jiang, G. H. Chen, X. Y. Wang, and K. T. Chau, "A novel high power density permanent magnet motor drive for electric vehicles," in *Proc. EVS11*, paper 8.06, 1992, pp. 1-12.

[20] T. M. Jahns, R. C. Becerra, and M. Ehsani, "Integrated current regulation for brushless ECM drive," *IEEE Trans. Power Electronics*, vol. 6, no. 1, pp. 118-26, Jan, 1991.

[21] R. C. Becerra, M. Ehsani, and T. M. Jahns, "Four-quadrant brushless ECM drive with integrated current regulation," *IEEE Trans. Industry Applications*, vol. IA-28, no. 4, pp. 202-209, July/August, 1992.

[22] K. J. Bins, K. M. Al-Aubidy, and D. W. Shimmin, "Implicit rotor position sensing using search coils for system-commutation permanent magnet drive system," *IEE Proceedings*, vol. 137, Pt. B, no. 4, pp. 253-258, July, 1990.

[23] P. W. Lee and C. Pollac, "Rotor position detection techniques for brushless permanent-magnet and reluctance motor drive," *Proceedings of IEEE-IAS Annual Meeting*, Houston, 1992, pp. 448-455.

[24] T. J. E. Miller, "Switched Reluctance Drive", Short Course, *IEEE-IAS Conference*, Seattle, 1990.

[25] M. Ehsani, "Position sensor elimination technique for the switched reluctance motor drive," U.S. patent No. 5,072,166, Dec. 1991.

[26] M. Ehsani, "Phase and amplitude modulation techniques for rotor position sensing in switched reluctance motors," U.S. patent no. 5,291,115, March 1994.

Advantages of Switched Reluctance Motor Applications to EV and HEV: Design and Control Issues

Khwaja M. Rahman	Babak Fahimi	Gopalakrishnan Suresh	Mehrdad Ehsani*
Student Member, IEEE	Student Member, IEEE	Student Member, IEEE	Fellow, IEEE

Texas A&M University
Texas Applied Power Electronics Center
Department of Electrical Engineering
College Station, TX 77843-3128
Tel: (409) 845-7582
Fax: (409) 862-1976
Email: ehsani@ee.tamu.edu

Abstract- Land vehicles need their drivetrain to operate entirely in constant power in order to meet their operational constraints, such as initial acceleration and gradability, with minimum power rating. The internal combustion engine (ICE) is inappropriate for producing this torque-speed profile. Therefore, multiple gear transmission is necessary with the ICE in a vehicle. Some electric machines, if designed and controlled appropriately, are capable of producing an extended constant power range.

The purpose of this paper is to investigate the capabilities of switched reluctance motor (SRM) for EV and HEV applications. This investigation will be carried out in two steps. The first step involves the machine design and the finite element analysis to obtain the static characteristic of the motor. In the second step, the finite element field solutions are used in the development of a dynamic model to investigate the dynamic performance of the designed motor. Several 8-6 and 6-4 SRM geometries will be investigated. Effects of different stator and rotor pole widths and pole heights on the steady state as well as on the dynamic performance of the motor will be studied. The air gap for each motor will be made as small as manufacturally possible. Effects of different level of magnetic saturation on the steady state and on the dynamic performance of the motor will be also studied. The performances to be compared for each design motor are. i) the range of the constant power operation, ii) drive efficiency in this extended constant power range, iii) the energy ratio (power factor) in this operational range, and iv) the short time overload capability. The first performance index defines the rated power of the motor. Longer the constant power range lower is the power rating for the same vehicle performances. Hence, special emphasis will be given on this. The rest of the performance indices are self explanatory. In the high speed operation of the SRM, there will be considerable phase overlapping. Hence, special designing might be needed to prevent the back iron from saturating. However, since flux peaking of each phase occurs at different rotor positions, the phase overlapping might not necessitate special designing of the back iron. However, the possibility of back iron being saturated will not be neglected and will be investigated. An optimal control scheme of SRM will be presented which extends the constant power range beyond those of other motors. Performance comparison will be made based on this control scheme. This optimal control scheme aims at finding the optimal phase turn-on and turn-off angles which maximizes the constant power range with maximum torque per ampere. Simulation results of the designed SRM in the vehicle operation in standard highway and city driving will be presented. To demonstrate the effectiveness of the optimal control scheme experimental results will be presented, however, for a reduced size motor available commercially. Finally, the performance of the designed SRM will be compared with performances of other potential EV and HEV motors.

* corresponding author

Advantages of Switched Reluctance Motor Applications to EV and HEV: Design and Control Issues

I. Introduction

Switched reluctance motor (SRM) is gaining much interest as candidate for Electric Vehicle (EV) and Hybrid Electric Vehicle (HEV) electric propulsion for its simple and rugged construction, ability of extremely high speed operation, and hazard free operation. Perhaps in view of these characteristics, one of the early SRMs was designed and built for electric vehicle application [1]. In designing this SRM, the major attention was given on the efficiency of the drive. Later, an optimized design method of SRM was reported in [2] for EV application. The design optimization was based on an analytical model of SRM, similar to the one developed by Corda and Stephenson [3]. The inaccuracy of the analytical model based on which the optimization was carried out, was the major flaw of this method. Moreover, the efficiency optimization was carried out for the constant speed operation of the drive with non-optimal control. Like the previous design, the special emphasis was given in this design on the drive efficiency and additionally on the drive cost. Most recently, a 100 hp SRM was designed and built in [4] for electric vehicle application. No special control scheme, design method, or optimization technique were, however, presented.

While designing an SRM in all the previous methods, no attention were given to the vehicle dynamics. Vehicle dynamics dictate a special torque-speed profile for its propulsion system. Our recent study has shown that, a vehicle, in order to meet its operational constraints such as initial acceleration and gradability with minimum power, needs the powertrain to operate entirely in constant power [5]. The power rating of a motor that deviates from the constant power regime can be as much as two times that of a motor operating at constant power throughout its speed range in a vehicle. The hyperbolic constant power profile, shown in Fig. 1, therefore, represents the theoretically optimal torque-speed profile of any motor drive for vehicle application. Operation entirely in constant power is not possible for any practical drive. An extended constant power range is, however, possible if the motor is appropriately designed and its control strategy are properly selected.

This paper will investigate the capabilities of SRM for vehicle traction. For this purpose, several designed SRM and an optimal control scheme will be presented which will maximize the constant horse power range. A 2-D finite element analysis will be used to obtain the static characteristics of designed motors. The finite element field solutions will be then used in the development of a dynamic model to investigate the steady state and the dynamic performance of the designed motors. An optimal control scheme of SRM will be presented which extends the constant

power range beyond those of other motors. Performance comparison will be made based on this control scheme This optimal control scheme aims at finding the optimal phase turn-on and turn-off angles which maximizes the constant power range. Several 8-6 and 6-4 SRM geometries will be investigated. Effects of different stator and rotor pole geometries and the level of saturation on the steady state as well as on the dynamic performance of the motor will be studied. The air gap for each motor will be made as small as manufacturally possible. In the high speed operation of the SRM, there will be considerable phase overlapping. Hence, thicker back iron than normal might be needed to prevent it from saturating. However, since flux peaking of each phases occur at different rotor positions, the phase overlapping might not bring the back iron into saturation. However, the possibility of back iron being saturated will not be neglected and will be investigated especially, during the short time overloading of the motor. Besides the range of the constant power operation, the other performances which will be investigated for each designed motor are, i) the drive efficiency in this extended constant power range, ii) the energy ratio (power factor) in this operational range, and iii) the short time overload capability. Simulation results of the designed SRMs in the vehicle operation in standard highway and city driving will be presented. To demonstrate the effectiveness of the optimal control scheme experimental results will be presented, however, for a reduced size motor available commercially. Finally, the performance of the designed SRM will be compared with performances of other potential EV and HEV motors.

II. SRM Static Characteristics

To investigate the dynamic and steady state performances of each SRM geometry considered in this paper, the static torque and flux linkage characteristics as functions of stator current and rotor position are required. The non-linearity of the SRM owing to its saturation region of operation, however, complicates the analysis. Several non-linear analytic models of SRM are presented in the literature to obtain the static data [3,6-8]. For accuracy we will, however, rely on the finite element analysis to obtain the static data. Although, a two dimensional finite element analysis tends to give an inaccurate unaligned inductance value, to compromise accuracy of a three dimensional analysis over speed, we will use a two dimensional (2-D) analysis. Finite element analysis will be performed on several 6-4 and 8-6 SRM geometries with varying stator and rotor pole widths and heights and different level of magnetic saturations. Fig 2 shows field solutions of one SRM geometry obtained using 2-D finite element analysis. Later, the static torque and flux linkage data obtained from the finite element analysis will be used in the dynamic model to determine the drive performance with optimal control.

III. Dynamic SRM Model

A block diagram of the dynamic SRM model is shown in Fig. 3. The static flux linkage and torque data as a function of the stator current and rotor position obtained from the finite element analysis for each SRM geometry are used in the dynamic model in order to include the effect of magnetic non-linearity. This model is used to predict the drive performance at steady state and in the dynamics. The optimal control scheme is also established by using the dynamic model. A linear model of the converter is used in the dynamic model. The switch and diode parameters used in the dynamic model, are obtained from the manufacturer's provided data.

IV. Optimal Control Scheme

Base speed in any motor is defined as the speed at which the back emf equals the bus voltage. Motor also reaches its rated power at this speed for rated excitation (current). Torque in SRM below base speed, when the back emf is lower than the bus voltage is controlled, like all other motors, by the PWM control of current. Above base speed, due to the high back emf which can not be field weakened, PWM control of current is not possible. Operation in constant power is made possible in this motor by the phase advancing of the stator phase current until overlapping between the successive phases occurs [9]. Torque control below base speed can be optimized by the stator current profiling [10,11]. However, above base speed the only control parameters are the phase turn-on and the turn-off angles. The phase turn-on and the turn-off angles can be optimally controlled above base speed to maximize the range of the constant power operation with maximum torque per ampere. To find the optimal turn-on and the turn-off angles the dynamic model developed in the earlier section is used. The search procedure for the optimal angles is lengthy and time consuming. However, any standard root seeking methods, such as the Secant method [12], may be used to accelerate the speed of the searching process. After series of iterations, the dynamic model finds the optimal turn-on and turn-off angles. To implement the control scheme in real time, a Neural Network based controller may be implemented [10].

V. Simulation Results

Simulation results presented in this section are of a 8-6 SRM. This motor will be later used for the experimental verification of the optimal control scheme. The experimental motor is a much smaller motor than can be used for EV and HEV applications. However, for the experimental verification of the optimal control scheme only, the performance investigation of this motor should be adequate. The static characteristics data (of this motor) to be used in the dynamic model, is generated experimentally (Fig. 4.). The block diagram of the experimental setup for obtaining the static data is shown in Fig. 5. Fig. 6. shows the optimal turn-on and the turn-off angles, for an extended constant power operation of

the experimental motor, as a function of the rotor speed. These angles are obtained from the dynamic model after an extensive search using the Secant method. The developed average torque in this constant power operation is also shown in the figure. As we can see the range of the extended constant power operation is more than six times the base speed. The long constant power range is obviously desirable for vehicle application.

However, the high speed mode of operation causes torque to be pulsatory. This pulsatory torque may cause some speed vibration if the inertia is low. Developed torque and the phase current at a speed of five times the base speed is shown in Fig. 7. Torque pulsation for vehicle application may not be a major problem. The high frequency torque pulsation at high speed may not have enough energy to cause any speed vibration in the high inertia vehicle load. The rms current at the high speed operation is shown in Fig. 8 as a function of the rotor speed. Current needed to maintain constant power decreases as the speed increases. The decrease in current magnitude with the increase in the speed for the same output power, indicates an improvement on the power factor (energy ratio) of operation of the motor. The power factor in this range of operation is plotted in Fig. 9. In other words, more power than rated should be available from the motor without increasing the rated current of the motor or the bus voltage. To investigate this, a second set of search for turn-on and turn-off angles is performed which maximize the output torque when constant rated current is maintained throughout the high speed operation of the motor. It may be mentioned here that, to maximize output torque, the stator current is usually held constant for most other motors, such as induction, dc etc., during the constant power operation. The results of these search is made available in Fig. 10 (the dashed curves). The maximum output power is plotted as a percentage of the rated power and as a function of the rotor speed. The current through out the total speed range is maintained constant at its rated value in this high speed operation. The optimal phase turn-on and the turn-off angles for the power output of Fig. 10(a) (the dashed curve) are plotted in Fig. 10(b) (the dashed curves). The output power is increased beyond the rated power considerably as can be seen in the figure. The peak is about 1.6 times the rated power, which occurs for this motor at about four times the base speed. The output power falls below the rated power roughly beyond six times the base speed. The power factor is improved further in the over power mode of operation. The resulted power factor is plotted in Fig. 11. The energy loop computed at the peak power of Fig. 10 is plotted in Fig. 12. The power at the end of the over power operation falls sharply as we can see in Fig. 10(a) (the dashed curve). The constant power range is also slightly reduced if compared to the range of Fig. 6. From Fig. 7, we can see that current actually reduces at higher speeds to maintain constant power of Fig. 6. Which indicates that above a certain speed, at high speed operation, more power may be obtained from the motor by lowering the current below the rated

instead of maintaining the rated current at all speeds. To investigate this possibility another search is made using the dynamic model. The findings are also plotted in Fig 10 (the solid line curve). In this search, stator current is allowed to lower below the rated if that results in a higher torque. We can see that beyond a certain speed (5 pu, roughly), it is advantageous to lower the current below the rated value instead of maintaining the rated current. The current along with the turn-on and the turn-off angles are plotted in Fig. 10(b) (the solid line curves). Beyond this speed (5 pu), the negative torque starts to dominate if the rated current is maintained, hence, power can actually be increased by lowering the current. Finally, the phase current peaks are plotted in Fig. 13 in per unit (normalized to the rated current) as a function of the rotor speed. Current peaks, as shown in Fig. 13, are lower than the rated current for most of the speed range. Before the peak starts to increase beyond the rated current magnitude (roughly above speed 4.5 pu) we, however, reduce the current to obtain more power (Fig. 10). Hence, current peaks are expected to lie below the rated motor current at all speeds. More results will be presented for SRMs designed specifically for EV and HEV applications in the full paper.

The extremely long range (exceeding six times the base speed for this motor) of overpowering in SRM is possible due to the fact that it (SRM) has a high phase winding inductance when the poles start overlapping. The Ldi/dt drop in the inductance takes care the difference in voltage between the high back emf and the bus voltage in the high speed operation of the SRM. Since the inductance is high, rate of drop of current is not required to be high. Hence, positive torque over a longer period can be obtained provided, the phases are turned on and turned off in appropriate times. We would like to point out further that, although, the brushless dc (BLDC) motor in the constant power range is controlled similarly [13], neither overpowering nor an extended constant power range would be possible in BLDC. Surface mounting of the permanent magnets increases the air gap in BLDC motor. Hence, the stator inductance is reduced considerably in BLDC motor. The mutual inductances between phases reduce the stator inductance further. As a result, current in the high speed range drops rapidly (high di/dt to compensate for the lower inductance) resulting corresponding drop in the torque and the mechanical power output.

The torque-speed characteristics Fig. 10 will make SRM very attractive for EV and HEV applications. If the power rating of Fig. 10 can be scaled to the level of EV and HEV application, the SRM performance may be compared to the other potential EV/HEV motors. For this purpose we chose the following EV

- vehicle rated speed of 26.82 m/s (60 mi/h);
- required acceleration of 26.82 m/s in 10 s;

- vehicle maximum speed of 44.7 m/s (100 mi/h);
- vehicle mass of 1450 kg;
- rolling resistance coefficient of 0.013;
- aerodynamic drag coefficient of 0.29;
- frontal area of 2.13 m^2;
- wheel radius of 0.2794 m (11 in);
- level ground
- zero head wind

The motor data are shown in Table I. The motor data chosen for induction and BLDC are for the commercially available samples of these motors. Clearly, more specific motors can be designed for vehicle applications, but such data were not available for this paper. The constant power range for induction motor is usually limited to 3-4 times the base speed. The speed range of BLDC is restricted further. A range over two times the base speed is usually difficult with this motor. The interior permanent magnet synchronous motor is capable of producing a long constant power, however, with a rotor designed with high saliency [14]. The high saliency rotor (axial lamination), reduces the maximum speed of the motor considerably. Hence, the test data of constant power range was presented in that paper at a reduced power level (1/3 the bus voltage). The motor power for acceleration for each motors, considered here, are shown in Table II. Clearly, SRM is favorable among these motors for its unique torque-speed profile and its extremely high speed capability. However, a more valid comparison would require considerations of many other factors, such as the drive kVA rating, efficiency of operation etc. More specific SRMs will be designed for the full paper to make this comparison more realistic. The other factors will be addressed in detailed for each designed SRM. The more valid comparison with potential EV and HEV motors will be then made.

VI. Conclusion

Simulation results exhibit some interesting characteristics of an SRM when controlled optimally. Available power from the motor, with this control, can be increased beyond the rated power of the motor during the high speed operation, without increasing the bus voltage and exceeding the rated current of the motor. The range of this overpowering mode is more than six times the base speed for the experiment motor. It is also shown that beyond a certain speed, it is necessary to reduce the current below the rated value in order to get more power. This unique characteristic of SRM makes it highly attractive for vehicle application. Simulation results indicate that, superior

performances than BLDC and induction motor may be possible with SRM. In the full paper, more specific 6-4 and 8-6 SRM geometries will be designed for EV and HEV applications. Their performances will be investigated based on the presented optimal control scheme. More realistic conclusion regarding the capabilities of SRM in vehicle application would then be made.

Acknowledgments

The support of Texas Higher Education Coordinating Board Advanced Technology Program, Texas Transportation Institute, and Texas Instrument Digital Control Systems Division, for this research is gratefully acknowledged.

VII. References

[1] P. J. Blake, R. M. Davis, W. F. Ray, N. N. Fulton, P. J. Lawrenson, and J. M. Stefenson, "The control of switched reluctance motors for battery electric road vehicles," *International Conference on PEVD*, pp. 361-364, May, 1984.

[2] J. H. Lang and F. J. Vallese, "Variable reluctance motor drives for electric propulsion," *United States Department of Energy Report*, DOE/CS-54209-26, May, 1, 1985.

[3] J. Corda and J. M. Stephenson, "Analytical estimation of the minimum and maximum inductances of a doubly-salient motor," *on Proc. Int. Conf. Stepping Motors Syst. (University of Leeds)*, 1979, pp. 50-59.

[4] T. Uematsu and R. S. Wallace, "Design of a 100 kW switched reluctance motor for electric vehicle propulsion," *APEC*, pp. 411-415, 1995.

[5] M. Ehsani, K. M. Rahman, and H. Toliyat, "Propulsion system design of electric and hybrid vehicles," *IEEE Trans. on Industrial Electronics*, vol. 44, no. 1, February 1997.

[6] J. V. Byrne, and J. B. O'dwyer, "Saturable variable reluctance machine simulation using exponential functions," *Proceedings of the International conference on Stepping Motors and Systems*, University of Leeds, UK, 1976, pp. 11-16.

[7] T. J. E. Miller and M, McGlip, "Nonlinear theory of switched reluctance motor for rapid computer-aided design," *IEE Proceedings*, vol. 137, Pt. B, No. 6, pp. 337-347, Nov. 1990.

[8] D. A. Torrey, X.-M. Niu, and E. J. Unkauf, "Analytical modeling of variable-reluctance machine magnetization characteristics," *IEE Proc. Electr. Power Appl.*, vol. 142, no. 1, pp. 14-22, Jan. 1995.

[9] T. J. E. Miller, "Switched reluctance motor and their control," Clarendon Press, 1993.

[10] K. M. Rahman, A. V. Rajarathnam, and M. Ehsani, "Optimized instantaneous torque control of switched reluctance motor by neural network," *IEEE IAS Conference Record*, New Orleans, Oct. 1997.

[11] I. Husain, K. R. Ramani, and M. Ehsani, "Torque ripple minimization in switched reluctance motor drives by PWM current control," *IEEE Trans. on Power Electronics*, vol. 11, no. 1, pp. 83-88, January, 1996.

[12] A. Ralston and P. Rabinowitz, *A First Course in Numerical Analysis*, 2nd ed. New York: McGraw-Hill, 1978.

[13] T. J. E. Miller, *Brushless Permanent-Magnet and Reluctance Motor Drives*, Oxford Science Publication, Oxford, 1989.

[14] W. L. Soong and T. J. E. Miller, "Field weakening performance of brushless synchronous AC motor drives," *IEE Proc.-Electr. Power Appl.*, Vol. 141, No. 6, pp. 331-340, November 1994.

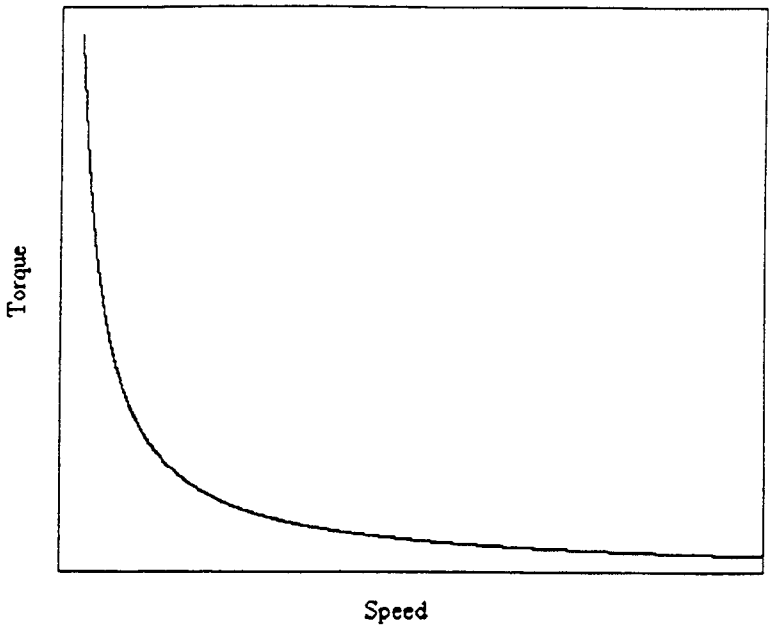

Fig. 1. Optimal Torque Speed Profile for EV and HEV drivetrain.

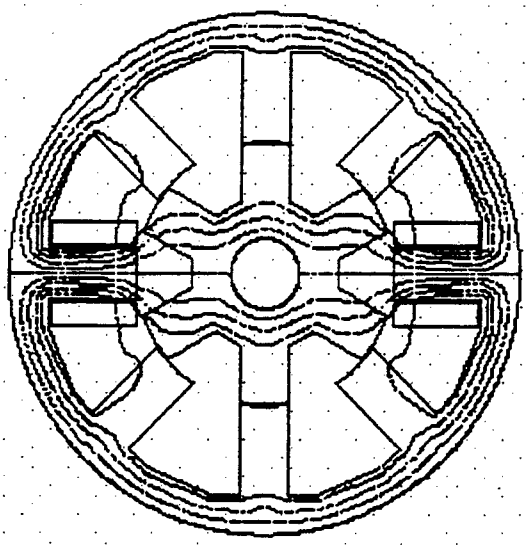

Fig. 2. A 2-D finite element field plot for a 8-6 SRM.

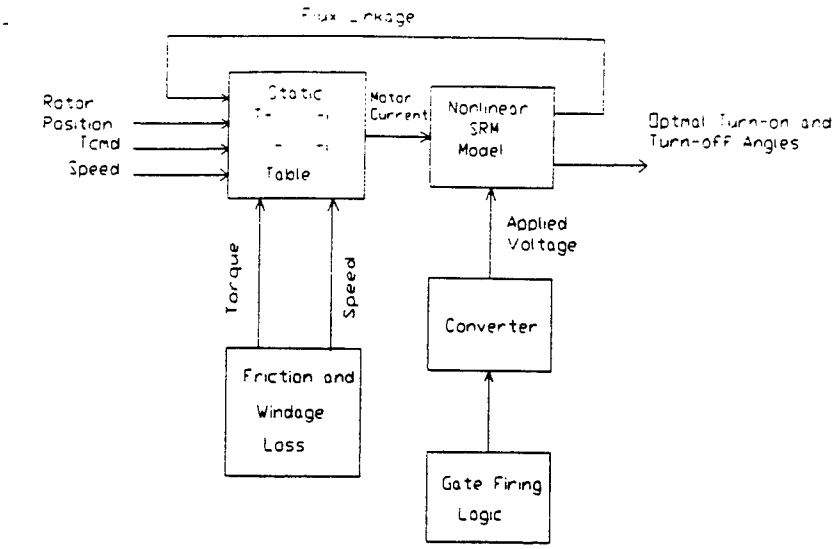

Fig. 3. A block diagram of the dynamic SRM model.

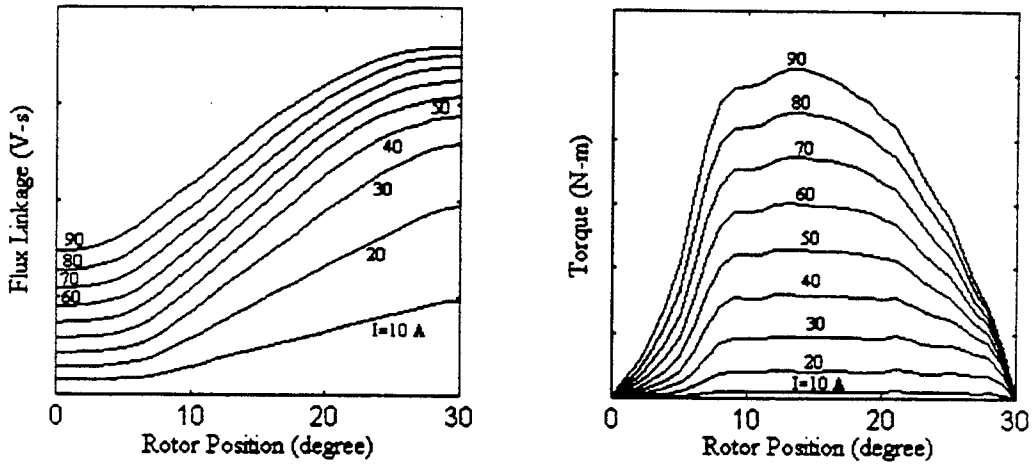

Fig. 4. Static flux linkage (a) and torque (b) data as a function of current and rotor position.

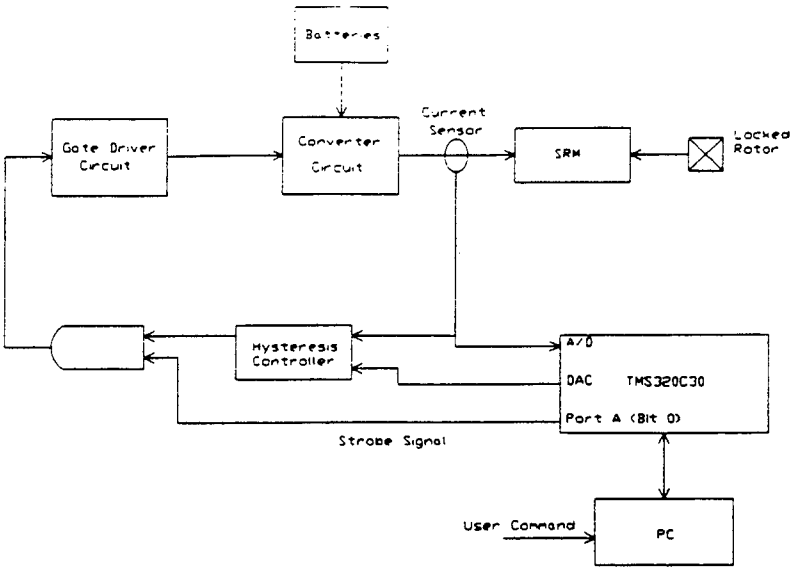

Fig. 5. DSP setup for generating static torque and flux linkage data.

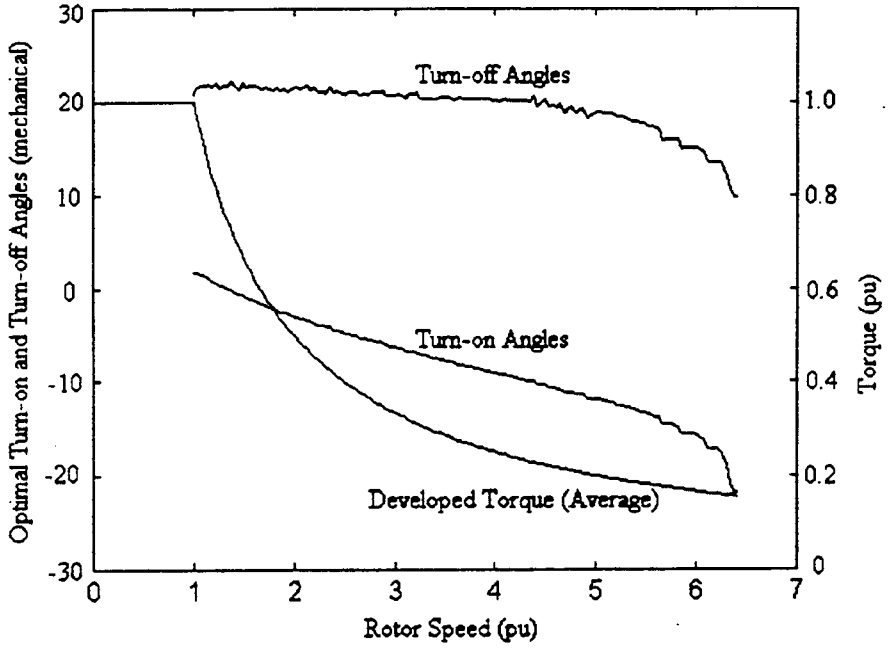

Fig. 6. Optimal turn-on and turn-off angles for extended constant power operation.

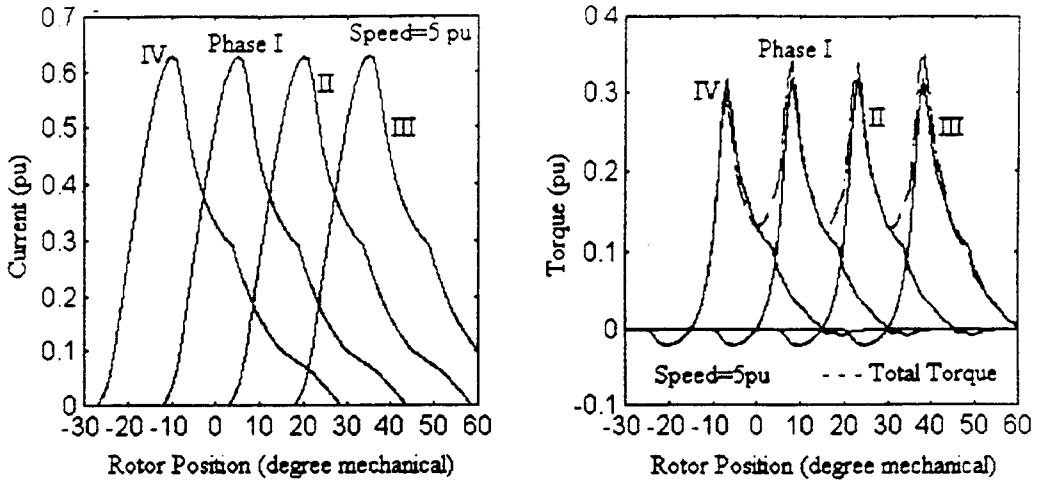

(a) (b)

Fig. 7. Phase current (a) and developed torque (b) at high speed.

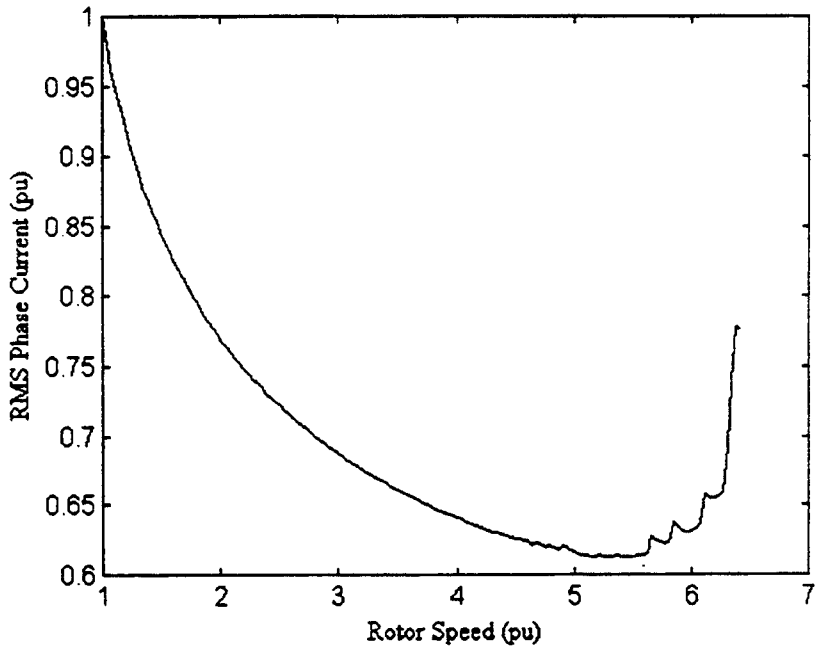

Fig. 8. Phase current (rms) at high speed.

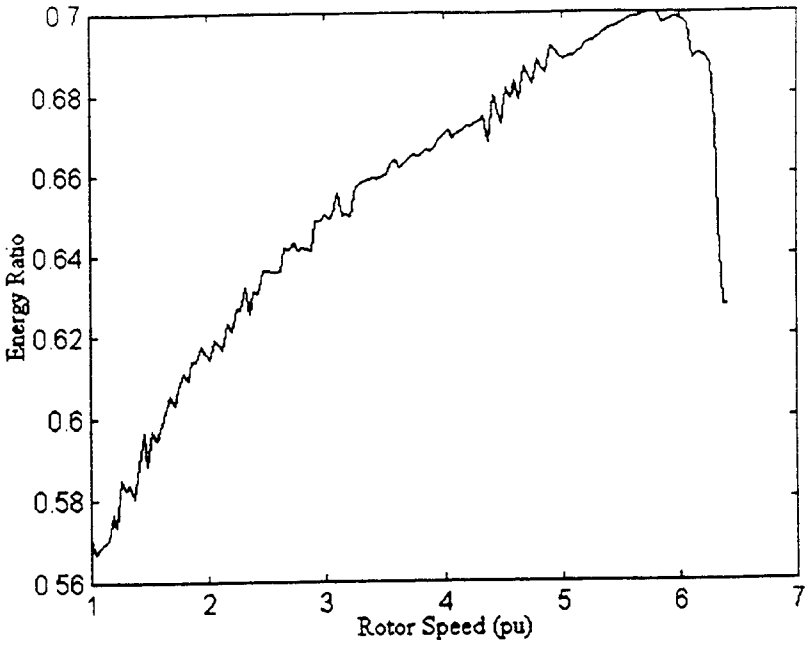

Fig. 9. Motor energy ratio (power factor) at high speed.

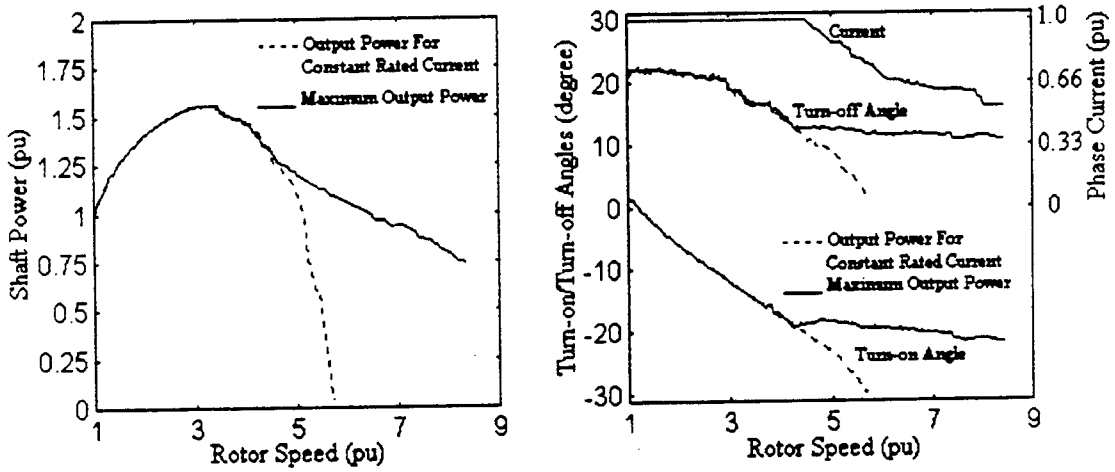

(a) (b)

Fig. 10. Output power (a) and turn-on, turn-off and phase current (b) for maintaining rated current (dashed curve) and for maximum power (solid line curve).

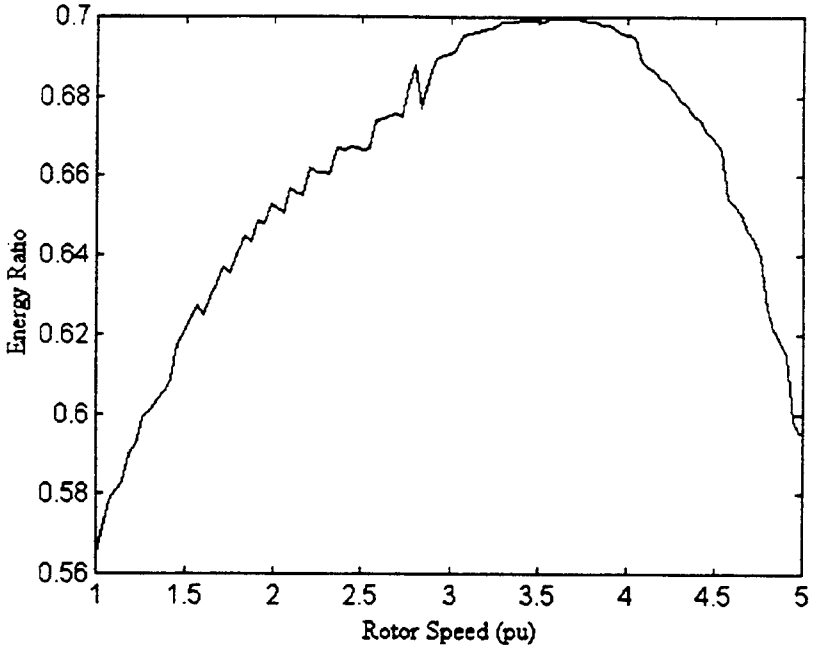

Fig. 11. Energy ratio (power factor) for constant current operation at high speed.

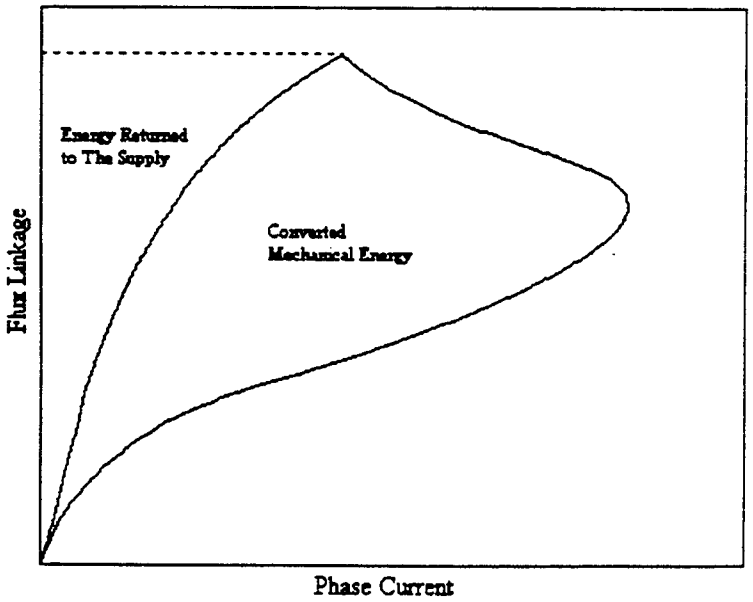

Fig. 12. The energy conversion loop for the peak power of Fig. 10.

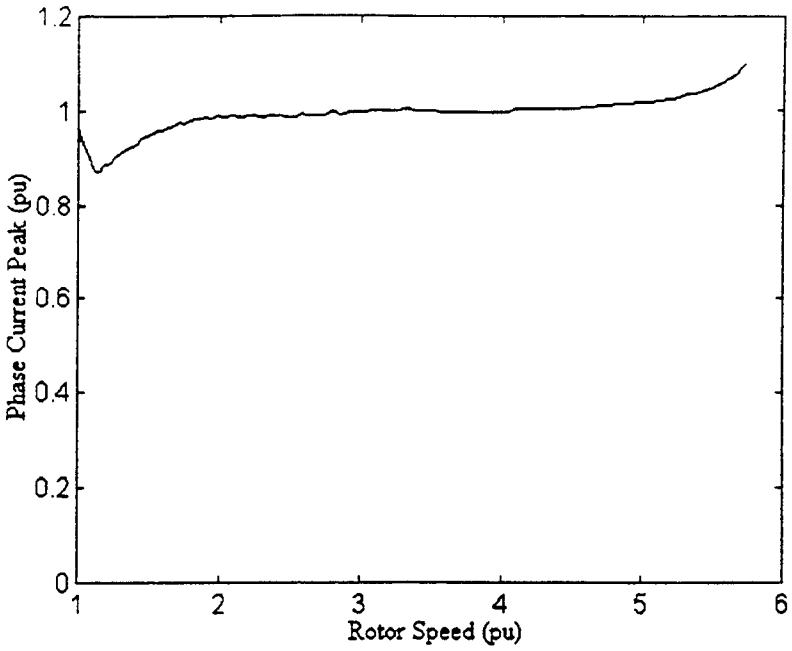

Fig. 13. Phase current peak (normalized to the rated current) as a function of the rotor speed.

Table I

Motor Data

	Rated Speed (rpm)	Maximum Speed (rpm)	Constant Power Range
Induction	1750	7000	1:4
BLDC	2000	4500	1:2.25
SRM	2000	13000	1:6.5

Table II

Rated Power Requirements For The Motors of Table I For A Typical EV Application

	Gear Ratio	Power Rating (kW)
Induction	4.55	67
BLDC	2.925	87
SRM	8.45	46

Current Status and Future Trends of More Electric Cars' Power Systems

A. Emadi
Student Member, IEEE

A. V. Rajarathnam
Student Member, IEEE

M. Ehsani*
Fellow, IEEE

*corresponding author
Texas Applied Power Electronics Center
Department of Electrical Engineering
Texas A&M University
College Station, TX 77843-3128
Phone:(409)845-7582
Fax:(409)862-1976
E-mail:ehsani@ee.tamu.edu

Abstract- The More Electric Cars (MEC) concept is based on utilizing electric power to drive automobile subsystems which historically have been driven by a combination of mechanical, hydraulic, and electric power transfer systems. Increasing use of electric power (More Electric) is seen as the direction of technological opportunity for automotive power systems based on rapidly evolving technology advancements in power electronics, fault tolerant electrical power distribution systems, and electric-driven machines. This paper will address the fundamental problems faced in automotive power systems. Furthermore, a brief description of the conventional automotive power systems, their disadvantages, scope for improvement, future electric loads, advanced distribution system architectures, role of electronics and microprocessors, stability analysis, and current trends in automobile power system research will be given. Finally, this paper conclude with a brief outline of the advancement to be made in the future.

I. INTRODUCTION

The electrical systems in the early automobiles were introduced mainly for lighting, cranking, and battery charging purposes. But, in the recent years, electrical and electronic system components, circuits and accessories in an automobile have steadily increased, both in complexity and quantity. In addition, the electrical systems in a modern automobile perform more duties as some of the conventional mechanical loads are being replaced by electric loads [1]-[3].

The need for improvement in comfort, convenience, entertainment, safety, security, communications, and environmental concerns necessitates the need for improved electrical systems. This has motivated the research in restructuring the entire power system architecture in the automobiles [4]-[8].

At present most automobiles use a 12V DC electrical system with point-to-point wiring. Since the capability of this architecture in meeting the needs of future electrical loads is questionable, alternative architectures must be considered [4]-[6]. One way to simplify the architecture is by changing the control strategy [4]. Also, there is a need for advanced automotive power systems which includes multi-voltage level system, separate

power and signal buses, replacement of mechanical loads with electrical loads [5]-[7]. In [9] insertion of a DC/DC converter between the automobile battery and electrical loads is proposed. This would allow gradual conversion to higher battery voltage, regulation of DC distribution voltage, and multiple distribution voltage levels. However, a higher voltage system that is compatible with the current 12V DC architecture will be preferred during the transition to new system design [8]-[11].

There are opportunities in the following areas of the automotive power system - improved starting, integrated management of power generation and demand, higher system integrity, higher efficiency, and improvement of the vehicle electrical environment, giving benefit in component cost. These can be achieved by multi-voltage level system, a distribution architecture with a separate communication bus and replacement of some conventional, engine driven, mechanical loads with electric loads to provide an improved efficiency and packing flexibility among several advantages. There will be considerable increase in power requirements due to introduction of new functions like active suspension and catalyst preheater, and the electrification of the present functions like power steering and engine valves.

The role of power electronics in the automobiles will make significant impact in the future automobiles [3]. Further, the future for automotive electronics is bright. Electronic solutions have proven to be reliable over time and have enabled carmakers to solve problems otherwise unsolvable [12]-[15]. Now, it is obvious that electronics could provide the capability to solve automotive problems that defined conventional mechanical or electromechanical approaches [13]-[15]. On the other hand, microprocessor technology has become an essential technology for future automotive electronics. As advances in semiconductor technology allow more functions on a single chip, issues of reduced design cycle times have become a serious challenge [16].

This paper briefly discusses about the conventional automotive power systems, their disadvantages, scope for improvement, future electric loads, advanced distribution system architectures, role of electronics and microprocessors, stability analysis, current trends in automobile power system research and concludes with a brief outline of the advancement to be made in the future.

II. HISTORY OF AUTOMOTIVE POWER SYSTEMS

Electrical systems for vehicle lighting appeared about 80 years ago, using first 4V and then 8V batteries, which were charged from an external supply such as low tension radio batteries. When dynamos began to be fitted, at the beginning of the first world war, there were 6, 8 and 12V systems. Electric starting came into general use between the wars, and the car electrical system standardized on 12V-except for the Ford, which followed American practice and continued to use 6V into the 1950s. Cars with 6V systems had the starting problems: connectors that went open circuit, trafficators that had to be thumped on the door pillar to make them work and wiring that overheated.

In the 1960s, alternators were gradually introduced in place of dynamos, so that by 1975 they were a standard fitment. This allowed the use of a wide range of electrical accessories, ranging from heated rear windows to electrically driven radiator cooling fans. More recently, electronic fuel injection has added to the electrical load by requiring an

electrically driven fuel pump. Air conditioning adds to the electrical loads and is now being fitted to top models.

Diodes were the first solid state electronic device to be used in the automobiles. They accompanied the introduction of the alternator in the early 60's, and the application of transistors was extended to the regulator. It was not until the late 70's that the microprocessor was introduced, allowing the extensive use of sensors and controls to accommodate increasingly sever emissions and fuel economy regulations [1].

III. CONVENTIONAL AUTOMOTIVE ELECTRICAL SYSTEMS

Fig. 1 shows the conventional electrical distribution system for automobiles [2]. This has a single voltage level i.e., 12V DC, with the loads being controlled by manual switches and relays. This distribution network is a point-to-point topology in which all the electrical wiring aggregates at one or two fuse boxes from which it is distributed to different loads through relays and switches of the dashboard control. This kind of distribution network leads to expensive, complicated and heavy wiring circuits.

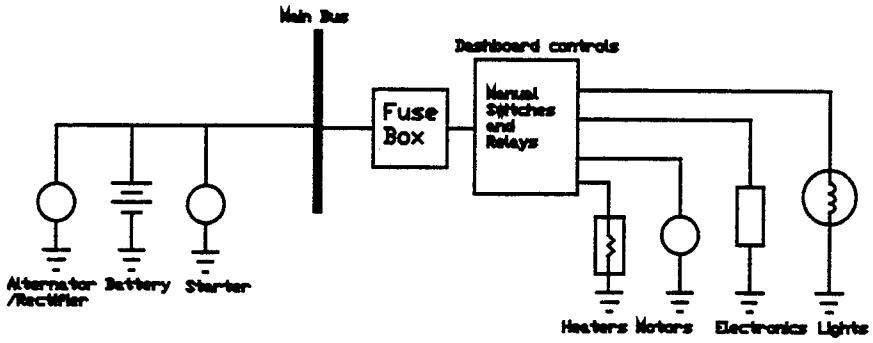

Fig. 1. Conventional 12V DC distribution system architecture

The present average power demand in an automobile is around 800W. The voltage in a 12V system actually varies between 9V and 16V, depending on the alternator output current, battery age and state of charge and other factors. The conventional electrical system in an automobile can be divided into the following subsystems.

A. Energy Storage System

Batteries are used in the automobiles for energy storage purposes. They are needed because the automobile requires a high quality power source for the vehicle to be independent and self starting. Their primary functions are to provide large current to crank the engine, supply electrical power for accessories for a reasonable period of time when the engine is not running or when the system demand exceeds that of generator/alternator output, and act as stabilizer, maintaining voltage levels for electrical distribution circuits.

Batteries commonly used in automobiles are the electro-chemical secondary cells in which the chemical reactions are reversible. Lead-acid batteries are commonly used because of their relatively low cost, high voltage per cell and good power capability, acceptable constant voltage charging characteristics, less or no maintenance, and their capability of delivering high currents in a short period of time. However, they have some

disadvantages: relatively low energy storage per unit weight, not very robust, poor performance at low temperatures , and explosive nature.

Experiments using a 20 Amps supply demonstrate just how dependent the battery is on the actual charging voltage. Typically, a car may require to be driven for either 500 or 100 miles to recharge its battery from 50% to 90% if the alternator output is held to either 13.2 or 14.0 volts. This effect shows how important it is for the charging circuit to be improved and any means of increasing the voltage at the battery considered.

Alternative batteries like Ni-Cd has better performance and life but are expensive. Also super capacitors are used in automotive applications. Their advantages include more rapid recharge and discharge capabilities, much larger life charge/discharge cycle life, and energy available directly measurable in terms of terminal voltage. However, they have certain limitations like high leakage current, failure modes and life expectancy yet to be determined, and cost unknown [10].

It seems there won't be any cost effectiveness for general energy storage other than the lead acid battery unless there is a drastic improvement in the development of new advanced battery technology.

In future cars equipped with electronic components we come into critical situations, when the battery state of charge is low and the voltage in the system breaks down during cold cranking. Beside of the possibility to protect every electronic part, like memories, by individual small batteries it seems to be more economic to think about a central small battery which is able to avoid a break-down of the voltage in the branches of the electrical network which contain sensitive parts [11]. This solution becomes even more advantageous when the amount of electronic equipment in standard cars is increasing. These batteries may be of nominal tensions below 12V, for example 8V, and contain only small capacities (Fig. 2).

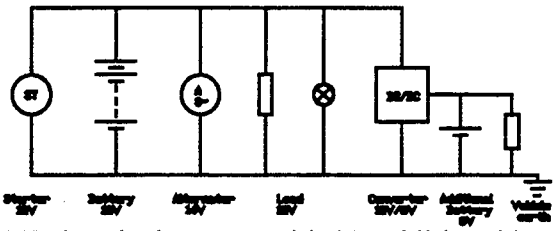

Fig. 2. 12V electrical system with 8V additional battery [11]

B. Charging System

Their primary task is to charge the battery while supplying electrical energy to operate other accessories. This is an integrated system of alternator, three-phase diode bridge rectifier and regulator. The voltage is regulated to a nominal of around 14.2V DC. The alternator used in automobiles has a poor characteristics with efficiency of around 50% and a high armature reactance. This means a poor fuel economy and the machine has to withstand a thermal stress of around 1.5kW. The high armature reactance implies that the stator core must be designed for unnecessary high flux for the terminal voltage, adding to cost and weight. Also, since the voltage has to be regulated at 14.2V DC independent of the speed, the machine capability is being restricted to low voltage output even at high speeds because of the system architecture. The present alternator can supply

effectively only up to 120A. With the increase in electrical loads in the future, a better design of the alternator is necessary.

The field circuit is energized by the battery at lower alternator speeds. The field relay is essential in those applications to prevent the battery from being discharged when engine is not in operation. Regulator operating current drawn from the battery is too low to cause a battery rundown. The regulator provides limiting by turning off the field current when the system voltage reaches a predetermined value. Some regulators provide temperature compensation that reduces the system voltage at high temperatures to reduce battery overcharge current.

C. Cranking System

This consists of a cranking motor, battery, control switches and interconnecting wiring. A typical 12/24V charging and 24V cranking system used in trucks is shown in Fig. 3. Cranking motors are DC series motors supplied by the battery which rotates the engine crankshaft through a pinion and flywheel ring gear. Cranking currents can be as high as 1600A with a peak reaching around 2500A for a fraction of a second at starting. This current is transferred from the battery through cables, terminals, and connectors. Resistance of this path has to be restricted to prevent excessive voltage drop that may result in malfunction of the motor. Control circuits that energize the motor include solenoid, switches and relays.

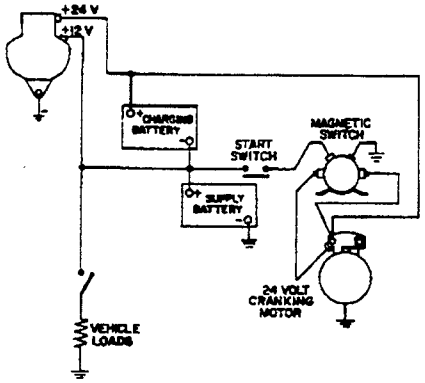

Fig. 3. Typical 12/24V charging and 24V cranking system for trucks [7]

D. Ignition System

The primary tasks of an ignition system are generating a voltage spike using the low battery voltage, delivering the voltage surge to each spark plug with correct timing to give maximum power, good fuel economy and low exhaust emissions, and establishing spark with enough intensity and for sufficient duration to ignite fuel/air mixture.

A typical 12V DC ignition system includes a battery charging system, a distributor with a shaft that runs at half the speed of the engine speed, a pulse transformer to transform the low system voltage to high voltage to establish an arc at the spark plugs, a secondary system with cables and insulation for high voltages. They must withstand deterioration due to high temperatures, moisture, oil, fuel, corona discharge etc., and spark plugs which place a gap in the combustion chamber between the center electrode and ground wires to ignite fuel mixture. The length and mass of the insulating material surrounding the

electrode which projects into the combustion chamber determines the spark plug heat range.

E. Lighting System

The majority of loads presently in a car are lamps. In terms of size, number of individual circuits and length of wire, the vehicle lighting system is by far the most extensive of all vehicle electrical sub-systems. These loads include head lamps, stop lamps, tail lamps, turn signal lamps, dashboard illumination, vehicle interior illumination, fog lamps, parking lamps, and warning lamps for emergency vehicles.

The trend is generally based on photometric regulation set by the government. Tungsten is the universal lamp filament material used for light source. It has high melting point and retains structural strength while incandescent lamps are nonlinear devices for which light output, life, color, and current depend on the voltage applied. They in life of the lamp with voltage is drastic. So it is important to maintain the voltage at the design value. The length of the filament depends on its diameter and voltage applied. Filament failure due to mechanical shock or vibration represents a large portion field problems today. Because short filaments are physically more rugged and optically easier to focus than long filaments, automotive applications favor low voltage tungsten lamps, and any future architecture will have to make 6V or 12V available for them. Headlamps, however, are seeing the introduction, on a limited basis, of High Intensity Discharge (HID) lamps [1]. These lamps require high striking voltages and electronic ballasting. Should their efficiency and optical advantages ever justify their high cost relative to tungsten lamps, they will represent a large market for power electronics.

F. Instrumentation System

Instrumentation in automobiles classified based on the functions include Fuel indicator, Temperature indicator, Speedometer, Pressure indicator, Ammeter and Voltmeter. According to their operating principles they can be classified as Mechanical or Magnetic.

Mechanical Instrumentation are mainly used for speed, temperature, and pressure measurement. Pressure and temperature gauges are usually based upon the bourdon tube or diaphragm as the basic operating principle. Speedometer uses the centrifugal force created to the rotating weights identical to a classical flyball governor provides action to move gearing and linkage. The electrical part this instrumentation is simply the illumination light required at the dashboard.

Magnetic Instrumentation include electro-magnetic devices which is based on the combined interaction of the current flow and magnetic fields. Since these type of gauges are connected to the sensor by means of wire, they provide flexibility in location and routing. Temperature sensors are thermistors which changes its resistance with temperature. Pressure sensors make use of mechanical diaphragm with a linkage that moves across a card containing coil of wires. Fuel gauges are similar with the float moving the linkage. Voltmeters and ammeters use the basic electro-magnetic principles for its operation. In the electro-magnetic gauges, temperature compensators are in-built through a resistive shunt that change with temperature.

G. Other Systems

The majority of loads presently in a car are motors and lamps. Motors present a somewhat different situation with lamps. At 12V, present motors loose 15% of their

energy in the brushes alone. In applications such as fans and blowers, where speed control and efficiency are important, but stall torque is not, brushless DC motors are an attractive alternative to brushed motors, especially at higher voltages. Where low speed, high torque is required, e.g., for window lifts and wipers, the ultrasonic motor with its low profile, pancake-like from-factor has recently been receiving attention [3]. Both the brushless and ultrasonic motors require power electronic drivers, and the cost and reliability of these drivers will influence considerably the large scale acceptance of the motors by the auto industry.

IV. FUTURE ELECTRICAL LOADS

In the future, throttle actuation, power steering, anti-lock braking, rear-wheel steering, and ride-height adjustment will all benefit from electrical power assistance, being compatible with electrical control systems, which are becoming essential to provide the ideal control function. For example, optimum fuel economy, performance and emissions cannot be achieved without interposing the fueling and ignition computer between the driver's foot and the throttle.

Many of the future electrical loads would replace existing engine power consumers, such as power-assisted steering and water and oil pumps, where the electrical drive can in fact require a lower engine power, being used only when needed. Some others are a response to government mandates, such as the electrically heated catalyst, and some are motivated by driver convenience, such as windshield.

However, there is a trend towards replacement of more engine driven mechanical loads with electrical loads due to regulatory measures, safety requirements, and driver's comfort. Some of the loads considered are air-conditioning system, active suspension system, electromechanical valve control, and electrically heated catalytic converter.

Also, DC motors with or without brushes will be used for applications like fans and pumps because of its efficiency at high voltage in addition to reduced cost, flexible control, high quality and reliability.

Most of future loads require power electronics controls. Indeed, power electronics will be used in future automobiles to perform two classes of functions. The first, which call a class I function, is the simple on/off control of loads now performed by mechanical switches and relays. This is a replacement function. The second, call a class II function, provides more sophisticated control of loads and requires a more complicated power electronic system, such as an inverter or DC/DC converter [2].

In aggregate these new loads represent an increase from the present average electric power requirement of more than 150%. Moreover, all of these loads would benefit from a voltage higher than 12V DC, and several, such as the electromechanical valves, active suspension and heated windshield, require substantially higher voltages.

V. POWERING UP A HIGHER SYSTEM VOLTAGE

As modern cars take in more and more electrical accessories, it may be time to consider increasing the base system voltage to cope with the greater loads. The optimum choice of voltage involves complex trade-off between cost, safety, economy, performance, and function. The most suitable voltage for one device will certainly not

suit all devices. A dual-voltage system is inevitable; in fact, three voltages may be necessary, as vehicles already have a separate 6V supply for instruments and electronic control units for engine management.

The most obvious choice for an increased voltage is that used on the larger commercial vehicles-24V. However, the rapid rise in electrical loads suggest that something higher than 24V could be needed in future.

Increased voltage benefits the starter commutator and brushgear, but, above about 50V, the increased number of armature conductors cancels this advantage and results in increased weight and cost. However, an increased system voltage, up to 50V, offers considerable reductions in the weight and cost. Switches and relays would carry lower currents so that voltage drops would cause less parasitic loss in the system. MOSFETs are now being used in solid state relays; although low cost devices are currently available only for 12 and 24V systems, demand for higher voltage devices is expected to make them available for 42V systems [8].

VI. ELECTRICAL DISTRIBUTION SYSTEM ARCHITECTURES

At present most Automobiles use a 12V electrical system with point-to-point wiring. The capability of this architecture in meeting the needs of future electrical loads is questionable. Furthermore, with the development of More Electric Vehicles (MEV) there is a greater need for better architectures.

A. Conventional Electrical Distribution System Architectures

Fig. 4 shows the conventional point-to-point automotive electrical distribution system [4]. Since the conventional architecture uses a 12V distribution and point-to-point wiring, the wiring harness is heavy and complex. The assembly process, therefore, becomes difficult and time consuming, leading to higher labor costs. Also retrofitting, fault tracing and repairing are more time consuming and expensive. The bulky harness also places constraints on the vehicle body design as the wires have to go through door hinges and other tight cavities. The large number of wires requires a proportionally large number of connectors; since the failure rate of connectors is high, system reliability is compromised. Fuses are needed to prevent fire in the wiring harness and must be placed in an easily accessible location. The conventional architecture has a central fuse box. Since this box contains all the fuse plugs, it is large and difficult to place. Furthermore, the fuse plugs are expensive. Another problem is that the system voltage varies over a wide range. As a result automotive loads have to be designed to function over a wide voltage range, making them heavy and expensive [4]. Also there is a problem of load-dump transient - a voltage spike caused due to sudden load loss on a fully loaded alternator. This requires overrated switches and loads for transients. Other disadvantages are: at 12V, motors losses about 15% of energy in the brushes alone and the 12V system cannot handle future electrical loads to be introduced in automobiles as it'll be expensive, heavy and inefficient.

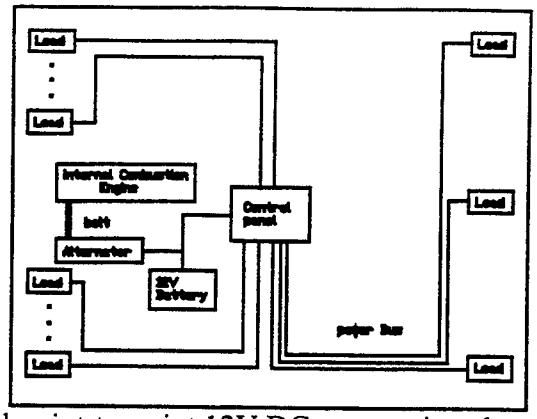

Fig. 4. The conventional point-to-point 12V DC automotive electrical distribution system

Changes in existing design may allow specialized designs to be used more effectively to improve overall cost reliability in an integrated system. On the other hand, there is a need for advanced automotive power systems which include multi-voltage level systems, separate power and signal buses, replacement of mechanical loads with electrical loads. These are motivated by the following factors:

- Continuing electrification of the automobile
- Currently 25% of a midsize car's fuel are used for electrical loads. If the some mechanical loads like air-conditioning and steering are electrified this percentage increases to about 50%. With these type of loads, power can be more effectively distributed and utilized at voltages much higher than 12V
- The automotive electricity is considerably expensive compared to the home electricity. Higher voltage levels improve electric efficiency by reducing ohmic losses and reducing copper requirement
- Improved electric efficiency reduces the automobile weight.
- Separate buses for signal and power
- Safety issues such as suspension, power steering, electric brakes, collision avoidance, back-up aide, and telematics
- Regulatory issues-higher fuel economy and lower emissions
- Interface between alternator and distribution system through power electronic circuits eliminates the need for overrated components
- The alternator can be allowed to generate unregulated voltage according to the varying engine speed, while the power conditioning circuit will provide a regulated, spike-free voltage
- Advance in the development of advanced power devices for cars capable of high-side switching, automatic shutdown on excessive temperature rise and integrated overcurrent protection
- Development power MOSFETs with low on-resistance
- Reduction in cost of power electronic component in the recent years

B. Advanced Electrical Distribution System Architectures

Since the conventional architecture does not adequately address the needs of a modern automobile, alternative architectures must be considered. One way to simplify the

architecture is by changing the control strategy [4]. In the conventional system each load is controlled by a dedicated wire. Alternatively a single wire multiplexed architecture can be used. In a multiplexed architecture the loads are controlled remotely by intelligent remote modules, as shown in Fig. 5. The control signal and power are sent through wires shared by many loads. Multiplexed topologies, therefore, reduce the number and length of wires in the harness. Furthermore, with communication between remote modules it will be practical to have a power management system, which can turn off unessential loads when there is not enough power. There are a number of multiplexed topologies, but the basic one are linear, star and ring.

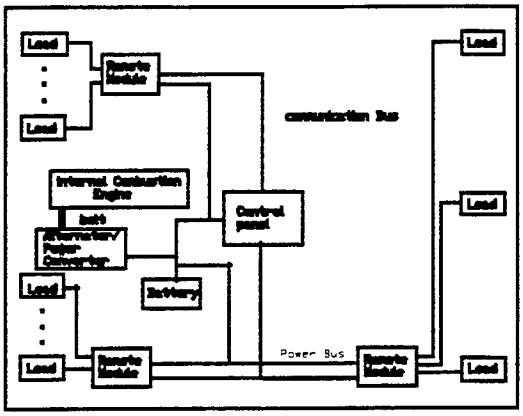

Fig. 5. Advanced automotive power system architectures of the future

A detailed diagram of a suggested advanced distribution system with high voltage level and medium frequency AC bus is shown in Fig. 6 [5]. Intelligent load control may avoid flat batteries by preventing lights left on, security system drains etc. This can be achieved by Power Management System (PMS). The primary functions of the PMS are battery management and charging strategy in a multiple battery system, load management, management of the alternator including the regulator, and provision and control of a high integrity supply system.

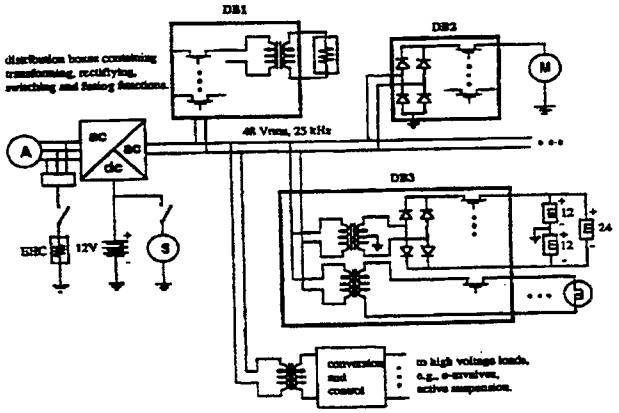

Fig. 6. High voltage, medium frequency AC distribution system

Distribution control networks simplifies vehicle physical design and assembly process and offer additional benefits from the amalgamation with intelligent power management control:

- They put all loads under intelligent control, therefore power management feature can be readily integrated into existing control with minimal cost
- Power management strategy can help optimize the size of the batteries and alternator
- Communications inherent with networked vehicle system can give improved performance with minimal increase in complexity and cost
- Vehicle economy can be improved using the knowledge of the battery state in a networked system

Further, the form in which power is distributed is important. A higher voltage will reduce the weight and volume of wiring harness. In addition, motor loads will be more efficient at higher voltages. A high voltage would also allow sheet-resistance based heated windshields, which require voltages greater than 60V, to be directly connected to the distribution bus. However, the advantage of a higher distribution voltage must be balanced against the cost of additional solution and shock protection, since voltage above 65V DC constitute a safety hazard [4]. Furthermore, lamps and electronics operate better at low voltage; hence in the case of a high voltage distribution bus it may be necessary to have a second low voltage bus. The main distribution can also be changed from DC to AC. The latter offers not only easy conversion to different voltage levels by the use of transformers, but also the ability to transfer power without contact. In this case, a DC power bus would also exist since a battery would be needed to start the engine and power essential loads when the engine is switched off.

In [9] insertion of a DC/DC converter between the automobile battery and electrical loads is proposed (Fig. 7). This would allow gradual conversion to higher battery voltage, regulation of DC distribution voltage, and multiple distribution voltage levels. Switching loss arising from parasitic inductance is a serious problem in this application. The nonlinear resonant switch can remove this source of loss, achieving zero current switching without sacrificing conduction loss or MOSFET switch utilization.

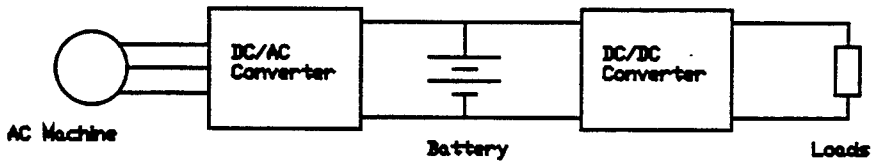

Fig. 7. New electrical system employing high-efficiency AC machine and isolated battery and load busses

The DC/DC load converter can provide the benefits of constant regulated voltage, higher automotive distribution voltage, and multiple load voltages. All of these benefits can considerably improve the automotive electrical system efficiency.

Also, it may be possible to improve the electrical system by replacing the components used in the conventional architecture. Permanent Magnet (PM) DC motors can be replaced by brushless DC, induction or variable reluctance motors. Similarly,

incandescent and halogen lamps can be replaced by more efficient and longer lasting High Intensity Discharge (HID) lamps [4]. Solid state relays can replace electromechanical relays, and fuse plugs can be replaced by fusing conductors or electronic fuses.

VII. THE ROLE OF ELECTRONICS AND MICROPROCESSORS IN ADVANCED AUTOMOTIVE ELECTRICAL SYSTEMS

In the early 1970s, other than radios and tape players, the only standard electronic components and systems on most automobiles were alternator diodes and voltage regulators. By the fall of 1974, there were twelve electronic system available, none of which were across the board standard production items. The twelve electronic systems were: alternator diodes, voltage regulators, electronic fuel injection, electronic controlled ignition, intermittent windshield wipers, cruise control, wheel lock control, traction control, headlamp control, climate control, digital clocks and air bag crash sensors [12].

The 1980s could be described as the decade of the emergence of automotive electronics. During this time the increase of electronic functions in passenger cars was quite dramatic. Among the first applications were the amplifier-type contact breaker ignition systems, then came breakerless units. Other systems include electronically controlled engine fueling, giving unprecedented performance or economy [13]. Electronic Anti-lock Braking Systems (ABS) are now becoming commonplace on highline cars, as are electronic instrumentation and driver information. Many more such functions are planned for future generations of cars, including electric actuation of brakes, steering and suspension.

Further vehicle functions can be implemented by the interaction of existing electronically controlled functions. One example of this type of interaction is in traction control where the ABS unit, on detecting wheel slip, can instruct the engine management unit to reduce engine torque until the car has recovered from the slip condition. Another example is the interaction between suspension, steering and braking controllers to maintain vehicle stability during braking and cornering. The interaction required can be achieved with dedicated links, but complexity and diagnosis advantages can be gained by the use of vehicle-wide local area networks, or data bus system [13].

Electronic engine management systems are becoming widely accepted, as is electronic ABS. Many more advanced systems are being planned. As roads become more heavily loaded, automotive electronic systems have their part to play in improving the safety and efficiency of road transport.

Reference [14] describes the electronically controllable system of valve actuation. It presents some performance predictions and results, and discusses some of the real life aspects of component performance requirements. The action of that system is referred to as Electronic Valve Timing (EVT). Valve motion has strong influence on the performance of diesel and spark ignition engines. The advantages of this relationship can be taken by designing valve motion to suit engines' application via EVT.

Current demands for shift comfort and driveability, and the need for interaction between the transmission and other vehicle electronic systems provide the impetus for introducing electronic control systems for transmission. The standard functions of such

systems have proven their worth and contributed towards satisfying these demands. For this reason, despite the additional cost involved, most automatic transmissions will be electronically controlled within next years. This is not only aimed at improving comfort and drivebility, but also at reduction fuel consumption, especially as automatic transmissions have always come off worse in tests than manual transmissions in this respect [15].

The future for automotive electronics is bright. Electronics solutions have proven to be reliable over time and enabled carmarkers to solve problems otherwise unsolvable. Some other predictions for the future are:

- Expansion of the airbag system to include side impact protection
- Magnetic transistors and diodes that can be directly integrated with signal conditioning circuits
- Electronic switched stop lamps involving a rate-of-closure detector system to determine if the vehicle's speed is safe for objects ahead of it. If the closure rate is unsafe, the stop lights could be activated to alert trailing drivers to a pending accident
- The integration of watchdog and fail-safe functions onto a microcontroller
- Microcontrollers that operate at frequencies of 24MHz or 32MHz to allow more code to be executed in the same amount of time
- A move from switching units to stepped operation actuators and the substitution of continuous for discrete time control
- Electroheological and magnetorheogical fluid actuators
- Micromechanical valves as actuators for converting low control power as in regulating the flow of fluids in hydraulic or pneumatic systems

After the introduction to automotive electronics in the 1970's, microprocessor-based automotive technology matured quickly in the 1980's. Now, it is clear that microprocessor technology has become an essential technology for future automotive electronics. It provides for automotive designers and engineers the opportunity to solve many problems and the unprecedented flexibility to innovate beyond mechanical limitations.

Newer architectures such as the Reduced Instruction Set Computer (RISC) and the Digital Signal Processor (DSP) promise higher levels of performance and, thereby, open the doors for new applications. DSP application to the exhaust will soon enable more efficient operation by cancellation of exhaust output pressure wave. In the future, microprocessor could alter engine mount characteristics in real time to reduce the coupling of engine vibration to the vehicle chassis. DSP technology already sophisticated dynamic suspension controls for high-performance cars and will soon be practical for most vehicles.

Microprocessor systems can accurately modify spark timing to optimize engine performance at all engine speeds. Also, they can eliminate the carburetor by direct control of fuel injection, the distributor contact points by use of a magnetic flux sensor, and the distributor itself by direct control of spark advance for each cylinder. A next logical step will eliminate the cam and all of its associated bearings, rods, and adjustments by

electronic control of valve openings and closings, producing an engine fully controlled by electronics.

Microprocessor technology makes it possible to explore engine technologies that were previously considered impractical for cars. Reasonable mechanical control systems could not produce adequate fuel economy or pollution reduction from two-cycle engines. Using leading edge microprocessor technology, an Australian company has produced a practical two-cycle engine that is suitable for a passenger car. This engine is much smaller than a traditional four-cycle engine of comparable horsepower [16].

In a few cars now, and in most future cars, microcontrollers will pass command signals over high speed serial data links using standardized communications protocols. Multiplexed wiring uses microprocessor technology to drastically reduce the amount of copper wiring, interconnection, and mechanical hardware in the car [16].

VIII. STABILITY ANALYSIS

There are many definitions of stability when considering linear, non-linear, discrete, and continuous systems. Linear system stability analysis is commonly performed using Routh-Hurwitz, root locus, Bode plot methods, and the Nyquist criterion. Another well known method of providing linear or non-linear system stability is the use of Lyapunov's second method [17]. Difficulty arises, however, in developing Lyapunov functions for many non-linear systems. Thus in determining the stability of a large system, more state-specific definitions are desirable. Stability considerations in non-linear systems require the consideration of initial conditions, external inputs, and their effects on non-linear components of the system. No known general analytical approach for the solution of non-linear systems is presently available.

The definition of stability in this paper considers the asymptotic stability as in the case of Lyapunov. However, we will not search for a suitable Lyapunov function, but instead consider the conditions of voltages and currents on the inputs and outputs of the subsystems. One form of instability is the divergence of one or more of these input or output voltages or currents (signals) from a desired value to some value which is outside the zone of tolerance, and the failure of the signal to return to within the zone of tolerance within a predefined period of time, i.e. unboundedness.

The common approach is to develop small signal linearized equivalent circuits and simulate the system to determine system stability. System stability is thus defined as the absence of instabilities on the main nodes. This linearized method governs small signal stability of the integrated system, but do not guarantee large signal stability for the entire system. For large signal stability, it is important to explicity include two other techniques in designing and building an automotive power system. Computer analysis and hardware testing form the other legs of a stability trial which should always be applied to the development of a complex system.

Large-signal stability refers to the ability of the system to move from one steady state operating point following a disturbance to another steady state operating point. Of prime concern is the way that the automotive power system will respond to dynamics caused by interconnecting between equipments and also to both a changing power demand and to various types of disturbance (loss of generation, short circuits, open circuits, etc).

However, for large-signal stability studies, time domain simulations using reliable large-signal models are inevitable. It depends on the actual control and protection circuit dynamics which may include, but is not limited to undervoltage lookout, overvoltage and overcurrent protections, cycle-by-cycle limiting, and nonlinearities due to magnetic saturation, leakage, semiconductor operation, temperature variations, aging, and castostrophic failures.

The stability of an automotive power system can be enhanced, and its dynamic response improved, by correct system design and operation. For example, the following features help to improve stability:

- the use of protection equipments that ensure the fastest possible fault clearing
- the use of a system configuration that is suitable for the particular operating conditions (e.g. avoiding long, heavily loaded links)
- ensuring an appropriate reserve in power capacity
- avoiding operating the system at low voltage
- avoiding weakening the network by the simultaneous outage of a large number of loads

In practice, financial considerations determine the extent to which any of these features can be implemented and there must always be a compromise between operating a system near to its stability limit and operating a system with an excessive reserve of generation and transmission. The risk of losing stability can be reduced by using additional elements inserted into the system to help smooth the system dynamic response.

IX. CONCLUSIONS

There is no doubt that the automobile power system architecture is heading for a drastic change which is imminent. Recent advances made in the area of power electronics, electric drives, electronic control, microprocessors, and microcontrollers are already providing the impetus to improve the automobile electrical and electronic systems. The extent of this change will certainly depend on the cost effective production of power electronics and other automotive electric components. The future automotive power systems will employ multi-voltage level systems, separate buses for power and communication, and an intelligent load management system. There is no question that power electronics will play an increasingly important role in automotive electrical systems. The extent of this role will be determined by how successful the power electronics industry is in producing apparatus at costs competitive with the alternatives. Electronic engine management systems will become widely accepted and automotive electronic systems, microprocessors and microcontrollers will have their considerable part to play in improving the efficiency and safety of automobiles.

REFERENCES

[1] J. G. Kassakian, H. Wolf, J. M. Miller, and C. J. Hurton, "The future of automotive electrical systems," *Proc. of IEEE Workshop on Power Electronics in Transportation*, Dearborn, Oct. 1996, pp. 3-12.

[2] J. G. Kassakian, "The future of power electronics in advanced automotive electrical systems," *Proc. of IEEE Power Electronics Specialist Conf.*, 1996, pp. 7-14.

[3] L. A. Khan, "Power electronics in automotive electrical systems." *Proc. of IEEE Workshop on Power Electronics in Transportation*, Dearborn, Oct. 1996, pp. 29-38.
[4] K. K. Afridi, R. D. Tabors, and J. G. Kassakian, "Alternative electrical distribution system architectures for automobiles," *Proc. of IEEE Workshop on Power Electronics in Transportation, Dearborn*, Oct. 1994, pp. 33-38.
[5] J. G. Kassakian, H. C. Wolf, J. M. Miller, and C. J. Hurton, "Automotive electrical systems-circa 2005," *IEEE Spectrum*, pp. 22-27, Aug. 1996.
[6] J. M. Miller, "Automotive power systems: present and future technologies," *Seminar at Texas A&M University*, Oct. 1997.
[7] E. Heller, "Truck electrical systems," *SAE 23rd L. Ray Buckendale Lectures*, 1997.
[8] J. G. W. West, "Powering up - a higher system voltage for cars," *IEE Review*, pp. 29-32, Jan. 1989.
[9] S. W. Anderson, R. W. Erickson, and R. A. Martin, " An improved automotive power distribution system using nonlinear resonant switch converters," *IEEE Trans. on Power Electronics*, vol. 6, no. 1, Jan. 1991, pp. 48-54.
[10] A. G. A. Guthrie, "The size of batteries to come," *IEE Colloquium on Vehicle Electrical Power Management and Smart Alternators*, 1988.
[11] R. Aumayer and G. L. Penna, "Batteries for new concepts of electrical systems in passenger cars," *IEE Colloquium on Vehicle Electrical Power Management and Smart Alternators*, 1988.
[12] R. Jurgen, *Automotive Electronics Handbook*, McGraw-Hill Inc., 1994.
[13] C. R. Boyce, "Automotive local area networks," *IEE Computing & Control Engineering Journal*, pp. 128-130, May 1990.
[14] M. E. Behr, "Potential for lost motion electronic valve timing," *Proc. of the International Congress on Transportation Electronics*, Oct. 1990, pp. 325-333.
[15] M. Schwab, "Electronically controlled transmission systems - current position and future developments," *Proc. of the International Congress on Transportation Electronics*, Oct. 1990, pp. 335-342.
[16] M. A. Goldman, S. E. Groves, and J. M. Sibigtroth, "The role of microprocessors in future automotive electronics," *Proc. of the International Congress on Transportation Electronics*, Oct. 1990, pp. 121-130.
[17] R. E. Kalman and J. E. Bertram, "Control system analysis and design via the second method of Lyapunov: I. continuous time systems," *American Society of Mechanical Engineering*, 1960.

Advantages of Switched Reluctance Motor Applications to EV and HEV: Design and Control Issues

K. M. Rahman, Student Member, IEEE
B. Fahimi, Student member, IEEE
G. Suresh, Student Member, IEEE
A. V. Rajarathnam, Student Member, IEEE
M. Ehsani, Fellow, IEEE

Texas A&M University
Department of Electrical Engineering
College Station, TX 77843-3128

Abstract- **Land vehicles need their drivetrain to operate entirely in constant power in order to meet their operational constraints, such as initial acceleration and gradability, with minimum power rating. The internal combustion engine (ICE) is inappropriate for producing this torque-speed profile. Therefore, multiple gear transmission is necessary with the ICE in a vehicle. Some electric machines, if designed and controlled appropriately, are capable of producing an extended constant power range.**

The purpose of this paper is to investigate the capabilities of switched reluctance motor (SRM) for EV and HEV applications. This investigation will be carried out in two steps. The first step involves the machine design and the finite element analysis to obtain the static characteristic of the motor. In the second step, the finite element field solutions are used in the development of a nonlinear model to investigate the dynamic performance of the designed motor. Several 8-6 and 6-4 SRM geometries will be investigated. Effects of different stator and rotor pole widths and pole heights on the steady state as well as on the dynamic performance of the motor will be studied. The air gap for each motor will be made as small as manufacturally possible. The performances to be compared for each design motor are, i) the range of the constant power operation, ii) drive efficiency in this extended constant power range, iii) the power factor in this operational range, and iv) the short time overload capability. The first performance index defines the rated power of the motor. Longer the constant power range lower is the power rating for the same vehicle performances. Hence, special emphasis will be given on this. In the high speed operation of the SRM, there will be considerable phase overlapping. Hence, thicker back iron than usual might be needed to prevent the back iron from saturating. However, since flux peaking of each phase occurs at different rotor positions, the phase overlapping might not necessitate special designing of the back iron. However, the possibility of back iron being saturated will not be neglected and will be investigated. The optimal control parameters of SRM, which maximize the constant power range with maximum torque per ampere, will be calculated. Performance comparison will be made for this optimal operation. Simulation results of the designed SRM will be presented for vehicle acceleration. To demonstrate SRM's capability in producing an extended constant power range, experimental results will be presented, however, for a reduced size motor available commercially.

I. INTRODUCTION

Switched reluctance motor (SRM) is gaining much interest as candidate for Electric Vehicle (EV) and Hybrid Electric Vehicle (HEV) electric propulsion for its simple and rugged construction, ability of extremely high speed operation, and hazard free operation. In view of these characteristics, one of the early SRMs was designed and built for electric vehicle application [1]. In designing this SRM, the major attention was given on the efficiency of the drive. Later, an optimized design method of SRM was reported in [2] for EV application. The design optimization was based on static analytical model of SRM, similar to the one developed by Corda and Stephenson [3]. Moreover, the efficiency optimization was carried out for the constant speed operation of the drive with non-optimal control. Like the previous design, the special emphasis was given in this design on the drive efficiency and additionally on the drive cost. Most recently, a 100 hp SRM was designed and built in [4] for electric vehicle application. No special control scheme, design method, or optimization technique were, however, presented.

While designing an SRM in all the previous methods, no attention was given to the vehicle dynamics. Vehicle dynamics dictate a special torque-speed profile for its propulsion system. Our recent study has shown that, a vehicle, in order to meet its operational constraints such as initial acceleration and gradability with minimum power, needs the powertrain to operate entirely in constant power [5]. The power rating of a motor that deviates from the constant power regime can be as much as two times that of a motor operating at constant power throughout its speed range in a vehicle. Operation entirely in constant power is not possible for any practical drive. An extended constant power range is, however, possible if the motor is appropriately designed and its control strategy is properly selected.

This paper will investigate the capabilities of SRM for vehicle traction. For this purpose, several SRMs will be designed and their optimal control parameters, which maximize the constant horse power range, will be calculated. A 2-D finite element analysis will be used to obtain the static characteristics of designed motors. The finite element field solutions will be then used in the development of a nonlinear model to investigate the steady state and the dynamic performance of the designed motors. The nonlinear model will also be used to search for the optimal control parameters (turn-on and turn-off angles) of each designed SRM which

extends the constant power range with maximum torque per ampere. Performance comparison will be made for this optimal operation. Several 8-6 and 6-4 SRM geometries will be investigated. Effects of different stator and rotor pole geometries on the steady state as well as on the dynamic performance of the motor will be studied. In the high speed operation of the SRM, there will be considerable phase overlapping. Hence, thicker back iron than normal might be needed to prevent it from saturating. However, since flux peaking of each phases occur at different rotor positions, the phase overlapping might not bring the back iron into saturation. However, the possibility of back iron being saturated will not be neglected and will be investigated. Besides the range of the constant power operation, the other performances which will be investigated for each designed motor are, i) the drive efficiency in this extended constant power range, ii) the power factor in this operational range, and iii) the short time overload capability. Simulation results of the designed SRMs in vehicle acceleration will be presented. To demonstrate that the SRM is capable of producing a long constant power range when controlled optimally, experimental results will also be presented, however, for a reduced size motor available commercially.

II. SRM Static Characteristics

To investigate the dynamic and steady state performances of each SRM geometry considered in this paper, the static torque and flux linkage characteristics as functions of stator current and rotor position are required. The non-linearity of the SRM owing to its saturation region of operation, however, complicates the analysis. Several non-linear analytic models of SRM are presented in the literature to obtain the static data [3,6-8]. For accuracy we will, however, rely on the finite element analysis to obtain the static data. Finite element analysis will be performed on several 6-4 and 8-6 SRM geometries with varying stator and rotor pole widths and heights. Later, the static torque and flux linkage data obtained from the finite element analysis will be used in the dynamic model to determine the drive performance with optimal control parameters.

III. Non-linear SRM Model

A block diagram of the non-linear SRM model is shown in Fig. 1. The static flux linkage and torque data as functions of the stator current and rotor position, obtained from the finite element analysis for each SRM geometry, are used in the dynamic model in order to include the effect of magnetic non-linearity. This model is used to predict the drive performance at steady state and in the dynamics. The optimal control parameters are obtained by using the dynamic model. A linear model of the converter is used in the dynamic model. The semiconductor switch and diode parameters used in the dynamic model, are obtained from the manufacturer's provided data. The core loss model presented in [15] is used with the SRM non-linear model to predict the core losses of each designed SRMs.

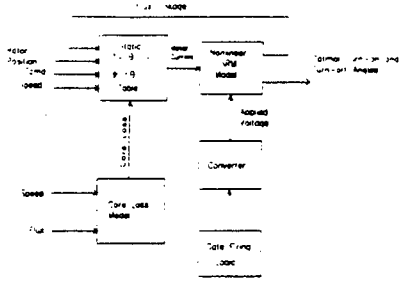

Fig. 1. A Block Diagram of the Dynamic SRM Model

IV. Determination Of The Optimal Control Parameters

Base speed in any motor is defined as the speed at which the back emf equals the bus voltage. Motor also reaches its rated power at this speed for rated excitation (current). Torque in SRM below base speed, when the back emf is lower than the bus voltage is controlled, like all other motors, by the PWM control of current. Above base speed, due to the high back emf which can not be field weakened, PWM control of current is not possible. Operation in constant power is made possible in this motor by the phase advancing of the stator phase current until overlapping between the successive phases occurs [9]. Torque control below base speed can be optimized by the stator current profiling [10,11]. However, above base speed the only control parameters are the phase turn-on and the turn-off angles. The phase turn-on and the turn-off angles can be optimally controlled above base speed to maximize the range of the constant power operation with maximum torque per ampere. To find the optimal turn-on and the turn-off angles, the dynamic model developed in the earlier section is used. The search procedure for the optimal angles is lengthy and time consuming. Any standard root seeking methods, such as the Secant method [12], may be used to accelerate the speed of the searching process. After series of iterations, the dynamic model finds the optimal turn-on and turn-off angles. To implement the control scheme in real time, a Neural Network based controller may be implemented [10].

V. Design Methodology

The design process starts with the hand calculation of several SRM geometries with varying pole numbers and pole dimensions. A 2-D finite element analysis is then performed to obtain the nonlinear field solutions within the motor. The finite element field solutions are used in the development of a nonlinear SRM model. The developed model is used to search the optimal control parameters which extends the constant power range of each motor with maximum torque per ampere. The steady state and the dynamic performances of each designed SRM are investigated for these optimal control parameters. These steps are repeated for each designed SRM in an attempt to determine an appropriate

SRM geometry for EV and HEV applications. In this paper, we will consider only the 8-6 and 6-4 SRM geometries. SRM geometries with more stator and rotor poles will have less space for phase advancing. As a consequence, motor will suffer from limited constant power range. Moreover, the ratio of the aligned to un-aligned inductance will reduce with increased number of rotor and stator poles. This will reduce the static torque and increase the converter volt-ampere [9].

VI. Design Examples

In this section we will present several SRM designs and will investigate their performances when controlled optimally. Our goal is to extend the constant power range with maximum torque per ampere. Special attention will also be given on the drive efficiency. All the design examples considered in this paper have almost the same stator outer dimension and stack length. We begin with the 6-4 SRM designs.

A. 6-4 SRM Design

First we will examine the effect of the pole widths on the SRM performances. The minimum stator and rotor pole widths of a 6-4 SRM should be 30° in order to have adequate starting torque from all positions. To maximize the room available for winding placement, we will keep the stator pole width fixed at 30° and while the rotor pole widths will be varied. The considered SRMs have the following dimensions

- Stator outer diameter, 13.58 inch.
- Rotor outer diameter, 7.4694 inch.
- Stack length, 7.4694 inch.
- Air gap, 0.0373 inch.
- Stator slot height, 1.7166 inch.
- Rotor slot height, 0.9763 inch.
- Stator core thickness, 1.3017 inch.
- Rotor core thickness, 1.3517 inch.
- M19 steel.
- Shaft diameter, 2.8135 inch.
- Number of turns per pole, 14.
- DC bus voltage, 240 V.
- Rated phase current, 168.3 ampere (Air cooled, 4 A/mm^2).
- Stator pole arc, 30°.
- Rotor pole arcs, 30.31° (same pole width as the stator), 31.5°, 34°, and 36°.

The dimensions of the four SRMs are same except for the rotor pole arc, which varies from 30.31° (same as the stator pole width) to 36°. For convenience, we will label these designs as design 1 through design 4. Finite element analysis is performed on each of these motors in order to obtain the nonlinear field solutions. These field solutions are then used in the nonlinear model to determine the steady state and the dynamic performances of each designed SRMs. Fig. 2(a) shows the constant power ranges of these motors. The optimal turn on and the turn off angles and the phase rms currents for the constant power operation of Fig. 2(a) are shown in Fig. 2(b). An extended speed constant power

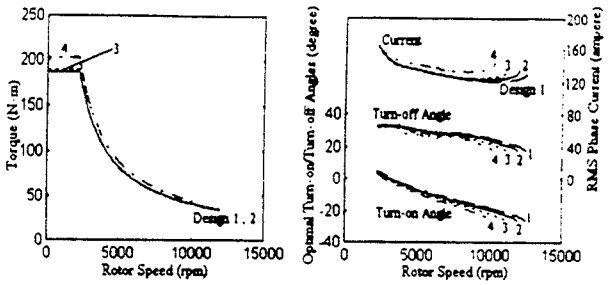

(a) (b)

Fig. 2. Extended constant power range (a) and optimal control angles and rms phase current (b) for SRM designs 1-4.

ranges are obtained for these designs when controlled with the optimal parameters. The extended constant power range is maximum (5.7 times the base speed) for design 1 (narrowest rotor pole), while it is minimum (4.7 times the base speed) for design 4 (widest rotor pole). However, the rated torque is minimum for design 1 and maximum for design 4. The long constant power range available from motor 1 will make it highly favorable for vehicle applications, despite the fact that it has a lower rated torque (power). The vehicle performance analysis for all these motors will be presented later. We can see in Fig. 2(b) that lower than rated rms current is needed at higher speeds to maintain constant power at the output. This is a direct consequence of the fact that the power factor (pf) of operation of the motors is improving at higher speed. The power factors and the drive efficiencies for theses motors are presented in Fig. 3 for the constant power operation. We have used the following definition for calculating the pf.

$$\text{pf} = \frac{\text{Output Shaft Power}}{\text{Input RMS VoltAmpere}} \qquad (1)$$

Design 1 exhibit both the best efficiency and the pf among these designs.

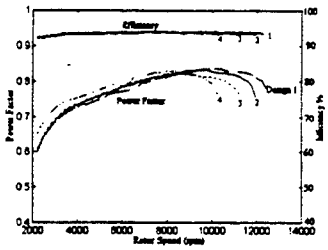

Fig. 3. Efficiency and pf of motors 1-4 for constant power operation.

Since the rms phase current decreases during high speed constant power operation, it should be possible to obtain more than the designed rated powers from these motors at high speed without exceeding the bus voltage and the rated current of each motors. This is shown in Fig. 4. Fig. 4(a) shows the maximum power available from these motors and 4(b) shows the phase current and the control angles for

the maximum power outputs. The output shaft powers are shown as a ratio of the ideal output power (unity pf) which is only possible from a separately excited dc motor. The power curves shown in Fig. 4 are the maximum powers these motors are capable of delivering, given the voltage and the

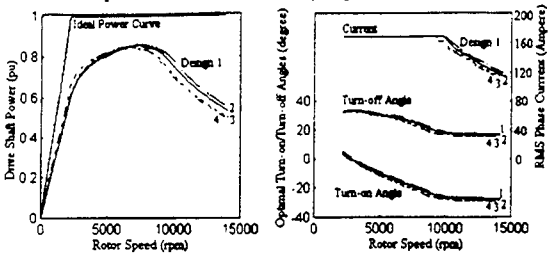

(a) (b)

Fig. 4. Maximum output power (a) and optimal control angles and rms phase current (b) for SRM designs 1-4.

current limitations. Again, design 1 is exhibiting better performance (higher power) at higher speeds. It may be noted that almost 40% more than the design rated power is obtained. The difference between the ideal power and the actual power is narrowing at the high speed. It is interesting to note that, beyond a certain speed the rms phase current is reduced from the rated value in order to obtain more power. Any current higher than this will actually reduce the output torque due to the development of more negative torque. Hence, beyond that speed it is advantageous to reduce the current rather than maintaining the rated current. Motor efficiency and power factor for its operation on the maximum power curve of Fig. 4(a) are shown in Fig. 5. Although the rated pf is low for SRM, this difficulty is greatly overcome at higher speeds and the SRM output power approaches the ideal power (Fig. 4). This will make SRM attractive for applications requiring high speed operations, *e.g.*, the vehicle propulsion system.

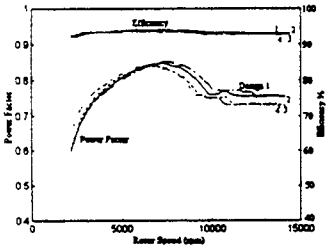

Fig. 5. Efficiency and pf of motors 1-4 for maximum power output.

Vehicle application also requires short term overload capability from its propulsion system. Hence, finally, we will examine the overload capabilities of these motors. SRM does not have any break down torque like the induction motor. The overload capability, however, would depend on how much current can be pushed in to the motor against the high back emf and how fast it can be pushed. Obviously, a low unaligned inductance will be favorable for both these conditions. Design 1 which has narrow poles (low unaligned inductance) will have like it's extended power capability a good overload capability. This is shown in Fig. 6 in pu of the rated power. As expected, maximum overload capability decreases as the speed increases. Peak overload capability for design 1 at the rated speed is almost 4.5 times its rated

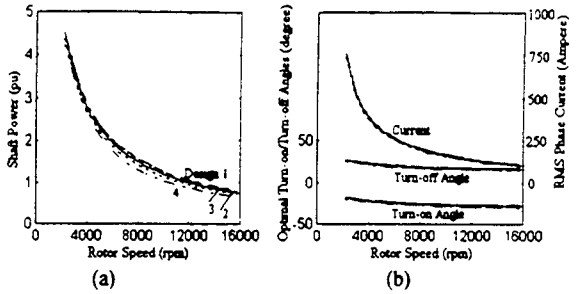

(a) (b)

Fig. 6. Maximum overload power (a) and rms phase current and optimal angles (b) for SRM designs 1-4.

power. RMS phase current and optimal control angles are shown in Fig. 6(b). These phase currents for the overload condition may be compared with the currents of Figs. 2 and 4, to understand the extent of overload from thermal (cooling requirement) point of view. We would, however, like to point out that the actual overload power would be less than this theoretically predicted overload power. When the motor is severely overloaded, the back iron will saturate. This will introduce strong coupling between phases, which is neglected in the developed model of this paper. Due to this phase couplings, torque and hence power will be reduced. Efficiency and pf during motor overloading are shown in Fig. 7.

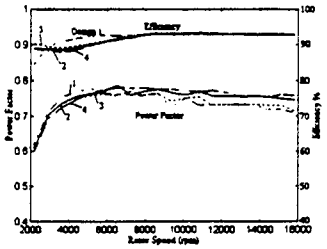

Fig. 7. Efficiency and pf of motors 1-4 during the overloading condition.

Next, we will investigate the effect of rotor pole height on the SRM performance. If the stator outer diameter is fixed, an increase in rotor pole height, however, will decrease the stator slot area. As a consequence, winding area will decrease. Hence, the rated current of the motor will decrease. In the unaligned position, flux also fringes through the side of the rotor pole. Hence, making the rotor pole very long will not be very useful in reducing the unaligned inductance. We will consider four more designs. The rotor pole height of design 2 (rotor pole arc 31.5°) is increased 10% and 20%, these two designs will be labeled design 5 and design 6 respectively. Also, the rotor pole height of design 3 (rotor pole arc 34°) is increased 10% and 20%. These two designs will be labeled design 7 and design 8 respectively.

As before, the finite element analysis is performed on these motors to obtain the field solutions. The non-linear field solutions are then used in the non-linear SRM model to examine the drive performance. For better understanding, the

performance of designs 5-8 will be presented along with the performance of design 2 and 3. Fig. 8 shows the constant power ranges of these motors when controlled optimally. Design 6, which has the narrowest and longest rotor poles

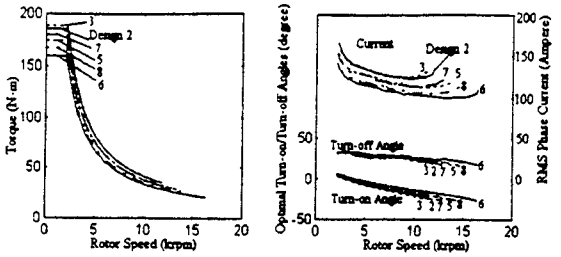

(a) (b)

Fig. 8. Extended constant power range (a) and optimal control angles and rms phase current (b) for SRM designs 5-8.

among these designs, has the longest constant power range (7.75 times the base speed!), however, the lowest rated torque. On the other hand, design 3, which has the widest and shortest rotor pole, has the highest rated torque but the shortest constant power range (5.1 times the base speed). The pf and the efficiency of these designs for the constant power operation are shown in Fig. 9.

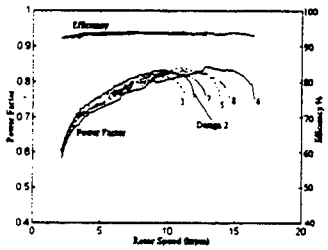

Fig. 9. Efficiency and pf of motors for constant power operation.

The maximum power available from these motors, operating within the voltage and the current limitations, is shown in Fig. 10 and the corresponding efficiencies and power factors are shown in Fig. 11. The overload capabilities of these motors are shown in Fig. 12 and the power factors and the efficiencies are shown in Fig. 13. Design 6 has an overloading capability of almost seven times the rated power.

Among the 8 designs we have presented so far, design 6 has the longest constant power range, however, the lowest power rating, while design 4 has the shortest constant power range, however, the highest power rating. A valid comparison between these motors, however, should be made in terms of the vehicle performances, which we will make in the next section. We will present two 8-6 SRM designs next.

B. 8-6 SRM Design

We will present two 8-6 SRM designs in this sub-section. These two designs have the following dimensions

- Stator outer diameter, 13.66 inch.
- Rotor outer diameter, 7.5156 inch.
- Stack length, 7.5156 inch.
- Air gap, 0.0376 inch.
- Stator slot height, 1.9303 inch.
- Rotor slot height, 1.3152 inch.
- Stator core thickness, 1.1066 inch.
- Rotor core thickness, 1.1987 inch.
- M19 steel.
- Shaft diameter, 2.4878 inch.
- Number of turns per pole, 11.
- DC bus voltage, 240 V.
- Current density 4 A/mm^2 (Air cooled).
- Stator and rotor pole arcs 21°, 23° (Design 9), and 19°, 21° (Design 10).

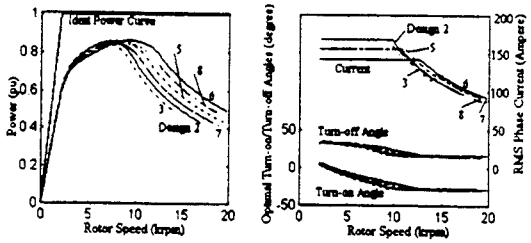

(a) (b)

Fig. 10. Maximum output power (a) and optimal control angles and rms phase current (b) for SRM designs 5-8.

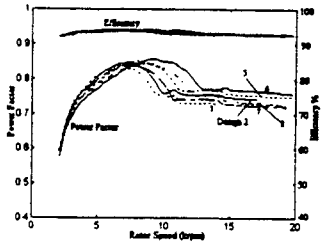

Fig. 11. Efficiency and pf of motors 5-8 for maximum power output.

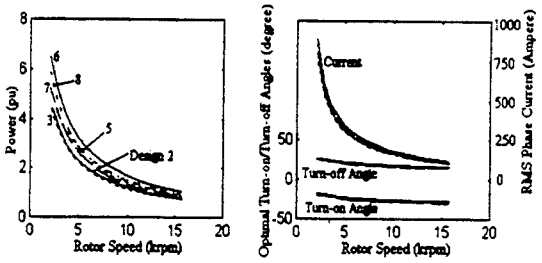

(a) (b)

Fig. 12. Maximum overload power (a) and rms phase current and optimal angles (b) for SRM designs 5-8.

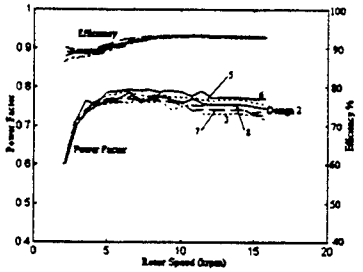

Fig. 13. Efficiency and pf of motors 5-8 during the overloading condition.

We have labeled the two SRM designs presented in this sub-section as design 9 and design 10. After performing the finite element analysis, the optimal constant power ranges are

calculated using the dynamic model. Fig. 14 shows the constant power ranges of these motors along with the rms phase current and the optimal angles. Design 9 which has wider poles produces higher rated torque, however, a constant power range of only 3.2 times the base speed. Design 10 has slightly lower rated torque and rated power than design 9, but has a much longer constant power range (4.125) than 9. The rms phase current also decreases while maintaining the constant power operation. The power factor and motor efficiency for the constant power operation are shown in Fig. 15. Power factor improves considerably in the

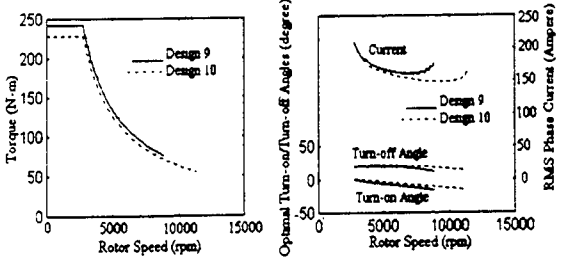

(a) (b)

Fig. 14. Extended constant power range (a) and optimal control angles and rms phase current (b) for 8-6 SRM designs 9 and 10.

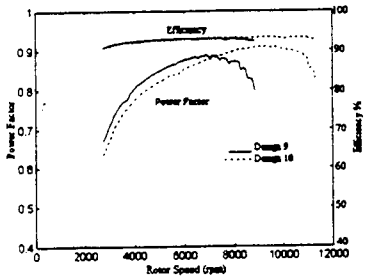

Fig. 15. Efficiency and pf of operation for motors 9 and 10 for their operation on the constant power profile.

high speed constant power operation of the motors. Design 10 has a lower power factor than design 9 at the rated speed, however, improves rapidly and shows better power factor than design 9 roughly after 7000 rpm. The 8-6 designs, although have shorter constant power range, are showing better power factor and much better power ratings than the 6-4 designs (Fig. 2,3). The 8-6 SRMs, due to their narrower pole widths than the 6-4 SRMs, operate in higher saturation level (6-4 and the 8-6 designs have comparable winding areas). Moreover, the higher phase overlapping in 8-6 motors are contributing more to the average torque. The back iron in 8-6 designs are, however, saturating. The stator and rotor back iron thickness in both the design are chosen 80% of the design 9 respective pole widths. The back irons in both the design, especially in the design 10 (design 10 has higher ampere-turn rating), saturate for the rated torque and near the rated speed of the motor. To prevent this from happening, design 9 would require 6% more core thickness, whereas design 10 would require 20% more core thickness.

Next, we will examine the maximum power capability operating within the rated voltage and current of the motors. Fig. 16 shows the maximum power capability of these two motors in per unit of their ideal output power. Design 10 has higher and wider power capability at high speeds. This is obviously desirable for EV and HEV applications. Efficiency and power factor for this operation are shown in Fig. 17. Design 10 i also showing higher power factor and efficiency at higher speeds.

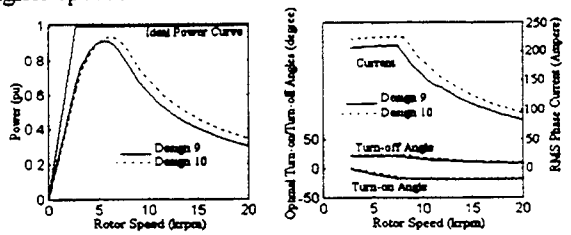

(a) (b)

Fig. 16. Maximum output power (a) and optimal control angles and rms phase current (b) for SRM designs 9 and 10.

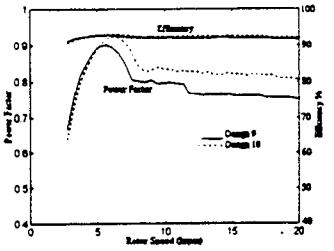

Fig. 17. Efficiency and pf of motors 9-10 for the maximum power output.

Finally, in Fig. 18 we show the overload capabilities of these designs. The power factors and efficiencies for the overloaded operation are shown in Fig. 19. Design 10 has better pf, better efficiency, and also better overload capability. Due to the higher unaligned inductance, the overload capability of the 8-6 designs are, however, lower than the 6-4 designs.

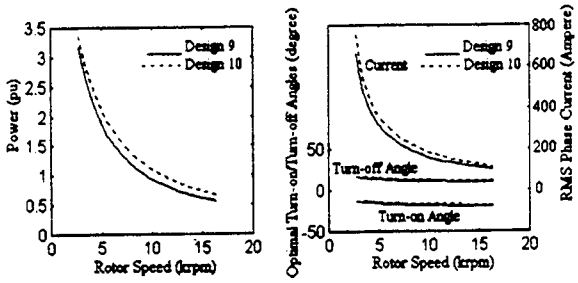

(a) (b)

Fig. 18. Maximum overload power (a) and rms phase current and optimal angles (b) for SRM designs 9 and 10.

In this section, we have presented eight 6-4 SRM designs and two 8-6 SRM designs. The 6-4 designs are showing much longer constant power capability and much higher overload capability than the 8-6 designs. The 8-6 designs, however, have higher rated torque and power. They also exhibit better power factor and efficiency. A valid comparison between these designs can only be made if we compare the vehicle performances, *e.g.* the initial acceleration performance, when these motors are used as the

propulsion system. This comparison will be made in the next section.

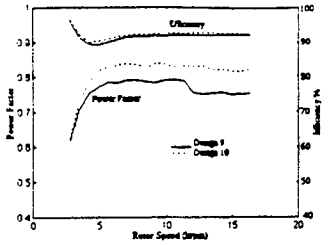

Fig. 19. Efficiency and pf of motors 9 and 10 during overloading condition.

VII. Vehicle Performance Analysis

In this section, we will compare the performances of the designed SRMS for a vehicle propulsion system by calculating the 0-60 mph acceleration time. The SRM performance will also be compared with the performances of induction motor (IM) and brushless dc (BLDC) motor. For the later comparison, we will calculate the power and the input volt-ampere requirements of IM and BLDC motor for the 0 to 60 mph acceleration in times specified by the SRMs. For this purpose, we consider the following vehicle

- vehicle rated speed of 26.82 m/s (60 mi/h);
- vehicle maximum speed of 44.7 m/s (100 mi/h);
- vehicle mass of 1450 kg;
- rolling resistance coefficient of 0.013;
- aerodynamic drag coefficient of 0.29;
- frontal area of 2.13 m^2;
- wheel radius of 0.2794 m (11 in);
- level ground
- zero head wind

For calculating the acceleration time, the maximum power capabilities of SRMs, presented in Figs. 4, 10, and 16, will be assumed. For calculating IM power and volt-ampere we will assume a constant power capability of 4 times the base speed and a pf of 0.8. While, a constant power range of 2.2 times the base speed and a pf of 0.9 will be assumed for BLDC motor.

Table I is listing the 0-60 mph acceleration time, power, and input KVA ratings of the IM, BLDC motor, and SRMs.

Table I
Motor power ratings and vehicle acceleration time

SRM Design #	Accl. time (s)	SRM Power (kW)	SRM KVA	IM Power (KW)	IM KVA	BLDC Power (KW)	BLDC KVA
1	13	42.1	69.8	57.88	72.35	75.5	83.9
2	13.25	42.56	69.86	56.9	71.13	74.43	82.7
3	13.48	42.61	69.9	56	70	73.27	81.41
4	13.58	45.88	69.85	55.68	69.6	72.78	80.86
5	13.85	39.1	64.76	54.7	68.38	71.46	79.4
6	14.78	34.6	59.35	51.68	64.6	67.39	74.88
7	14.1	38.98	64.68	53.85	67.3	70.34	78.15
8	15.01	35.38	59.32	50.1	62.6	66.4	73.77
9	10.1	68.12	101.4	72.7	90.88	95.67	106.3
10	8.74	69.95	109.3	83.04	103.8	109.6	121.8

Among the 6-4 designs, design 1, which has the narrowest rotor poles requires least amount of time for the acceleration. Design 6, which has the longest constant power range, is requiring longer time for the initial acceleration due to its lower power rating. The 8-6 designs have much higher power rating than the 6-4 designs, the acceleration time is therefore much lower for the 8-6 designs, despite their relatively lower constant power range. The 6-4 SRMs have better overload capability than the 8-6 designs. They also operate in a lower level of saturation. Their performance, therefore, can be improved significantly by increasing the current density. However, more efficient cooling of the motor would be required. The rotor pole height of designs 1-4 can also be reduced to make more room for phase windings. This will, however, increase the unaligned inductance and consequently, the constant power range, the overload capability, as well as the pf will be reduced. SRMs are exhibiting equal or better performances than the induction and BLDC motors.

VIII Experimental Result

SRM designs presented in section VI show that an extremely long constant power range is possible if the motor is designed appropriately and controlled optimally. A range of three to seven times the base speed has been demonstrated with different designs. In this section, we will present experimental results to demonstrate that an extended constant power range is possible from SRM. The experimental motor, however, is a small motor available commercially. The motor was not designed specifically following the methodology presented in this paper. However, it will be controlled with the optimal control parameters. The optimal control parameters are calculated from the dynamic model. The nonlinear field solutions for this motor is calculated from the experimentally collected data. Simulation results for this motor show that an extended range exceeding 6.5 times the base speed is possible. A detailed simulations results of this motor can be obtained in our other paper [16].

Fig. 20 shows the experimentally measured torque and rms phase current at high speed when the motor is controlled

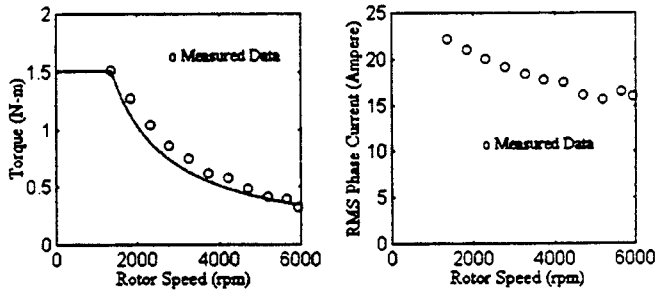

(a) (b)

Fig. 20. Experimentally measured torque (a) and rms phase current (b) at high speed.

optimally. The experimental setup has a maximum speed limitation of 6000 rpm. Therefore, we limited our experiment to 6000 rpm. The measured constant power range is almost 4.35 times the base speed. There is still some room available for phase advancing. This can be seen from the phase current waveform near 6000 rpm (Fig. 21). The measured rms phase current decreases while maintaining constant power, indicating, as predicted theoretically, an improvement in the power factor.

IX. Conclusion

High speed capabilities of several 6-4 and 8-6 designs are presented in this paper. Simulation results are showing some interesting characteristics of the SRM. An extremely long constant power ranges are available from the 6-4 designs. Power factor improves significantly at the high speeds from its low speed values. Almost 40% more than the design rated power is obtained at high speed without exceeding the voltage and the current ratings of the motors. Excellent efficiencies are exhibited by these designs at high speed. The design examples presented in this paper by no means are the best design geometries. Nevertheless, a design methodology is presented and the potential of SRM for vehicle application is clearly demonstrated. SRM definitely shows the potential to perform superior to brushless dc and induction motors. A constant power range of more than four times the base speed is demonstrated by the 8-6 experiment motor. The experimental result also demonstrate the improvement of pf at the high speed operation.

Acknowledgment

The support of Texas Higher Education Coordinating Board Advanced Technology Program, Texas Transportation Institute, and Texas Instrument Digital Control Systems Division, for this research is gratefully acknowledged.

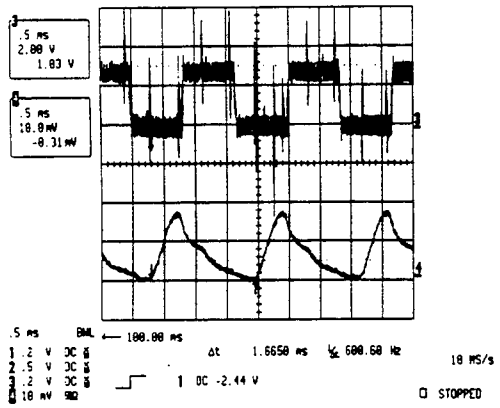

Fig. 21. Actual (the lower trace) and the commanded (the upper trace) current at 6000 rpm. The oscilloscope scales are 21 and 20 amperes per division for the commanded and the actual current respectively.

X. Reference

[1] P. J. Blake, R. M. Davis, W. F. Ray, N. N. Fulton, P. J. Lawrenson, and J. M. Stefenson, "The control of switched reluctance motors for battery electric road vehicles," *International Conference on PEVD*, pp. 361-364, May, 1984.

[2] J. H. Lang and F. J. Vallese, "Variable reluctance motor drives for electric propulsion," *United States Department of Energy Report*, DOE/CS-54209-26, May, 1, 1985.

[3] J. Corda and J. M. Stephenson, "Analytical estimation of the minimum and maximum inductances of a doubly-salient motor," *on Proc. Int. Conf. Stepping Motors Syst. (University of Leeds)*, 1979, pp. 50-59.

[4] T. Uematsu and R. S. Wallace, "Design of a 100 kW switched reluctance motor for electric vehicle propulsion," *APEC*, pp. 411-415, 1995.

[5] M. Ehsani, K. M. Rahman, and H. Toliyat, "Propulsion system design of electric and hybrid vehicles," *IEEE Trans. on Industrial Electronics*, vol. 44, no. 1, February 1997.

[6] J. V. Byrne, and J. B. O'dwyer, "Saturable variable reluctance machine simulation using exponential functions," *Proceedings of the International conference on Stepping Motors and Systems*, University of Leeds, UK, 1976, pp. 11-16.

[7] T. J. E. Miller and M, McGlip, "Nonlinear theory of switched reluctance motor for rapid computer-aided design," *IEE Proceedings*, vol. 137, Pt. B, No. 6, pp. 337-347, Nov. 1990.

[8] D. A. Torrey, X.-M. Niu, and E. J. Unkauf, "Analytical modeling of variable-reluctance machine magnetization characteristics," *IEE Proc. Electr. Power Appl.*, vol. 142, no. 1, pp. 14-22, Jan. 1995.

[9] T. J. E. Miller, "Switched reluctance motor and their control," Clarendon Press, 1993.

[10] K. M. Rahman, A. V. Rajarathnam, and M. Ehsani, "Optimized instantaneous torque control of switched reluctance motor by neural network," *IEEE IAS Conference Record*, New Orleans, Oct. 1997.

[11] I. Husain, K. R. Ramani, and M. Ehsani, "Torque ripple minimization in switched reluctance motor drives by PWM current control," *IEEE Trans. on Power Electronics*, vol. 11, no. 1, pp. 83-88, January, 1996.

[12] A. Ralston and P. Rabinowitz, *A First Course in Numerical Analysis*, 2nd ed. New York: McGraw-Hill, 1978.

[13] T. J. E. Miller, *Brushless Permanent-Magnet and Reluctance Motor Drives*, Oxford Science Publication, Oxford, 1989.

[14] W. L. Soong and T. J. E. Miller, "Field weakening performance of brushless synchronous AC motor drives," *IEE Proc.-Electr. Power Appl.*, Vol. 141, No. 6, pp. 331-340, November 1994.

[15] P. N. Materu and R. Krishnan, "Estimation of Switched Reluctance Motor Losses," *IEEE Trans. on Industry Applications*, Vol. 28, No. 3, pp. 668-679.

[16] K. M. Rahman, G. Suresh, B. Fahimi, A. V. Rajarathnam, and M. Ehsani, "Optimized torque control of switched reluctance motor at all operational regimes using neural network," *IEEE IAS Annual Meeting*, St. Louis, 1998.

970294

Parametric Design of the Drive Train of an Electrically Peaking Hybrid (ELPH) Vehicle

Yimin Gao[1], Khwaja M. Rahman, and Mehrdad Ehsani
Texas A&M Univ.

ABSTRACT

The operation of an electrically peaking hybrid vehicle (ELPH) can be divided into two basic modes. • Constant or cruising speed mode in which a small internal combustion engine (ICE) is used to power the vehicle. • Peak power mode in which the combination of an electric motor and ICE is used to supply peak power for acceleration and limited-duration steep hill climbing of the vehicle.

A method, by which the engine size and the speed reduction ratio from the engine to drivewheels can be developed based on the cruising mode, is presented in this paper. The electric motor power rating and the motor gear ratio to the drive wheels can then be determined, based on the acceleration and gradeability. The results show that a simple single-gear transmission would be a good selection for overall performance.

INTRODUCTION

Petroleum fueled, internal combustion engine powered vehicles are the most popular means of transportation, because of their high energy density and relatively high power density. However, in recent years, increasing concern over air pollution, caused by tailpipe emissions of the petroleum-based vehicles, and the dwindling petroleum resources have caused the automotive engineers and automakers to re-evaluate the designs of the conventional internal combustion engine powered vehicles. The conventional automotive drive train suffers from a number of disadvantages :

1. The inherently mismatched speed-torque characteristic of the engine and the vehicle necessitates a complicated transmission, with its associated losses and inflexibility.

2. In order to have ample power for acceleration and gradeability with a limited number of transmission gears, the engine must be oversized to roughly ten times that required for cruising at *100 Km/h* on a level road and three or four times that required for maintaining *100Km/h* on a *6%* grade.[1]

3. Today's internal combustion engines show a significant difference in specific fuel consumption between partial load and the optimal operating point, which is close to full load as shown in *Fig. 1*. An oversized engine moves the cruising operating point away from the optimal operation point. Consequently, ICE vehicles have low efficiency [2].

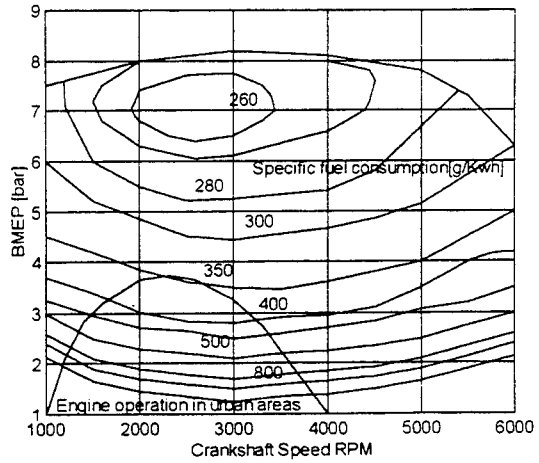

Fig. 1. Typical SI-engine SFC Map with Actual Operation Point[2]

The electric motor, in addition to its clean, quiet and efficient operation, has inherent flexibility in its speed-torque control. *Fig. 2* shows a typical torque-speed characteristics of the electric motor with power electronic drive. The motor can operate anywhere within this torque-speed boundary. This

[1] Visiting scholar from Jilin University of Technology, China

allows the motor to meet the vehicle torque-speed requirements at all times, without a variable gear transmission. However, pure electric vehicles (Ev's) suffer from other disadvantages[9].

1. The heavy and bulky battery pack, with its relatively small energy storage, makes the EV limited in range, and load carrying capacity.

2. Long charging time limits the EV's practicality.

Therefore, commercial success of the EV depends strongly on the development of advanced batteries. However, progress in batteries over the past several decades has not been adequate.

The hybrid configurations, in which two power sources are applied to propel the vehicle, show significant promise[7,8]. The hybrid electric-internal combustion engine drive train, if properly configured, can combine many of the advantages of both EV and ICE vehicles [9].

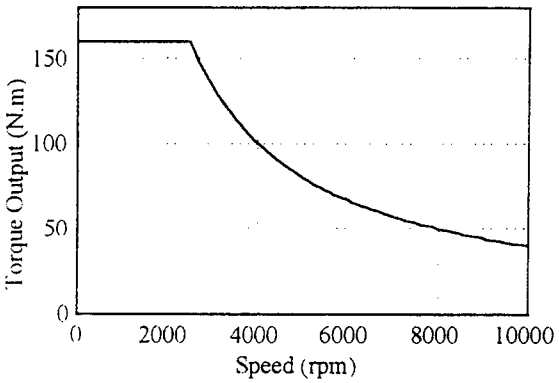

Fig. 2. The Speed-torque Characteristic of Electric Motor

ELECTRICALLY PEAKING HYBRID CONFIGURATION

The operation of passenger vehicles can be divided into two basic modes: constant speed (cruising), and acceleration (peak power). In cruising mode, relatively low power is required from the drive train. However, large amount of energy is consumed in a long trip. In acceleration mode, high peak power is required but not much energy is consumed, due to its brief and transient occurrence. Proper parallel combination of ICE, for cruising operation, and electric motor with a small battery pack, for acceleration, can satisfy these requirements in a viable drive train. The motor with a small chemical battery pack optimized for high power would have acceptable power capability and power density for acceleration[3]. A small ICE with a small fuel tank would have the energy density for cruising and recharging the battery for the next acceleration.

A configuration of such an electrically peaking hybrid (ELPH) vehicle is shown in *Fig. 3* in which the base power unit is the engine and peaking power unit (or load leveling device) is the electric motor.

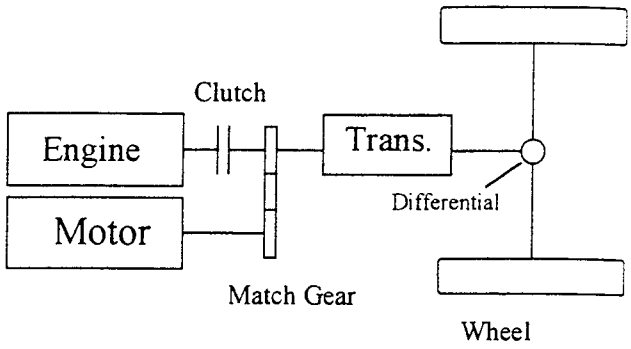

Fig. 3 The Configuration of an Electrically Peaking Hybrid (ELPH) Vehicle

The ELPH configuration, in addition to satisfying the requirements of acceleration and gradeability, has the ability to recover braking energy with the electric motor functioning in regenerating mode. Furthermore, when the vehicle operates with light load, such as at a low constant cruising speed or going down a slight hill, the engine can recharge the battery pack to maintain adequate state-of-charge. More beneficially, this enhances the engine load, for operation close to its optimal point. A well designed ELPH vehicle may never use an external source to charge its battery pack and can achieve an excellent fuel economy.

In this paper, the following specification of the Electrically Peaking Hybrid (ELPH) vehicle prototype, which is being developed at Texas A&M University, will be taken as the example.

Curb weight	*1700 kg,*
Rolling resistance coefficient of tire	*0.013,*
Aero-dynamic drag coefficient	*0.29,*
Front area	*2.13 m^2,*
Wheel radius	*0.2794 m.*

CRUISING MODE

As described above, when the vehicle operates on level ground with a constant cruising speed, the engine alone delivers power to the drivewheels. Consequently, the performance of the vehicle is determined only by the engine power and speed reduction ratio from the engine to the drivewheels.

ENGINE POWER REQUIREMENT- The determination of the engine power plays a very important role in the design of ELPH vehicle. An oversized engine would lose its fuel-saving advantage as in the conventional vehicles. On the other hand, an undersized engine can not deliver enough power to meet the requirements of the vehicle. Therefore, a large battery pack and a large motor would be needed to compensate for the shortage of engine power. Consequently, the ELPH vehicle would suffer from the same problems as an EV.

When the vehicle operates on a level ground with a constant cruising speed, the engine must deliver enough power to overcome the vehicle load power which includes the rolling resistance power and the aero-dynamic drag power. Thus, the required engine power output is

$$Pe = \frac{v}{1000\eta_{et}}\left(mgf + \frac{1}{2}\rho C_D A v^2\right) \qquad (1)$$

where, v = speed of vehicle, *m/s*,
η_{et} = efficiency of the transmission form engine to drivewheels, *0.9*
m = vehicle mass, *Kg*,
f = rolling resistance coefficient,
g = gravity acceleration, *9.81 m/s²*,
C_D = aero-dynamic drag coefficient,
A = front area of the vehicle, m^2,
ρ = air density, *1.228 Kg/m³*.

Fig. 4. shows the vehicle load power as a function of the vehicle speed in cruising mode This figure indicates that not much power is needed to maintain the vehicle operation in cruising mode. About *30 Kw* of power capacity will be plenty to meet the requirement of the vehicle at a speed of *130 Km/h (81.5 mph)*. This *30 Kw* of engine power capacity is quite small in comparison to the average *50* to *70 Kw/1000Kg* specific power of conventional cars More precise selection of the engine power capacity will be made with consideration of recharging of the peaking battery pack

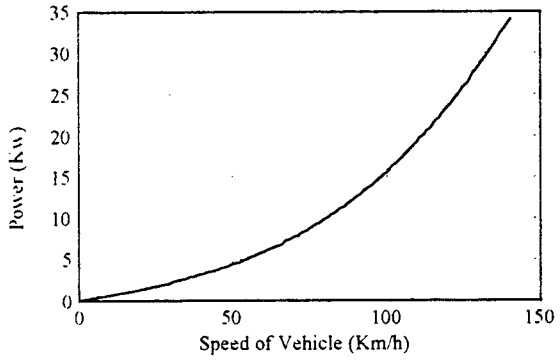

Fig. 4. Required Engine Power Versus Constant Speed on A Level Road

DIFFERENTIAL GEAR RATIO-*Fig. 5.* shows the speed-power characteristics of a typical gasoline SI engine. Equation (2) gives the vehicle speed for a single-gear transmission or a top gear operation of a multi-gear transmission. By equation (2), *Fig. 5* can be transformed into a vehicle speed-power profile, as shown in *Fig. 6.*

$$v = \frac{\pi r N}{30 r_d} \quad (m/s) \qquad (2)$$

where, r_d = differential gear ratio drivewheels,
r = radius of the drivewheel, m
N = speed of engine, *rpm*.

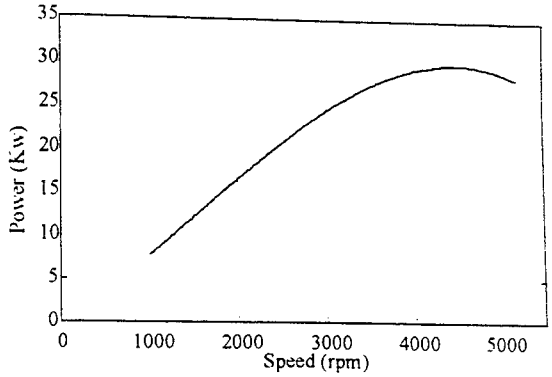

Fig. 5. Typical Characteristics of SI Engine

In *Fig. 6.* several engine power curves with different differential gear ratios are shown along with the vehicle resistance power curve. The top speeds of the vehicle with different differential gear ratios are represented by the crossing points of engine power curves with resistance curve (such as v_{2max}, v_{3amx} and v_{4max} corresponding to r_{d2} , r_{d3}, and r_{d4}) or by the maximum rpm of the engine (such as v_{1max} corresponding to r_{d1}). *Fig. 6* indicates that, with r_{d3}, the vehicle has a highest top speed which corresponds to the peak power of the engine. However, with r_{d2}, the vehicle has more remaining power, defined as the difference between the engine power curve and vehicle resistance power curve only a slight top speed reduction. The remaining power can be used for acceleration or grade climbing or battery charging . As shown in *Fig. 6*, with a gear ratio of r_{d2} and at a speed of *100 Km/h*, the engine has about half of its power remaining. A large gear ratio, such as r_{d1}, will allow the vehicle to have more remaining, but the top speed will suffer a significant reduction. In contrast, too small a gear ratio, such as r_{d4}, will allow the vehicle to have a small remaining power. For a small engine with the addition of battery charging load, the differential gear ratio of r_{d2} is a suitable selection.

ACCELERATION MODE

When the vehicle experiences acceleration or steep hill climbing, high traction peak power is needed. This high transient power (peaking power) is supplied by both the engine and the motor working together. In the ELPH vehicle, the contribution of the electric motor drive to the peak power should be dominant. Thus, the acceleration and maximum gradeability of the ELPH drive train is mainly determined by the electric motor drive and battery power rating.

ACCELERATION-The ideal characteristic of a power unit for vehicular application is constant power output over the full speed range[4,5,6,]. A vehicle with this kind of power unit does not require a multi-gear transmission to enhance its acceleration and gradeability performance. A well controlled electric motor has speed-torque characteristics that are close

to this ideal, as shown in *Fig. 2*. Here the motor has a constant power output over a large range of speed and a constant torque output over the low speed range. Therefore, the acceleration performance of the ELPH vehicle will be determined by the power rating of the electric motor and is only slightly influenced by the gear number and gear ratios of the transmission.

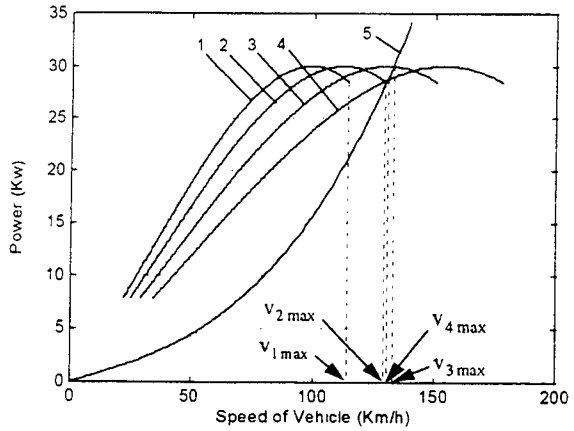

1---r_{d1}=4.78, 2---r_{d2}=4.22,
3---r_{d3}=3.64, 4---r_{d4}=3.08
5--- vehicle resistance power

Fig. 6. Engine Power Output And Resistance Power Versus Vehicle Speed with Different Differential Gear Ratios

The vehicular acceleration on a level ground can be expressed as:

$$\frac{dv}{dt} = \frac{F_t - F_w - F_f}{\delta m} \quad (m/s^2) \qquad (3)$$

where, $F_t = (T_e + T_m r_m) r_t r_d \eta_t / r$, the thrust force of ground acting on the drivewheels (T_e and T_m are engine torque and motor torque respectively; r_t and r_d are the transmission and differential gear ratios, respectively; r_m is gear ratio from motor to driveshaft.). $F_w = 0.5\rho C_D A v^2$, the aero-dynamic drug, and $F_f = mgf$, the rolling resistance. δ is the rotational inertia coefficient.

The accelerating time from zero to a desired speed , v^*, can be expressed as:

$$t = \int_0^{v^*} \left(\frac{dt}{dv}\right) dv = \int_0^{v^*} \frac{\delta m}{F_t - F_w - F_f} dv \qquad (4)$$

The calculation of the vehicle acceleration time is somewhat difficult due to the speed-torque characteristic of the engine which, generally, can not be expressed by an explicit formula. However, it may be completed by numerical methods with a computer.

Fig. 7 shows a plots of acceleration times from zero to *96 Km/h* vs. electric motor power with different gear ratios from the motor to the driveshaft, r_m. The assumptions are a *30 Kw* engine, motor characteristics as shown in *Fig. 2*, a differential gear ratio of r_d = *4.23* and transmission gear ratio of r_t = *1.0*.

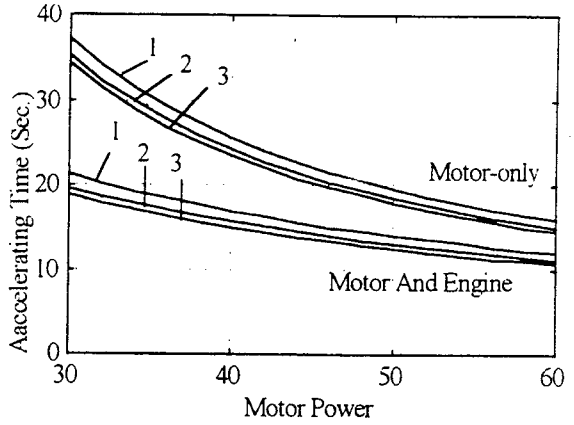

1---r_m=1.5, 2---r_m=1.9, 3---r_m=2.3

Fig. 7. The Accelerating Time Versus Electric Motor Power

As we expected, the gear ratio from the motor to the driveshaft has a small influence on the acceleration time and, the electric motor power plays a dominant role in the acceleration of the vehicle.

Using a computer program, the acceleration time of the vehicle with a multi-gear transmission can also be calculated, as shown in *Fig. 8*. The results indicate that the number of gears in the transmission has a small influence on the acceleration of the vehicle when the differential gear ratio is greater than *4*. This result is desirable because a single-gear transmission can greatly simplify the drive train and the control system.

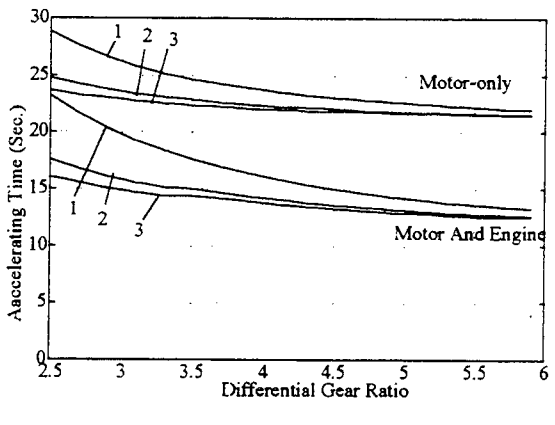

1- gear transmission, gear ratio, 1
2--2-gear transmission , gear ratios , 1.6,1
3--3-gear transmission , gear ratios, 2.54, 1.6 and 1
Engine power = 30 Kw,
Electric motor power = 42 Kw
Gear ratio from motor to driveshaft, r_m=1.7

Fig. 8. Accelerating Time with Different Number of Gears and Different Differential Gear Ratios

GRADEABILITY-The gradeability of the vehicle is determined by the maximum thrust forces acting on the drivewheels. The gradeability of a vehicle can be expressed by

$$\sin\alpha = \frac{F_t - F_w - F_f}{mg} \qquad (5)$$

where α is the road angle in degrees .

Due to the small aero-dynamic drag at low speeds, the gradeability of the vehicle is mostly determined by the maximum torque of the motor and the engine as well as the gear ratios of the transmission. *Fig. 9* shows the gradeability of the vehicle with a three-gear transmission in which the parameters used are the same as in *Fig. 8*. *Fig. 9* indicates that the gradeability will be greatly enhanced by using a multi-gear transmission. However, in real applications, the vehicle would seldom use the first or second gear for climbing a grade, because, normally, such large grades are seldom encountered in highway and urban driving. This also means that a single-gear transmission would serve the gradeability well.

Fig. 10 shows gradeability versus different power outputs with a single-gear transmission in which the parameters are the same as in *Fig. 8*. Actually, the gradeability can be enhanced, without a need for increasing the gear ratio or applying a multi-gear transmission, by decreasing the base speed of the electric motor. This is accomplished in the low speed, constant torque region of the motor operation

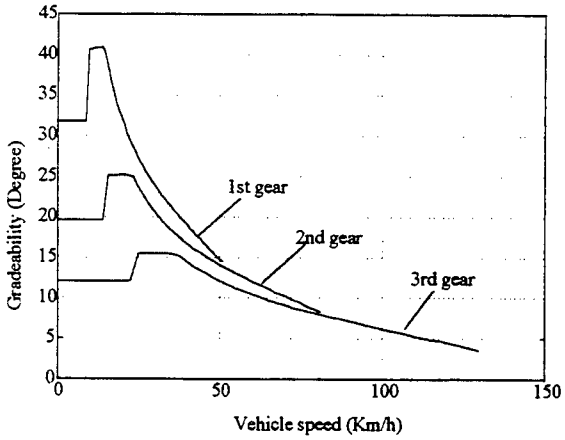

Fig. 9. Gradeability with A Multi-gear Transmission

CONCLUSION

The ELPH vehicle can combine many advantages of conventional and electric vehicles. A well designed ELPH vehicle would have a comparable performance to the conventional vehicle and excellent fuel economy and emission characteristics.

Using the method presented in this paper, the power capacity of a small internal combustion engine and a single speed reduction gear can be used to achieve a satisfactory performance and a excellent fuel economy at cruising speed. Properly selected electric motor power and speed reduction gear can eliminate application of the complicated multi-gear transmission with satisfactory acceleration and hill climbing performance.

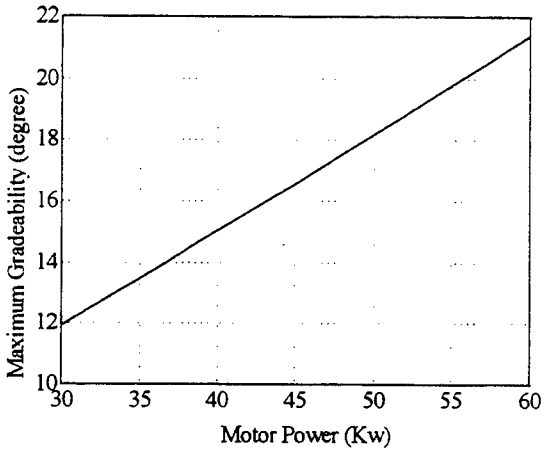

Fig. 10. Gradeability of the Vehicle with Different Motor Power Output And A Single-gear Transmission

ACKNOWLEDGMENT

The financial support of Texas Higher Education Coordinating Board and Texas Transportation Institute for the ELPH project is gratefully acknowledged.

REFERENCE

[1] Timothy C. More and Armory B. Loind, *Vehicle Design Strategies to Meet and Exceed PNGV Goals*, SAE 951906.

[2] Martin Endar and Philipp Dietrich, *Duty Cycle Operation as a Possibility to Enhance the Fuel Economy of an SI Engine at Part Load*, SAE 960229.

[3] A.F. Burke, *Battery Availability for Near Term (1998) Electric Vehicle*, SAE 911914.

[4] J.Y. Wong , *The Theory of Ground Vehicle* , John Wiley & Sons Inc. Press, 1978.

[5] M.Ehsani, K. M. Rahman, and H. Toliyat, *Propulsion System Design of Electric & Hybrid Vehicle*, accepted for publication in the IEEE Tran. on Industrial Electronics.

[6] H.A. Toliyat, K. M. Rahman, and M. Ehsani, *Electric Machine in Electric & Hybrid Vehicle Application*, Proceeding of ICPE, 95, Seoul, pp 627--635.

[7] M.Ehsani, *Electrically Peaking Hybrid System And Method*, U.S. Patent pending.

[8] J. Howze, M. Ehsani and D. Buntin, *Optimizing Torque Controller for a Parallel Hybrid Electric Vehicle*, U.S. Patent pending.

[9] Proceedings of the ELPH Conference, Texas A&M University, College Station, Texas, Oct. 1994.

960448

An Empirically Based Electrosource Horizon Lead-Acid Battery Model

Stephen Moore and Merhdad Eshani
Texas A&M Univ.

ABSTRACT

A empirically based mathematical model of a lead-acid battery for use in the Texas A&M University's Electrically Peaking Hybrid (ELPH) computer simulation is presented. The battery model is intended to overcome intuitive difficulties with currently available models by employing direct relationships between state-of-charge, voltage, and power demand. The model input is the power demand or load. Model outputs include voltage, an instantaneous battery efficiency coefficient and a state-of-charge indicator. A time and current dependent voltage hysteresis is employed to ensure correct voltage tracking inherent with the highly transient nature of a hybrid electric drivetrain.

INTRODUCTION

The behavior of a battery in the hybrid electric vehicle enviroment is complex and demands detailed analysis of battery characteristics. Lead-acid battery behavior is notorious for its dynamics under load conditions and varying state of charge levels. Because of these peculiar dynamics, a transient lead-acid battery model must be based on a series of detailed experiments executed at varying state of charge conditions and power levels. In addition, experiments must be run to evaluate charging transients as well, due to the peaking properties of the hybrid electric drive train.

The battery model is a critical component in the simulation of a hybrid electric drive train. With current lead-acid battery technologies, on which the ELPH model is based, the battery must be treated with special care to not damage cycle life by avoiding deep discharge, over-charging and gassing [1]. These limitations make the battery's operating region fairly narrow. The battery must unfailingly supply peaking power each time it is called upon and must be able to accept charge back to prepare for the next transient. This peaking/charging cycle is very demanding on the battery and must stay within the battery's narrow operating bandwidth to avoid damage. This special care treatment must be considered when modeling the drive train.

Under the hybrid peaking philosophy, it must also be considered that the battery is completely responsible for vehicle performance during transient situations. The battery must provide large amounts of energy in short bursts and must recover as much energy as possible when charging opportunities exists. Wild voltage swings occur with the massive power demands, resulting in difficult to predict performance. These high power effects must be modeled with confidence to give the simulation realistic transient performance results.

HISTORIC AND AVAILABLE BATTERY MODELS

The most basic battery model is based on the electrochemistry of the lead-acid reaction. From these equations one can derive energy storage and electromotive forces given reactant masses and geometries. Unfortunately, the basic electrochemical reaction equations do not take into account thermodynamic or quantum effects that result in phenomenons such as the time rate of change of voltage under load. It is because of these extremely complex processes that most battery models are empirical rather than based on first principle.

The Peukert equation can be used to estimate state of charge and make a fairly confident battery model. Peukert's

equation simply states that the battery capacity decreases with increasing current [2,3]:

(1) $K = I_n - T_i$

(2) $QD = K \times I^{-(n-1)}$

Where QD is the capacity of the battery in Ampere-hours, dependent on current I and battery constant n. The constant n is usually n = 1.35 for lead-acid battery types. T_i is the amount of time to discharge at current I. For example, if I is increased, QD will decrease. The problem with this equation is that it cannot model variable rate discharges, intermittent discharges or voltage behavior. It is only a fixed-rate state of charge estimator.

There are several models available that use electrical circuit equivalents to predict battery performance. Two of these models, the Kleckner Model and the Zimmerman-Peterson model uses capacitors as charge storing elements. The Kleckner model is limited because it is a discharge only model. Also complicating the use of this model is that its electrical equivalent equation terms must be recalculated and updated every time the instantaneous current draw changes. [4]

The most widely known and used model is the Shepherd model. This empirical model is used in conjunction with the Peukert equation to obtain battery voltage and state of charge given power draw variations [5,6,7]:

(3) $E_T = E_s - Ri - Ki\dfrac{Q}{Q - \int idt}$

Where Q is the capacity of the battery in Ampere-hours, E_S is the open circuit voltage, Ri is the internal resistance, K_i is the polarization resistance, and $\int idt$ is the accumulated Ampere-hours. E_T is the battery terminal voltage. The capacity Q and instantaneous current i are then related to the Peukert equation to derive QD, fractional state of charge. State of charge is found by Q / QD * 100%. Notice that this model has a interdependence of battery voltage, current draw and state of charge, very like a real battery displays. The Shepherd model has been improved upon with the addition of extra terms to describe additional phenomenon, such as the improved internal resistance calculations afforded by the Lindstorm model. The Wood model incorporates secondary equations to describe overcharging and gas generation, along with a self discharge term which is not insignificant given the current lead acid battery technology.

Another widely used battery model is the fractional discharge model. This model is based on the premise that as capacity changes with current demands the peak power availability changes as well. This can be observed directly from the Shepherd model by observing the voltage and current as the capacity decreases. However, the fractional discharge model derives state of charge directly from the incremental power and energy densities rather than comparing capacities. This is a very intuitive way of obtaining the state of charge because the experiments required to analyze the power and energy densities are relativity easy. Experiments are run at several different state of charge levels and loads, and as the data points are collected they are curve fit to form an equation for power density. The results of this model do not include specifics about voltage and current but rather only power and state of charge. [8]

ELPH 2.0 BATTERY MODEL

The ELPH 2.0 battery model is a combination of the battery modeling techniques described above. Experiments similar to the ones required by the fractional state of charge model were run to characterize battery performance. Batteries were subjected to varying degrees of load at specific state of charge conditions. Using experimental results from several batteries, important relationships were developed. This model is based on results from more than a single sample to eliminate the possibility of modeling manufacturing aberrations in a single example from the manufacturer.

Key relationships used in constructing the model includes the voltage dependence on current draw and state of charge. A high confidence voltage modeling is a requirement of the ELPH simulation. Another key relationship is the battery efficiency's dependence from power draw and state of charge. According to Peukert's equation, at high currents the battery energy capacity will decrease more than the amount of energy removed. The difference between the change of amount of available energy and the amount of energy removed can be expressed as an efficiency. Battery efficiency is described as:

(4) $\eta = \dfrac{\Delta QD}{E_T \times i \times \Delta T}$

Where η is efficiency, ΔQD is the change of battery capacity, E_T is the battery voltage at the terminals, i is the instantaneous current, and ΔT is the time step. Notice that E_T * i * ΔT is energy. This equation can be rewritten as:

(5) $\eta = \dfrac{\text{energy capacity decrease}}{\text{energy removed}}$

Through experimentation, a mathematical surface consisting of a grid of measured data points was constructed. An equation was surface-fitted to these points, resulting in a η(SOC,P) relationship where η is efficiency, SOC is the state of charge, and P is the instantaneous power demand.

The next relationship developed is the E_T(SOC,i) relationship, describing the terminal voltage of the battery E_T given a current draw and the state of charge. Measured data points were obtained by subjecting the battery to several tests under different loads and state of charge conditions while monitoring voltage. Again, a mathematical grid was constructed and an equation was surface-fitted (see Figure 1 and 2 for characteristic surfaces).

Horizon Discharge

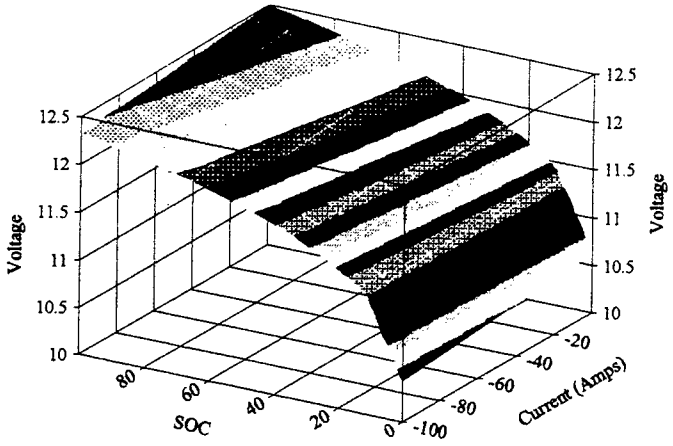

Figure 1. Notice that the voltage is nearly independent of current. This "flat" profile is very surprising and shows the Horizon's excellent suitability for electrically peaking applications.

Horizon Charge

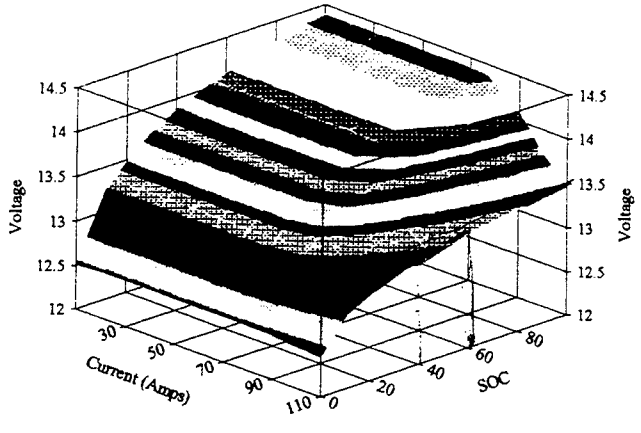

Figure 2. The recharge curve has the expected broad characteristic of being able to absorb large amounts of current at low states of charge.

A battery does not exhibit an instantaneous change in voltage with change of load. This differential change of voltage over time ($\Delta E_T/\Delta T$) had to be taken into account because the ELPH model requires very rapid peaking transients with extreme power demands. Inaccurate voltage modeling would lead to poor performance predictions. Most models that take this voltage hysteresis into account generalize the time constant to be about τ = 0.08 seconds. After experimental measurements were made, a fixed time constant τ could not be assumed, rather the $\Delta E_T/\Delta T$ is variable, dependent on power demand. At low or near zero currents, the battery can take several seconds to approach a steady voltage. At high power demands, the battery voltage reacts much more quickly:

(6) $\tau = f(\Delta T, i)$

(7) $E_T^* = E_T \times e^{-\frac{\Delta T}{\tau}} + E_T(SOC,i) \times (1 - e^{-\frac{\Delta T}{\tau}})$

This allows the voltage to track power demands with a hysteresis with a current dependent variable time constant (Figure 3)

The ELPH battery model operates by combining each of these terms to calculate terminal voltage and state of charge given a current demand. Outputs from the model include battery voltage Es, instantaneous current demand i, instantaneous power demand, battery efficiency η, $\Delta E_s/\Delta_T$ monitoring and state of charge SOC.

10 Second 5 kW Spike

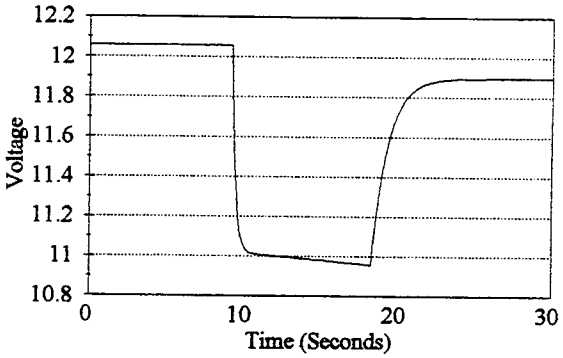

Figure 3 Voltage Hysteresis

MODEL LIMITATIONS

The current revision of the ELPH 2.0 battery model is capable of performing simulations of an Electrosource Horizon 95 Ampere-hour battery. Simulations have a number of restrictions to be eliminated in future revisions.

A major limitation to the present revision is that the charge equation relating efficiency to power demand and state of charge η(SOC,P) can be made more accurate. This is due to the difficulty of experimentation and available resources. With the advent of the ELPH stationary and mobile testbeds, this phenomenon will be readily observable in a vehicle environment, facilitating much more pertinent data and empirical measurements. The next revisions are expected to predict charging performance much more confidently.

Secondary equations that include battery inefficiencies such as heat and gas generation will also be added. The current revision of the model does not allow for overcharging, which imposes the restriction that the model must never experience charging conditions once the battery is fully charged. This problem must also be addressed because the hybrid electric drive train will expose the batteries to charging extremes as well as discharging extremes.

CONCLUSION

The ELPH 2.0 battery model is capable of high confidence performance prediction under a restricted operating bandwidth. The model takes into account variable efficiencies of charging and discharging under different and instantaneous situations, critical in a hybrid peaking drive train. State of charge is accurately predicted and overall battery efficiency over particular load scenarios can be calculated.

Battery voltage tracking is maintained by implementing a variable hysteresis dependent on current draw. Peak power and power density characteristics can be properly calculated, otherwise vehicle performance prediction would be skewed due to excessive or deficient power availability from the battery.

During the summer of 1994 the ELPH research team was awarded a 1994 Dodge Neon for the 1995 HEV Challange. The stock engine was removed and replaced by a parallel drivetrain consisting of a Honda CV250 motorcycle engine modified for compressed natural gas and an Advanced DC eight inch motor. Ten Electrosource Horizon batteries supply electrical power to a standard Curtis DC motor controller with regenerative capability. The control strategy, implemented by an Alan-Bradly programmable logic controller, was developed by the ELPH team during modeling and simulation studies. The vehicle is currenly being outfitted with a comprehensive data aquasition system to collect the neccesary data for model validation. With the accession of the ELPH mobile testbed, numerous improvements can be made to the model with the amount of data that will be available from an in-vehicle prototyping platform.

A stationary testbed consisting of electrical drive components will provide high precision data for further model validation. The stationary testbed features a 7.5 kW vector controlled induction motor connected in series with a 11 kW DC dynamometer. Power is supplied by a 144 volt battery pack. The DC dynamometer will be programmed with vehicle dynamics to simulate a road load. This testbed, expected to demonstrate electric vehicle driving scenarios by January 1996, will provide data on the performance of electric motors and batteries in EV and HEV environments.

ACKNOWLEDGMENT

The financial support of Texas A&M University, Texas Transportation Institute and Texas Higher Education Coordinating Board Advanced Technology Program for the work done in the ELPH project is gratefully acknowledged.

REFERENCES

1. Eshani, M., *et al.*, "Executive Summary of the ELPH Project", ELPH Conference Proceedings, 1994
2. White, K.E., "A Digital Computer Program for Simulating Electric Vehicle Performance", SAE 780216, 1978
3. Van Donegan *et al.*, "Theoretical Prediction of Electric Vehicle Energy Consumption and Battery State of Charge During Arbitrary Driving Cycles", EVC Symposium VI, EVC paper 8115, Baltimore, Oct. 1981
4. W. Facinelli, "Modeling and Simulation of Lead Acid Batteries for Photovoltaic Systems", Proceedings of the 18th IECEC, 1983
5. Unnewehr, L.E., and Freedman, R., "A Comparative Evaluation of Battery Models for Electric Vehicle Simulation", Industry Application Society Conf., 1979, IEEE IAS 79-31B
6. Shepherd, C.M., "Design of Primary and Secondary cells: An Equation Describing Battery Discharge", J. Electrochemical Soc., 1965, 112, pp. 644-657
7. Taylor, D.F., and Siwek, E.G., "The Dynamic Characterization of Lead Acid Batteries for Vehicle Applications", SAE 730252, 1973
8. Bumby, J.R, Forster, I., *et al.*, "Computer Modeling of the Automotive Energy Requirements for Internal Combustion Engine and Battery Electric Powered Vehicles", IEEE Proceedings, Vol 132, Pt. A, No. 5, Sept. 1985

OTHER REFERENCES

1. Manwell, J.F., and McGowan, J.G., "Lead Acid Battery Storage Model for Hybrid Energy Systems", Solar Energy, Vol. 50, No. 5, pp. 399-405, 1993
2. Salameh, Z.M., *et al.*, "A Mathematical Model for Lead-Acid Batteries", IEEE Transactions on Energy Conversion, Vol. 7, No. 1, March 1992, pp. 93-97
3. Hornstra, F., and Yao, N., "Standard Test Procedures for Electric Vehicle Batteries at the National Battery Test Laboratory", SAE Paper No. 820401, 1982

ABOUT THE AUTHOR

Stephen Moore is an electrical engineering graduate student at Texas A&M University doing research for the ELPH team under the supervision of Dr. Merhdad Ehsani. His main area of focus is computer modeling and simulation of energy storage systems. The ELPH team can be reached by FAX at 409-862-1976.

(6 P

Design Considerations For EV And HEV Motor Drives

Khwaja M. Rahman
Student Member, IEEE

Mehrdad Ehsani
Fellow, IEEE

Texas Applied Power Electronics Center
Texas A&M University
College Station, TX 77843-3128
Tel: (409) 845-7582
Fax: (409) 862-9173
Email: ehsani@ee.tamu.edu

Abstract: Vehicle load dictates an extended range constant power operation from its propulsion system in order to meet its operational constraints such as initial acceleration, gradability etc., with minimum power rating. The internal combustion engine (ICE) fails miserably in generating this torque profile. Multiple gearing, therefore, is necessary with the operation of the ICE for vehicle application. An indefinite extension of the constant power range, however, has some undesirable effects on the overall system. The total system cost may go up with the extension, beyond a certain point, of the constant power range. It may be possible, for each motor type and its design, to arrive at some optimal number for the extended constant power range which will minimize the total system cost. To help in obtaining the extended constant power range special design and control of the electrical propulsion system would be necessary. This design process would include selection of motor type, its size, maximum speed, control strategy etc. This paper will discuss the necessity of the extended constant power range and its effect on the system. The relevant electric motor design and control issues will be discussed. Several commonly used motors, with special emphasis given to switched reluctance motor (SRM), will be studied to determine their performances for vehicle applications.

I. Introduction

Electric and hybrid electric vehicles offer the most promising solutions to reduce vehicular emission. Electric vehicle (EV) constitute the only commonly known group of automobiles that qualify as zero emission vehicles (ZEVs). These vehicles use an electric motor for propulsion, and batteries as electrical energy storage devices. Although, there have been significant advancements in motors, power electronics, microelectronics, and microprocessor control of motor drives, the advancement in battery technology has been relatively sluggish. Hence, the handicap of short range, associated with EV's still remains. Given these technology limitations, hybrid electric vehicle (HEV) seems to be the viable alternative to ICE automobile at the present. HEVs qualify as ultra low emission vehicles (ULEVs), and do not suffer from the range limitations imposed by the EVs. These vehicles combine more than one energy source to propel the automobile. In the heat engine/battery hybrid systems, the mechanical power available from the heat engine is combined with the electrical energy stored in a battery to propel the vehicle. These systems also require an electric drive train to convert electric energy into mechanical energy, just like the EV. Hybrid electric system can be broadly classified as series or parallel hybrid systems.

In series hybrid systems, all the torque required to propel the vehicle is provided by an electric motor. In parallel hybrid systems the torque obtained from the heat engine is mechanically coupled to the torque produced by an electric motor [1]. In the electric vehicle, the electric motor behaves exactly in the same manner as in a series hybrid. Therefore, the torque and the power requirements of the electric motor are roughly equal for an EV and series hybrid, while they are lower in parallel hybrid.

Designing an electrical propulsion system for EV and HEV is a difficult job. Special design and control of a motor would generally be required in order to optimize its performance for vehicle applications. An extended constant power range operation is necessary from the electric motor to minimize the acceleration power of the vehicle. This paper will discuss this necessity of the extended constant power range and its effect on the propulsion system. The design and control issues for extending the constant power range of operation for few commonly used motors will be discussed with paying special attention to the switched reluctance motor.

II. Optimal Torque Speed Profile of the EV and HEV Propulsion System

Our recent study has shown that, a vehicle, in order to meet its operational constraint such as initial acceleration and gradability with minimum power needs its propulsion system to operate in constant power [2]. The power rating of the motor that is deviating from the power source regime can be as much as two times that of a motor operating in constant power through out its speed range in a vehicle. Fig. 1. represents theoretically the optimal torque-speed profile of any motor drive for vehicle application.

The importance of the extended constant power range can be better understood by a numerical example comparing the required acceleration power for different constant power speed range (as a multiple of its base speed). Let us consider the following vehicle:

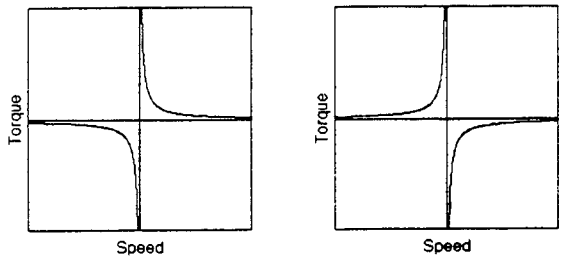

(a) (b)

Fig. 1. Optimal torque-speed profile for EV and HEV propulsion systems, (a) motoring, (b) generating.

- 0-26.82 m/s (0-60 mi/h) acceleration in 10 s;
- vehicle mass of 1450 kg;
- rolling resistance coefficient of 0.013;
- aerodynamic drag coefficient of 0.29;
- wheel radius of 0.2794 m (11 in);
- level ground;
- zero head-wind velocity;
- maximum motor speed 10,000 r/m;
- maximum vehicle speed 44.7 m/s (100 mi/h);

Table I shows the example of power requirement to meet the above acceleration requirements for several

Table I

	Constant Power Range					
	1:1	1:2	1:3	1:4	1:5	1:6
Motor Rated Power (kW)	110	95	74	67	64	62

constant power ranges of the propulsion power train. The result of Table I clearly shows the importance of extended constant power range. The electric motors capable of performing longer constant power ranges meet the acceleration requirement with lower power rating. A detailed study of the propulsion system design of EV and HEV can be obtained in [2]. Fig. 2 shows the power rating of the propulsion system for the required initial acceleration as shown in Table I. however, as a function of the motor rated speed. The power requirement is minimum as we can see in Fig. 2 when the motor rated speed is zero, i.e. the operation is entirely in constant power. The other extreme of the curve shows the power requirement for operation of the propulsion system entirely in constant torque.

We have already seen that the longer constant power range of operation of the electrical propulsion system reduces the power requirement for initial acceleration. However, with the increase of the constant power range of the electrical motor, for the same maximum speed of the motor, the rated torque of the motor increases despite the fact that motor power is decreasing. This is illustrated in Fig. 3 for a motor with maximum speed of 10,000 rpm. Therefore, although the converter power (volt-ampere) requirement hence the converter cost will decrease with increasing constant power range, the motor size, volume, and

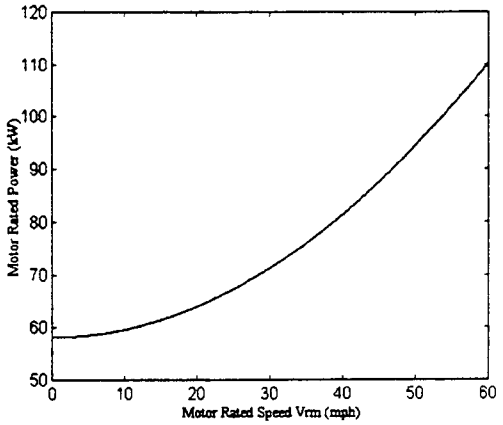

Fig. 2. Initial acceleration power requirement.

cost will increase with increasing constant power range. The motor size can only be reduced in this case by picking a

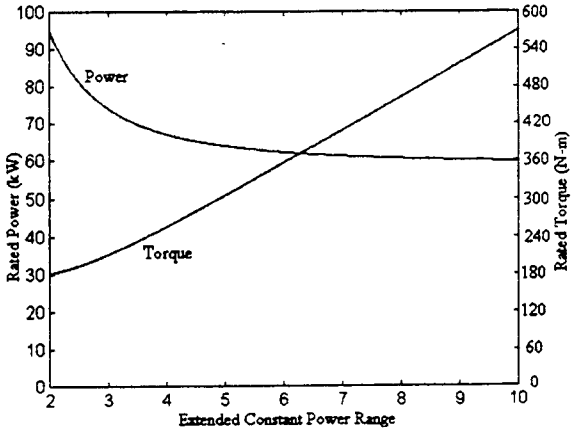

Fig. 3. Rated power and torque of the motor as a function of the constant power speed range.

motor capable of running at a higher speed. The motor maximum speed, in one hand, can not be increased indefinitely without incurring more cost. On the other hand, high maximum motor speed would require a bigger transmission. Hence, there exist multitude of system level conflicts with the extension of the constant power range. However, for different motor (different motor has different high speed capability) it may be possible to arrive at an optimal constant power range number base on the cost and the performance analysis. This analysis is, however, beyond the scope of this paper.

III. Design Considerations for EV and HEV Motor Drives

In light of the above discussion we would expect the following characteristics from EV and HEV motor drives

- a wide speed constant power range
- high maximum speed capability
- good efficiency
- low cost
- low maintenance
- safety/reliability
- ease of control

Modern electric motor is benefited from design and material innovations. Availability of low loss, high grade, stress relieved, coated electrical steel laminations have contributed significantly to the improvement of efficiency and reduction in size of modern electric motors. In the recent EVs and HEVs the dc commutator motors, ac induction motors, and permanent magnet (PM) brushless dc motors are common. Recently, there is also an interest in using switched reluctance motor.

Two most important characteristics for the EV and HEV motor drives are the wide speed constant power capability and the high operational efficiency. Efficiency is particularly important for the operation of the electric vehicle. The electric machines for electric and hybrid electric vehicle applications should be designed and controlled for better efficiency. For instance, the high speed operation of the motor would increase the iron losses. Motors for vehicle application should, therefore, be designed with very thin laminations. As far as the efficiency is concerned, the permanent magnet motors have an upper hand over all other motors. The absence of rotor winding eliminates the rotor losses. Furthermore, due to the presence of the permanent magnet field, the rotor excitations are not required to be fed through the stator as are the cases for the induction and the switched reluctance motor. However, at speeds beyond the base speed weakening of the permanent magnet field requires an additional stator current component. This would lower the efficiency of the permanent magnet motors at higher speeds. Switched reluctance motors can be also designed and controlled for improved efficiency. For example, motors designed with narrower stator pole widths will have more room for winding placement. This would result in a lower copper loss. However, other impacts for this simple modification should be studied.

Extended constant power capability, on the other hand, is motor type, its design, and the control dependent. DC commutator motors are inherently suited for extended constant power operation. However, poor efficiency, low maximum speed capability, and bulky nature limit their operation in vehicle applications. The constant power capability of ac motors depends largely on the motor type its design and also on the control strategy. The design and control issues for obtaining an extended constant power range are discussed next for few potential EV and HEV motors.

A. Induction Motor

The control of induction motor for EV and HEV applications is predominantly the field oriented control (FOC) [3]. Break down torque in induction motor, however, limits their extended speed constant power capability. A machine designed with a high breakdown torque, e.g. four times the rated torque, allows a constant power range of four times the base speed. The constant power range, therefore, can be extended by designing motor with a high breakdown torque. Induction motors designed with lower leakage inductance have higher breakdown torque. This method of designing an induction motor was presented by Boglietti [4] for spindle application. Induction motor designed with low leakage inductance, however, has higher harmonic components and experience more copper loss. Two other methods of control of induction motor are also presented which extend the constant power range. One method involves magnetic contacts and tapping in the windings [5]. As the speed increases beyond the base speed, the magnetic contacts are used with the tappings to progressively cut some part of each phase windings. This way the back emf is reduced and a long constant power range is obtained. The other method involves the winding pole changing. By changing the winding connection a four pole winding can be changed to a two pole winding and a designed constant power range of two times the base speed can be extended, in theory, to four times the base speed. Most recently [6], a contactor less pole changing scheme is presented which uses two inverters with the two sets of winding of the induction motor. By changing the direction of current flow in one of the windings, four pole winding configuration is changed to a two pole configuration and vice versa.

B. Permanent Magnet ac (PMAC) Motor

Two types of permanent magnet motors are generally built. One is the trapezoidal back emf type while the other is the sinusoidal back emf type. The trapezoidal motors usually have magnets mounted on the surface. The surface mounting of the magnets reduces the stator inductance. As a consequence, these motors suffer from poor field weakening capability. By adding external inductance and then by the usual phase advancing technique the range can be extended [7]. The additional cost and the bulkiness make this method not very attractive. A specially designed multi-pole multi-phase trapezoidal motor which claims to eliminate the phase coupling, has been demonstrated to obtain a range of three times the base speed [8].

The sinusoidal PM motors designed with salient rotor by the interior magnet placement are capable of exhibiting an extended constant power range. Some design rules for sinusoidal PM motors and the synchronous reluctance motor for obtaining a long constant power range were presented in [9]. An optimal design line as functions of rotor saliency and magnet usage was also presented. As mentioned there, the key to obtaining a long constant power range is to design the rotor with high saliency, if one wants to minimize the magnet usage. The high saliency rotors are, however, usually axially laminated. Hence, the rotor construction will be costly, moreover, the rotor will have speed limitations.

C. Switched Reluctance Motor (SRM)

The SRM relies upon reluctance torque rather than the more conventional reactive torque of wound field synchronous, surface magnet PM, and induction machines. The SRM is a doubly salient reluctance machine with independent phase windings on the stator. The rotor does not have any winding, and is usually made of steel lamination. The stator and rotor have unequal number of poles with three phase 6/4, four phase 8/6, and three phase 12/8 being common configuration. Due to the absence of rotor windings this motor is very simple to construct, has low inertia, and allows an extremely high speed operation. A cross sectional view of a 6-4 SRM is shown in Fig. 4.

The absence of rotor copper loss eliminates the problem, as in an induction motor, associated with rotor cooling which has a poor thermal path. Moreover, due to unipolar excitation, the SRM core is subjected to a magnetic reversal at a much reduced frequency than the stator excitation. This results in a reduced hysteresis loss in the SRM core unlike the permanent magnet (PM) motors and the induction motor.

SRMs normally are low cost machine for their extremely simple construction. Moreover, due to the unipolar excitation, it is possible to design SRM converters which requires a minimum of one switch per phase. SRM operation is extremely safe and this motor is particularly suitable for hazardous environment. The SRM drive produces zero or small open circuit voltage and short circuit current. Furthermore, most SRM converters are immune from shoot through faults, unlike the inverters of induction and brushless dc motors.

Rapid acceleration and extremely high speed operation in SRM is possible for its low rotor inertia and simple construction. SRM operates in constant torque from zero speed upto the rated speed. Above rated speed upto a certain speed, the operation is in constant power. The range of this constant power operation depends on the motor design and its control. Beyond constant hp operation and up to the maximum speed, the motor operates in the natural mode, where the torque reduces as the square of the speed. Because of this wide speed range operation, SRM is particularly suitable for gearless operation in EV/HEV propulsion.

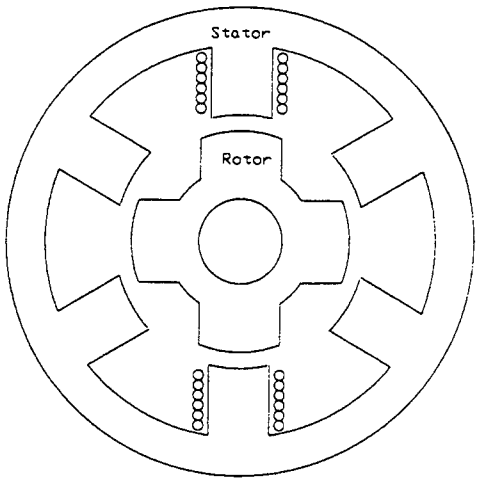

Fig. 4. Cross sectional view of a 6-4 SRM.

Motor current in the SRM drive below base speed can be controlled from zero to the maximum by chopping with a fixed phase excitation. The excitation angle can be controlled to optimize efficiency and torque ripple. Operation beyond base speed in constant hp is possible by phase advancing the firing angle until an overlapping between the two successive phases occurs.

To extend the constant power range the motor should be designed appropriately and controlled optimally. In order to obtain the optimal control parameters which maximize the constant power range it is necessary to obtain an accurate model of SRM. The highly non-linear nature of operation of SRM, however, complicates the analysis. The non-linear field solutions within the motor are needed to be solved in order to

develop a non-linear model of SRM. For accuracy, finite element (FE) analysis should be performed for the field solutions. The design methodology presented next may be followed in order to obtain an appropriate SRM geometry for EV and HEV applications.

1. SRM Design Methodology

The design methodology suggested in this paper has the following steps

i) Designing, using hand calculation, of several SRM with varying stator and rotor pole numbers and geometries.
ii) Investigation of the static performance characteristics of each SRM designed geometries using finite element analysis.

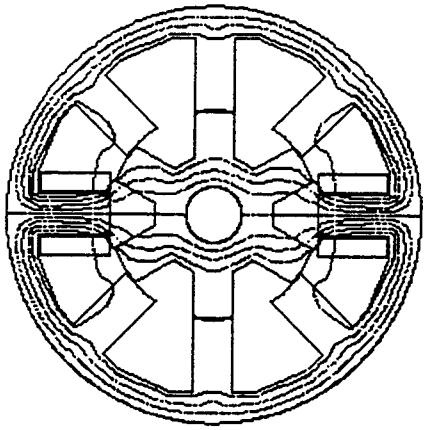

Fig. 5. A 2-D finite element field plot for an 8-6 SRM.

iii) Development of a non-linear SRM model using the generated static flux linkage and torque characteristics.
iv) Development of an optimal control scheme using the dynamic model. More about the optimal control algorithm will be discussed later.
v) Investigation, using the dynamic model, the steady state and dynamic performance of each SRM geometry with the optimal control.
vi) Repeat step i) through v) until the desired performance is achieved.

The desired performances for EV and HEV motors have been discussed earlier. We are more concerned here to obtain a long constant power range. The proposed design methodology is a powerful approach to investigate the SRM capability for EV and HEV applications, however, is extremely time consuming. We next talk about the non-linear modeling of SRM and development of the optimal control algorithm.

2. SRM Non-linear Model

The SRM voltage equation is

$$V = iR + \frac{d\psi}{dt} \quad (1)$$

where i is the phase current, R is the phase coil resistance, and ψ is the flux linkage. $\psi(i,\theta)$ is a nonlinear function of phase current i and the rotor position θ. The finite element analysis can be used to obtain the non-linear solution of the $\psi(i,\theta)$. One such static solutions of the non-linear field and the developed torque are shown in the Fig. 6.

These static flux (Ψ-θ-i) and torque (T-θ-i) data are used to develop a dynamic model of SRM. A block diagram of the dynamic model is shown in Fig. 7.

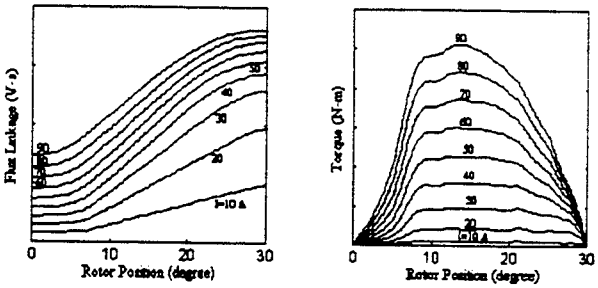

Fig. 6. Static flux linkage and the torque as functions of rotor position and stator current.

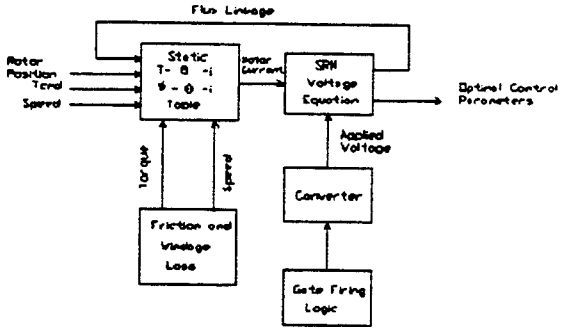

Fig. 7. A block diagram of the non-linear model of SRM.

SRM experience much higher commutation frequency than other motors of same speed and pole counts. Moreover, the flux waveform at different core and pole segments of SRM have different frequencies and different shapes, rich in harmonics. As a consequence, the core loss at high speed can very well become the dominant loss component in the motor. Therefore, for better accuracy the core loss model should be included in the dynamic model. Due to the non-linear and non-sinusoidal nature of operation, development of the core loss model is difficult for SRM, nonetheless, core loss models are presented in the literature [10,11]. The developed dynamic model is used to obtain the optimal control parameters which will

maximize the constant power range with maximum torque per ampere.

3. Optimal Control Algorithm

SRM high speed control parameters are the

- phase turn-on angle.
- phase turn-off angle.

these control parameters need to be controlled optimally to extend the constant power range with maximum torque per ampere. The developed non-linear model is used in this purpose. The necessary process is a search process or a root seeking process which will examine all the possible control parameters for each torque and speed to obtain the optimal ones. As can be understood, this is also a time exhaustive process.

4. Design Example

One 30 kW 6-4 SRM design along with its steady state performance with the optimal control will be presented in this sub-section. The presented SRM design is one design, not necessarily the SRM design, however, the constant power range performance is quite impressive for the presented SRM. A more systematic study of the SRM design methodology will be presented elsewhere.

Design Geometry:

- Power 30 kW
- Bus voltage 270 V
- Corner Speed 2500 rpm
- Peak torque, 114.6 N-m
- Maximum Speed 12,500 rpm
- Rotor pole angle 32.5°
- Stator pole angle 31°
- Air gap 0.04 inch
- Rotor outer diameter, 5.7 inch
- Stack length, 5.7 inch
- Stator inner diameter, 8.6 inch
- Stator outer diameter, 10.5 inch
- Number of turns per pole, 30
- RMS phase current, 104 amps (4 A/mm^2)
- M-19 steel, 14 mill thickness

The average torque along with the optimal angles are shown in Fig. 8. The phase current at high speed is shown in Fig. 9. As we can see the, the phase current decreases during constant power high speed operation, when controlled optimally. This is a direct consequence of the fact that the power factor is increasing during the high speed operation of the SRM.

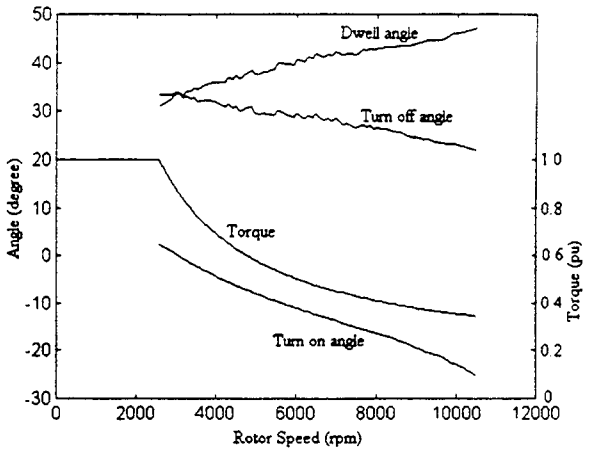

Fig. 8. Average torque and the optimal angles for high speed operation of SRM.

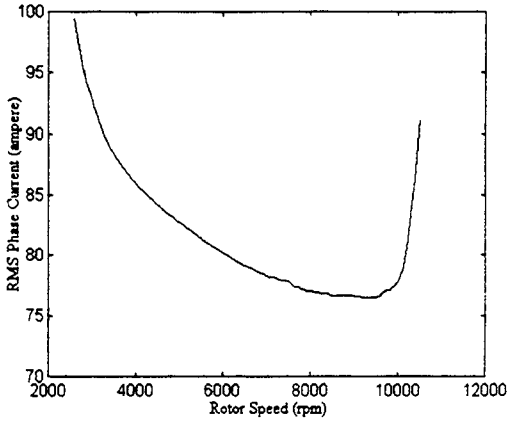

Fig. 9. Phase current during high speed constant power operation.

IV. Conclusion

The extended range constant power capability of different motors are discussed. Different means to extend the constant power range are also discussed. The design methodology and the control strategy for obtaining an extended constant power range for SRM are presented. The presented SRM design shows a good constant power range with improved power factor over its low speed operation.

V. References

[1] A. F. Burke, "Hybrid/Electric vehicle design options and evaluations," *SAE paper # 920447*, Feb., 1992.

[2] M. Ehsani, K. M. Rahman, and H. Toliyat, "Propulsion system design of electric and hybrid vehicles," *IEEE Trans. on Industrial Electronics*, vol. 44, no. 1, pp. 19-27.

[3] A. M. Trzynadlowski, *The Field Orientation Principle in Control of Induction Motors*, Kluwer Academic Publishers, Boston, 1994.

[4] A. Boglietti, P. Ferraris, M. Lazzari, and F. Profumo, "A new design criteria for spindle induction motors controlled by field oriented technique," *Electric Mach., Power Syst.*, vol. 21, pp. 171-182, 1993.

[5] T. Kume, T. Iwakane, T. Sawa, and T. Yoshida, "A wide constant power range vector-controlled ac motor drive using winding changeover technique," *IEEE Trans. on Industry Applications*, vol. 27, no. 5, Sept./Oct. 1991.

[6] M. Osama, and T. A. Lipo, "A new inverter control scheme for induction motor drives requiring wide speed range," *IEEE Trans. Industry* Applications, vol. 32, pp. 938-944, 1996.

[7] T. Sebastian and G. R. Slemon, "Operating limits of inverter-driven permanent magnet motor drives," *IEEE Trans. Industry Applications*, vol. 23, pp. 327-333, 1987.

[8] C. C. Chan, J. Z. Jiang, G. H. Chen, X. Y. Wang, and K. T. Chau, "A novel polyphase multiple square-wave permanent magnet motor drive for electric vehicles," *IEEE Trans. on Industry Applications*, vol. 30, no. 5, pp. 1258-1266, Sept./Oct. 1994.

[9] W. L. Song, and T. J. E. Miller, "Field weakening performance of brushless synchronous AC motor drives," *IEE Proc. Electric Power Application*, vol. 141, no. 6, pp. 331-340, 1994.

[10]

Evaluation of Soft Switching for EV and HEV Motor Drives

Mehrdad Ehsani, *Fellow, IEEE*
Khwaja M. Rahman, *Student Member, IEEE*
Maria D. Bellar, *Student Member, IEEE*
Alex Severinsky, *Senior Member, IEEE*

Texas A&M University
Department of Electrical Engineering
College Station, TX 77843-3128
Phone: (409) 845-7582
Fax: (409) 862-1976

Abstract-**Soft switching has the potential of reducing switch stresses and of lowering the switching losses as compared to hard switching. For this reason, several soft switching topologies have been presented in the literature. Each topology has some advantages. Their operation, however, requires additional active and/or passive elements. This introduces additional cost and complexity. To understand the effectiveness of the soft switching technique, when applied to electric vehicle (EV) and hybrid electric vehicle (HEV) systems, it may be necessary to first evaluate their system requirements and performances. This evaluation process would require knowledge of the vehicle dynamics. The vehicle load requires a special torque-speed profile from the drive train for minimum power ratings to meet the vehicle's operational constraints such as, initial acceleration and gradability. The selection of motor and its control for EV and HEV applications is dictated mainly by this special torque-speed requirement. As a consequence, this requirement will have a strong influence on the converter operation. This paper makes an attempt to evaluate EV and HEV running in both standard FTP75 city driving cycle and highway driving cycle. The analysis will be carried out for several most commonly used electric motors operating on the optimal torque-speed profile. Special attention will be given to the converter losses. Features of the soft switching will be evaluated in the context of the dynamic vehicle power flow and the system losses, as well as the power converter requirements. The relative significance of soft switching for EV and HEV systems will then be established.**

I. Introduction

Power switches are an integral part of any power converter circuit. Unfortunately, they are also the major source of power dissipation in the circuit. This power dissipation is caused by two features. One is conduction voltage drop in the switch while the switch is conducting. Some devices have lower conduction drops (MCT, BJT), hence lower conduction losses, while other devices have medium to high conduction drops (IGBT, MOSFET), hence medium to high conduction losses. The other cause of energy dissipation in a power switch is the dynamics of the switching. Switching of current in the presence of a switch voltage and vice versa, commonly referred to as hard switching, causes power losses in the switch. The switching loss increases with the switching frequency. To reduce the switching loss very fast devices are built. These devices have very fast turn-on and turn-off characteristics. However, high di/dt and dv/dt associated with this fast switching increase stresses on the switch and causes EMI. To alleviate the difficulties associated with hard switching, the concept of soft switching was introduced. The main underlying principle in soft switching is to switch the power device at the instant when the switch current is zero, known as zero current switching (ZCS), or switch the device when switch voltage is zero, known as zero voltage switching (ZVS). This way both the switching loss and switch stresses can be reduced. Many soft-switched converter topologies have been presented in the literature [1-6]. The followings are usually claimed with respect to the operations of the soft-switched converter topologies:

- higher efficiency,
- better device utilization,
- reduced size of filtering elements,
- higher power density,
- reduced acoustic noise,
- reduced EMI,
- fast dynamic response,
- reduced torque and current ripple.

However, the operation of the soft-switched converters requires additional active and/or passive elements. This introduces additional cost and complexity. Moreover, some of the advantages listed above may be questionable and some may not be very critical for some applications. Therefore, it may be necessary to assess the effectiveness of soft switching compared to hard switching, in connection to specific applications. This paper, therefore, makes an attempt to evaluate soft switching for electric vehicle (EV) and hybrid electric vehicle (HEV) drivetrain applications. This evaluation is based on the systems performance and on the power converter requirements. First knowledge of the vehicle dynamics will be needed. A study of vehicle dynamics reveals that, the vehicle powertrain is required to exhibit a special torque-speed profile for minimizing the power requirement to meet the vehicle's operational constraints [7]. The selection of the electric motor and its control will be governed by this special torque-speed requirement. As a consequence, the converter operation will be greatly influenced by this special requirement. A simplified analysis is carried out on a system level for induction motor, switched reluctance motor (SRM), and brushless dc (BLDC) motor operating on the optimal

torque-speed profile. Efficiency is a maior issue, especially for EV operations. Hence, special attention will be given to the converter losses, as a means to evaluate the improvement in the system efficiency that could be achieved by using soft switching. The loss estimation will be carried out for the vehicle running in both standard FTP75 city driving cycle and highway driving cycle. The relative significance of soft switching for EV and HEV systems will then be established.

II. EV and HEV Characteristics

A. EV and HEV Architecture

Electric vehicles (EVs) use an electric motor for propulsion and battery as the only source of energy. These vehicles constitute the only commonly known group of automobiles that are classified as Zero Emission Vehicles (ZEVs). However, EVs suffer from range limitations. As a consequence, efficiency is a major issue for EV, since it relates directly to the range of the vehicle.

Hybrid electric vehicles (HEVs) are classified as Ultra Low Emission Vehicles (ULEVs), and do not suffer from the range limitations imposed on the EVs. This is due to the fact that the power train combines more than one energy source to propel the vehicle. There are many different power train configurations for hybrids, but in general, they fall into two categories: series and parallel. In series hybrid the ICE engine is normally used to charge a battery pack through a generator, while the electric motor propels the vehicle powered by the battery. It is also possible to direct the ICE power directly to the wheels through the motor generator pair when the battery is fully charged. Thus, the engine can be decoupled from the wheel and always run in the optimal efficiency region. However, the several stages of energy conversions have their associated power losses. In contrast, the parallel hybrid system connects both the ICE and the electric motor in parallel. These two components directly provide the power into the wheel.

In series hybrid system, the electric motor behaves exactly in the same manner as in an electric vehicle. Therefore, the torque and power requirements of the electric motor are roughly equal for an EV and series hybrid, while they are comparatively lower for parallel hybrid. For HEVs, electrical efficiency is not as critical as it is in the case of EVs.

B. Optimal Torque Speed Profile for EV and HEV Drivetrain

Our recent study has shown that, a vehicle, can meet its performance requirements with minimum power rating if the powertrain operates mostly in constant power [7]. The power rating of a motor that deviates from the constant power regime can be as much as two times that of a motor operating at constant power throughout its speed range in a vehicle.

The electric motor in its normal mode of operation can provide constant rated torque up to its base or rated speed. At this speed, the motor reaches its rated power limit. The operation beyond the base speed, up to the maximum speed, is limited to this constant power region. The range of this constant power operation depends primarily on the particular motor type and its control strategy. It is obvious from the previous discussion that an electric machine must be capable of performing a long constant power operation in order to be suitable for EV and HEV applications. A range of six times the base speed in constant power would generally be required in order to reduce the power requirement to an appreciable level [7]. Clearly, for normal vehicle operation the optimal motor will operate mainly in constant power range. In our study, therefore, special attention will be given to the converter operation for high speed constant power operation of the drivetrain.

The specification of the power of the motor along with its power factor (pf) of operation will define the VA rating of the converter. Since different types of motors have different constant power capabilities and have different pf of operation, the converter VA rating will be different for each motor.

C. Methods of Torque Control at Low Speed and High Speed

The method of torque control below base speed, when the back emf is lower than the DC bus voltage, is similar for all motors. It usually involves PWM chopping of the current for the control of the torque. However, the torque control method above base speed, when the back emf exceeds the bus voltage, is motor and control dependent.

In the case of the induction motor, the usual practice is to begin field weakening once the motor speed exceeds the base speed. This way, the back emf is not allowed to build up beyond the bus voltage. Nevertheless, in order to retain the PWM current control capability at high speed, the electric motor would need to enter the field weakening before reaching the base speed. This would, however, reduce the available torque at high speed. To maximize the torque capability at high speed, six-step mode of operation seems to be inevitable because of the limited bus voltage [8]. Torque control in this mode and smooth transition between current regulated PWM mode and six-step mode becomes an important issue.

SRM is a singly fed motor as is the induction motor. Both the excitation current and the torque current are fed through the stator. However, unlike the induction motor, no control method is known that can isolate the torque component of current from the field component of current. Hence, field weakening is not possible in the SRM. Operation in constant power is made possible in this motor by the phase advancing of the stator current conduction angle until overlapping between the successive phases occurs [9]. Due to the high back emf, which cannot be weakened, PWM control of current is not possible in the extended speed range of operation.

Operation of the BLDC motor in the extended speed constant power range is similar to SRM. Due to the presence of the permanent magnet field which can only be weakened through a production of a stator field component which opposes the rotor magnetic field, field weakening is difficult in BLDC motor. Extended constant power operation is possible through the advancing of the commutation angle [10-12].

In summary we conclude that the switching of the DC bus by the converter is dictated by the torque control method. That is, the torque at low speed will be controlled by the PWM

control of the current. However, to maximize the torque capability of electric motor drives for EV and HEV applications, torque at high speed will be controlled by controlling the phase of the input voltage (phase-shift control). Since the control operation influences the number of switchings performed by the converter, it will influence the switching losses. Hence, torque control scheme of each motor will be studied in detail in this paper in an attempt to estimate the switching losses for EV and HEV application.

III. EV and HEV Drivetrain Model Considerations

In this section, some vehicle characteristics, motor and power converter considerations for modeling EV and HEV drivetrains are presented. The main objective is to calculate the converter switching and conduction losses for both systems. Also, the use of induction motor (IM), brushless dc (BLDC) motor and switched reluctance motor (SRM) is considered in the study of the two systems.

The vehicle characteristics of a typical 4-seat passenger car are given below:

- 0-26.82 m/s (0-60 mph) in 10 seconds.
- vehicle mass of 1700 kg.
- rolling resistance coefficient of 0.013.
- aerodynamic drag coefficient of 0.29.
- wheel radius of 0.2794 m (11 inch).
- level ground.
- zero head wind velocity.

In the series hybrid system, the electric motor behaves exactly in the same manner as in an electric vehicle. In both cases, the electric motor provides the necessary power to the drive shaft. Whereas, in the case of the parallel hybrid vehicle, the necessary wheel power is provided by the ICE and the electric motor. Therefore, the torque and power requirements of the electric motor are roughly equal for EV and series hybrid, while due to power sharing they are comparatively lower for parallel hybrid. The amount of power sharing in parallel hybrid, however, depends on the relative size of the ICE and the electric motor, and on the control strategy. In this study, the system mode of control assumes the ICE is providing the base power for cruising the vehicle, and the electric motor is used to provide the peak power during acceleration and hill climbing [13]. The ICE size is determined based on this mode of control. The electric motor size, however, depends on the particular motor in use, on the optimal motor control, and also on the above mentioned system mode of control. The detailed analysis of it can be found in [7].

In the calculation of the conduction and switching losses of the converter, PWM operation with hard switching is considered. The maximum switching frequency is assumed to be 10 kHz. The voltage and current rating of each switch of the inverter module used in the simulation are 600V and 400A respectively. For the calculation of the switching loss, the manufacturer's data on the switch turn on and turn off profiles, including reverse recovery effects of anti-parallel diodes, are used. The on-state characteristic of each switch module is simulated by a dc source, representing the saturation voltage, in series with an on-state resistance. This simplified model is used for the calculation of the conduction loss. The control strategy, the pf of operation, and the high speed-constant power capability are different for each type of motor. Consequently, the converter losses will be different for each case. In the simulations, IM, BLDC motor, and SRM are considered. Torque control below the base speed is achieved through the PWM chopping of current. As mentioned earlier, to maximize the available torque at high speed, phase control of the input voltage is used to control the torque. This control technique has the advantage of requiring only few switchings per electrical cycle. On the other hand, it has the disadvantages of being sluggish in response and having higher torque ripple. These drawbacks, however, are expected to have minimal effect on the vehicle operation due to the high vehicle inertia. Simulation results of the converter losses are presented in the next section.

IV. Simulation Results

In this section, the converter switching and conduction losses of a simulated electric and hybrid electric vehicle are calculated. For both systems, the cases when the vehicle runs on the FTP75 urban drive cycle (Fig. 1(a)) and on the highway drive cycle (Fig. 1(b)) are studied.

A. Losses in an HEV

The converter losses in an HEV depend on the energy sharing between the ICE and the electric motor. Figures 2(a) and 2(b) show the total energy through put and the energy distribution between the ICE and the electric motor, when the vehicle is running in the two drive cycles. In these figures, the energies are calculated cumulatively by integrating each power component over the drive cycle time. It is possible to recover, at least partially, the kinetic energy released by the vehicle when it decelerates. This is achieved by running the electric motor as a generator and charging the battery pack. This mode of control is referred to as regenerative braking in the literature. For obvious reason, the regenerative braking energy, which has its associated converter losses, is considered positive. This energy is added to the electric motor energy. In this analysis, it is assumed that all the kinetic energy released during the vehicle deceleration is recovered through regeneration, except for the amount lost in the process of regeneration. However, this is not practical for a very rapid braking of the vehicle. The electric motor and the battery pack are not capable of handling the huge amount of power released in a short burst during the harsh braking. In that case the mechanical brake needs to be engaged in addition to the regenerative braking. However, for the drive cycles considered in this study (Figs. 1(a) and 1(b)), the above assumption is valid. It is obvious, from the simulation results of Fig. 2(a), that the energy flow through the electric motor of the hybrid vehicle, running in highway drive cycle, is extremely small when compared to the total energy. Any amount of energy savings, by soft switching, in this case will not have much impact on the total energy savings. The urban drive cycle (Fig. 1(b)), however,

requires the electric motor more frequently, to supply the acceleration power of the hybrid vehicle. Moreover, the energy released during vehicle deceleration in the urban drive cycle is also recovered by the electric motor (generator), converter set.

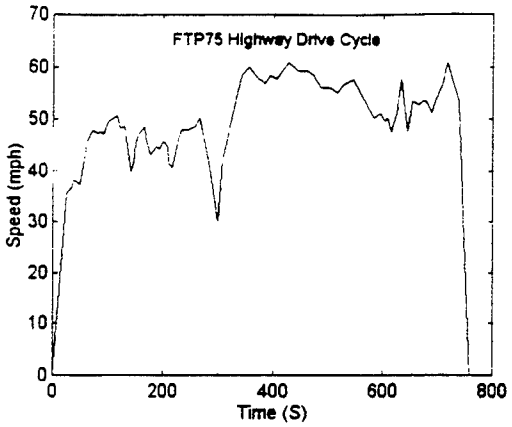

(a)

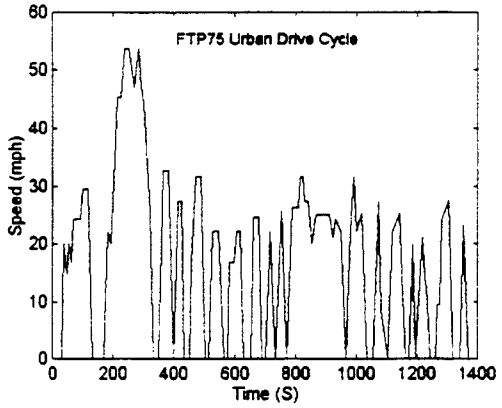

(b)

Fig. 1. FTP75 highway (a) and urban (b) drive cycles.

In the case of EV, since the battery is the only source of energy, the total energy required to run the vehicle is handled by the electric motor. Special assessment of energy savings due to soft switching is, therefore, necessary for the EV operation in both drive cycles. For the HEV operation, it might be important only in the urban drive cycle.

The calculated values of the conduction (the solid line curve) and switching (the dashed curve) losses of HEV drivetrain systems using IM, BLDC, and SRM are presented in Figs. 3(a) and 3(b) for the urban drive cycle. Fig. 3(a) considers the case when the vehicle deceleration energy is recovered through regenerative braking, and Fig. 3(b) is for the case when the regeneration is not considered. The losses of Figs 3(a) and 3(b) are shown as a percentage of the total expended energy of the propulsion system. The converter energy losses and the total energy are calculated cumulatively, integrating the losses and the system power over the drive cycle time. Hence, loss percentage shown at any point in these figures indicates the average loss (in percent) up to that time of the drive cycle. The losses shown at the end of the drive cycle are, therefore, the average losses for the whole drive cycle. In figures 3(a) and 3(b) we can see two spikes at the beginning of the drive cycle. These spikes are due to the two initial accelerations of the vehicle. As time progresses, the cumulative energy builds up and any local fluctuation, due to subsequent car accelerations, does not show up in the global

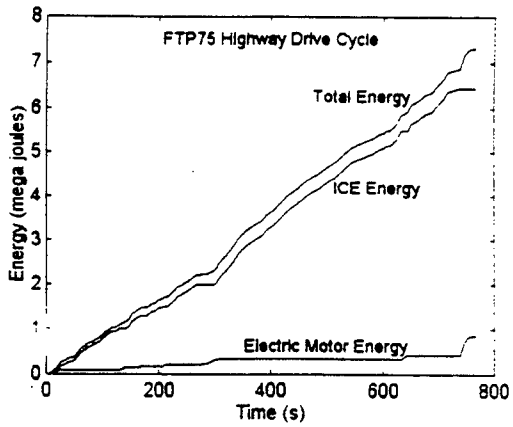

(a)

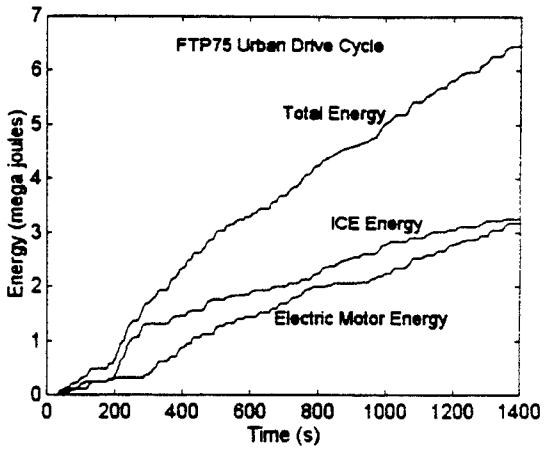

(b)

Fig. 2. Energy consumption in HEV for highway (a) and urban (b) drive cycles.

picture. Due to the lower pf of operation of SRM, its conduction loss is higher in both cases. However, the switching loss of SRM converter is comparable to those of IM and BLDC inverters. High speed capability of SRM, besides the fact that the torque control at high speed is attained by the phase control of the input voltage, have helped to lower the switching losses in SRM converter, despite its lower pf of operation. For the HEV urban drive cycle the average switching losses (Fig. 3(a) and Fig. 3(b)), for all motors considered here, are less than 2% of the total energy for the case with regenerative braking and less than 1% for the case without regenerative braking. In some soft switched topologies the conduction loss can be higher than in a hard-switched converter [14]. Although the switching loss can be reduced considerably, it is not totally eliminated. Hence, if one assumes zero switching losses by using a soft switching

technique, for this drive cycle, the maximum gain in energy would, therefore, be less than 2%.

Now, let us examine the impact of soft switching on the operation of HEV in terms of the gasoline saved per 100 miles of travel. The total energy spent for the operation of the vehicle in

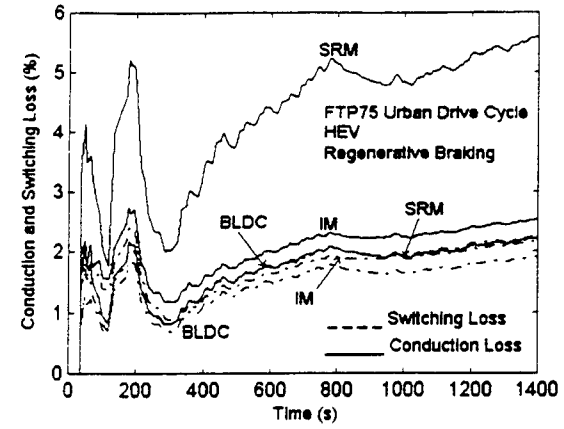

(a)

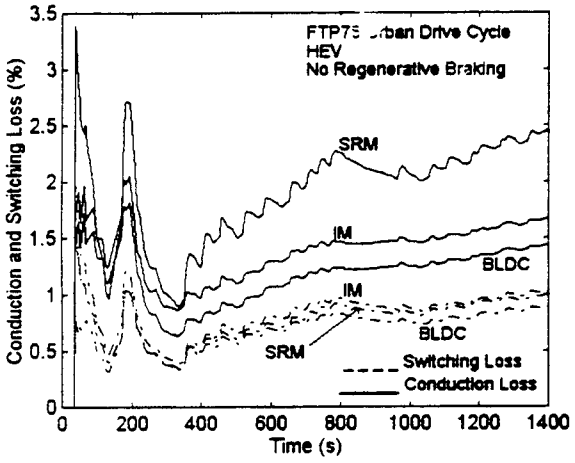

(b)

Fig.3. Converter losses for HEV in urban drive cycle with (a) and without (b) regenerative brakings.

the urban drive cycle is 6.45 mega joules. Total distance traveled by the vehicle in this drive cycle is 6.6 miles. Energy density per gallon of gasoline is 121 mega joules. Assuming an efficiency of 20% in the operation of the ICE, the total savings in the gasoline is only 0.0808 gallons per hundred miles traveled in the urban drive cycle. Total savings for an average urban driving of 10,000 miles in a year is only 8.08 gallons of gasoline. Since HEV is not energy limited, we conclude, the extra cost and complexity associated with the operation of a soft switched converter do not justify soft switching for HEV.

In highway driving cycle, except for few accelerations and few cases of regenerative braking, the electric motor is seldomly used . Calculated values of the switching losses for the operation of HEV in the highway drive cycle are shown in Figs. 4(a) and 4(b) with and without the consideration of regenerative braking, respectively. These losses are not significant and do not warrant any special effort in converter efficiency improvement.

B. Losses in EV

The energy recovered through regenerative braking is the same in EV as in HEV. However, since the battery is the only source of energy, the energy flow out of the battery pack is higher in case of EV. Due to this increased energy flow through the electric motor, the converter incurs more losses in both conduction and switching. Hence, losses as a percent of total energy is higher in case of EV. This is shown in Fig. 5(a) and 5(b) for urban driving cycle with and without the consideration

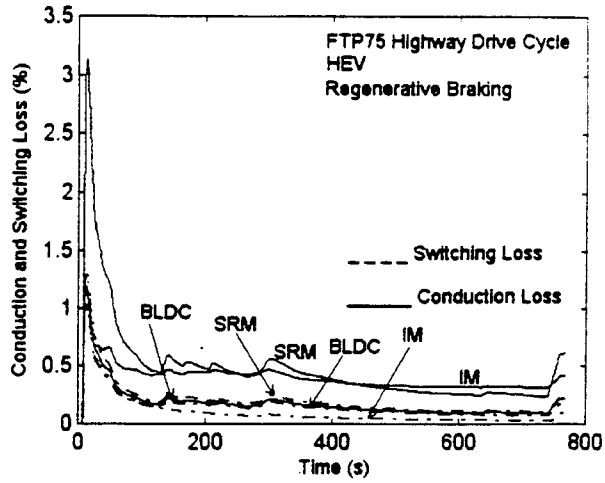

(a)

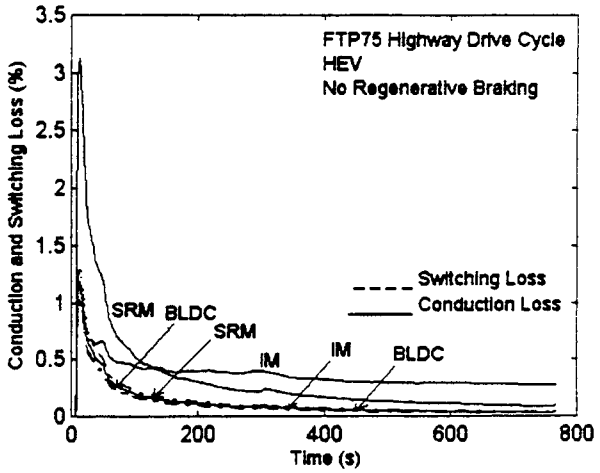

(b)

Fig.4. Converter losses for HEV in highway drive cycle with (a) and without (b) regenerative brakings.

of regenerative braking respectively. In both cases the switching and the conduction losses are increased for the operation of EVs when compared to those of HEVs. The switching loss is close to 3% with regenerative braking and close to 2% without regenerative braking. Although, the losses in EV are not greatly increased compared to the losses of HEV, EV losses have severe

consequences since they are related directly to the range of the vehicle. Therefore, the energy savings through soft switching may justify the additional cost, complexity, and lower reliability associated with its operation.

Finally, we consider the highway driving for EV. Although, EVs are not best suited for highway driving, the losses can be calculated for completeness. Figs. 6(a) and 6(b)

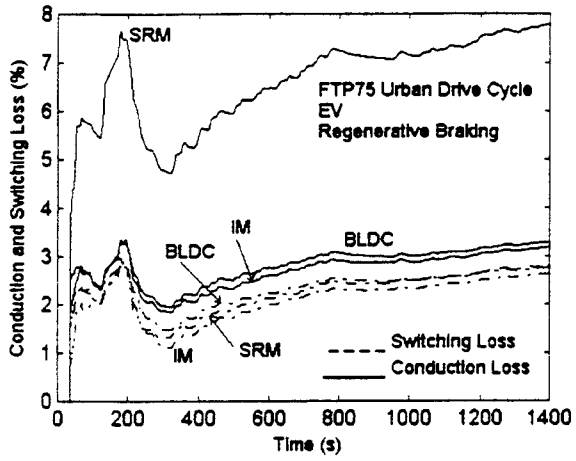

(a)

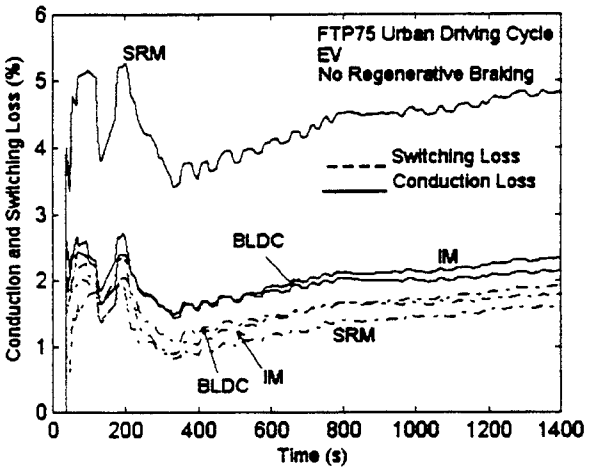

(b)

Fig.5. Converter losses for EV in urban drive cycle with (a) and without (b) regenerative brakings.

show the converter losses for the operation of the EV in the highway drive cycle with and without the consideration of the regenerative braking. Since the electric motor (battery) supplies all the energy in the operation of the EV, the losses are higher than in the case of HEV operation in the same drive cycle. However, the switching loss percentage is lower in highway driving as compared to the city driving of the EV (Figs. 5(a) and 5(b)) . It can be seen in Figs. 6(a) and 6(b), that the switching losses are actually less than 1% in both cases. The energy savings in the hypothetical highway driving of EV, therefore, may not justify the adoption of soft switching for its driving in the highway cycle.

V. Discussion

The simulation results of section IV give little incentive for soft switching in HEV, as far as the efficiency of the drivetrain is concerned. However, EV is a different issue. Since

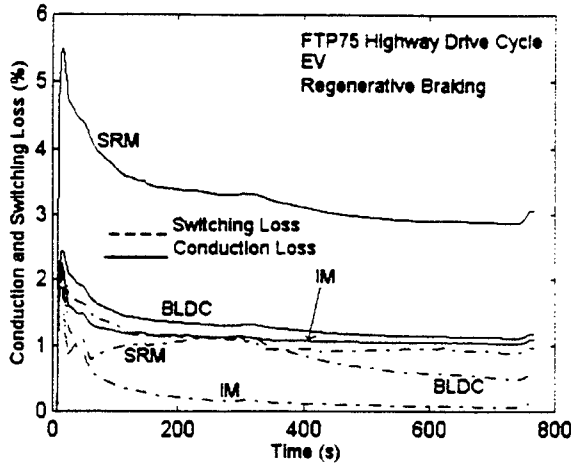

(a)

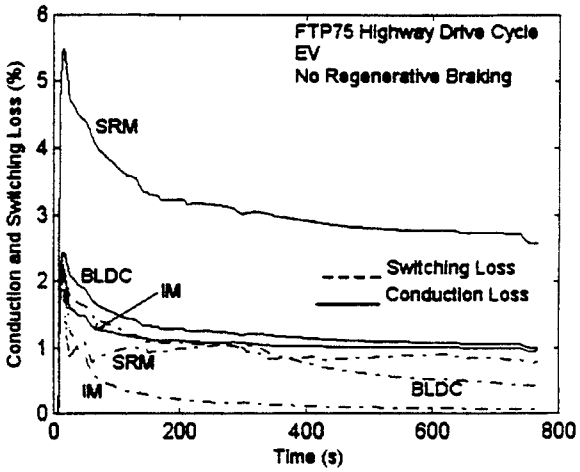

(b)

Fig.6. Converter losses for EV in highway drive cycle with (a) and without (b) regenerative brakings.

EV is energy limited, any gain in efficiency, by adopting soft switching, is directly related to the range of the vehicle. Hence, the marginal 3% gain in efficiency shown in the previous section for the urban driving cycle still may justify soft switching for EV electrical drive train. In other papers, e.g., [6] , the soft switching operation is shown to provide more gain in the efficiency of the converter than it is shown here. Those results should not be confused with the concepts presented in this study. Here we have evaluated the converter efficiency from the system prospectives. The gain in efficiency shown in this paper is based on the specific application to EV and HEV drivetrains with a special (optimal) mode of control, especially at the high speed operation of the vehicle (motor), as opposed to the fixed

frequency PWM switching operation for a fan or resistive load used in the other works.

Faster switches are developed to reduce the switching power losses. However, the high di/dt and dv/dt associated with the faster switching cause voltage and current spikes due to stray inductance and capacitance in the circuit. This phenomenon causes high current and voltage stresses in the switch, and can also produce severe EMI problems. The use of snubbers can reduce the switching stresses in the switches, but they are lossy and add parts count. Another approach, as suggested in [8], is to use slower switches for vehicle applications. This would reduce both the EMI problem and switch stresses. But it will increase the switching losses. The additional switching losses caused by the slower switches should not have much impact on the operation of the HEV, however, it may favor soft switching for EV applications.

Soft switching with high switching frequency can produce a fast converter dynamic response. This may be difficult to achieve with hard switching without sacrificing efficiency. However, vehicle has a slow dynamics. Faster dynamic response, therefore, is not necessary from the electrical propulsion system of the EV and HEV. On the contrary, a deliberate damping may be required to suppress the possible excitation of any mechanical resonances [15].

Slower switching, in an attempt to reduce the switching losses, will introduce higher torque and current ripples. Nevertheless, the vehicle inertia is expected to smoothen the effect of torque ripple on the speed ripple.

The audible noise for switching at frequencies lower than 20 kHz is another issue. Switching over 20 kHz with hard switching may not be practical for high power drives. The audible noise, however, may not be unacceptable to the users who are already accustomed to the noisy operation of the conventional automobiles. It may also be particularly tuned to be pleasant to the ear.

VI. Conclusions

An evaluation of the soft switching inverters for EV and HEV motor drives is presented. Simulation results of the converter losses are presented for the operation of the EV and the HEV in the FTP75 city and highway drive cycles. Operation of induction, brushless dc, and switched reluctance motors are considered for the electrical propulsion system of the EV and the HEV. The simulation results show that the energy savings by using soft switching is less than 2% of the total energy for the operation of the HEV in the standard highway as well as in the urban driving cycles. Since, HEV does not have any energy limitation, this small saving in energy does not justify the extra cost and complexity associated with the soft switched converter. The simulation results for the operation of the EV in the urban driving cycle reveal that the maximum savings in energy would be up to 3% with soft switching. These savings, although marginal, may justify soft switching for EV applications until high energy density batteries with extremely quick charging characteristics are developed in the future. The energy savings for EV with soft switching in highway driving is less than 1% of the total energy. Since, EVs are not designed for primary highway driving, the small energy savings may not justify soft switching for this case. We can summarize our findings as follows:

- Soft switching is not recommended for the design of HEV.
- Soft switching is not recommended for the design of EV in highway driving.
- Soft switching may be recommended for EV operation in urban driving. However, a specialized soft switched topology would be needed for the particular vehicle load.

To reduce the EMI problem and the switch stresses due to fast switch turn-ons and turn-offs, slower switches may be used. The additional losses incurred by these slow switches are not expected to have any major impact on the operation of the electrical propulsion system of the HEV. The other characteristics of soft switching with high switching frequency such as, faster dynamic response, torque and current ripple, audible noise etc., do not have any appreciable effect on the design and operation of the EVs and the HEVs.

VII. REFERENCES

[1] Y. Murai and T. A. Lipo, "High Frequency Series Resonant DC Link Power Conversion", *IEEE IAS Annual Meeting Conference Record*, 1988, pp. 772-779.

[2] D. M. Divan, "The Resonant DC Link Converter - A New Concept in Static Power Conversion", *IEEE Transactions on Industrial Applications*, Vol.25, No.2, pp. 317-325, 1989.

[3] William McMurray, "Resonant Snubbers with Auxiliary Switches", *IEEE Transactions on Industry Applications*, Vol.29, No.2, March/April 1993.

[4] M. Ehsani and T. S. Wu, "Zero Current Soft Switched Capacitively Coupled DC-AC Converter for High Power", *IEEE Industry Application Society Annual Meeting Records*, Toronto, pp. 800-805, 1993.

[5] T. S. Wu, M. D. Bellar, A. Tchamdjou, J. Mahdavi and M. Ehsani, "A Review of Soft-Switched DC-AC Converters", *IEEE IAS Annual Meeting Conference Record*, 1996, Vol.2, pp.1133-1144.

[6] J. S. Lai, "Resonant Snubber-Based Soft-Switching Inverters for Electric Propulsion Drives", *IEEE Transactions on Industrial Electronics*, Vol. 44, No.1, pp. 71-80, February 1997.

[7] M. Ehsani, K. M. Rahman, and H. Toliyat, "Propulsion System Design of Electric and Hybrid Vehicle," *IEEE Trans. on Industrial Electronics*, vol. 44, no. 1, pp.19-27, February 1997.

[8] X. Xu, V. A. Sankaran, "Power Electronics in Electric Vehicles: Challenges and Opportunities," *IEEE IAS Annual Meeting Conference Record*, 1993, pp. 463-469.

[9] T. J. E. Miller, "Switched Reluctance Drive," Short Course, *IEEE-IAS* Conference, Seattle, 1990.

[10] T. M. Jahns, "Torque Production in Permanent Magnet Synchronous Motor Drives with Rectangular Current Excitation," *IEEE Trans. Industry Application*, vol. 20, no. 4, pp. 803-813. July/Aug., 1984.

[11] R. C. Becerra and M. Ehsani, "High Speed Torque Control of Permanent Brushless DC Motors," *IEEE Trans. Industrial Electronics,"* vol. IE-35, no. 3, pp. 402-406, August, 1988.

[12] C. C. Chan, J. Z. Jiang, G. H. Chen, X. Y. Wang, and K. T. Chau, "A Novel High Power Density Permanent Magnet Motor Drive for Electric Vehicles," in *Proc. EVS11*, paper 8.06, 1992, pp.1-12.

[13] Y. Gao, K. M. Rahman, and M. Ehsani, "Parametric Design Of The Drive Train Of Electrically Peaking Hybrid (ELPH) Vehicle," *SAE Journal Publication SP-1243, paper no. 970294*, 1997.

[14] J. S. Lai, R. W. Young, and J. W. McKeever, "Efficiency Consideration of DC Link Soft-Switching Inverters for Motor Drive Applications," *IEEE PESC Annual Meeting*, 1994

[15] H. A. Toliyat, K. M. Rahman, and M. Ehsani, "Electric Machines in Electric and Hybrid Vehicle Applications," *ICPE*, Seoul, Korea, 1995.

Fundamentals of Energy and Power Storage and Production in HEV Architectures

Stephen W. Moore
Texas A&M University

Mehrdad Ehsani
Texas A&M University

ABSTRACT

Fundamentals of hybrid electric vehicle architecture and component selection are presented in this paper. Current hybrid and electric vehicle topologies include numerous architectural arrangements ranging from the all-electric drive to parallel and series types. Each architecture features a novel arrangement of engines, motors, batteries, or some other source of varying different sizes. However, each architecture can be abstracted into basic concepts of power production and energy storage.

This paper presents a fundamental concept of designing a vehicular hybrid drivetrain by separating the concepts of power and energy production and storage. A fundamental drive cycle featuring the basic building blocks of vehicle performance is presented and analyzed. The boundaries for maximum and minimum transient power expenditures and absorption are established. Total energy consumption, generation, and storage requirements are identified.

Each individual drivetrain component's power and energy production and storage characteristics are identified and are combined in such a way to satisfy the vehicle's performance criteria. A series hybrid is presented as an example of the conceptual separation of power and energy for a given drive cycle.

INTRODUCTION

The hybrid automotive drivetrain can be conceptually abstracted into two components: a power source and an energy source. The power source is responsible for instantaneous transients such as providing brief power for accelerations or regenerative braking and for passing maneuvers or hill climbing. The energy source is responsible for contributing average power. These concepts are most easily illustrated with a series hybrid (Figure 1) [1].

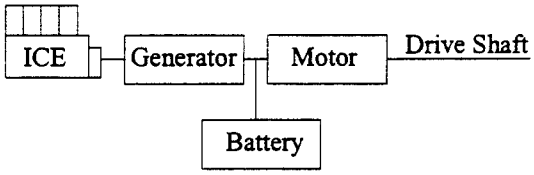

Figure 1. Series Hybrid Architecture

The series hybrid is much like an electric vehicle with the exception of on-board electricity production. The ICE and generator produce the average energy requirement of the vehicle and additional transient power is provided by the battery pack. This architecture will be studied more in the next section. Notice that the series hybrid is not limited to ICE and generator. Many options exists such as fuel cells, thermoelectric cells [2], and turbine generators.

The traditional method used to evaluate or simulate vehicle performance is with the use of a drive cycle. A drive cycle is a set of pre-defined driving profiles with different performance requirements that can be used to represent the majority of driving expectations. There are many popular drive cycles available varying in intensity and length (Table 1)[3]:

Table 1. Various US Drive Cycles

Name	Abbreviation	Time (sec)	Length (km)
EPA Highway Cycle	HWY	765	16.5
EPA City Cycle	LA4	1372	12.0
Unified LA92 Cycle	LA92	1435	15.8
New York City Cycle	NYCC	599	1.9
US06 Cycle	US06	600	12.9

Please notice that the EPA City Cycle LA4 is also known as the FTP cycle, or the Federal Urban Driving Schedule (FUDS). The LA4 was developed in the early 1970s to simulate urban driving conditions. Later urban driving scenarios include the California Air Resources Board Unified LA92 Cycle [4], developed in 1992. The

US06 was developed by the EPA to include some additional features over the earlier LA4 [5]. Pictured below is the LA4 driving cycle.

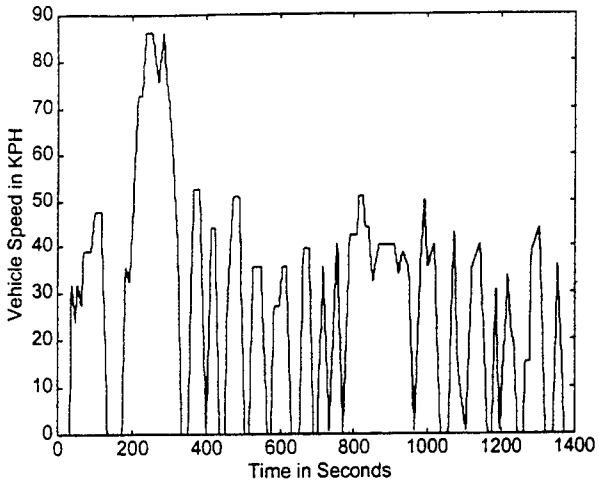

Figure 2. EPA City Cycle LA4

Other countries and agencies have developed similar driving cycles for testing and evaluation purposes. However, it is presented that all driving cycles share three common characteristics:

1. Maximum and minimum power transients.
2. Average energy consumption.
3. Maximum deviation between instantaneous power consumption and average energy production.

These three characteristics will be evaluated in the following sections.

VEHICLE DYNAMICS MODEL

To illustrate the concept of abstracting a drive cycle into power and energy characteristics, a simplified vehicle model is used. The vehicle load (F_w) consists of rolling resistance (f_{ro}), aerodynamic drag (f_l), and climbing resistance (f_{st}) [6].

$$F_w = f_{ro} + f_l + f_{st} \quad \text{(Eq. 1)}$$

The rolling resistance (f_{ro}) is caused by the tire deformation on the road:

$$f_{ro} = f \cdot m \cdot g \quad \text{(Eq. 2)}$$

where f is the tire rolling resistance coefficient. It is nonlinear and increases with vehicle velocity, and also during vehicle turning maneuvers. These nonlinearities are not taken into account in this model. Vehicle mass is represented by m, and g is the gravitational acceleration constant.

Aerodynamic drag, f_l, is the viscous resistance of air acting upon the vehicle:

$$f_l = 0.5\xi C_w A(v + v_0)^2 \quad \text{(Eq. 3)}$$

where ξ is the air density, C_W is the aerodynamic drag coefficient, A is the vehicle frontal area, v is the vehicle speed, and v_0 is the head wind velocity.

The climbing resistance (f_{st} with positive operational sign) and the down grade force (f_{st} with negative operational sign) is given by

$$f_{st} = m \cdot g \cdot \sin\alpha \quad \text{(Eq. 4)}$$

where α is the grade angle.

A typical simplified road load characteristic as a function of vehicle speed is shown in Figure 3.

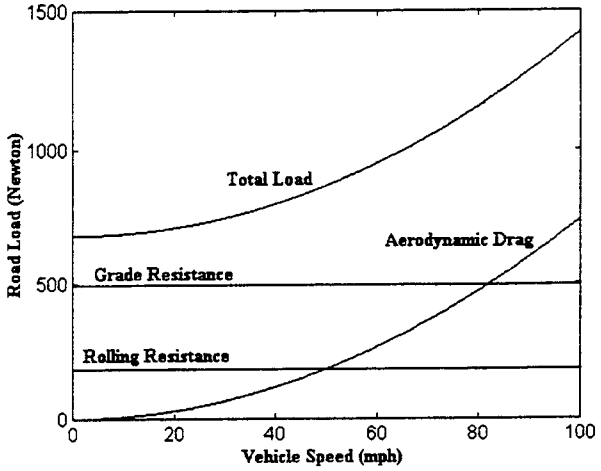

Figure 3. Typical Vehicle Load Function

This graph represents the load function of the vehicle with the characteristics of Table 2. Notice that this graph does not take into account a headwind, a variable grade, or the nonlinearities of tire deformation and rolling resistance.

Table 2. Example Vehicle

Parameter	Value
Mass	1450 kg
Rolling Resistance Coefficient	0.013
Aerodynamic Coefficient	0.29

SERIES HYBRID EXAMPLE

A simple series hybrid topology was simulated using the LA4 drive cycle to examine power and energy consumption. Figure 4 illustrates the kinetic energy of the vehicle during the drive cycle:

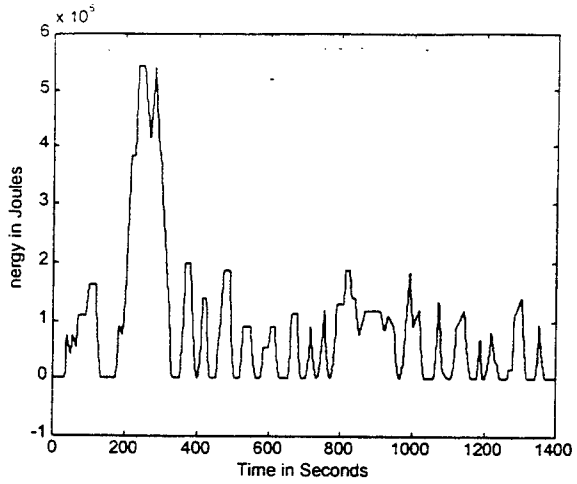

Figure 4. Kinetic Energy of the Vehicle

Adding in the aerodynamic and rolling resistance losses, the total amount of energy the vehicle consumes over the drive cycle can be plotted (Figure 5):

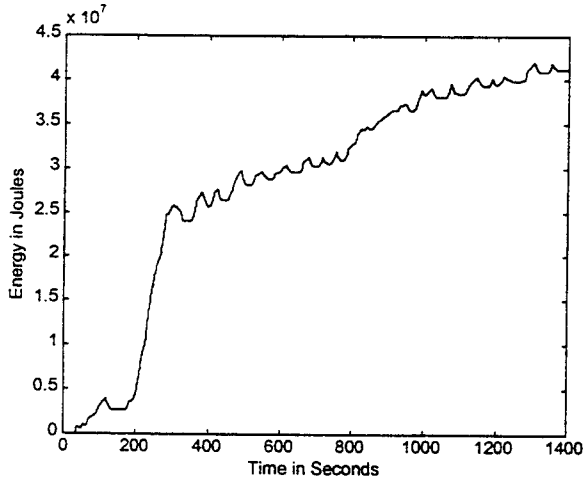

Figure 5. Cumulative Vehicle Energy Consumption

Taking the derivative of the energy consumption we can size the traction motor for the peak power requirement (Figure 6):

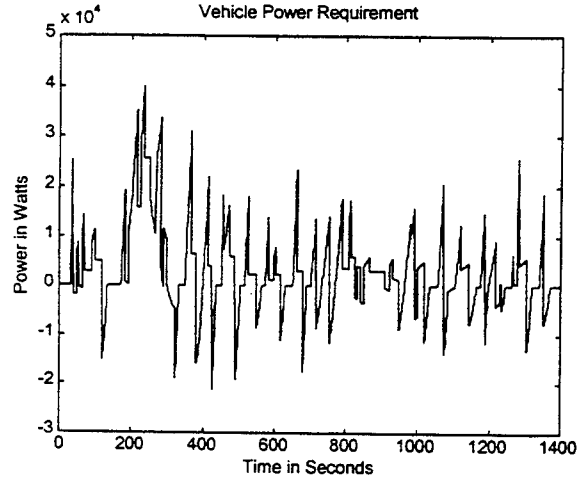

Figure 6. Instantaneous Power Requirement

Thus this vehicle requires a 41 kW peak power traction motor capable of 22 kW of regeneration to perform adequately on the LA4 driving cycle in zero wind, zero grade conditions. Looking at Figure 5, we see that the average energy consumption was 1.7e+7 joules, which means an average power consumption of 29 kW. Thus the traction motor must be sized to continuously dissipate the heat associated with the average load in addition to the heat produced by the peak loads.

Assuming that this series hybrid has an ICE and generator producing electrical energy at a continuous rate equal to the average consumption (29 kW), a plot of the cumulative energy production and the cumulative energy consumption can be made (Figure 7):

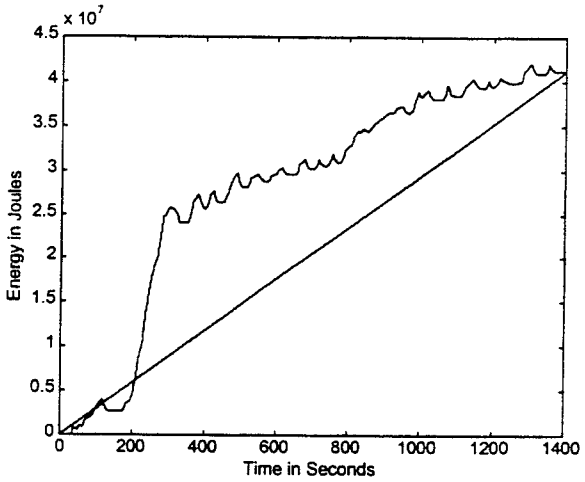

Figure 7. Energy Consumption and ICE Production

Notice how the ICE/generator energy production *exactly equals* the energy consumption of the vehicle. However, because the ICE/generator produces energy at a constant rate and the vehicle consumes energy at a variable rate, a transient energy storage device (the 'battery,' or some other type of storage device) is required. Illustrated on Figure 8 is the amount of energy stored in the battery of the vehicle (assuming the battery is at zero condition at the beginning of the cycle):

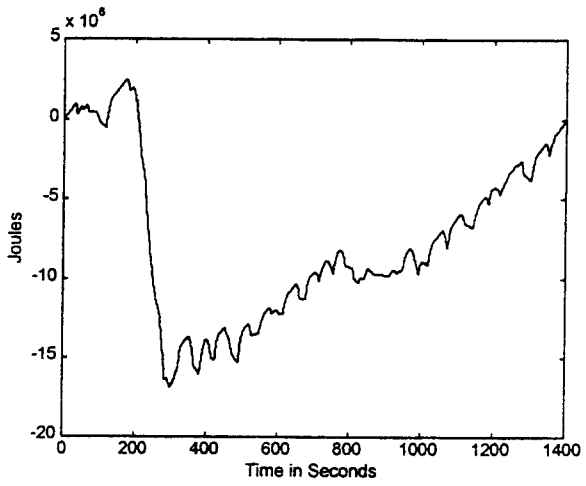

Figure 8. Energy Content of Battery

The battery discharges rapidly with the initial acceleration and cruise in the LA4 profile, then is slowly recharged by the series ICE/generator. The power requirement of the battery can be found by taking the derivative of the battery energy balance (Figure 9):

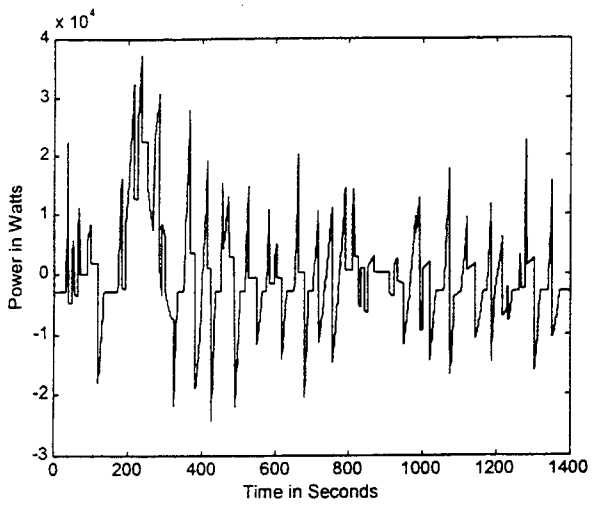

Figure 9. Power Requirement of Battery

Thus with an ideal (100% efficient) energy storage device, this vehicle will require a battery with 1.7e+7 Joules (4695 watt-hours) of storage and be able to stand 39 kW watt discharge and 25 kW (depending on regenerative braking performance as well) recharge power. The ICE/generator produces 29 kW continuously. Using a non-ideal energy storage device (a simplified ultracapacitor model was used for this scenario), the energy loss is apparent (Figure 10):

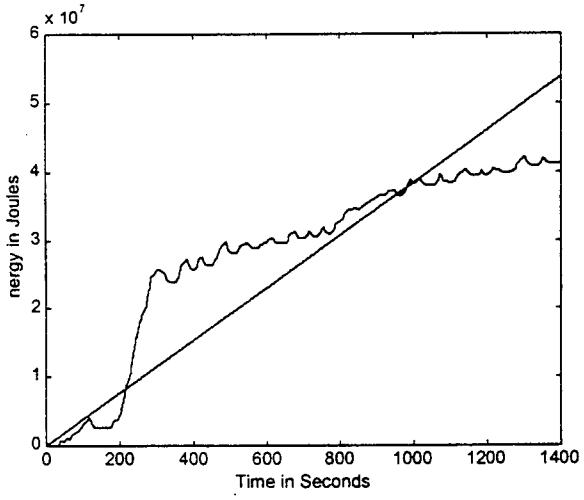

Figure 10. Vehicle Energy Consumption and ICE Production

Notice that the ICE/generator is required to produce more energy than the vehicle dynamics consume to compensate for losses in the energy storage device. The peak power and energy capacity criteria of the storage device are also increased (up to 44 kW peak discharge power and 5.2 kWhr capacity).

DRIVE CYCLE ANAYLSIS

As discussed in the introduction, drive cycles share three common characteristics:

1. Maximum and minimum power transients.
2. Average energy consumption.
3. Maximum deviation between instantaneous power consumption and average energy production.

Inspection of Figure 6 reveals that the series hybrid with the characteristics of Table 2 has a maximum peak power of 41 kW. Figure 5 illustrates the cumulative energy consumption, which can be divided by the total time to find the average energy consumption of 29 kW. Figure 7 illustrates the difference between the cumulative energy consumption and the cumulative energy production. The maximum difference between these two values at any time denotes how much energy the vehicle must store above average to deliver power for peak loads. In this example, the maximum deviation is 1.7e+7 joules for the ideal case and 1.9e+7 joules for the non-ideal case.

Each of these values relate to component sizing. The traction drive motor must be capable of 41 kW peak power and 29 kW of average power. The ICE/generator must be capable of producing 29 kW continuously and the battery must be at least 4.7 kWhr in size (ideal case example). Many series hybrid implementations allow for the ICE to operate intermittently. In this case, the ICE must produce an average of 29 kW over its on/off cycle, and the battery capacity must be increased to accommodate operating the vehicle then the ICE is not operating. Under these conditions, the battery peak charge and discharge rates will also be much higher, because the battery will be supplying all the power to the traction motor during the ICE off cycle.

This type of analysis can be implemented on any hybrid architecture, series or parallel. In parallel operation, the energy production always comes from the ICE, but the ICE also serves as a traction (power) device as well.

Several drive cycles that appear to be vastly different may exhibit similar characteristics when analyzed in this fashion. Drive cycle top speed is a serious issue in aerodynamic and maximum component RPM ratings, but becomes irrelevant in this type of analysis. Two different drive cycles with different top speeds may compute to be equal in terms of maximum power and energy consumption. In this case, the traction motor peak power, ICE/generator sizing and battery capacity requirements are all the same. However, in the case of the drive cycle with the higher top speed, the traction motor must be rated to the proper RPM.

CONCLUSIONS

Any hybrid vehicle architecture can be broken down into two abstract components: energy and power storage and production. Each drivetrain component contributes one or both of these elements. A simplified series hybrid example was presented in which the energy consumption of the vehicle was compared to the energy production of the ICE/generator. The difference in these energies was identified as the amount of energy the vehicle's battery would have to store. In addition, the amount of energy the ICE/generator would have to produce was identified, as well as the maximum peak power requirement of each component

The EPA LA4 drive cycle (the Federal Urban Driving Schedule) was used as an example drive cycle in this illustration. However, the specifics of the LA4 cycle are irrelevant in this type of analysis, because a drive cycle with vastly different characteristics could very well show the same results, as long as it required the vehicle to consume the same amount of average energy and have a similar global maximum power requirement. However, some specific features of the drive cycle are important for other considerations, such as aerodynamics or component RPM ratings.

This method of analyzing system energy and power flow can be applied to other HEV architectures other than series. Hybrid architectures which incorporate an energy storage device such as a battery or ultracapacitor fall in this category.

REFERENCES

1. A.F. Burke, "Hybrid/Electric Vehicle Design Options and Evaluations," SAE Paper 920447.
2. Michael Seal, et al., "Thermophotovoltaic Generation of Power for Use in a Series Hybrid Vehicle," SAE Paper 972648.
3. Feng An, M. Barth, and G. Scora, "Impacts of Diverse Driving Cycles on Electric and Hybrid Electric Vehicle Performance," SAE Paper 972646.
4. T. Austin, et al., "An Analysis of Driving Patterns in Los Angeles During 1992," Proceedings of the Third Annual CRC-APRAC On-Road Vehicle Emissions Workshop, San Diego, CA, 1992.
5. US Document, "Support Document to the Proposed Regulations for Revisions to the Federal Test Procedure: Detailed Discussion and Analysis," EPA Office of Air and Radiation, 1995.
6. Automotive Handbook, Germany: Robert Bosch Gmbh, 1986.

Effect on Vehicle Performance of Extending the Constant Power Region of Electric Drive Motors

Stephen W. Moore
Texas A&M University

Khwaja M. Rahman
Texas A&M University

Mehrdad Ehsani
Texas A&M University

ABSTRACT

The effect on vehicle performance of extending the constant power operating mode of electric drive motors for electric and hybrid vehicles is presented in this paper. Modern electric and hybrid vehicle designers have the selection of several technologies to choose from when selecting an electric drive motor. Each motor technology exhibits a particular torque vs. speed characteristic. Many of these technologies, most notably the switched reluctance machine, have capitalized on iron and copper utilization, extending their useful speed range. However, the extended speed capabilities of these motor drives have vehicle performance consequences.

It is presented that vehicle performance is affected by changing the torque-speed characteristics of the drive motor. The extended constant power speed range motor can have smaller rated power than otherwise but suffer high speed passing performance. Traditional extended constant power range motors (about two times the rated speed) have to have a higher rated power but exhibit superior performance capability.

INTRODUCTION

The electric motor is of primary importance to the electric and hybrid vehicle designer. In an electric or a series hybrid vehicle the electric drive is the only propulsion mechanism and much attention needs to be paid to cost, weight, and performance. Depending on the architecture, electric motor drives in parallel hybrid designs can be utilized as peak power devices, load sharing devices, or only as a small transient torque source. Some parallel hybrid concepts even allow the drivetrain to revert to an electric-only mode, relegating all propulsion to the electric drive. In parallel applications like these, the motor technology is equally critical as in the cases of EV or series HEVs.

An electric motor can operate in two modes, the normal mode and the extended mode (Figure 1). In the normal mode, or the constant torque region, the motor exerts constant torque (rated torque) over the entire speed range until the rated speed is reached. Once past the rated speed of the motor, the torque will decrease proportionally with speed, resulting in a constant power (rated power) output. The constant power region eventually degrades at high speeds, in which the torque decreases proportionally with the square of the speed. This is known as the 'Natural Mode' and is usually neglected for most motor technologies. Please note that Figure 1 denotes a 1:3 type motor, where the constant power region extends beyond the constant torque region by a factor of 3.

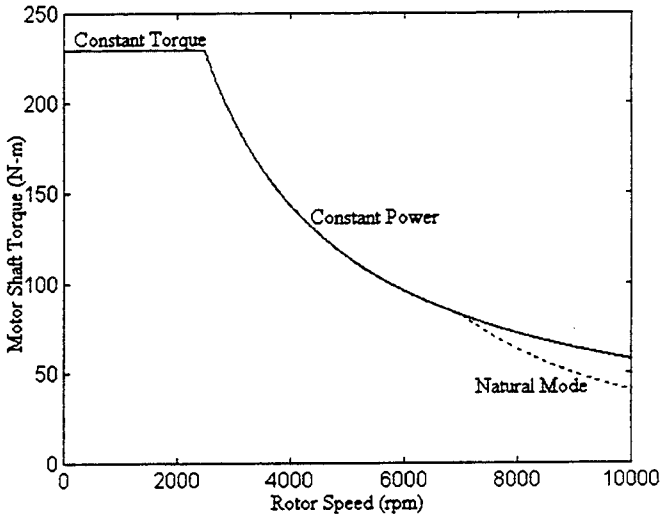

Figure 1. Typical Motor Characteristics

Three major motor technologies were chosen for illustrative purposes: the induction motor, the brushless DC (BLDC) motor, and the switched-reluctance (SRM) motor. Specifications for each motor technology were chosen from commercially available samples, and do not represent maximum possible performance for each technology.

	Rated Speed	Maximum Speed	Power Ratio
Induction	1750	8750	1:5
BLDC	4000	9000	1:2.25
SRM	4000	20000	1:3

Table I. Electric Motor Technologies

It must be noted that the SRM is capable of operating in the natural mode up to 20,000 rpm.

Induction machine drives are the present leading technology for EV and HEV power trains [1,2]. Both the GM EV-1 and Nissan FEV employ the induction motor. Permanent magnet (PM) motors are particularly known for their high efficiency and high power density. PM motors can be broadly classified into sinusoidally fed PM synchronous motor (PMSM) and rectangular fed brushless dc (BLDC) motor. The high efficiency of operation of these motors has attracted EV applications. Specially designed varients of these motors are used in the BMW E1/E2 and U2001, whereas the Ford/GE ETX-II use PMSM motor [3-5]. The major shortcoming of PM motors is the cost due to the high energy magnets. Safety is another issue because the PM field may cause severe consequences during a short circuit fault [6]. BLDC motors suffers from poor field weakening capability due to the surface mounting of the permanent magnet field that may necessitate a multi-gear transmission with the operation of this motor [6]. The interior magnet PMSM motor has reluctance torque in addition to reaction torque and this may help in getting a long constant power operation [7]. However, interior mounting of the permanent magnets further increases the cost and may reduce the maximum speed.

The switched reluctance motor is gaining lot of attention for its simplicity and safe operation. This motor is commercially used in the Chloride Lucas EV. Test results showed superior operation and higher power density when compared to an induction motor [8]. Because of its simple construction and low rotor inertia, the SRM has very rapid acceleration and extremely high speed operation. Because of its wide speed range operation, the SRM is particularly suitable for gearless operation in EV/HEV propulsion.

VEHICLE DYNAMICS

A simple vehicle dymanics model to evaluate vehicle performance is presented. A simplified vehicle model load (F_w) consists of rolling resistance (f_{ro}), aerodynamic drag (f_l), and climbing resistance (f_{st}) [9].

$$F_w = f_{ro} + f_l + f_{st} \qquad \text{(Eq. 1)}$$

The rolling resistance (f_{ro}) is caused by the tire deformation on the road:

$$f_{ro} = f_r \cdot m \cdot g \qquad \text{(Eq. 2)}$$

where f_r is the tire rolling resistance coefficient. It is nonlinear and increases with vehicle velocity, and also during vehicle turning maneuvers. These nonlinearities are not taken into account in this model. Vehicle mass is represented by m, and g is the gravitational acceleration constant.

Aerodynamic drag, f_l, is the viscous resistance of air acting upon the vehicle)

$$f_l = \frac{1}{2} \cdot \rho_e \cdot C_D \cdot A_f \cdot (v + v_0)^2 \qquad \text{(Eq. 3)}$$

where ρ_e is the air density, C_D is the aerodynamic drag coefficient, A_f is the vehicle frontal area, v is the vehicle speed, and v_0 is the head wind velocity.

The climbing resistance (f_{st} with positive operational sign) and the down grade force (f_{st} with negative operational sign) is given by

$$f_{st} = m \cdot g \cdot \sin\alpha \qquad \text{(Eq. 4)}$$

where α is the grade angle.

A typical simplified road load characteristic as a function of vehicle speed is shown in Figure 2.

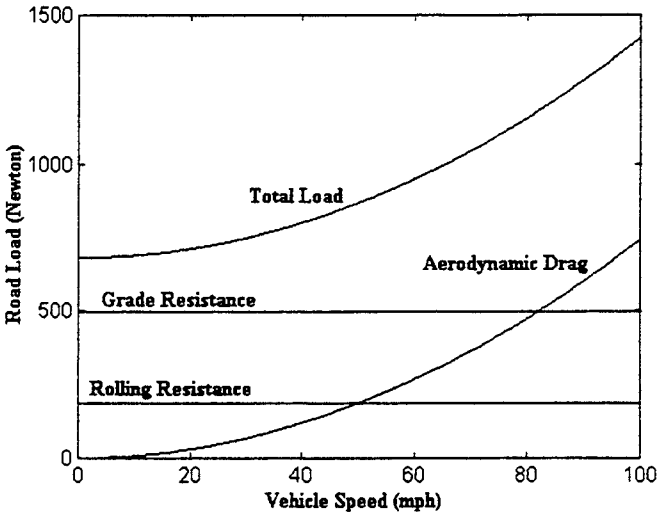

Figure 2. Typical Vehicle Load Function

This graph represents the load function of the vehicle with the characteristics of Table 2. Notice that this graph does not take into account a headwind, a variable grade, or the nonlinearities of tire deformation and rolling resistance. A gear ratio between the motor and the driveshaft is specified for a later example.

Table 2. Example Vehicle

Parameter	Value
Mass	1450 kg
Rolling Resistance Coefficient	0.013
Aerodynamic Coefficient	0.29
Gear Ratio	0.71
Wheel Radius	0.279 m

MOTOR SIZING

An electric vehicle with the basic characteristics given in Table 2 will be used to evaluate the desirability of extending the constant power range of electric machines. First, the required power must be computed. Starting with the definition of acceleration where F is defined as the amount of available propulsion force,

$$a = \frac{dv}{dt} = \frac{F}{m} \qquad \text{(Eq. 5)}$$

and integrating over a time interval t_f to a terminal velocity of v_f,

$$m\int_0^{v_{rv}} \frac{dv}{F} = \int_0^{t_f} dt \qquad \text{(Eq. 6)}$$

the rated power P_m can be found. The left hand side of the equation can be broken into separate constant torque (motor speeds up to v_{rm}) and constant power (motor speeds from v_{rm} to v_{rv}) integrals:

$$m\int_0^{v_{rm}} \frac{dV}{P_m / V} + m\int_{v_{rm}}^{v_{rv}} \frac{dV}{P_m / V} = t_f \qquad \text{(Eq. 7)}$$

Now solving for the required motor power P_m, we get:

$$P_m = \frac{m}{2t_f}(v_{rm}^2 + v_{rv}^2) \qquad \text{(Eq. 8)}$$

where the motor operates in constant torque mode until speed v_{rm} is reached, and then operates in constant power until terminal velocity v_{rv} is reached at time t_f. For our example vehicle to reach 60 mph (26.8 m/s) in 10 seconds (v_{rv} = 26.8 $^m/_s$ and t_f = 10 sec), the required rated motor power P_m is dependant on the ratio of v_{rm} and v_{rv} (Figure 3 and Table 3):

Table 3: Power Requirement as a Function of the Constant Power Range Ratio

	Extended Constant Power Range							
	1:1	1:2	1:3	1:4	1:5	1:6	1:7	1:8
Motor Power (kW)	110	94	74	67	64	62	61	60.6

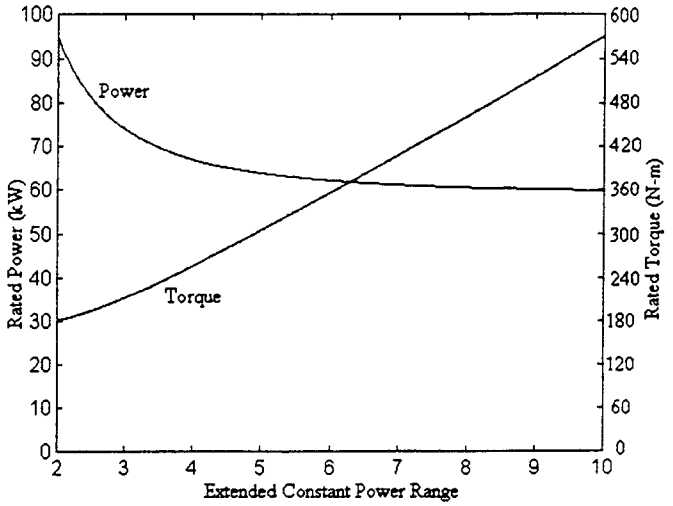

Figure 3. Rated Power and Torque vs. Extended Constant Power Range

Notice that the required torque ratings of extended constant power range motors must be significantly higher, but the required power is lower. After a ratio of about 1:4, the benefit of getting to use a lower power motor begins to become less significant.

PERFORMANCE ANAYLSIS

As shown in Table 3, the required power to reach velocity v_{rv} in time t_f is dependent on the ratio of the constant torque region and the constant power region of the electric motor. Even though the vehicle will reach v_{rv} in time t_f in each case, the nature of the acceleration is variable.

To compute a time t_a for an acceleration to an arbitrary speed v_a while operating in the constant torque region,

$$t_a = \int_0^{V_a} \frac{m \cdot \delta}{F_m - f_{ro} - j_l} \cdot dV \qquad \text{(Eq. 9)}$$

where F_m is the force from the electric motor, f_{ro} is the rolling resistance force (Eq. 2) and f is the areodynamic losses (Eq. 3). Headwinds and climbing resistance are assumed to be negligible in this example, but can easily be added in.

$$t_a = \int_0^{Va} \frac{m \cdot \delta}{\frac{T_{rm} \cdot i_t \cdot \eta_e}{r} - m \cdot g \cdot f_r - \frac{1}{2} \cdot \rho_e \cdot C_D \cdot A_f \cdot V^2} \cdot dV$$

where T_{rm} is the rated torque, i_t is the gear ratio between the motor and the driveshaft, and r is the wheel radius. η_e is the speed of the motor, which is dependent on the instantaneous velocity of the vehicle:

$$\eta_e = \frac{60 \cdot V \cdot i_t}{2 \cdot \pi \cdot r} \qquad \text{(Eq. 11)}$$

To compute the distance S_a covered during this acceleration,

$$S_a = \int_0^{Va} \frac{m \cdot \delta \cdot V}{\frac{T_{rm} \cdot i_t \cdot \eta_e}{r} - m \cdot g \cdot f_r - \frac{1}{2} \cdot \rho_e \cdot C_D \cdot A_f \cdot V^2} \cdot dV$$

To compute the time t_b to accelerate from the rated speed of the motor v_{rm} to any greater speed v_b in the constant power region of operation,

$$t_b = \int_{Vrm}^{Vb} \frac{m \cdot \delta}{\frac{P_m \cdot i_t}{r} - m \cdot g \cdot f_r - \frac{1}{2} \cdot \rho_e \cdot C_D \cdot A_f \cdot V^2} \cdot dV$$

where P_m is the rated power of the motor. Distance can be computed with an equation similar to the constant torque case. Now, by varying the ratio between the constant torque region and the constant power region but keeping the same 0-60mph acceleration in 10 seconds, the acceleration profiles can be seen (Figure 4):

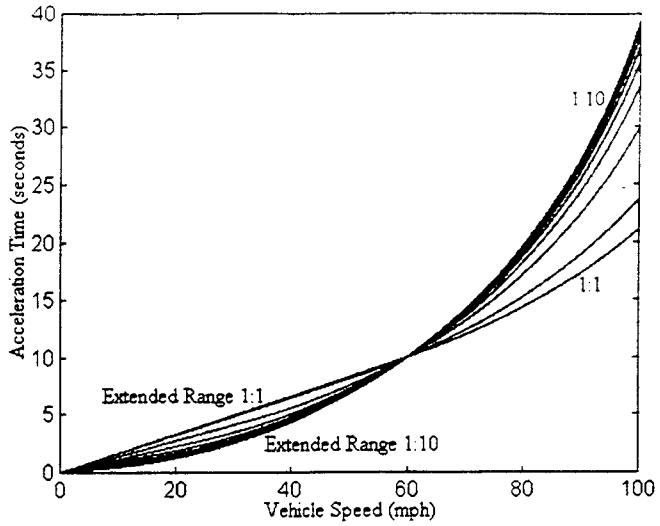

Figure 4. Acceleration Profiles for Different Ratios

Notice that all motors will accelerate to 60 mph in the 10 Seconds but the acceleration curves are different. The extended speed range motors accelerate much more quickly in the beginning and then the acceleration becomes slower at higher speeds. This uneven acceleration affects the distance covered (Figure 5):

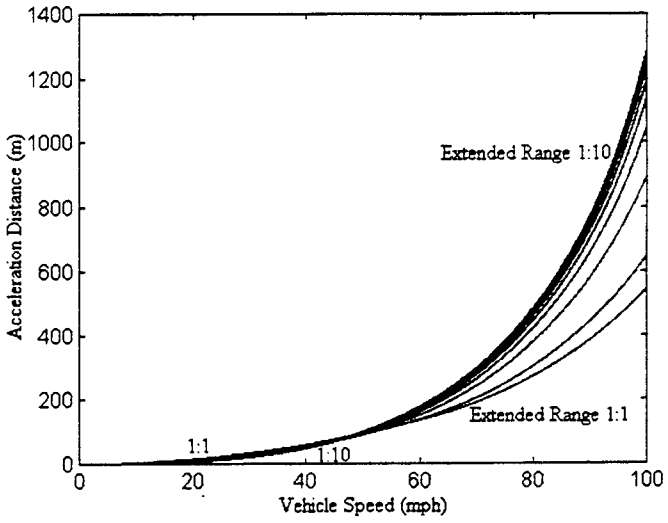

Figure 5. Distance Covered

Notice that vehicles with very low extended constant power ranges (which requires a higher P_m according to Table 3) accelerate to 60 mph in the 10 Seconds but in less distance. This affects passing performance significantly (Figure 6):

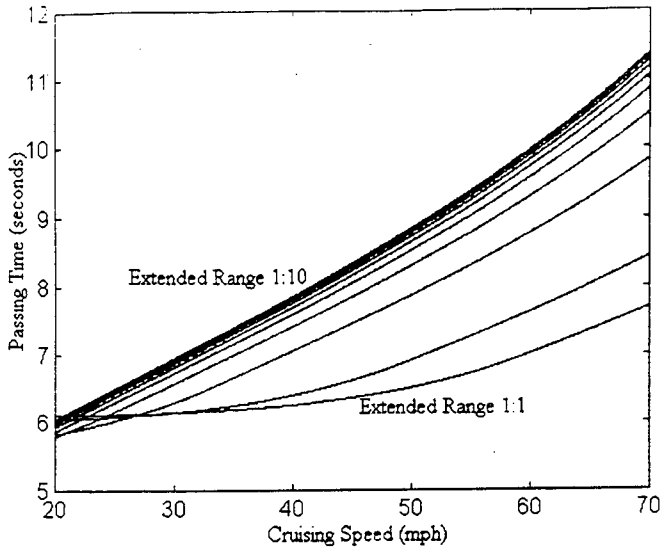

Figure 6. Passing Times

The motors with longer constant power range perform better (shorter passing time) at lower speeds (20 mph), however, the higher power motors (shorter constant power range) perform better at higher speeds. The total distances covered during passing are shown in Figure 7:

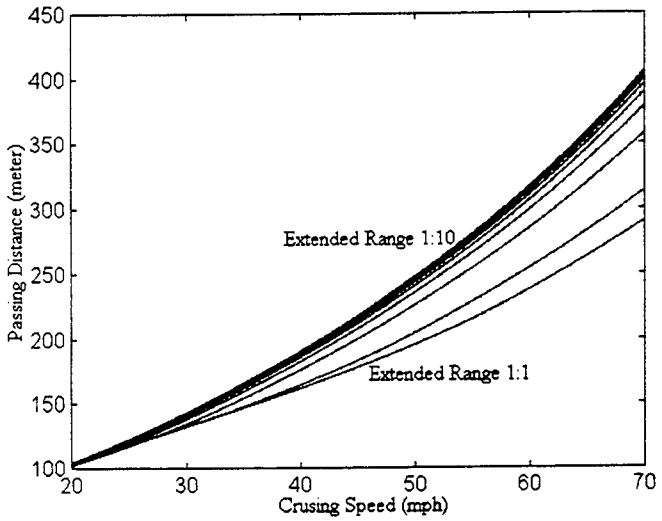

Figure 7. Passing Distance

CONCLUSION

In summary, for simple EV or series HEV designs,

- The power requirement for acceleration decreases as constant power region ratio increases. This results in a smaller motor controller.
- Conversely, the torque requirement for acceleration increases as the constant power region ratio increases. This results in a larger motor size and volume.
- Passing performance suffers considerably as the constant power region ratio increases.

A motor's maximum speed has a pronounced effect on the required torque of the motor. Low speed motors with extended constant power speed range have a much higher rated shaft torque. Consequently, they need more iron and copper to support this higher flux and torque. As motor power decreases (due to extending the range of constant power operation), the required torque is increasing. Therefore, although the converter power requirement (hence the converter cost) will decrease when increasing the constant power range, the motor size, volume, and cost will increase. Increasing the maximum speed of the motor can reduce the motor size by allowing gearing to increase shaft torque. However, the motor maximum speed can not be increased indefinitely without incurring more cost and transmission requirements. Thus there is a multitude of system level conflicts when extending the constant power range.

Several candidate motor technologies were discussed for EV or HEV applications, the induction motor, the brushless DC motor (BLDC) and the switched reluctance motor (SRM). The induction motor has a clear advantage of achieving very high constant power range ratios, but suffers by requiring a very high torque rating. The relatively low maximum speed of the induction motor compounds this problem, because the motor cannot be geared down to the driveshaft an appreciable amount.

The SRM achieves a balance of a modest extended constant power range and a very high maximum speed. Extending the constant power range beyond what the SRM offers yields very little additional benefits (Table 3 and Figure 3). The high maximum speed allows for the SRM to be geared at twice the gear ratio of the induction or BLDC motors, halving the required maximum torque.

The examples presented in this paper form a methodology for evaluating tradeoffs between the power requirement, torque requirement, acceleration performance, and passing performance for different motor technologies. Initial studies indicate that the switched reluctance motor is a good candidate by achieving an optimal balance of these criteria. The same evaluation techniques can be implemented on more complex designs, including parallel or series-parallel type hybrid electric vehicles.

CONTACT

Stephen Moore and Dr. Mehrdad Ehsani can be reached by calling the Department of Electrical Engineering, Texas A&M University, at (409) 845-7441, or email smoore@ee.tamu.edu and ehsani@ee.tamu.edu.

REFERENCES

[1] C. C. Chan, and K. T. Chau, "Advanced ac propulsion systems for electric vehicles," in *Proc. Int. Symp.*

Automotive Technology Automation, 1991, pp. 119-125.

[2] J. L. Oldenkamp, and S. C. Peak, "Selection and design of an inverter-driven induction motor for a traction drive system," *IEEE Trans. on Industry Applications,* Vol. IAS-21, No. 1, Jan./Feb., 1985, pp. 259-265.

[3] C. C. Chan, J. Z. Jiang, G. H. Chen, and K. T. Chau, "Computer simulation and analysis of a new polyphase multipole motor drive," *IEEE Trans. Industrial Electronics,* Vol. 40, 1993, pp. 570-576.

[4] C. C. Chan, W. S. Leung, and K. T. Chau, "A new permanent magnet motor drive for mini electric vehicle," in *Proc. Int. Electric Vehicle Symp.,* 1990, pp. 165-174.

[5] C. C. Chan, J. Z. Jiang, G. H. Chen, X. Y. wang, and K. T. Chau, "A novel polyphase multipole square wave permanent magnet motor drive for electric vehicle," *IEEE Trans. Industry Applications,* 1994, pp. 1258-1266.

[6] T. J. E. Miller, *Brushless Permanent Magnet and Reluctance Motor Drives,* London, U.K., Oxford Univ. Press, 1989.

[7] W. L. Soong and T. J. E. Miller, "Field weakening performance of brushless synchronous AC motor drives," *IEE Proc.-Electr. Power Appl.,* Vol. 141, No. 6, pp. 331-340, November 1994.

[8] P. J. Blake, R. M. Davis, W. F. Ray, N. N. Fulton, P. J. Lawrenson, and J. M. Stefenson, "The control of switched reluctance motors for battery electric road vehicles," *International Conference on PEVD,* pp. 361-364, May, 1984.

[9] Automotive Handbook, Germany: Robert Bosch Gmbh, 1986.

99P-220
A Charge Sustaining Parallel HEV Application of the Transmotor

Stephen W. Moore
Texas A&M University

Mehrdad Ehsani
Texas A&M University

ABSTRACT

An electromechanical gear is presented along with design examples utilizing the electromechanical gear in hybrid electric vehicle drive trains. The designs feature the electromechanical gear (the Transmotor) in place of traditional mechanical transmissions and/or gearing mechanisms. The transmotor is an electric motor suspended by its shafts, in which both the stator and the rotor are allowed to rotate freely. The motor thus can provide positive or negative rotational energy to its shafts by either consuming or generating electrical energy.

A design example is included in which the transmotor is installed on the output shaft of an internal combustion engine. In this arrangement the transmotor can either increase or decrease shaft speed by applying or generating electrical power, allowing the ICE to operate with a constant speed. A torque splitting device is then employed to absorb excess torque produced by the engine or to create supplementary torque when needed, allowing the ICE to operate with constant torque. Thus a constant speed constant torque engine can be directly coupled to the output drive shaft by using electric machines.

The governing equations, a control strategy and an analysis corresponding to each operating mode of the architecture are presented. The operating regions and boundaries of individual components are investigated and engine, motor and energy storage system sizing are identified.

INTRODUCTION

An ordinary automobile transmission is presently the most common method utilized to match the speed of the powerplant (usually an internal combustion engine) to the speed of the driveshaft [1]. Transmissions face the problem of having to constantly switch gear ratios as the vehicle's speed changes. A type of automobile transmission called the Continuously Variable Transmission (CVT) overcomes the traditional problems of having to switch gears.

The electromagnetic gear offers superior characteristics for the automotive designer over the traditional transmission and the CVT. Both types of mechanical transmissions are a 'two-port' design, meaning that there are two connections, the input shaft and the output shaft. The transmotor is a 'three-port' design, meaning that there are three connections, the input shaft, the output shaft, and an electrical connection. The addition of the extra connection allows for design and operational flexibility over the mechanical designs. This allows the electromagnetic gear to actively generate or absorb electrical or mechanical power, whereas the traditional transmissions only allow the passage of mechanical power.

The electromechanical gear is a rotating electric machine in which both the rotor and the stator are free to rotate [2,3,4], with the electrical energy being delivered with brush or slip ring mechanisms. The machine can operate as either a motor if it converts electrical energy into mechanical energy or as a generator if it converts mechanical energy to electrical energy. Furthermore, depending on the relative speeds of the rotor and stator and the direction of the torque developed on the rotor, the transmotor can operate in all four modes (forward motoring, forward generating, reverse motoring, reverse generating).

THE ELECTROMECHANICAL GEAR

An ordinary electric motor features two connections, one electrical and one mechanical. Ordinary motors can operate in four possible scenarios:

- Output shaft rotating clockwise while providing positive torque (forward motoring),
- Output shaft rotating counterclockwise while providing positive torque (reverse motoring),

- Output shaft rotating clockwise while absorbing torque (forward generating),
- Output shaft rotating counterclockwise while absorbing torque (reverse generating).

In comparison, the electromechanical gear features three connections, the rotor shaft, the stator shaft, and the electrical connection (Figure 1).

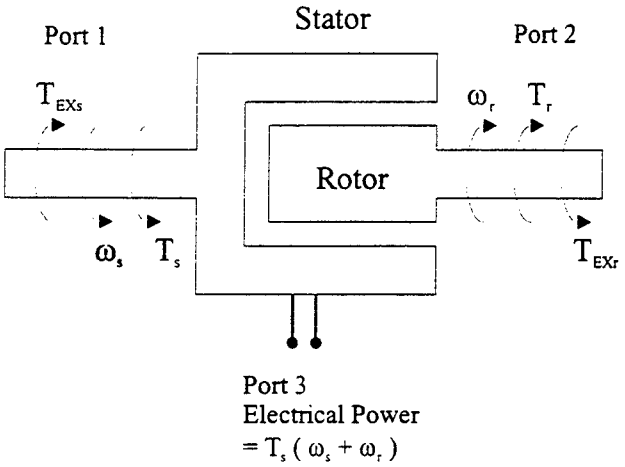

Figure 1. Electromechanical Gear

Where ω_s is the rotational speed of the stator, ω_r is the rotational speed of the rotor and T_{EXs} and T_{EXr} are the external torques applied to the shafts. Since the transmotor is suspended in space, torque is conserved. When torque is produced in the transmotor, it acts equally on the stator and the rotor in opposite directions. In Figure 1 the electromechanical torque developed in the machine is T_r, which acts on the rotor as shown. An equal but opposite torque T_s, acts on the stator. Although the electromechanical torques on the rotor and stator are equal in magnitude, they interact with the externally applied torques T_{EXr} and T_{EXs} to result in different angular speeds for the rotor and stator. Thus in Figure 1, the rotor speed ω_r, and the stator speed ω_s, can be different in magnitude as well as direction. Depending on the relative speed between the rotor and stator and the electromechanical torque developed in the machine, the electromechanical gear can operate in four possible quadrants similar to a traditional electric machine (Figure 2):

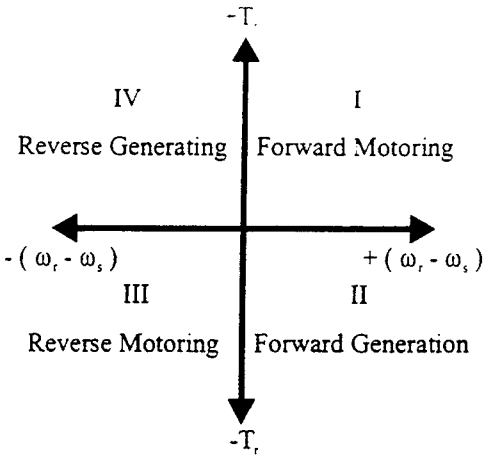

Figure 2. Four Quadrants of Operation

In Figure 1, $T_r = T_s$ and is equal to the electromechanical torque developed in the machine. The stator is assumed to be rotating at speed ω_s, in an opposite direction to the rotor speed ω_r. The law of conservation of energy holds true for any electromechanical system. Applying instantaneous power balance to the electromechanical gear shown in Figure 1:

Electrical Power Input + Mechanical Power Input = Electrical Power Output + Mechanical Power Output

which implies,

Electrical Power at Port 3 = Mechanical Power at Port 1 + Mechanical Power at Port 2

Applying values to these quantities,

Electrical Power $= T_s \omega_s + T_r \omega_r$ (Eq. 1)
Electrical Power $= T_r (\omega_r + \omega_s)$ (since $T_r = T_s$) (Eq. 2)

Thus it is observed that the electrical power input into the electromagnetic gear is split into mechanical power output at the stator and rotor shafts. The four possible operating modes of the machine are shown in Figure 2 and are classified as:

- Quadrant I. Forward motoring
- Quadrant II. Forward generating
- Quadrant III. Reverse motoring
- Quadrant IV. Reverse generating.

In the forward motoring quadrant, the rotor moves in the positive direction with respect to the stator. The electromechanical torque developed on the rotor acts in the positive direction in this mode. In the forward generating quadrant the rotor still moves in the positive direction relative to the stator, but now the electromechanical torque acting on the rotor is in the negative direction. The electromagnetic gear operates in the reverse motoring quadrant when the rotor moves in

the negative direction with respect to the stator, and the electromechanical torque acts in the negative direction on the rotor. In the reverse generating quadrant, the rotor moves in the negative direction relative to the stator, while the electromechanical torque acts in the positive direction on the rotor.

The electromagnetic gear can operate in any one of the four quadrants shown in Figure 2 depending on the relationship between T_r, ω_r, and ω_s. Notice that the clockwise direction of rotation is considered to be positive. Because there are three ports, there are nine possible (3^2) major operating modes consisting of 21 minor modes of operation.

If the stator is held in place (i.e. $\omega_s = 0$) by an infinite external torque T_{Exs}, the transmotor performs like an ordinary electric machine. The rotor will spin at the speed ω_r and produce torque T_r. It will operate in all four quadrants in this manner. The same holds true if the rotor is held fixed ($\omega_s = 0$) by an external torque T_{EXr}. Then the stator will spin at the speed ω_s and produce torque T_s. The electrical power consumed would be T_s ω_s.

If the stator and rotor speeds are exactly matched ($\omega_s = \omega_r$) then the motor will simply rotate in place producing nor consuming any torque or electrical energy. It is in this mode that the transmotor can perform as an electrical clutch, because the external torques applied to the motor can not exceed the transmotor's torque rating without slipping. By varying the transmotor's magnetic field, the torque threshold can be adjusted.

If the stator and the rotor are spinning in the same direction but one is faster than the other, the transmotor operates in all four quadrants depending on the applied and produced torques. For example, consider the transmotor stator attached to an ICE producing T_{EXs} torque and spinning at speed ω_s (Figure 3). If the driveshaft is at zero speed ($\omega_r = 0$) then the transmotor is *generating* electrical power (Quadrant III). If the vehicle is traveling at high speeds and the rotor speed is faster than the stator speed ($\omega_r > \omega_s$) then the transmotor is *consuming* electrical power (Quadrant I). In both scenarios, the transmotor does not contribute torque, and the torque applied to the driveshaft is T_{EXs}. Similar scenarios take place under regenerative braking.

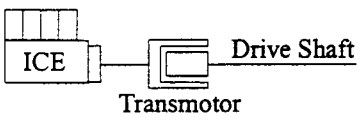

Figure 3. Simple Application of the Transmotor

The closest mechanical system to the transmotor is the planetary gear. A planetary gear has three mechanical ports as does the transmotor (Figure 4):

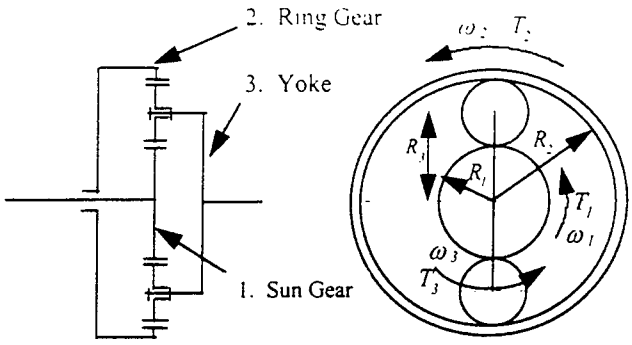

Figure 4. Planetary Gear

There are three major components of the planetary gear, the sun gear (1), the ring gear (2), and the yoke (3). The torque and speed relationships for the planetary gear are:

$$\omega_3 = \frac{R_1}{2R_3}\omega_1 + \frac{R_2}{2R_3}\omega_2 \qquad \text{(Eq. 3)}$$

$$T_3 = \frac{2R_3}{R_1}T_1 = \frac{2R_3}{R_2}T_2 \qquad \text{(Eq. 4)}$$

where R_1, R_2 and R_3 are the radii of the different gears. Ignoring the effects of gear sizing, the fundamental operation of the planetary gear system is:

$$\omega_3 \approx \omega_1 + \omega_2 \qquad \text{(Eq. 5)}$$

$$T_3 \approx T_1 \approx T_2 \qquad \text{(Eq. 6)}$$

These equations state that when torque is applied on two of the ports, the third port must also have that same torque (or a factor of those torques when given gear sizing). They also state that when speeds are applied to two ports, the third port will display a sum of those speeds. These equations compare with the transmotor governing equations:

$$\omega_r = \omega_s + \omega_e \qquad \text{(Eq. 7)}$$

$$T_r = T_s \qquad \text{(Eq. 8)}$$

where ω_e is the speed produced by the electrical port. Notice that these equations are a dual of the planetary gear equations. Attaching an electric motor to one of the planetary gear ports, a transmotor equivalent can be made (Figure 5):

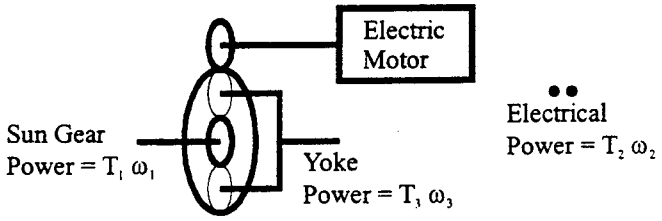

Figure 5. Transmotor Equivalent

Notice that this duality does not take into account the torque and speed translations due to the differing radii of the planetary gears.

EXAMPLE HYBRID ARCHITECTURES

There are almost an unlimited ways in which electric motors, gears, engines, and other drivetrain components can be arranged into vehicle powertrains. This section will describe a few example architectures featuring the transmotor. First, the basic hybrid architectures are presented:

- Series Hybrid

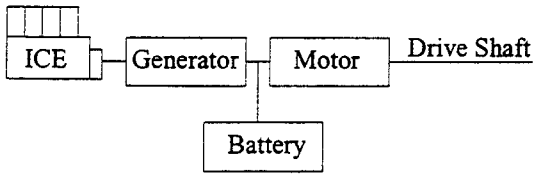

Figure 6. Series Hybrid

The series hybrid is much like an electric vehicle with the exception of on-board electricity generation [5]. The ICE and generator produce the average energy requirement of the vehicle and additional transient power is provided by the battery pack. A series hybrid is not limited to ICE and generator. Many options exists such as fuel cells, thermoelectric cells, and turbine generators.

- Parallel Torque Summing Hybrid

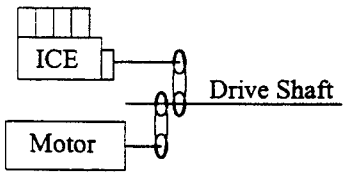

Figure 7. Parallel Torque Summing Hybrid

The torque summing hybrid uses a drive shaft with belts [6] or gears to combine the torques of the ICE and electric machine. The torque summing hybrid can operate in two basic modes. When the ICE torque is too low, the electric machine can add power to the driveshaft by increasing the torque. When the ICE torque is more than the vehicle demand, the electric machine can absorb energy from the driveshaft by producing electricity. More modes of operation can be created by the addition of clutches, transmissions, and electromagnetic locks, but the two basic modes of operation remain the same. A pass-though type motor can be used in place of the belt or gear torque summing device [7,8,9,10,11]:

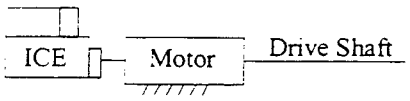

Figure 8. Torque Summing Hybrid

A Torque summing hybrid allows the ICE to be sized smaller than the peak torque demand of the vehicle, however, the ICE is forced to operate over its entire torque and speed ranges. In this case, the ICE is sized for the average torque and the electric motor sized for the peak torque requirement. A version of this design is also known as the Petro Electric Drivetrain [12].

- Parallel Speed Summing Hybrid

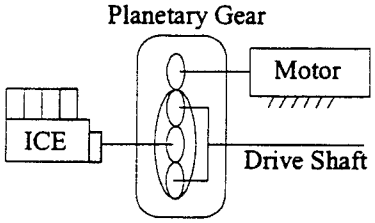

Figure 9. Speed Summing Hybrid

This speed summing hybrid uses a planetary gear system to combine the speeds of the ICE and electric machine. The electric machine cannot contribute or subtract torque from the system, only rotational speeds. With the transmotor, the planetary gear system can be removed:

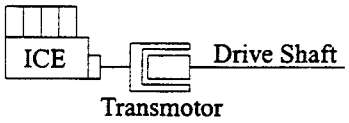

Figure 10. Simplified Speed Summing Hybrid

The speed summing hybrid has two basic modes. When the ICE's speed is too low, the electric machine can add power to the driveshaft by increasing rotational speed. When the ICE is operating too fast, the electric machine can absorb rotational energy from the driveshaft by generating electricity. More modes of operation can be created by the addition of clutches and locks, but the two basic modes remain the same. Notice the ICE can operate at a single speed in this configuration, but must vary its torque production.

- Parallel Speed Summing Hybrid with Transient Torque Sink

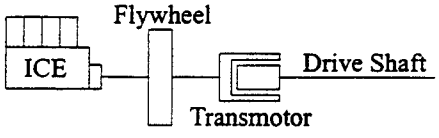

Figure 11. Speed Summing with Torque Sink

The addition of the flywheel provides the transmotor with a transient torque sink in which it can act against to add torque to the driveshaft. This allows for the ICE to be sized smaller than the peak required torque because transient torque can be obtained from the flywheel's rotational energy. However, the torque sink is limited and gradability and load carrying capability is limited to ICE sizing.

- Series/Parallel Hybrid

The disadvantages of a parallel torque summing hybrid vehicle are substantial. The ICE is not operated strictly in its peak efficiency region, but instead its operation varies as a function of vehicle speed. The electric machine in the torque summing hybrid is the primary torque device, providing transient and peak power. The engine serves as a secondary torque device and average power source. The inverse of these properties are true with a speed summing hybrid. The ICE is allowed to operate at an optimal speed, but the torque output is variable, forcing the engine to operate outside of its peak efficiency region. The engine in this case is the only torque device, thus forcing the designer to match the ICE to the torque demands of the vehicle. These disadvantages are eliminated with the series hybrid architecture. The ICE is coupled directly to a generator and operated at an optimal speed and torque. Thus the ICE does not contribute power directly to the vehicle drive shaft. This arrangement puts the full burden of powering the vehicle on the propulsion motor(s). Series hybrids tend to be costly due to the large generator and propulsion motor sizes.

A possible hybrid design methodology to allow the ICE to operate at a constant optimal torque and speed is to combine the parallel and series architectures:

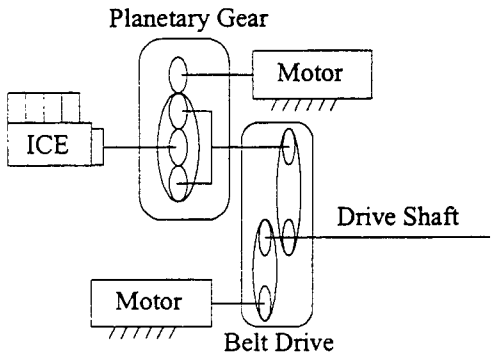

Figure 12. Series/Parallel Hybrid

This series/parallel hybrid architecture has been demonstrated roughly in the Toyota Prius, the first mass-produced hybrid electric vehicle. There are several other combinations of series/parallel designs [13]. The architecture is capable of four basic modes of operation with the ICE operating at a constant torque and RPM:

1. Slow vehicle speed and accelerating. The planetary gear/motor subtracts speed from the ICE by generating electricity to match its speed to the driveshaft speed. The driveshaft motor adds extra torque for acceleration.
2. Slow speeds decelerating. The planetary gear subtracts speed from the ICE shaft and the driveshaft motor subtracts torque from the driveshaft by generating electricity.
3. Fast vehicle speed and accelerating. The planetary gear motor supplements the ICE speed and the driveshaft motor adds extra torque for acceleration.
4. Fast speeds decelerating. The planetary gear adds speed to the ICE shaft and the driveshaft motor subtracts torque.

Additional modes are available as well:

5. Electric mode only. In this mode, the driveshaft motor provides all the power required by the vehicle.
6. Series mode only. The planetary gear consumes all available power from the ICE to charge the batteries. The driveshaft motor provides all traction power requirements.

The series/parallel architecture can be improved upon by the use of a transmotor:

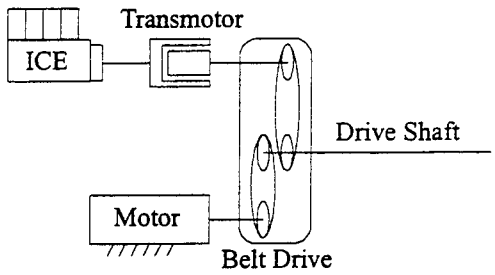

Figure 13. Transmotor Application

This arrangement removes the necessity of the planetary gear system, thus improving the mechanical efficiency of the system. However, the mechanical torque summing device (gears, belts, ect.) still imposes design and efficiency penalties. The torque summing device can be replaced with an in-line motor mounted in series with the transmotor:

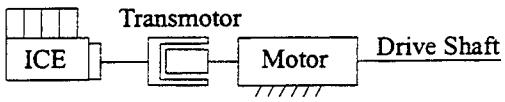

Figure 14. Simplified Series/Parallel Architecture

This architecture has four basic modes of operation similar to the four listed previously. In addition, there are five other significant modes:

5. Cruise. The transmotor matches the ICE speed to the driveshaft (consumes electrical power) and the in-line motor absorbs excess torque from the ICE (generates electrical power), resulting in a net electrical energy flow of zero.
6. Charging Cruise. The ICE operates outside of its optimal region to produce excess RPM and torque, which is converted to electrocute by the motors.
7. Engine Mode. The ICE operates with variable speed and torque, thus minimizing the work required by the electric motors.
8. EV Only Mode (requires a lock or clutch). The shaft of the ICE is locked in place and the motors are used in series are a primary mover, powered by the battery pack.
9. Standstill Charging. The transmotor absorbs all energy from the ICE to charge the battery and the in-line motor is used to lock the driveshaft.

Major design obstacles for the implementation of the transmotor in this architecture are not trivial. The foremost concern is the requirement for two motors and two motor controllers, which results in an increase of system cost. However, this penalty is reduced slightly because each motor and controller does not have to carry the full propulsion load of the vehicle and can be sized smaller. Initial simulations suggest that although the transmotor has to be rated for the full torque of the ICE, its rated power can be a third of the rated power of the traction motor.

Other design considerations involve the actual construction of the transmotor unit. Because the transmotor floats on its shafts, it presents a challenge to deliver the electrical power to the stator and rotor. The bearings and mechanical support for the motor are also an issue.

Since the transmotor and traction motor are configured to be in series with this design, it is plausible that the stator of the transmotor be extended outwardly and serve as a flywheel. An addition of a flywheel to the series/parallel architecture would create an additional torque sink, allowing smaller component sizing.

CONCLUSION

The transmotor is an electric motor suspended by its shafts, in which both the stator and the rotor are allowed to rotate freely. Electric power is supplied to the rotor or stator (or a combination of the two, depending on the motor technology implemented) using a delivery mechanism such as slip-rings. In this manner, the transmotor can be used to consume or generate electrical power given a rotational speed differential between the rotor and the stator. Because the transmotor is suspended, it cannot contribute a torque component (positive or negative) to the driveshaft.

The transmotor can operate in all four quadrants: forward motoring, forward generating, reverse motoring, and reverse generating like an ordinary electric machine. In addition, these four modes can be broken down into 21 minor modes, which allows the hybrid designer a high degree of flexibility in his control scheme.

The transmotor's speed summing property makes it an ideal active replacement for traditional mechanical transmissions. Traditional transmissions are a 'two-port' design, meaning that there are two connections, the input shaft and the output shaft. The transmotor is a 'three-port' design, meaning that there are three connections, the input shaft, the output shaft, and an electrical connection. The addition of the extra connection allows for design and operational flexibility over the mechanical designs.

Many modern hybrid architectures feature planetary gears as speed summing devices to match the output speed of an ICE to the rotational speed of the driveshaft. The transmotor is the electromechanical dual of the planetary gear system.

Design obstacles facing hybrid designers wanting to implement speed summing parallel hybrid topologies

CONTACT

Stephen Moore and Dr. Mehrdad Ehsani can be reached by calling the Department of Electrical Engineering, Texas A&M University, at (409) 845-7441, or email smoore@ee.tamu.edu and ehsani@ee.tamu.edu.

REFERENCES

1. Davis, Gregory W., "The Development of an Electo-Hydraulically Controlled, Five-Speed Transmission for a Hybrid Electric Vehicle," SAE Paper No. 980830.
2. Sodhi, Sameer, "Electromagnetic Gearing Applications in Hybrid Electric Vehicles," Ph.D. Dissertation, Texas A&M University, August, 1994.
3. Wakefield, E. H., "History of the Electric Automobile," SAE Publication, 1994.
4. Weisenburger, G.E., "Electric Motor", U.S. Patent #667,275, Filed Feb. 1900.
5. A. F. Burke, "Hybrid/electric vehicle design options and evaluations," *SAE Journal Publications,* Paper No. 920447, Feb., 1992.
6. Johnston, B., et al, "The Continued Design and Development of the University of California, Davis Future Car," SAW Paper 980487.
7. Ehsani, M., K.M. Rahman, and H.A. Toliyat, "Propulsion System Design of Electric and Hybrid Vehicles," IEEE Transaction of Industrial Electronics.
8. Toliyat, H.A., K.M. Rahman, and M. Ehsani, "Electric Machine in Electric and Hybrid Applications," Proceedings of ICPE, 1995, Seoul, pp. 627-635.
9. Ehsani, M., "Electrically Peaking Hybrid System and Method," U.S. Patent granted, 1996.
10. Howze, J., M. Ehsani, and D. Buntin, "Optimizing Torque Controller for a Parallel Hybrid Electric Vehicle," U.S. Patent granted, 1996.
11. Gao, Yimin, K. Rahman, and M. Ehsani, "Parametric Design of the Drive Train or an Electrically Peaking Hybrid (ELPH) Vehicle," ASE paper 970294.
12. Jeffries, P.N. and A.E. Corbett, "The Petro-Electric Drivetrain," IEEE Colloquium on Motors and Drives for Battery Powered Propulsion, digest no. 080, pp. 7/1-4, Apr. 1993.

13. Willis, F.G., and R.R. Radtke, "Hybrid Vehicle System Analysis," SAE paper 920447.

A Matlab-based Modeling and Simulation Package for Electric and Hybrid Electric Vehicles Design

Karen Butler, *Member,IEEE,* Mehrdad Ehsani, *Fellow,IEEE,* Preyas Kamath, *Student Member,IEEE*

Abstract - **This paper discusses a simulation and modeling package developed at Texas A&M University, V-Elph 2.01. V-Elph facilitates in-depth studies of electric (EV) and hybrid electric (HEV) vehicle configurations or energy management strategies through visual programming and by creating components as hierarchical subsystems which can be used interchangeably as embedded systems. V-Elph is composed of detailed models of four major types of components: electric motors, internal combustion engines, batteries, and support components which can be integrated to model and simulate drive trains having all electric, series hybrid, and parallel hybrid configurations. V-Elph was written in the Matlab/Simulink graphical simulation language and is portable to most computer platforms.**

This paper also discusses the methodology for designing system level vehicles using the V-Elph package. An EV, a series HEV, a parallel EV, and a conventional ICE driven drive train have been designed using the simulation package. The simulation results such as fuel consumption, vehicle emissions, and complexity are compared and discussed for each vehicle.

I. INTRODUCTION

Presently, only electric and low-emissions hybrid vehicles can meet the criteria outlined in the California Air Regulatory Board (CARB) regulations which require a progressively increasing percentage of automobiles to be ultra-low or zero emissions beginning in the year 1998 [1]. Though purely electric vehicles are a promising technology for the long range goal of energy efficiency and reduced atmospheric pollution, their limited range and lack of supporting infrastructure may hinder their public acceptance [2]. Hybrid vehicles offer the promise of higher energy efficiency and reduced emissions when compared with conventional automobiles, but they can also be designed to overcome the range limitations inherent in a purely electric automobile by utilizing two distinct energy sources to provide energy for propulsion. With hybrid vehicles, energy is stored as a petroleum fuel and in an electrical storage device such as a battery pack and is then converted to mechanical energy by an internal combustion engine (ICE) and electric motor, respectively. The electric motor is used to improve energy efficiency and vehicle emissions while the ICE provides extended range capability. Though many different arrangements of power sources and converters are possible in a hybrid power plant, the two generally accepted classifications are series and parallel [3].

Computer modeling and simulation can be used to reduce the expense and length of the design cycle of hybrid vehicles by testing configurations and energy management strategies before prototype construction begins. Interest in hybrid vehicle simulation began to pick up in the 1970's along side the development of several prototypes which were used to collect a considerable amount of test data on the performance of hybrid drive trains [4]. Also studies have been conducted to study the hybrid electric vehicle concepts [5-7]. Several computer programs have since been developed to describe the operation of hybrid electric power trains, including: Simple Electric Vehicle Simulation (SIMPLEV) from the DOE's Idaho National Laboratory [8], MARVEL from Argonne National Laboratory [9], CarSim from AeroVironment Inc., JANUS from Durham University [10], and ADVISOR from the DOE's National Renewable Energy Laboratory [11]. A previous simulation model, ELPH, developed at Texas A&M University was used to study the viability of an electrically-peaking control scheme and to determine the applicability of computer modeling to hybrid vehicle design [12] but was essentially limited to a single vehicle architecture. Other work conducted by the hybrid vehicle design team at Texas A&M University is reported in [13-17].

V-Elph [18-19] is a system level modeling, simulation and analysis package developed at Texas A&M University using Matlab/Simulink [20] to study issues related to electric vehicle (EV) and hybrid electric vehicle (HEV) design such as energy efficiency, fuel economy, and vehicle emissions. V-Elph facilitates in-depth studies of power plant configurations, component sizing, energy management strategies, and the optimization of important component parameters for any type of hybrid or electric configuration or energy management strategy. It uses visual programming techniques, allowing the user to quickly change architectures, parameters, and to view output data graphically. It also includes detailed models of electric motors, internal combustion engines, and batteries developed at Texas A&M University.

This paper discusses the methodology for designing system level vehicles using the V-Elph package. An EV, a series HEV, a parallel EV, and a conventional ICE driven drive train have been designed using the simulation package. The simulation results are compared and discussed for each vehicle.

II. DRIVE TRAIN DESIGN METHODOLOGY

Several levels of depth are available in V-Elph to allow users to take advantage of the features that interest them. At the most basic level, a user can run simulation studies by selecting one of the electric vehicles, series or parallel hybrid vehicles, or conventional vehicles provided and display the results using the graphical plotting tools. In addition to being able to change the drive cycle and the environmental conditions under which the vehicle operates, the user can switch components in and out of a vehicle model to try different types of engines, motors, and batteries models. The user can also change vehicle characteristics such as size and weight, gear ratios, and the size of the components that make up the drive train.

An intermediate user can create his/her own vehicle configurations using a blank vehicle drive train template as shown in fig. 1. This drive train was constructed graphically by connecting the main component blocks (drive cycle, controller, power plant, vehicle dynamics) using the Simulink visual programming methodology through the connection of the appropriate input and output ports. The power plant is blank and is designed using component models selected from a component library. Components can be isolated to run parameter sweeps that create performance maps which assist in component sizing and selection. A controller block is designed with logic statements which create the signals required to control the individual system-level components. A vehicle dynamics block is designed with input parameters such as road angle, mass, and drag coefficient necessary to compute vehicle output dynamic parameters such as engine speed and road speed. The drive cycle block is designed by selecting a drive cycle from those supplied by the package or creating a new drive cycle.

Finally, advanced users can pursue sophisticated design objectives such as the creation of entirely new component models and the optimization of a power plant by creating add-on features that are compatible with the modeling system interface.

V-Elph allows the interconnection of virtually any type of electrical or mechanical component utilized in a vehicle drive train, even experimental technologies such as ultra-capacitors. Component models can be created from look-up tables, empirical equations, and both steady-state and dynamic equations. Each component model is created from the general model and interface shown in fig. 2. The component models are stored in a library, called the library of components as shown in fig. 3. The speed at which the simulation executes is highly dependent on the complexity of the component models used in a vehicle design. The various detailed component models currently utilized in the V-Elph package were developed by members of the ELPH research team at Texas A&M University.

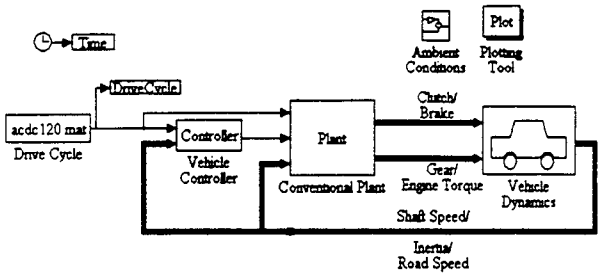

Fig. 1. System level representation of a general vehicle drive train in V-Elph

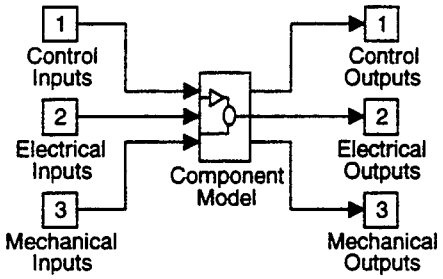

Fig. 2 Component Input/Output interface

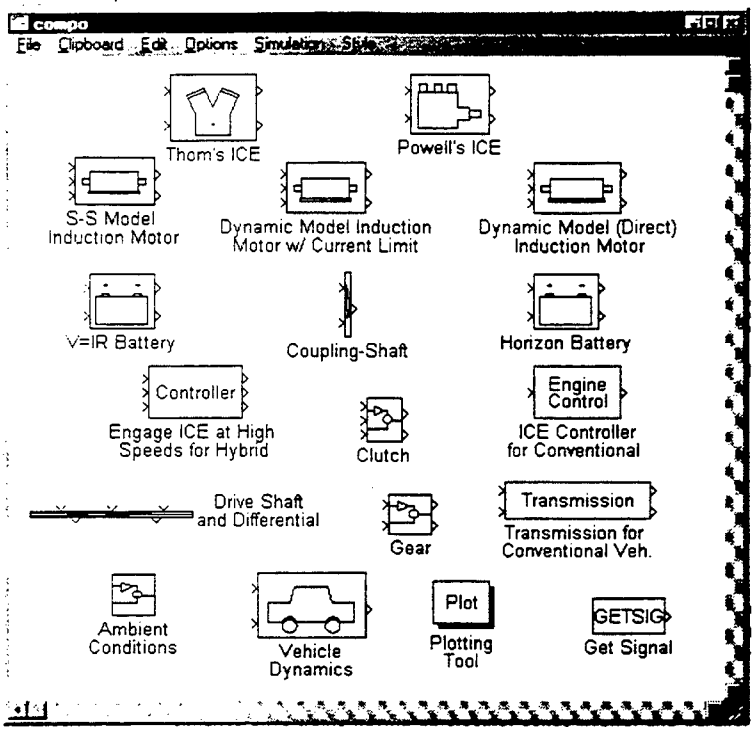

Fig. 3. Library of Components

I. DESIGN OF VEHICLE DRIVE TRAINS

In this section, the design and analysis of an electric vehicle drive train, two parallel hybrid vehicle drive trains with different control strategies, a series hybrid electric vehicle drive train, and a conventional internal-combustion-engine-driven vehicle drive train using the V-Elph package are discussed. A description is given of the performance specifications and the control strategy and power plant developed for each vehicle design. A typical mid-sized family sedan was used as the basis for each vehicle. The vehicles' components were sized to provide enough power to maintain a cruising speed of 120 km/h on a level road and acceptable acceleration performance of 0 to 100 km/h in 16 seconds for short time intervals. The vehicles were also designed to maintain highway speeds for an extended period of time and provide adequate performance on hills. The same ICE, motor, battery, and vehicle dynamics models were used for each vehicle design with appropriate changes made to the model parameters to meet the specific vehicle performance requirements.

Simulation studies were performed for each vehicle using a simple acceleration and deceleration drive cycle, an FTP-75 urban drive cycle, a federal highway drive cycle, and a commuter drive cycle. Various performance parameters generated during the simulation studies are graphically presented in the paper. Also a table is included which compares such performance parameters as fuel consumption and emissions for each simulation study.

A. ICE Conventional Drive Train Design

The conventional ICE-driven drive train was designed based on the specifications of a Buick LeSabre ('91 model) [21]. The vehicle's 4-speed automatic transmission was modeled as a manual transmission with a clutch, retaining the same overall gear ratios. It is a 4 door sedan, 6 passengers vehicle with a desired 0-60 mph in the 10 seconds range characteristic and a curb weight of 3483 lbs (1580 kgs). The power plant is shown in fig. 4. Table 1 shows the engine and vehicle specifications utilized to design the conventional drive train.

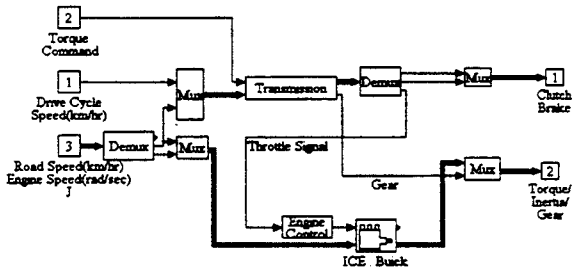

Fig. 4. Power plant representation of conventional vehicle drive train designed using V-Elph

TABLE I.
SPECIFICATIONS OF ICE DRIVE TRAIN

Engine Specifications			
Total Displacement		3.791 liter	
Max Torque		298 Nm at 3200 rpm	
Max Power		125 KW at 4800 rpm	
Vehicle Specifications			
Curb Weight		1580 kg	
Acceleration		0-60 mph in 10 s	
Overall Gear Ratios			
1st	2nd	3rd	4th
8.94	4.804	3.06	2.142

A. *Parallel Hybrid Electric Drive Train Design*

In a typical parallel design, consisting of an ICE and an electric motor in a torque-combining configuration, either the ICE or the electric motor can be considered the primary energy source depending on the vehicle design and energy management strategy. Also the drive train can be designed such that the ICE and electric motor are both responsible for propulsion or each is the prime mover at a certain time in the drive cycle. A component's functional role could change within the course of a drive cycle due to battery depletion or other vehicle requirements. Vehicle architecture decisions, control strategies, component selection and sizing, gearing, and other design parameters become considerably more complex in a parallel hybrid due to the sheer number of choices and their effect on a vehicle's performance given a particular mission.

The vehicle drive train configuration in fig. 5 was designed in V-Elph for a parallel HEV. It is based on a typical mid-sized family sedan with a gross mass of 1838 Kg that includes the additional batteries used in the hybrid power plant. The drive train includes a controller which manipulates the torque contributions of the electric motor and ICE. The battery provides power for the induction motor. The ICE model was sized to provide enough power to maintain a cruising speed of 120 km/h on a level road and the electric machine was sized to provide acceptable acceleration performance of 0 to 100 km/h in 16 seconds for short time intervals.

The ICE model was designed based on Powell's engine analysis [22]. The induction machine model [13] performs two functions in the drive train; as a motor it provides torque at the wheels to accelerate the vehicle and as a generator it recharges the battery during deceleration (regenerative braking) or whenever the torque produced by the power plant exceeds the demand from the driver. Vector control was utilized to extend the constant power region of the motor, making it possible to run the motor over a wide speed range. The motor can provide the requested torque up to the constant power threshold at speeds above the base speed of the motor; operation beyond this point is restricted to avoid exceeding the motor's power rating. The HEV design utilizes the wide speed range of the vector controlled induction motor to improve the overall system efficiency.

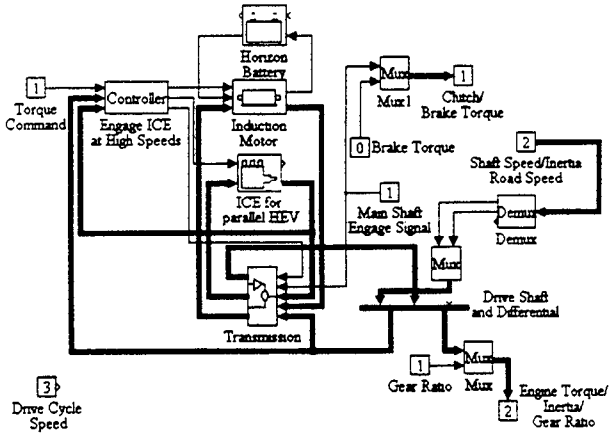

Fig. 5. Parallel HEV drive train configuration

The battery model [23] uses the current load and battery state of charge to determine dc bus voltage. Voltage tends to drop as the state of charge decreases and as the amount of current drawn from the battery increases. At low currents, the battery efficiency is reasonably high regardless of the state of charge. As the amount of current drawn from the pack increases, the battery efficiency drops rapidly to about 75% for a 400 A drain. At current levels up to about 100 A the battery recharge efficiency is relatively high but quickly drops off above this threshold because the physical and chemical processes in the battery can not react quickly enough to absorb the energy, resulting in battery degradation. It is thus desirable to perform battery charging at current levels of 100 A or less whenever possible.

Two parallel HEV drive trains were designed using a different control strategy, referred to as control strategy 1 and control strategy 2. Control strategy 1 operates such that the ICE runs at a constant fuel throttle angle and the electric machine makes up the difference between the torque requested by the driver and the torque produced by the ICE. This scheme aims to minimize the amount of time that the ICE is in use by maximizing the speed at which the ICE is engaged to the wheels while maintaining the battery state of charge over the drive cycle. Control strategy 2 operates such that the ICE runs over its entire speed range and makes the ICE throttle angle a function of speed to meet the steady-state road load. The general principle behind each strategy is that the electric motor provides power for propulsion during the transients, acceleration to deceleration, and the ICE provides propulsion during cruising.

The sizes of the components for the parallel hybrid drive train are stated in Table 2.

TABLE 2
COMPONENTS OF PARALLEL HYBRID DRIVE TRAIN

ICE	1.0 liter, 32.5 kW
Motor	Vector controlled, 40 kW
Battery	Thirteen, 12-volt, lead acid

A. Series Hybrid Electric Drive Train Design

In a series hybrid electric vehicle, only one energy converter provides torque to the wheels while the others are used to recharge an energy accumulator, usually a battery pack. In a typical series hybrid design, an ICE/generator pair charges the batteries and only the motor actually provides propulsion. The series hybrid drive train shown in fig. 6 includes a controller and power plant and was designed based on [24]. A vector controlled induction motor powered by a D.C. battery pack of 156 volts supplies the power at the drive wheels. In addition, there is an A.P.U. (auxiliary power unit) comprising of an ICE driving an induction generator. The A.P.U. supplies power to the battery when the demanded current by the induction motor exceeds a threshold value of 75 amperes. The local controller is responsible for the following tasks

- demanding a torque (positive or negative) from the induction motor depending on drive cycle requirements.
- for switching on/off the APU.

The torque demanded from the induction motor is positive during acceleration and cruise phases of the drive cycle (motoring mode) and is negative during the deceleration phase of the drive cycle (generator mode). During the motoring mode, current is drawn from the battery (discharging) and during generation mode current is supplied to the battery (charging).

When the APU is on, the ICE is running at its optimum speed and the induction generator supplies charges the battery; in the 'off' mode, the ICE idles. Thus the APU is responsible for decreasing the drain on the battery pack, especially during the acceleration phases of the drive cycle. The ICE control is based on a "constant throttle strategy" which was found to be optimum [24].

The system control strategy for a series hybrid is not required to be as complex as the controller for a parallel hybrid since there is only one torque provider. For the series design discussed in the paper, the classic proportional, integral, and derivative (PID) controller [25] is utilized.
The sizes of the components for the series hybrid drive train are stated in Table 3.

TABLE 3
COMPONENTS OF SERIES HYBRID DRIVE TRAIN

ICE	1.2 liter, 40 kW
Motor	Vector controlled, 40 kW
Generator	Vector controlled, 40 kW
Battery	13, 12-volt, lead acid

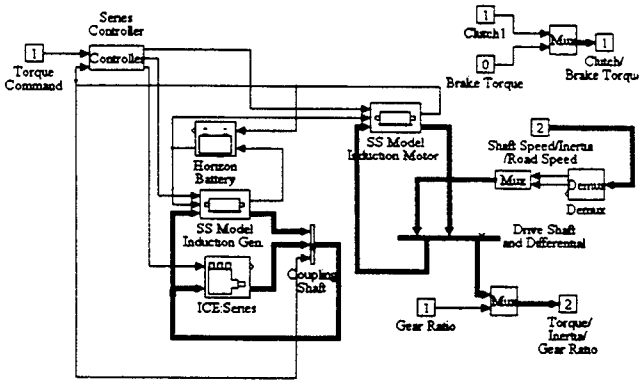

Fig. 6. Drive Train for Series hybrid vehicle

B. Electric Drive Train Design

In electric vehicles, all of the onboard systems are powered by batteries and electric motors. The electric drive train designed using V-Elph is shown in fig. 7.

In the electric vehicle, all the torque demanded at the drive wheels is solely met by a vector controlled induction motor powered by a D.C. battery pack of 240 volts. The controller demands a torque (positive or negative) from the induction motor, depending upon the torque demanded by the vehicle to meet the drive cycle speed. The induction motor tries to meet this demanded torque. Positive power is demanded from the induction motor (operating in motoring mode) during acceleration and cruise phases of the drive cycle and negative power is demanded during the deceleration phase of the drive cycle (operating in generator mode). During the motoring phase the induction motor draws current from the battery pack (discharging) and during the generator mode the induction motor supplies current to it (recharging) . The induction motor and battery pack are sized to satisfy the peak power requirements of the drive cycle.

The sizes of the components for the electric vehicle drive train are stated in Table 4.

TABLE 4
COMPONENTS OF ELECTRIC VEHICLE DRIVE TRAIN

Motor	Vector controlled, 40 kW
Battery	20, 12-volt, lead acid

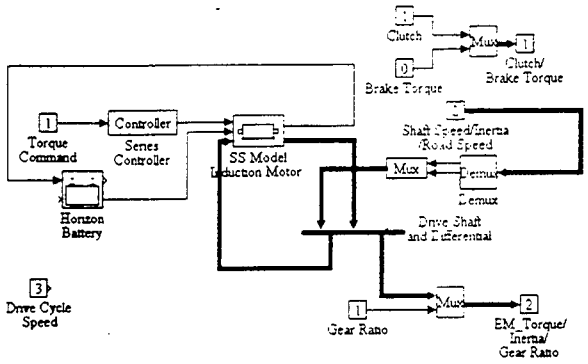

Fig. 7. Electric Vehicle Drive Train

I. SIMULATION STUDIES

Four drive cycles were applied to the various vehicle drive train designs. Drive cycle one consisted of a gradual acceleration to 120 km/h, cruise, and then a deceleration back to stop as shown in fig. 8. Drive cycles two and three were composed of the FTP-75 urban drive cycle and the federal highway drive cycle [226] as shown in figs. 9 and 10, respectively. Drive cycle four was a commuter drive cycle as shown in fig. 11 which was developed by combining three FTP-75 urban drive cycles with two federal highway drive cycles. The two highway cycles are inter-spaced between each of the urban cycles.

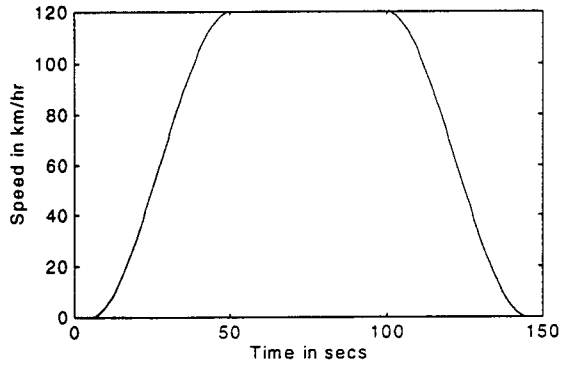

Fig. 8. Drive cycle one consisting of acceleration, cruise, and deceleration

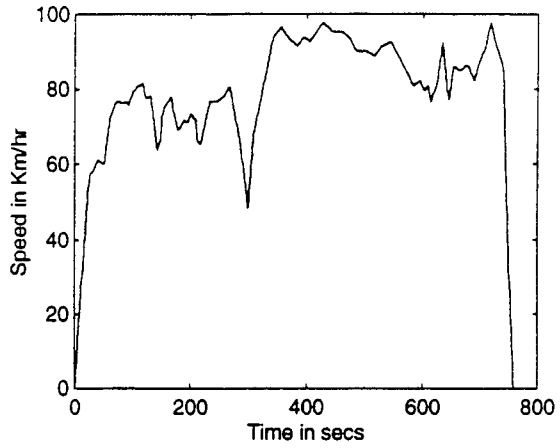

Fig. 9. FTP-75 Urban drive cycle – Drive Cycle Two

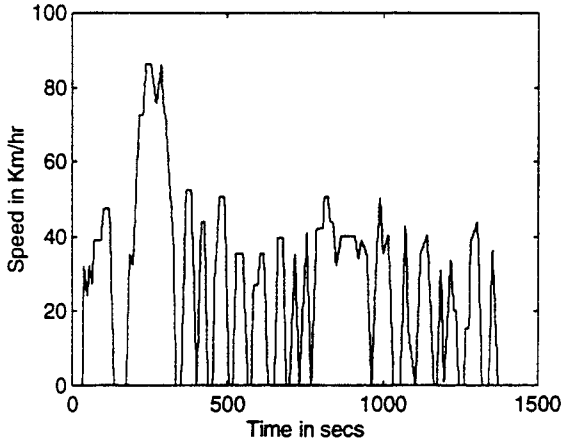

Fig. 10. Federal highway drive cycle – Drive Cycle Three

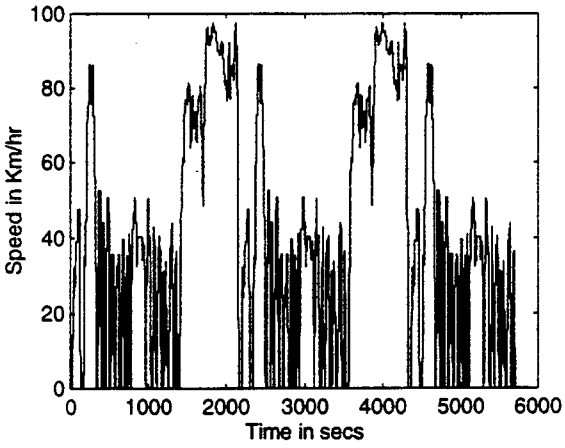

Fig. 11. Commuter drive cycle – Drive Cycle Four

The V-Elph package includes plotting tools that provide graphical displays of output variables generated during simulation studies. Also V-Elph provides a mechanism to facilitate the study of various aspects related to electric and hybrid electric vehicle drive train design such as control strategies and vehicle configurations (e.g. EV and HEV). The following figures illustrate the results of various simulation studies conducted using the four drive cycles with the five vehicle configurations.

Fig. 12 shows a plot of the electric motor (EM) torque and ICE torque versus time for the drive cycle one applied to the parallel vehicle using control strategy 1. It illustrates how the electric motor torque increases with the increase in vehicle speed. When the vehicle reaches cruising speed, the electric motor torque reduces to a slightly negative constant value while the ICE torque maintains a constant value. Then during the deceleration phase of the drive cycle, the ICE torque is at its idling torque while the electric motor torque is providing a negative torque, operating in generating mode.

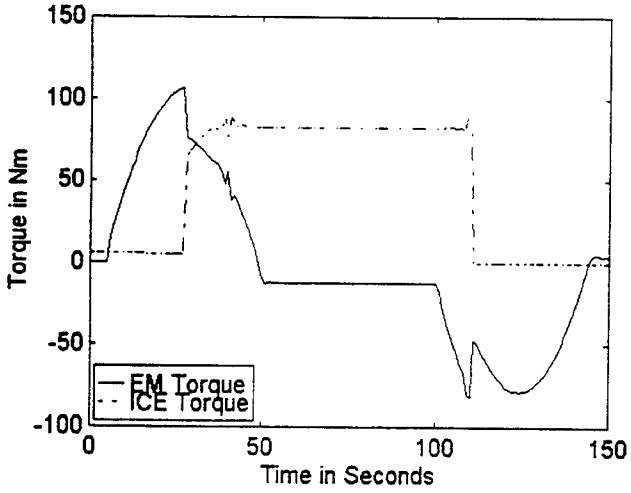

Fig. 12. EM torque and ICE torque for drive cycle one applied to the parallel vehicle with control strategy 1

Figs. 13 and 14 show the split of the ICE and electric motor torque for control strategies 1 and 2.

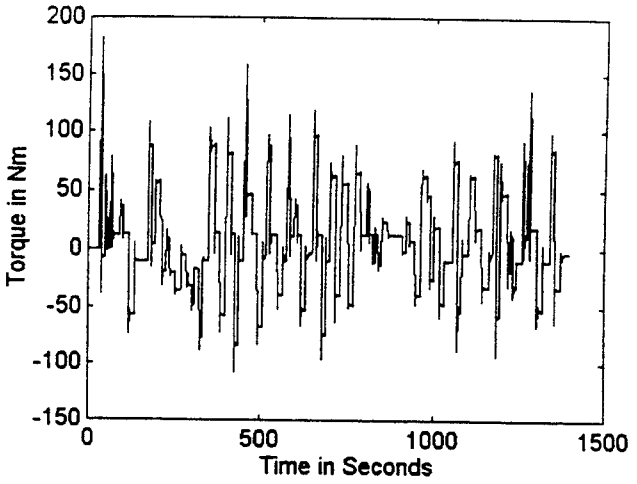

Fig. 13 (a). EM torque for federal urban drive cycle applied to parallel vehicle with control strategy 1

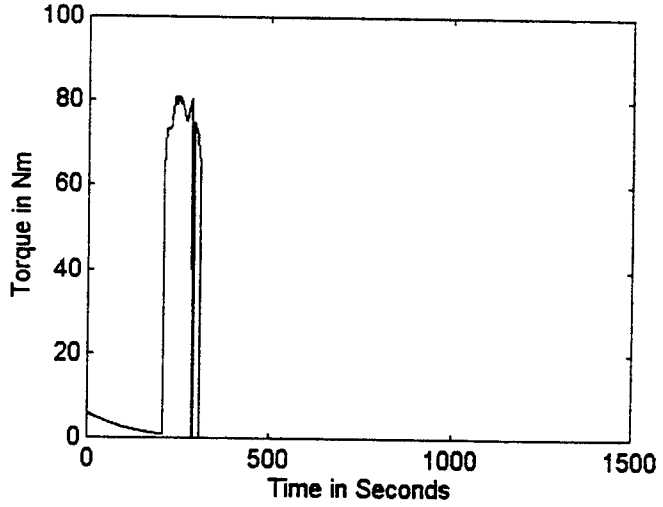

Fig. 13 (b). ICE torque for federal urban drive cycle applied to parallel vehicle with control strategy 1

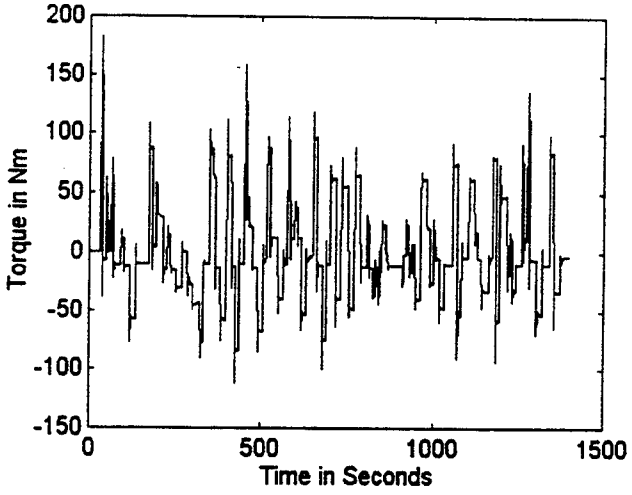

Fig. 14 (a). EM torque for federal urban drive cycle applied to parallel vehicle with control strategy 2

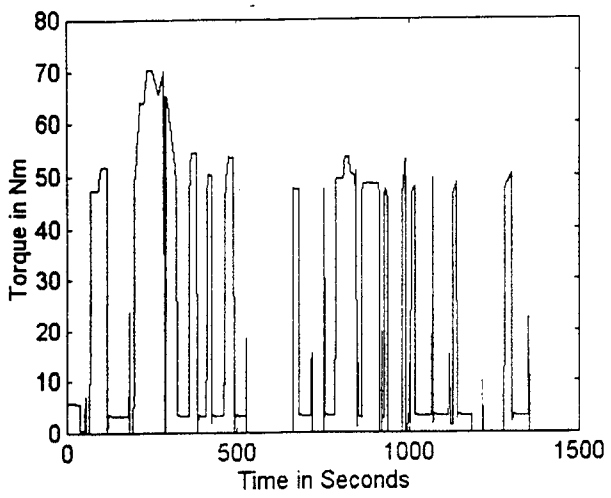

Fig. 14 (b). ICE torque for federal urban drive cycle applied to parallel vehicle with control strategy 2

Figs. 15 and 16 show the EM torque for the federal urban drive cycle applied to the series hybrid electric vehicle and electric vehicle which are virtually identical because for both vehicles the electric machine is the sole source of propulsion. In figs. 17 and 18, the differences in the battery current for the two test cases are illustrated; the battery current is larger for the electric vehicle than the series HEV.

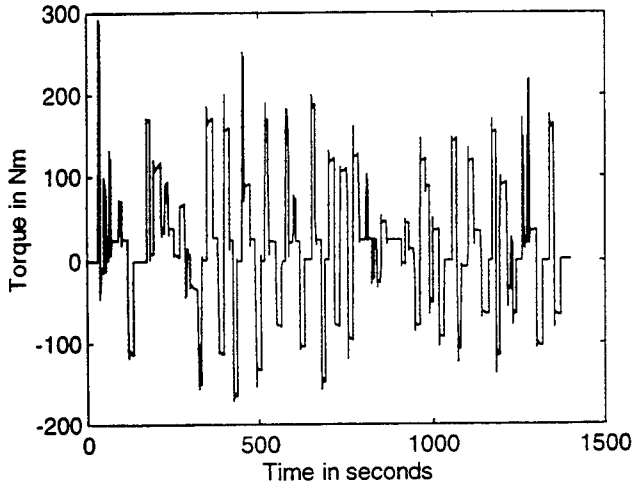

Fig. 15. EM torque for federal urban drive cycle applied to series HEV

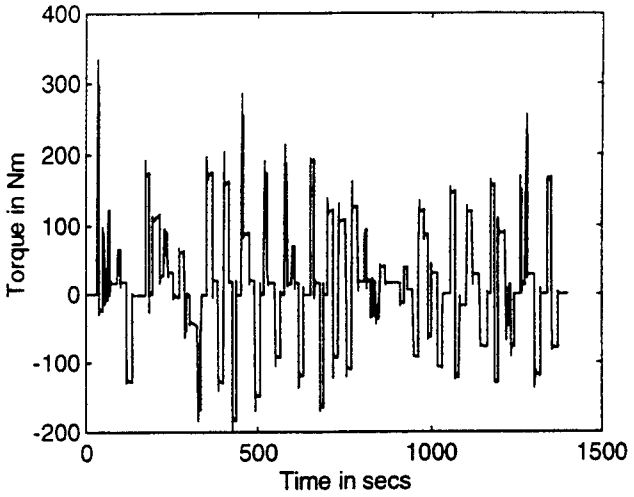

Fig. 16. EM Torque for federal urban drive cycle applied to electric vehicle

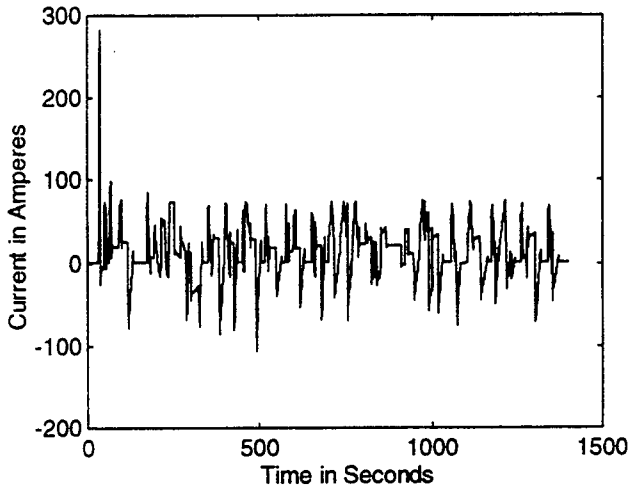

Fig. 17 Battery Current for federal urban drive cycle applied to series HEV

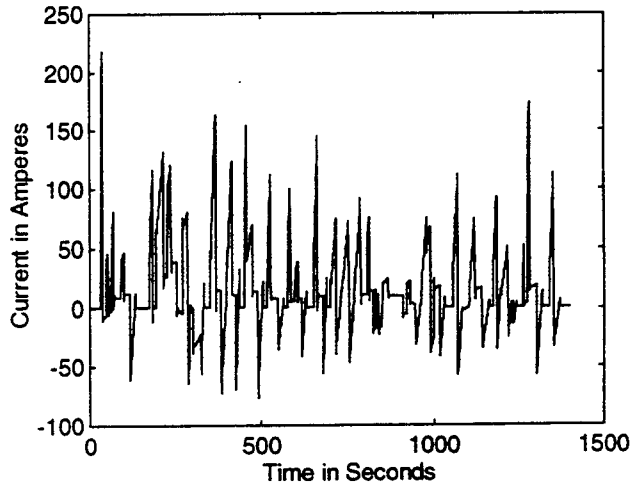

Fig. 18 Battery Current for federal urban drive cycle applied to electric vehicle

Table 5 shows a summary of results generated by the V-Elph package during the application of the four drive cycles to the five vehicle drive trains. The weight and control complexity is included in the table for each vehicle drive train. The control complexity was determined by assessing the complexity of the system controller used to manipulate the components providing propulsion to the wheels, e.g. the controller for the parallel HEV must control the ICE and electric machine. The total chemical emissions and fuel consumption of the engine and the change in the state of charge of the battery for the total drive cycle is tabulated for each vehicle.

The results for the urban drive cycle, which is composed of many quick acceleration and deceleration instances, show an improvement in the fuel consumption for the parallel HEV and series HEV. Also the engine emissions were greatly reduced. From figs. 15 and 16, it was noted earlier that the EM torque are identical for the federal urban drive cycle applied to the series HEV and electric vehicle. However, the difference in their change in the battery SoC as seen in the are due to the inclusion of the ICE in the series HEV which uses this fuel source to provide power to recharge the batteries.

The strategy of the controller for the parallel HEV using control strategy 1 was to minimize the use of the ICE. Figs. 13(a) and 13(b) shows the division of the ICE and EM torque for the urban drive cycle applied to the parallel vehicle drive train using control strategy 1. The ICE torque is only generated when the demanded vehicle speed is greater than 60 km/h. Hence the motor provides most of the power to the wheels during the drive cycle. This behavior can be seen by comparing the change in SoC for the EV of 7.58% and for the parallel HEV using control strategy 1 of 5.6% which shows that the motor in the parallel HEV is used almost as much as the motor in the EV. Also the fuel consumption (km/l) for the parallel HEV using control strategy 1 is extremely large.

Minimization of the ICE throttle is the control strategy for the parallel HEV using control strategy 2. The ICE throttle position is determined using the steady state load (aerodynamic drag and friction) required at a particular vehicle speed. In comparing the performance of this drive train using the urban and highway drive cycles, the fuel consumption, the kilometers traveled per liter, for the urban cycle is greater because the motor is used more during the urban cycle than the highway cycle.

Also the differences in the performance of the two control strategies for parallel HEV are also illustrated by the fuel consumption and change in state of charge (SoC) on the federal urban drive cycle.

Since the battery pack is the sole power supplying device in the electric vehicle, its drop in SoC is more than compared to the parallel or series hybrid vehicle.

TABLE 5 COMPARISONS BETWEEN VARIOUS VEHICLE DRIVE TRAIN CONFIGURATIONS

	Conventional	Parallel HEV control strategy 1	Parallel HEV control strategy 2	Series HEV	EV
control complexity	n/a	complex	complex	medium	simple
weight (kg)	1700	1838	1838	1908	2008
Drive Cycle One					
NOx (g/km)	2.451	1.447	1.421	2.096	NA
CO (g/km)	1.637	0.6125	0.6198	0.8544	NA
HC	0.03382	0.003336	0.00624	0.001963	NA
fuel consumption (km/l)	7.723	18.96	18.6	20.1	NA
% change in state charge	NA	+0.536	+0.3	-0.8384	-3.743
Drive Cycle Two: FTP-75 urban drive cycle					
NOx (g/km)	1.314	0.1875	0.3268	1.516	NA
CO (g/km)	1.994	0.1509	0.4926	0.6489	NA
HC	0.08234	0.01036	0.04289	0.01095	NA
fuel consumption (km/l)	5.808	56.02	21.18	19.68	NA
% change in state charge	NA	-5.6	-0.5396	-5.915	-7.58
Drive Cycle Three: Federal highway drive cycle					
NOx (g/km)	0.7071	1.04	0.86	1.574	NA
CO (g/km)	0.9732	0.7248	0.6528	0.6532	NA
HC	0.05544	0.02907	0.02962	0.002272	NA
fuel consumption (km/l)	12.4	16.5	17.23	21.89	NA
% change in state charge	NA	+10	+10.71	-9.734	-9.871
Drive Cycle Four: Commuter drive cycle					
NOx (g/km)	0.955	0.6304	0.6195	1.642	NA
CO (g/km)	1.439	0.4491	0.5907	0.6852	NA
HC	0.07379	0.01915	0.03665	0.005872	NA
fuel consumption (km/l)	6.228	24.75	18.69	20.36	NA
% change in state charge	NA	+4.2	+18.32	-34.22	-41.89

I. Conclusion

This paper discussed a new system-level modeling, simulation and analysis package developed at Texas A&M University using Matlab/Simulink to study issues related to electric vehicle (EV) and hybrid electric vehicle (HEV) design such as energy efficiency, fuel economy, and vehicle emissions. The package uses visual programming techniques, allowing the user to quickly change architectures, parameters, and to view output data graphically. It also includes detailed models of electric motors, internal combustion engines, and batteries.

The designs for four vehicle drive trains, an EV, a parallel EV, a series HEV, and a conventional ICE vehicle are presented. The results of applying a simple, a commuter, the federal urban, and the federal highway drive cycles are compared. These results illustrate the flexibility of the package for studying various issues related to electric and hybrid electric vehicle design. The simulation package can run on a PC or a Unix-based workstation.

II. Acknowledgments

Support for this work was provided by the Texas Higher Education Coordinating Board Advanced Technology Program (ATP), the Office of the Vice President for Research and Associate Provost for Graduate Studies, through the Center for Energy and Mineral Resources, Texas A&M University, and the Texas Transportation Institute.

III. References

[1] M. J. Riezenman, "Electric Vehicles," *IEEE Spectrum*, pp. 18-101, Nov. 1992.

[2] V. Wouk, "Hybrids: then and now," *IEEE Spectrum*, pp. 16-21, July 1995.

[3] A. Kalberlah, "Electric Hybrid Drive Systems for Passenger Cars and Taxis," *Tech. Rep. 910247, SAE*, 1991.

[4] B. Bates, "On the road with a Ford HEV," *IEEE Spectrum*, pp. 22-25, July 1995.

[5] M. Hayashida, and et al, "Study on Series Hybrid Electric Commuter-Car Concept," *SAE Journal SP-1243, Paper No. 970197*, Feb. 1997.

[6] A. Nikopoulos, H. Hong, and T. Krepec, "Energy Consumption Study for a Hybrid Electric Vehicle," *SAE Journal SP-1243, Paper No. 970198*, Feb. 1997.

[7] R.D. Senger, "Validation of ADVISOR as a Simulation Tool for a Series Hybrid Electric Vehicle using the Virginia Tech Future Car Lumina," Master's Thesis, Virginia Tech University, 1997.

[8] G. Cole, "Simple Electric Vehicle Simulation (SIMPLEV) v3.1," DOE Idaho National Engineering Laboratory.

[9] W.W. Marr and W.J. Walsh, "Life-cycle Cost Evaluations of Electric/Hybrid Vehicles," *Energy Conversion Management*, vol. 33:9, pp. 849-853, 1992.

[10] J.R. Bumby and et al, "Computer Modeling of the Automotive Energy Requirements for Internal Combustion Engine and Battery Electric-Powered Vehicles," *in Proceedings of IEE Pt. A*, vol. 132:5, pp. 265-79, 1985.

[11] K. B. Wipke and M. R. Cuddy, "Using an Advanced Vehicle Simulator (ADVISOR) to Guide Hybrid Vehicle Propulsion System Development," *http://www.hev.doe.gov*.

[12] D. Buntin, *Control System Design for a Parallel Hybrid Electric Vehicle*, Master's thesis, Texas A&M University, College Station, Texas, 1994.

[13] M. Ehsani, K.M. Rahman, and H.A. Toliyat, "Propulsion System Design of Electric and Hybrid Vehicles," *IEEE Transactions on Industrial Electronics*, vol. 44, Feb. 1997, pp. 19-27.

[14] H. A. Toliyat, K. M. Rahman, and M. Ehsani, "Electric Machine in Electric and Hybrid Vehicle Application," *Proceeding of ICPE '95*, Seoul, pp. 627-635.

[15] M. Ehsani, *Electrically Peaking Hybrid System and Method*, U.S. Patent granted in 1996.

[16] J. Howze, M. Ehsani, and D. Buntin, *Optimizing Torque Controller for a Parallel Hybrid Electric Vehicle*, U.S. Patent granted in 1996.

[17] *Proceedings of the ELPH Conference*, Texas A&M University, College Station, Texas, October 1994.

[18] K. M. Stevens, *A Versatile Computer Model for the Design and Analysis of Electric and Hybrid Drive Trains*, Master's thesis, Texas A&M University, College Station, Texas, 1994.

[19] K. L. Butler, K. M. Stevens, and M. Ehsani, "A Versatile Computer Simulation Tool for Design and Analysis of Electric and Hybrid Drive Trains," 1997 SAE Proceedings *Electric and Hybrid Vehicle Design Studies*, Book # SP 1243, Paper # 970199, pp. 19-25, February 1997, Detroit, MI.

[20] *Matlab/Simulink*, Version 4.2c.1/1.3c, The Mathworks Inc., Natick, Mass.

[21] D. Sherman, "Buick LeSabre Limited," *Motor Trend*, p. 65-73, July 1991

[22] B.K. Powell, "A Dynamic Model for Automotive Engine Control Analysis," in *Proceedings of the 18th IEEE Conference on Decision and Control*, pp. 120-126, 1979.

[23] S. Moore and M. Ehsani, "An Empirically Based Electrosource Horizon Lead-Acid Battery Model," *SAE Journal SP-1156, Paper No. 960448*, Feb. 1996.

[24] C. G. Hochgraf, M.J. Ryan, and H.L. Wiegman, "Engine Control Strategy for a Series Hybrid Electric Vehicle Incorporating Load-Leveling and Computer Controlled Energy Management," *SAE Journal SAE/SP-96/1156*, p. 11-24.

[25] G. Franklin, J. D. Powell, and M. Workman, *Digital Control of Dynamic Systems*, pp. 222-229, 1990, Addison-Wesley.

[26] U. Adler, ed., Automotive Handbook, Stuttgart, Germany: Robert Bosch GmbH, 2 ed., 1986.

Paper Number

A Study of Design Issues on Electrically Peaking Hybrid Electric Vehicles for Diverse Urban Driving Patterns

Z. Rahman, K. L. Butler and M. Ehsani
Texas A&M University

ABSTRACT

A vehicle's performance depends greatly on the operating conditions, such as journey type, driving behavior etc. Driving patterns vary with geographical location and traffic conditions. In today's global economy where automobile industries are concerned with both local and international markets, it becomes necessary to investigate vehicle performance for driving cycles of different countries and develop vehicle designs which are appropriate to the consumer's market. This paper concentrates on the issues related to designing hybrid electric vehicles. A method of optimizing the size of the principal hardware components of hybrid vehicles such as, electric motors, internal combustion engines, transmissions and energy storage devices based on the demands of different drive cycles is discussed in the paper. Driving cycles of five major countries around the globe were used for investigation: the ECE 15 used by United Nations Economic Commission for Europe (UN/ECE), the Japanese 10-15 mode, China's Beijing-11, Australian urban drive cycle and finally, the United States EPA75. The 'V-ELPH 2.01' EV-HEV computer simulation package developed at Texas A&M University was used for simulation testing.

INTRODUCTION

Hybrid electric vehicles (HEVs) are a viable alternative to conventional internal combustion engines (ICE)-based vehicles for the automobile industry due to environmental issues and exhausted petroleum resources. Recent efforts in HEV research are directed toward developing an energy efficient and cost-effective propulsion system [1,2]. But performance of automobiles depends not only on the vehicle drive train alone, but also on driving patterns such as journey type, driving behavior, etc. Moreover, while designing an HEV configuration, the constraints commonly imposed on optimizing critical component selection are: vehicle range, acceleration, maximum speed and road grades. All these factors are directly related to driving patterns. Hence, a comprehensive study on HEV performance over different driving conditions is very important for properly optimizing the key components in HEV design.

Consumer demand and driving patterns vary with geographical location and traffic conditions. For example, the rates of acceleration of the European standard driving cycles representing urban patterns of European drivers are lower than those drive cycles of United State's drivers [3]. Consumers of US demand extra ancillary loads, such as bigger air conditioners than other consumers. The impact of diverse driving conditions on vehicle performance is, in fact, delaying the introduction of Toyota's HEV model 'Prius' in US market. "Because the Prius was made for urban Japan's stop-and-go driving, the US model will most likely be completely different" - stated by Toyota's representative in Torrance [4].

The specifications required concerning HEV design may be divided into two categories. The first category is user-governed specification, which depends mostly on consumer's demand. The acceleration performance, maximum speed and fuel economy falls in this category. This category of specifications dictate the sizing of the vehicle components such as, the electric motor (EM), internal combustion engine (ICE) and transmission system. These are also the 'hardware' of HEVs. The second category is based on ecological issues such as vehicle emissions. The state or environment safekeeping organizations such as, Environmental Protection Agency (EPA) and California Air Regulatory Board (CARB) in US provide some regulations to automotive engineers concerning ICE exhausts. The EM-ICE control strategies developed by HEV designers should maintain vehicle emissions within the regulation limits. For charge-sustainable HEVs, the control mechanism should also take care of recharging the battery pack. The control strategy is the 'software' of the HEVs.

HEV design methodology may use a selective or general approach in defining vehicle specifications. In 'selective' designing the hardware specifications of HEV is optimized by selecting the minimum size of EM and ICE with a single gear transmission system to operate efficiently in a specific driving pattern. The control strategy is selected according to the requirement of the particular driving behavior. The 'general' design approach customizes the hardware and software specifications of the HEV so that it performs reasonably

well under diverse driving patterns. This approach, of course, will not give optimum result for any particular drive cycle. But it would be cost effective for automotive industries to generalize some of the design constraints, especially the hardware portion.

The concept of developing driving cycles for vehicle research technology was initially introduced to measure the fuel consumption and emissions of motor vehicles. Milkins and Watson [5] proposed other applications of drive cycles; 'evaluation of the merits of alternative vehicle design options' was one of them. In the same reference, the authors did a comprehensive statistical analysis on driving cycles of Japan, Europe, US and Australia. Later, Feng and Marc worked on analyzing driving patterns to model fuel economy of conventional ICE driven vehicles [6]. In [7], Feng and et al. presented simulation results on the impacts of driving patterns on EV and HEV performance in US conditions.

This paper focuses on the design issues of HEVs using the drive cycles of 5 major countries, i e United States, Japan, Australia, China and Europe. The drive cycles are analyzed to obtain the speed, acceleration performance and energy requirement of the vehicle. The peak power capacity of EM and ICE, and energy capacity of the battery pack is calculated for each drive cycle. The selective approach is taken to design parallel hybrid drive trains for each drive cycle. Simulation studies were done with the EV-HEV computer software package V-ELPH 2.01 [9] developed at Texas A&M University.

ELPH CONCEPT

HEV designers attempt to design a good control mechanism that will increase the fuel economy, reduce ICE emissions and accomplish charge sustainability of the energy pack of the vehicle. One of the focuses of the HEV research group of Texas A&M University is the design of parallel hybrids based on the electrically peaking hybrid (ELPH) concept [5]. In this type of control strategy the electric motor supplies the acceleration and deceleration power for the vehicle while the engine provides the average load power of the drive cycle. The main goal of this control technique is to use the ICE in the high speed region with almost smooth torque demand so that toxic emissions from the ICE is minimized and miles per gallon (mpg) fuel economy of the vehicle is optimized. Also measures to keep the state of charge (SOC) of the battery pack remaining within a specified limit during the driving period are taken into consideration. The objective of ELPH propulsion system is that the HEV should have comparable performance to conventional vehicles. The driving operation of the ELPH vehicles should also be similar to conventional vehicles.

HEV DYNAMICS

The power required to drive a vehicle depends on the following factors:

1. Rolling resistance of the tire with road
2. Aerodynamic drag
3. Inertial resistance in acceleration
4. Grade resistance
5. Transmission losses
6. Ancillary loads; i e, air conditioner, lights, stereo etc.

Since grade resistance is not included in all standard drive cycles, the effect of grade resistance in HEV design is neglected in this paper. The effect of air velocity is also eliminated from the simulations. Thus, total power demanded by the vehicle from its power plant is expressed as:

$$P = \frac{v(f_r Mg + \frac{1}{2}\rho C_d A_f v^2 + M\delta \frac{dv}{dt})}{\eta_t} + P_{aux} \quad (1)$$

where, P is vehicle power demand in watts, v is velocity of the car in m/s, f_r is coefficient of rolling resistance, M is vehicle weight in kg, g is acceleration of gravity in m/s^2, ρ is air density in kg/m^3, C_d is coefficient of air drag, A_f is frontal area of the vehicle in m^2, δ is mass factor which includes the effect of rotational inertia, η_t is transmission efficiency and P_{aux} is the power required to drive the ancillary (hotel) loads in watts.

CALCULATION OF ICE AND EM POWER FOR ELPH VEHICLES

For a conventional vehicle, all the power is supplied by the engine whereas in HEV, the driving power is supplied by the EM and the ICE. The ELPH concept mentions that the steady state portion of the driving power is provided by the ICE while the transient portion is supplied by EM. Hence, equation (1) is divided into two parts:

$$P_{ICE} = \frac{v(f_r Mg + \frac{1}{2}\rho C_d A_f v^2)}{\eta_t} + P_{aux} \quad (2)$$

$$P_{motor} = \frac{M\delta v \frac{dv}{dt}}{\eta_t} \quad (3)$$

where, P_{ICE} is the power provided by the ICE in watts and P_{motor} is the power provided by the EM in watts. The primary bottleneck considered in HEV development is the low power and energy density of the battery pack. To minimize loading on the battery pack and thus the EM, power required for auxiliary loads (P_{aux}) is considered to be delivered by the ICE. If we consider the mass and dimension for a typical vehicle model to be fixed then all the parameters except vehicle speed (v) in equation (2) and (3) becomes a constant. Hence, the engine power becomes a function of vehicle speed (v) only and motor power is proportional to the product of vehicle speed and

acceleration ($v\frac{dv}{dt}$): named as specific energy K. Therefore, the maximum engine capacity can be determined by the peak velocity (v_{max}) of the drive cycle. Similarly, the motor power rating can be determined by taking maximum specific energy (K_{max}) of the drive cycle.

CALCULATION OF BATTERY CAPACITY

The size of the battery pack is dependent on two factors. First, the battery pack should be capable of delivering motor peak power. Second, in case of charge sustainable HEVs, the battery energy should meet the requirement of keeping battery SOC within a specified limit. (For charge depleting EV/HEV, the size the of battery pack depends on the vehicle range specification). The peak power demand of the battery can be calculated by equation (3). But the energy requirement of the battery depends on the EM-ICE control strategy of HEV. Different control strategies will obtain different fuel economies and different battery energy capacities. Presently, the ELPH configuration is designed using one of two electrically peaking control strategies, referred to as control strategy 1 and control strategy 2. The descriptions of these control strategies are presented later.

In this paper, the method to determine battery energy capacity is followed from the concept [10] with an empirical model of the horizon lead-acid battery [11] developed for 'V-ELPH'. The energy supplied by the battery pack in a drive cycle at time t is:

$$E = \int_0^t P_b d\tau \qquad (4)$$

where, E is the net energy in watt-s supplied from battery pack at time t seconds and P_b in watts is the battery power. During positive motor power demand, such as acceleration and cruising, the motor power is delivered by the battery. Hence,

$$P_b = \frac{P_{motor}}{\eta_{bd}\eta_{motor}} \qquad (5)$$

where, η_{bd} is the battery discharging efficiency and η_{motor} is motor efficiency. During braking mode the motor delivers power back to the battery. But because of the chemical sluggishness involved in recharging the battery pack, the maximum regenerative braking power that the electric system can supply is limited by the maximum recharging current. Hence,

$$P_b = P_{motor}\eta_{bc}\eta_{gen} \quad ,I_b \le I_{rmax} \qquad (6.a)$$

$$P_b = P_{b\,max} \quad ,I_b > I_{rmax} \qquad (6.b)$$

where, η_{bc} is battery charging efficiency, η_{gen} is regenerating efficiency of EM, I_b is battery current in amperes, I_{rmax} is maximum recharging current in amperes and P_{bmax} is maximum regenerative braking power in watts. The time history of the energy delivered by the battery pack for a given drive cycle can be obtained from equations (4), (5) and (6).

For a charge sustainable HEV, the SOC of battery is always kept within a specified range. So, the battery should be capable of delivering energy with its SOC remaining within the range. Thus, the minimum energy capacity of the battery is:

$$C_b = \frac{|\Delta E_{max}|}{\Delta SOC} \qquad (7)$$

where, C_b is battery energy capacity in watt-s, ΔE_{max} is the maximum variation of battery energy in watt-s in time-energy profile, ΔSOC is the allowable range of SOC in percentage.

The equation to obtain the gear ratio between the driving units (ICE and EM) with the drive wheel is:

$$i_t = \frac{\pi n_{max} r}{30 v_{max}} \qquad (8)$$

where, i_t is the gear ratio, n_{max} is the maximum speed of ICE or EM in rpm, r is wheel radius in meters and v_{max} is maximum vehicle speed in m/s.

DRIVE CYCLES

Figure 1 presents the urban drive cycles of five countries: EPA75 of the United States, Australian urban (AU), ECE 15 of the EEC nations, M10-15 of Japan and Beijing-11 (Bj-11) of China. Drive cycles from US and Australia represent actual driving behavior while drive cycles from Europe, Japan and China were constructed by using constant accelerations and decelerations. Unusual driving conditions, such as hill climbing, load pulling, stormy weather, etc are not considered in these cycles.

ESTIMATION OF HEV HARDWARES

In this example, a typical 4 door, 5-seat family sedan was selected [10]. The vehicle specifications are:

- Weight, M — 1700kg
- Coefficient of rolling resistance, f_r — 0.013
- Coefficient of air drag, C_d — 0.29
- Frontal area, A_f — 2.13m^2
- Wheel radius, r — 0.2794m
- Ancillary load, P_{aux} — 5 kW

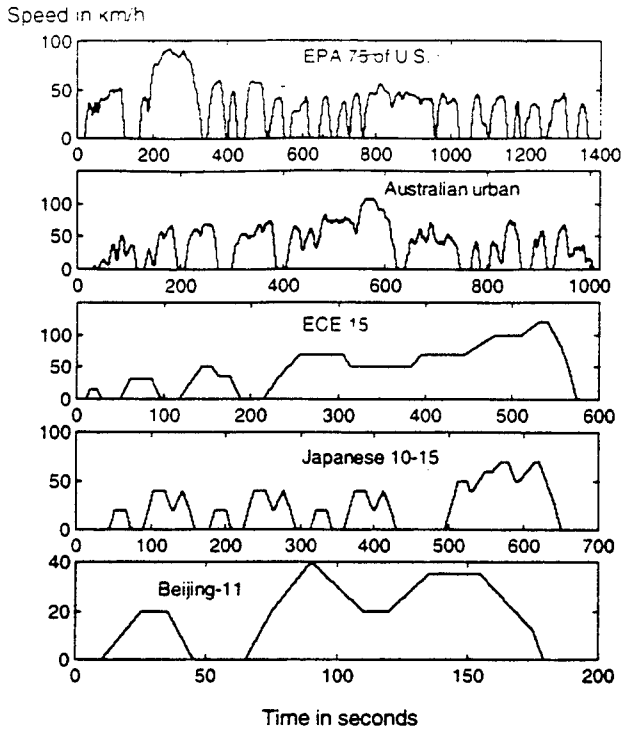

Figure 1. Velocity-time profile of the drive cycles. (See additional source section for reference).

DETERMINATION OF ICE, EM AND BATTERY POWER FOR ELPH VEHICLES

Table 1 shows the maximum speed v_{max} and maximum specific energy K_{max} of the five drive cycles. The power capacity of ICE and EM are calculated using equation (1) and (2). In the calculation, the transmission efficiency, η_t = 0.92, mass factor, δ = 1.035 and air density, ρ = 1.202kg/m^3. The peak power capacity of the battery can be calculated from equation (5) taking battery discharging efficiency, η_{bd} = 0.85 and motor efficiency, η_{motor} = 0.9.

Table 1. Determination of ICE, EM and battery power for different drive cycles.

Drive Cycles	v_{max} km/h	K_{max} m^2/s^3	P_{ice} kW	P_{motor} kW	P_b kW
EPA 75	91.2	20	17.53	38.25	50
AU	107.5	33.5	22.8	64	82
ECE 15	120	9.5	27.8	18	23.5
M10-15	70	10.7	12.55	20.5	26.8
BJ-11	40	4	8	7.65	10

The ratings specified in table 1 show a remarkable variation of ICE and EM power for different drive cycles. Because of a very simple driving pattern, ratings obtained for BJ-11 is found to be rather impractical. So, we restrain from further investigation on BJ-11. The Australian urban cycle requires the highest power rating for EM to satisfy the high acceleration demand of the Australian drivers. On the other hand, high speed limits in European countries demand high power ICE than EM. Table 1 also shows that the variation of motor power demand is more prominent than the variation in engine power demand. Electric motors have the capability to operate in overload for a short time. Motor power, P_{motor}, specified in table 1 is basically the peak power needed by the vehicle during the very short transient period of acceleration. Usually the continuous power rating of EM is half of the peak power rating. So, a parallel HEV requires a traction motor with the power rating of 20kW continuous/ 40 kW transient to satisfy the driving performance of EPA 75. The ICE ratings shown in table 1 are, actually, the minimum power demanded by the vehicle during cruising. Road grades, stormy weather conditions, load pulling, etc were not considered in the calculation. So to factor in these conditions the rated ICE power will need to be higher than the ratings stated in table 1. Furthermore, the engine produces its peak power at a shaft speed below its maximum shaft speed (see figure 2.a). The ICE power (P_{ICE}) stated in table 1 refers to engine power at maximum car speed, which is also the maximum shaft speed. Hence, the peak ICE power must be slightly larger than P_{ICE} stated in table 1 ($P_{ICEmax} > P_{ICE}$).

DETERMINATION OF BATTERY ENERGY

Before calculating battery energy capacity, the gear ratio for the motor and engine to the drive wheels need to be calculated. Figure 2.a and 2.b show the profile for torque and power of a typical engine and motor with their shaft speeds. These figures were derived using the empirical engine model and steady state vector controlled induction motor model available in the HEV simulation software V-ELPH 2.01. In this example, the engine operating speed is taken to be 1000 rpm to 6500 rpm (figure 2.a). Motor base speed is chosen 3000 rpm with an extended operating range up to 12000 rpm (figure 2.b). The gear ratios for the engine and motor is calculated by equation (8) taking the maximum shaft speed n_{max} to be 6500 rpm for the engine and 12000 rpm for electric motor. Table 2 shows the gear ratios obtained for different drive cycles.

In this example it was considered that the engine alone is responsible to deliver power to the ancillary loads. Therefore, considering a constant 5 kW of ancillary load operating over the driving schedule the idle speed of engine is determined by the speed in which ICE is capable of delivering 5 kW of power. As engine size will vary due to different power ratings for different drive cycles, the idle speed of the engine will, therefore, be different (see table 2) for different drive cycles. A steady state motor model is used in the simulation having

braking torque 2.5 times its rated torque. The advantage of overloading the electric motor to twice its continuous power rating was not considered in the simulation. But operation above the base torque limit for 1-minute period was allowed in the simulations. The motoring and regenerating profile was considered symmetrical and efficiency of regeneration (η_{gen}) was taken as 0.85. The regenerating current (I_{max}) of the battery was limited to 100 amperes.

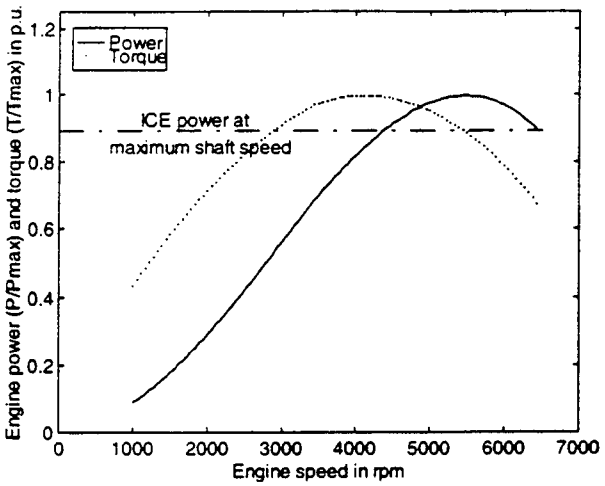

Figure 2.a Torque and power characteristics of Engine

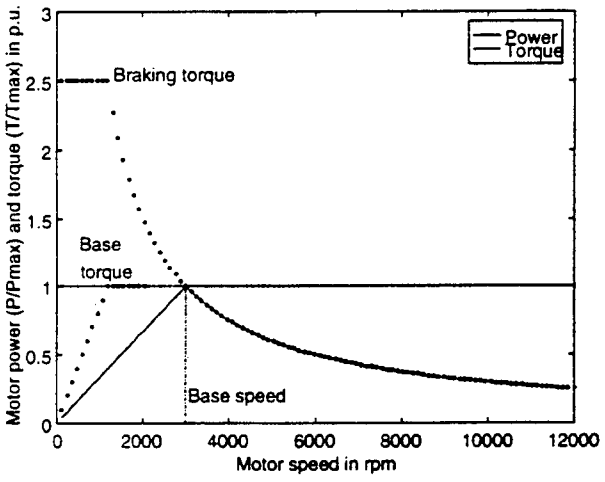

Figure 2.b Torque and power characteristics of Motor

A charge sustainable HEV requires a proper control strategy to maintain battery SOC over the driving schedule. In this example the initial SOC of battery was considered 60% and the allowable range of SOC fluctuation (ΔSOC) was taken as 20%. The two control strategies utilized in the simulations are explained below.

Control Strategy 1

Control strategy 1 (CS1) operates such that the ICE runs at a constant fuel throttle angle and the electric machine makes up the difference between the torque requested by the driver and the torque produced by the ICE. After overcoming the road load, the extra power produced by the ICE is used to charge the battery. This scheme aims to minimize the amount of time that the ICE is in use by maximizing the speed at which the ICE is engaged to the wheels while maintaining the battery state of charge of the drive cycle.

Control Strategy 2

Control strategy 2 (CS2) operates such that the ICE operates over its entire speed range and makes the ICE throttle angle a function of speed to meet the steady-state road load, as shown in figure 3. Since the battery would be depleted in a truly electrically-peaking design, the amount of power that the ICE produces needs to exceed the steady-state road load by some amount to implement a charge sustainable hybrid. In this control strategy, the gain of ICE throttle controller is varied until the battery SOC is maintained over the drive cycles.

$$\text{gain} = \frac{\text{ICE throttle command}}{\text{ICE throttle for steady state road load}} \quad (9)$$

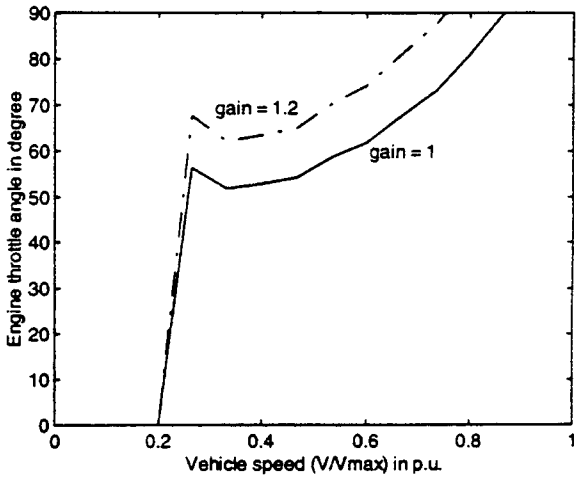

Figure 3. Variation of engine throttle angle with car speed with two different gains for control strategy 2.

The general principle behind each strategy is that the electric motor provides power for propulsion during the transients, acceleration and deceleration, and the ICE provides propulsion during cruising.

Results

Figure 4 to 7 shows the simulation results. The minimum engine and motor size corresponding to each drive cycles, as stated in table 1, was used in the simulations. Results show that the HEVs designed for each drive cycles met the driver's demand. Maximum change in battery energy is obtained from these figures. The minimum battery capacity was calculated by equation (7) taking the allowable variation in battery SOC to be 20%. A tabular presentation of the simulation results is given in table 2.

Table 2. The gear ratios and battery capacities obtained from simulation for control strategy 1 (CS1) and control strategy 2 (CS2) with four different driving cycles.

Drive Cycle	Gear ratio ICE	Gear ratio EM	ICE idle speed (rpm)	ICE engage speed for CS1 (rpm)	ICE throttle controller gain for CS2	Maximum change in battery energy (kW-hr) CS1	Maximum change in battery energy (kW-hr) CS2	Minimum battery capacity (kW-hr) CS1	Minimum battery capacity (kW-hr) CS2
EPA 75	7.51	13.86	2000	3000	1.05	0.15	0.12	0.75	0.6
AU	6.37	11.76	1500	2000	1.3	0.14	0.11	0.7	0.55
ECE 15	5.7	10.53	1500	3800	1.05	0.05	0.01	0.075	0.05
M10-15	9.78	18.06	2500	3700	1.2	0.01	0.01	0.05	0.05

The third column of table 2 shows a high ICE idle speed for the Japanese drive cycle. The reason is that the engine size for M10-15 of Japan was smaller compared to other drive cycles. To produce 5 kW of constant power for the auxiliary loads with this engine required it to operate in high speed. Frequent acceleration-deceleration in US and Australian drive cycles necessitated the ICE to be engaged with the drive wheel at a lower speed range than the European and Japanese drive cycles for CS1. High acceleration power demand of the Australian drive cycle required a throttle gain of 1.3 for CS2 to keep the change in battery energy level close to zero over the total driving period. Such a high throttle gain for the Australian driving pattern actually indicates that the engine was operating in almost wide open throttle position, which is similar to the concept of CS1. Figure 5.b, therefore, shows a very close resemblance with figure 5.a. On the other hand, driving patterns for Europe and US required a nominal throttle gain of 1.05 in CS2. The maximum variation of battery energy was less for CS2 than CS1 for all driving patterns. The reason is that in CS1 the ICE provides power in high magnitude but less frequently, whereas, in CS2 the ICE provides power in low magnitude but more frequently.

A typical 12-volt lead-acid battery cell has power density of 280 w/kg and energy density of 34 w-hr/kg. The battery energy capacity obtained in the simulation results indicates that a small size of battery pack is sufficient enough for ELPH HEVs. But the power requirement of the battery demands larger battery pack. For example, the Australian drive cycle requires a battery pack capable of producing peak power of 82 kW (= 293 kg), whereas, the energy requirement of the battery indicates a battery pack of 0.7 kW-hr (= 21kg) for CS1 and 0.55 kW-hr (= 16 kg) for CS2. The figures indicate that the battery pack needs to be sized by its peak power rating rather than the energy requirement. In fact, the acceleration performance of EV/HEVs are limited mostly because of the weight and volume of the battery pack.

In this example, transmission systems for all vehicles were considered to be single gear. A multigear transmission system will, of course, increase the acceleration performance and gradeability of the vehicle with the cost of increasing system complexity and weight.

COMPARISON STUDY

To compare the power ratings of the designed parallel HEVs for different driving conditions with a few of today's parallel HEVs manufactured by automobile industries, table 3 is presented below. The EM's peak power capacity and weight per piece of NiMH batteries used in 'Toyota Prius' was not available in [13] and hence is omitted from the table.

Table 3. ICE, EM and battery size of commercial parallel HEVs.

Manufacturer	Engine size (kW)	Motor Size Cont./Peak (kW)	Energy storage
Ford Werke AG Escort [12]	60	20/40	200 kg of NiCd, 7kWh
Subaru ElCapa [12]	48	10/19	302 kWs of capacitor + 5.7 kWh PbAcid
Toyota Prius [13]	45	30/-	40 pieces of NiMH, 55wh/kg

Comparing table 1 with table 3, it is evident that HEVs of Ford and Subaru tend to use larger engines and smaller motors compared to the ELPH based HEV designed in this paper. Using small size motors in HEV favors lower battery weight and volume. But small motors cannot produce the total accelerating power by itself. Therefore, the engine is required to operate in low speed operation, which requires multigear transmission system. The control strategies used in the three HEVs are, of course, different than the ELPH based CS1 and CS2. Yet, it is evident that Subaru's 'Elcapa' is suited more for European driving condition than the US and Australian

driving pattern. Ford's 'Escort' has ICE and EM ratings matched with US driving condition. But it might not be able to satisfy the Australian drive cycle with ELPH based strategies. The powerful engine of 'Escort' will be required to operate in acceleration modes. Toyota's 'Prius' is a truly parallel HEV with comparable ICE and EM power ratings. Of course, further studies are necessary in this area.

The engine sizes proposed for the drive cycles in table 1 are smaller than the engine size used in the vehicles of table 3. The reason is, that the five drive cycles do not include the influence of road grades, load pulling or air velocity. These factors will necessitate a larger size engine.

Drive cycles for Japan and Europe were developed with constant acceleration and deceleration. So, motor power obtained for these drive cycles show values smaller than values expected in real life. More realistic drive cycles including the effect of road grades, air velocity, load pulling will give more insight in HEV design issues.

CONCLUSION

This paper has shown the effect of diverse urban driving patterns in HEV hardware designing. Four parallel HEVs were developed for four urban areas around the globe by optimizing the size of the HEV components using ELPH concept. For conventional vehicles, resizing the engine is, more or less, the main issue as cars are imported to different driving environments. But for hybrid cars, the degrees of freedom involved in the arrangement and sizing of HEV components are so many that it becomes more complicated to design an HEV than a conventional vehicle to be compatible for different driving patterns.

This paper also emphasizes the importance of realistic and contemporary driving patterns. In this paper, the effect of the variation of auxiliary loads was not considered. But the impact of the variety of auxiliary vehicle loads on HEV performance is also another important issue as user demand will vary with geographical locations.

ACKNOWLEDGMENTS

The authors affirm their appreciation to all the students and faculty persons in the HEV research group of Texas A&M university in developing V-ELPH 2.01. Support for this work was provided by the Texas Higher Education Coordinating Board Advanced Technology Program (ATP) and the Office of the Vice President for Research and Associate Provost for Graduate Studies, through the Center for Energy and Mineral Resources, Texas A&M University.

The authors would specially like to thank Dr. Harry Watson, University of Melbourne, for providing the Australian urban drive cycle and Dr. Sado Imai, Mitsubishi motors, for providing Japan's 10 and 15 mode drive cycle.

CONTACT

K. L. Butler received the Ph.D. degree in May 1994 in electrical engineering from the Howard University where she was a NASA fellow. She received the B.S.E.E. degree in 1985 and M.S.E.E. degree in 1987 from Southern University in Baton Rouge and University of Texas in Austin, respectively. She is currently an assistant professor at Texas A&M University. She is a recent recipient of an NSF Faculty Early Career Development (CAREER) Award.

Dr. Butler was a member of technical staff at Hughes Aircraft Company from 1988-89. Her research interests are in the areas of intelligent systems, modeling and simulation, power distribution automation and system protection.

REFERENCES

1. M. Ehsani, K. M. Rahman and H. A. Toliyat, "Propulsion System Design of Electric and Hybrid Vehicles", *IEEE Trans. on Industrial Electronics, vol. 44, no. 1, Feb. 1997.*
2. A. F. Burke, "Hybrid/Electric Vehicle Design Options and Evaluations", *SAE 920447.*
3. Michel Andre' et al, "Driving Cycles for Emission Measurements Under European Conditions", *SAE 950926.*
4. D. E. Frey, "Toyota decides not to sell Prius in US this year", *http://texnews.com/1998.*
5. Milkins and Watson, "Comparison of Urban Driving Patterns", *SAE 830939.*
6. Feng An and M. Ross, "A Model of Fuel Economy and Driving Patterns", *SAE 930328.*
7. Feng An and et al, "Impacts of Diverse Driving Cycles in Electric and Hybrid Electric Vehicle Performance", *SAE 972646.*
8. M. Ehsani and et al, "Introduction to ELPH: A Parallel Hybrid Vehicle Concept", *Proceedings of the ELPH Conference, 1994.*
9. K. L. Butler, K. M. Stevens and M. Ehsani, "A Versatile Computer Simulation Tool for Design and Analysis of Electric and Hybrid Drive Trains", *SAE 970199.*
10. Y. Gao, K. M. Rahman and M. Ehsani, "The Energy Flow Management and Battery Energy Capacity Determination for the Drive Train of Electrically Peaking Hybrid Vehicle", *SAE 972647*
11. S. Moore and M. Ehsani, "An Empirically Based Electrosource Horizon Lead-Acid Battery Model", *SAE 960448.*
12. F. A. Wyczalek, "Hybrid Electric Vehicles (EVS-13 OSAKA)", *ISBN# 0-7803-3277-6, IEEE1997.*
13. "Toyota Prius", *http://www.acceleration - online.com/ toyota.htm*

ADDITIONAL SOURCES

The 'EPE 75' and 'ECE 15' drive cycles were obtained from the webpage of EPE. The 'Australian urban' was provided by Dr. Harry Watson, 'Japanese 10-15' was provided by Dr. Sado Imai. 'Beijing 11' drive cycle was reconstructed from the Ph.D. dissertation of Dr. Feng An.

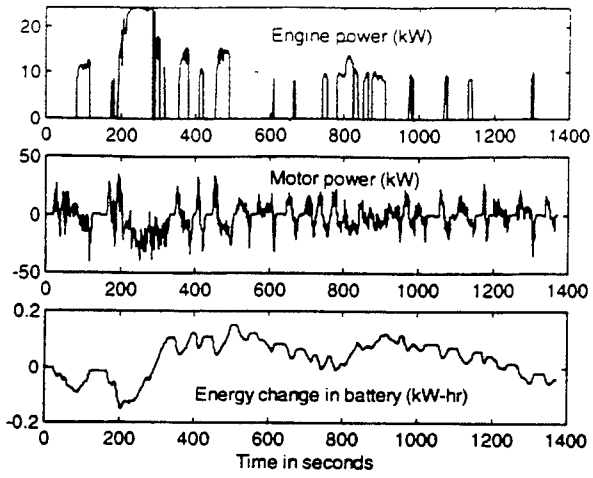

Figure 4.a Time history of engine power, motor power and energy change in battery for EPA 75 with CS1.

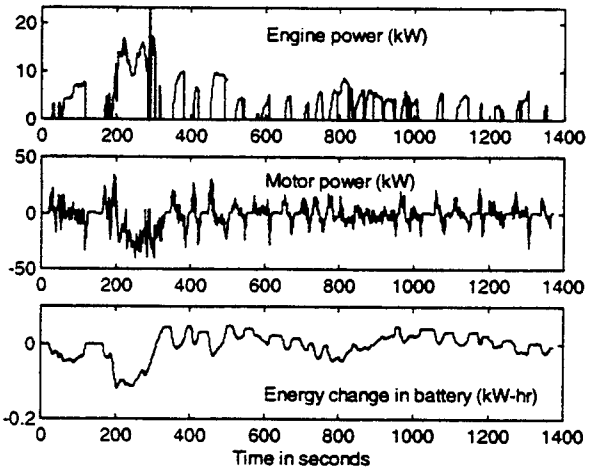

Figure 4.b Time history of engine power, motor power and energy change in battery for EPA 75 with CS2.

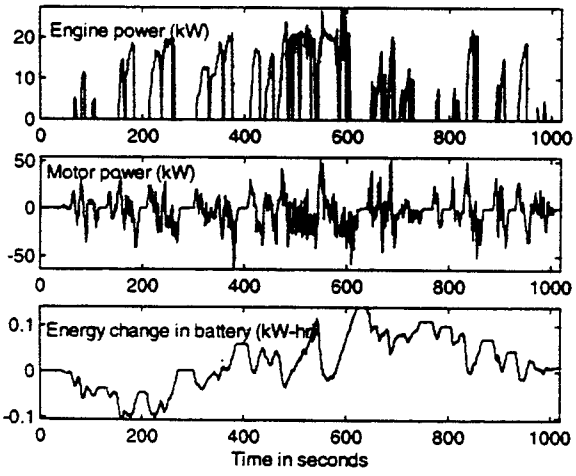

Figure 5.a Time history of engine power, motor power and energy change in battery for Australian urban with CS1.

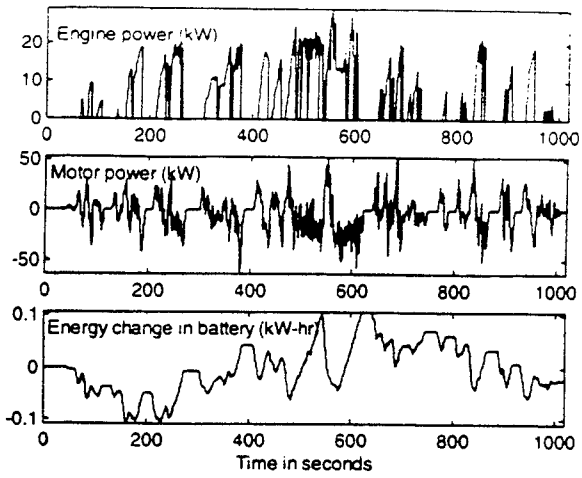

Figure 5.b Time history of engine power, motor power and energy change in battery for Australian urban with CS2.

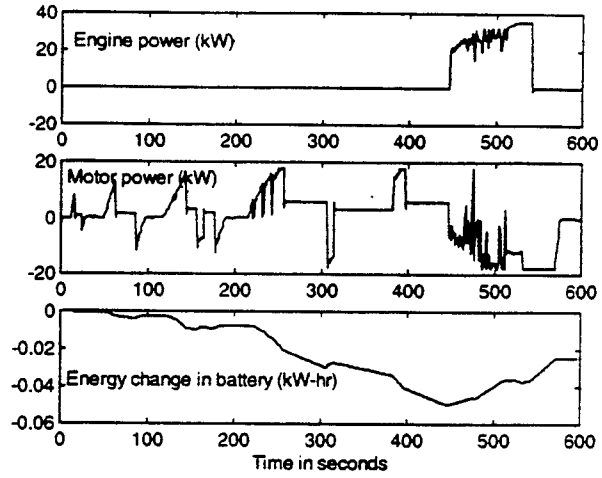

Figure 6.a Time history of engine power, motor power and energy change in battery for ECE 15 with CS1.

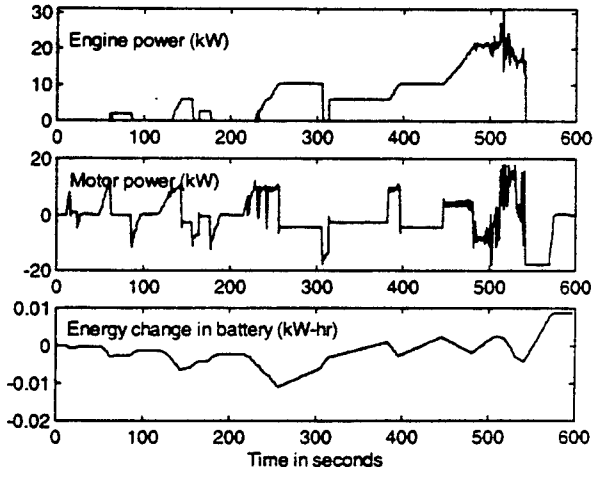

Figure 6.b Time history of engine power, motor power and energy change in battery for ECE 15 with CS2.

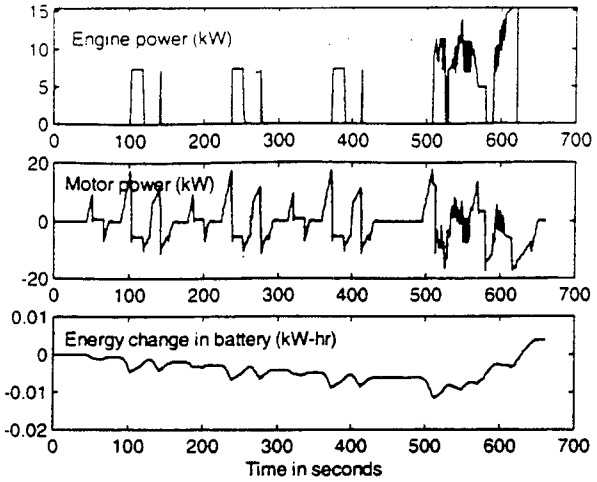

Figure 7.a Time history of engine power, motor power and energy change in battery for Japan 10-15 with CS1.

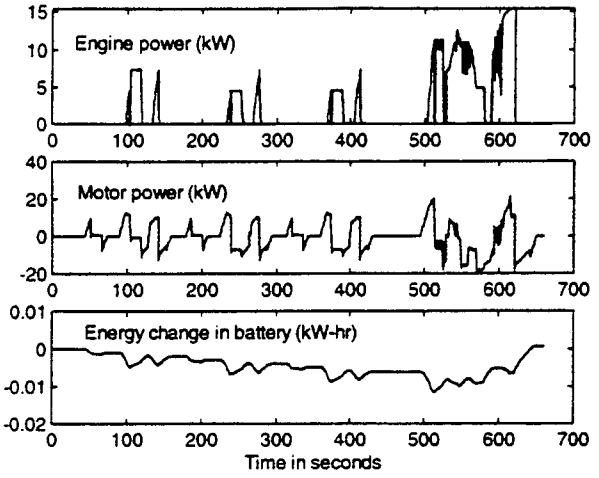

Figure 7.b Time history of engine power, motor power and energy change in battery for Japan 10-15 with CS2.